DISSERTATION ZUR ERLANGUNG DES DOKTORGRADES
DER FAKULTÄT FÜR CHEMIE UND PHARMAZIE
DER LUDWIG-MAXIMILIANS-UNIVERSITÄT MÜNCHEN


# Oil-Based Parenteral Depot Formulation for Veterinary Peptide Delivery

YORDANKA ZHIVKOVA YORDANOVA

aus

Shumen, Bulgarien

2018

**Erklärung**
Diese Dissertation wurde im Sinne von § 7 der Promotionsordnung vom 28. November 2011 von Herrn Prof. Dr. Wolfgang Frieß betreut.

**Eidesstattliche Versicherung**
Diese Dissertation wurde eigenständig und ohne unerlaubte Hilfe erarbeitet.
München, den 16.09.2018

.....
Yordanka Yordanova

**Dissertation eingereicht am 11.10.2018**

**1. Gutachter:** Prof. Dr. Wolfgang Frieß
**2. Gutachter:** Prof. Dr. Gerhard Winter

**Mündliche Prüfung am 30.10.2018**

*To my parents and my sister*

*Thank you for always being there for me in the moments when I am most scared to make the next step. Your never ending support has inspired me to carry on moving and never stop dreaming. I feel blessed and proud to have you by my side!*

***За моите родители и за моята сестра, които винаги са били до мен и са ми помагали да направя следващата стъпка, когато най-много ме е било страх. Вашата безкрайна подкрепа ме кара да продължавам напред и да не спирам да мечтая. Щастлива съм че ви имам!***

# CONTENTS

# PREFACE

I would like to tell you a short story of how the simplest ideas could turn into one's life's passion, without your knowledge. The following thesis summarizes my research work over the last 5 years and represents a work, which started way before that time. I was born and raised in a small town in Bulgaria called Shumen. I applied for studies in pharmaceutical sciences at the University of Frankfurt. At that time not many people could associate Frankfurt with science and research, since it is mainly a finance centre. When I enrolled for classes, at first I did not know what to expect. I still remember the welcoming speech of Prof. Steinhilber. I was sitting in the back of the B1 lecture room while he spoke passionately about the world of pharmaceutical science, research and drug discovery. This gave me some first insights into the world of research and practical application of science and was also the beginning of my path towards scientific research. I never regretted my choice of subject at the university, even if it was not always easy. Parallel to studying, I worked various part-time jobs and all these jobs helped me gain some valuable experience and offered me a different view in comparison to the academic one. During that time I met a lot of different people, many of whom I became good friends with. After passing the second state exam, I began the next chapter of my life. I finished my practical year in order to take and pass the third state exam and become a pharmacist. My PhD studies brought me to Munich.

The scientific knowledge which I had accumulated until then could be applied to my studies. I then stared working on the main project of my thesis, the development of an oil depot suspension. I learned to never underestimate a project just because it appears to be simple on the surface.

I believe in thinking differently and in the fact that progress comes from ideas that are put into action. Pharmaceutical technology is for me the kind of science that will give you the tools to turn an idea into applicable product.

Yordanka Yordanova

Munich,

September 16, 2018

# CHAPTER ONE

# **INTRODUCTION**

# 1 GnRH [6-D-Phe] acetate Oil Depot Suspension

Yordanka Yordanova[1], Johannes Kauffold[2], Wolfgang Zaremba[3], Wolfgang Friess[1]

1. Department of Pharmacy, Pharmaceutical Technology & Biopharmaceutics, Ludwig-Maximilians-Universitaet, Butenandtstrasse 5, 81377 Muenchen, Germany
2. University of Leipzig, Faculty of Veterinary Medicine, An den Tierkliniken 29, 04103 Leipzig, Germany
3. Veyx Pharma GmbH, Scientific Department, Soehreweg 6, 34639 Schwarzenborn, Germany

**The following chapter serves as an introduction to the research work of formulating a new parenteral depot of GnRH [6-D-Phe] acetate peptide for swine cycle synchronization, referred to as estrous cycle. It starts by covering the physiological principles underlying the estrous cycle in the swine and then continues with a brief overview of the current procedures employed for estrus synchronization. Their major drawbacks are outlined, making the research and development of alternative procedures for cycle synchronization necessary. On this basis, the requirements from a veterinary and swine physiology perspective were translated into formulation and studies from a galenic point of view.**

## 1.1 INTRODUCTION

Research efforts to synchronize the estrous cycle and ovulation in pigs with the ultimate goal of fixed time artificial insemination (AI) date back to 1949 and 1962. Tanabe et al[1] and Dzuik and Baker[2] reported the first seminal studies for the use of chorionic gonadotropin (hCG) to stimulate follicle development and ovulation. The results of these early studies facilitated the East German Research efforts into using protocols based on gonadotropins to induce puberty, synchronize estrous cycle and implement fixed time insemination strategies[3,4]. The ultimate goal of the synchronization protocols was to mimic the reproductive physiology of the pig with the advantage of a simultaneous and periodic batch wise AI based on the concept of all-in-all-out. The developed protocols provided animals in the same reproductive stage thus reducing the nonproductive days and labor with an improved economic outcome for the farm. The strive in the last years in the pig sector to further reduce the costs and labor as well as the enormous pressure to decrease the use of antibiotics has resulted in a demand for new approaches and formulations for manipulating the reproductive processes in the female pig. This reinforces the need of actively managing reproduction using simple and robust protocols. The development of such protocols requires the understanding of the reproductive cycle and the availability of hormones and hormonally active substances in suitable galenic formulations. In the following we will explain in short the reproductive cycle of a swine, which will then lead to the formulation requirements.

## 1.2 THE ESTROUS CYCLE IN PIGS

In general, the estrous cycle in pigs spans a period of 18-24 days (Figure 1.1). The cycle is strictly controlled through an integrated system, involving the hypothalamus, pituitary gland, ovary and reproductive tract. The hypothalamus exerts its action on the pituitary gland through a decapeptide gonadotropin releasing hormone (GnRH). GnRH is released in a pulsatile manner, approximately every 90 minutes, and stimulates the secretion of gonadotropins from the anterior pituitary gland, follicle stimulating hormone (FSH) and luteinizing hormone (LH). FSH and LH regulate the ovary and the production of estrogen and progesterone. These hormones feed back negatively to the hypothalamus suppressing the release of GnRH and directly influencing the secretion of FSH and LH by desensitizing the anterior pituitary gland to GnRH. In short, the systems is self-regulating and adjusting and working on the principle of a cruise control in order to maintain hormonal homeostasis. What happens within the cycle?

The cycle itself can be separated in two major phases, regulated by either FSH or LH. As shown in Figure 1.1, it consists of a LH- regulated 13 to 15 days corpus luteum formation period (luteal phase) and a FSH-regulated 5 to 7 days follicle growth and development period (follicular phase). During the luteal phase, ovarian production of progesterone has a negative influence on follicular growth by preventing the secretion of both FSH and LH. It basically hits the break on FSH and LH when it senses that the progesterone levels are too high. Around days 12 to 14 of the cycle, the progesterone concentration declines. Then the uterine production of prostaglandin $F_{2\alpha}$ ($PGF_{2\alpha}$) of non-pregnant animals causes the rapid regression of corpora lutea (luteolysis). With the destruction of the corpora lutea the progesterone production ceases. When the break is gone appropriate secretory patterns of FSH and LH resume, induced by the pulsatile release of GnRH. FSH and LH stimulate ovarian follicle development resulting in increased estrogen production, ultimately inducing behavioural estrus. The estrogen inhibits selectively only the production of FSH and induces a surge release of LH and subsequent ovulation[5].

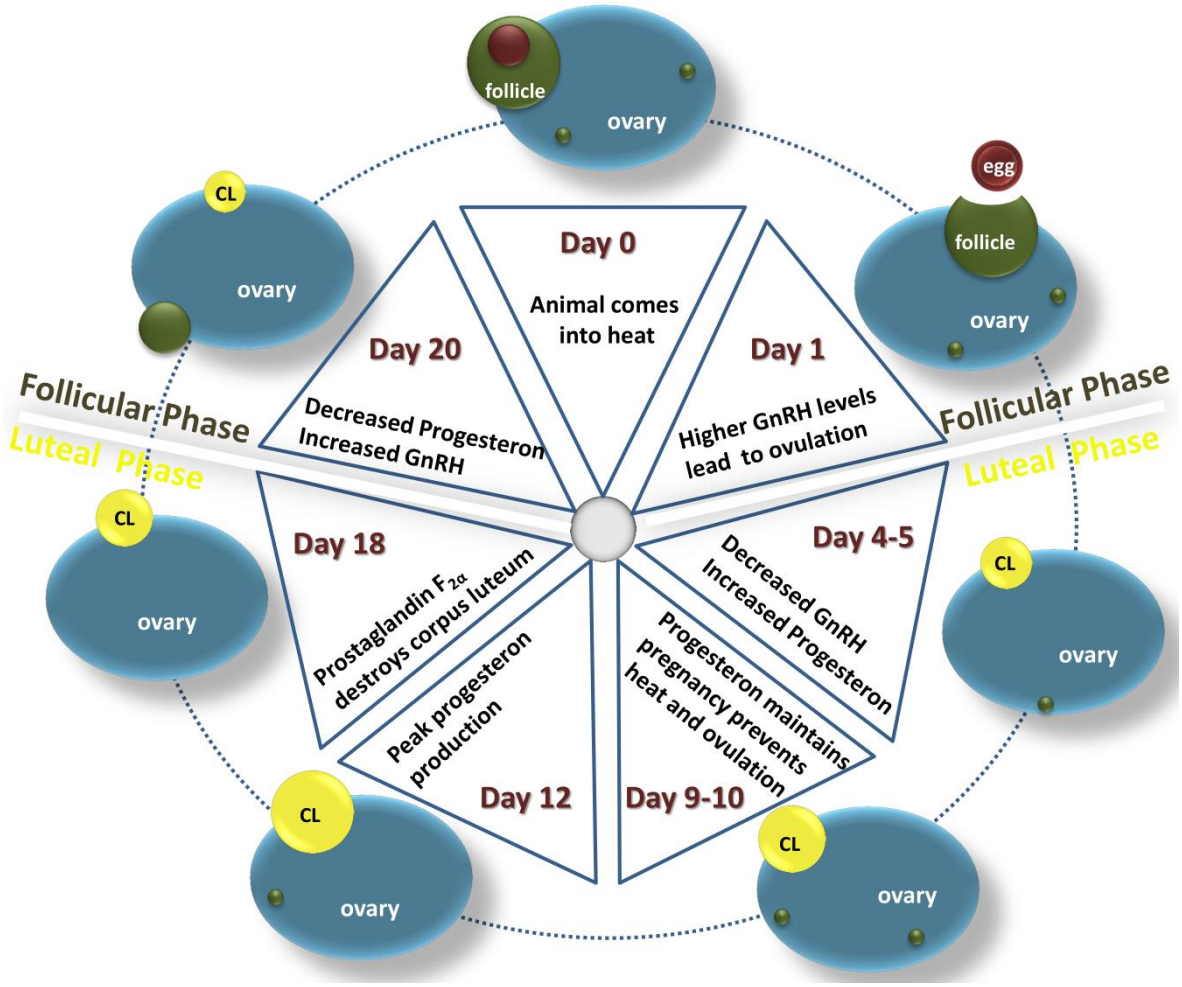


**Figure 1.1| Estrous cycle in the pig**
The image was modified from http://crinetsupport.blogspot.de/2015/07/dairy-synchronization-learning.html

## 1.3 CURRENT SYNCHRONIZATION TREATMENTS

The current estrous synchronization treatments are based on protocols for suppressing the follicle development and/or mimicking the luteal phase, the post ovulation phase. The treatments used in these synchronization protocols can be classified in 3 major groups depending on their pharmacological effect on the cycle.

### *1.3.1 Estrus synchronization*

As the physiological luteal phase is characterized by high concentrations of progesterone, the phase can be mimicked by treatment with a gestagen derivative. Earlier studies used progesterone and its derivatives and did not prove fully effective for synchronizing the estrus[6]. At present a synthetic gestagen derivative, allyl trenbolone, also known as altrenogest (Regumate® in Europe and Matrix® in North America) is the only licensed substance, which can successfully suppress the follicle development in randomly cycling gilts[7]. It is fed in a dose of 15 to 20 mg/day/gilt over a period of 14 to 18 days[8–10]. The precision of estrus synchronization is greater in gilts after a treatment for 18 days compared to 14 days. After

discontinuing the altrenogest treatment, gilts usually show estrus within 5 to 7 days[3,11]. Other approaches to extend the lifespan of corpora lutea and suppress ovarian activity included GnRH agonists in a slow release device[12–16]. In a recently published study an implant of the GnRH analog deslorelin was applied to suppress the ovarian activity in gilts. However, the deslorelin implant failed to succeed and produced a permanent anestrus in the treated gilts, which was not reversible through the administration of 400 IU equine chorionic gonadotropin (eCG) and 200 IU of human chorionic gonadotropin (hCG)[17]. It basically induced an undesirable menopause in the treated animals for an unknown duration of time.

### *1.3.2 Stimulation of follicular development*

The onset of the follicular phase can be induced by administration of gonadotropins-like pure eCG (with predominantly FSH and minor LH activity) or a mixture of eCG and hCG (with predominantly LH and minor FSH activity). The latter combination is commercially available as PG 600® (400 IU eCG and 200 IU hCG) in the United States and is used in non-cycling animals to induce follicular growth and ovulation. PG 600® acts in a similar way as FSH and LH during the follicular phase of the estrous cycle. However, such combinations increase the risk of inducing ovarian cysts and premature luteinization of the follicles, which comes from the extra hCG and the increased LH activity. This is also the reason why pure lyophilized eCG (also known as PMSG-pregnant mare serum gonadotropin) (Pregmagon®, Intergonan®) is preferred in synchronization protocols at 800-1000 IU[7]. Synthetic GnRH analoga, Perforelin, Maprelin® (Veyx Pharma) exhibited selective FSH releasing activity in barrows[18].

### *1.3.3 Induction of ovulation*

For a fixed-time AI, the ovulation needs to be induced with compounds with predominantly LH activity such as hCG or a short-term GnRH analogue. If hCG is to be applied, the interval between the eCG and hCG administration is crucial. hCG should be given as close as possible to the endogenous LH peak in order to induce ovulation. This poses a risk for variability in the treatment. In contrast to hCG, the GnRH treatment resembles a more biologically relevant event, since the pulsatile release of the peptide hormone is part of the follicle phase within the reproductive cycle. A GnRH agonist analogue GnRH [6-D-Phe], under the tradename Gonavet® 50 µg/mL Veyx Pharma was more effective in synchronizing the ovulation in swine compared to earlier applied GnRH[19]. 50 µg of GnRH [6-D-Phe] proved to be appropriate to synchronize the ovulation of swine diagnosed as non-pregnant[20].Porceptal® 4 µg/mL MSD/Intervet containing another GnRH agonist analogue buserelin (GnRH-[6-D-Ser($Bu^t$)] [10-Pro-NHEt] acetate]) has proved as well successful to induce ovulation in pigs 30 to 33 hours after application[21].

## 1.4 GENERAL FORMULATION REQUIREMENTS FROM A VETERINARY PERSPECTIVE

Currently all swine estrus synchronization protocols require the administration of large amounts of altrenogest (17-α-allyl-17-β-hydroxyestra-4, 9, 11-trien-3-one). The environmental disrupting potential of this synthetic progestin is of a growing concern[22–24].

Exposure to levonorgestrel, a human contraceptive, at 0.8 ng/mL reduces fecundity in fish[24]. Compared to levonorgestrel, altrenogest is utilized at an even larger scale[25–27]. In a typical synchronization protocol a swine receives 210-360 mg dose of altrenogest over 12 to 18 days. The doses recommended by the manufacturer translate then into several thousands of kg of annual altrenogest usage among 66 000 000 pigs. Consistent with the agricultural adaptation practices, additional extensive use is to be expected in Asian and Pacific regions[28]. Presumably because of its veterinary use, altrenogest has been overlooked in the last couple of years in environmental reviews of progestin pharmaceuticals[29].

Which are the other procedures currently used parallel to altrenogest? One is the use of intravaginal progesterone releasing insert, like CIDRs which are under development for cattle and sheeps[30]. However, progesterone is another gestagen product with a detrimental effect on the environment. A second option is the serial administration of estradiol between day 11 and 14 of the estrous cycle to induce pseudo-pregnancy, prolong the luteal phase and then induce lyteolysis. The estradiol mimics the early embryonic signaling to the mother. A major disadvantage, however, is that this procedure is labor intensive and estradiol is not cleared for use in pigs[31]. A third possibility of induction of a prolonged luteal phase is the administration of a single dose hCG on the 12 day of the cycle[32]. The hCG induces the follicle development and thereby production of estradiol to mimic early embryonic signaling. However, this last treatment is still being researched since the duration of the inter-estrus intervals varies[33,34].

The focus from a veterinary perspective is therefore the development of an environmentally sound product, which can reduce the hormone load coming from the swine sector. This can be achieved through a single dose injection, which can reduce the labor involved with feeding altrenogest over 14 to 18 days. The single dose injection should contain a luteal phase prolonging active substance, which is easily metabolized into inactive compounds with no environmental impact. A suitable candidate fulfilling this requirement is the long acting GnRH analogue, GnRH [6-D-Phe] acetate[35,36]. The peptide has shown an effect in earlier synchronization protocols as a single dose injection of 50 µg/mL Gonavet® for the successful induction of ovulation in pigs[20]. GnRH [6-D-Phe] acetate is a synthetic superagonistic decapeptide, analogue to the physiological GnRH that possesses greater potency than the natural hormone. It contains D-Phe$^6$ in place of Gly$^6$, which hinders the enzymatic degradation and prolongs its plasma half-life. Compared to the natural hormone it possesses an increased affinity to the GnRH receptors in the pituitary gland. As mentioned earlier, the GnRH release from the hypothalamus occurs in a pulsatile manner.

What happens when GnRH [6-D-Phe] acetate is administered in pharmacological doses each day over a longer period of time? According to the cruise control analogy, FSH and LH levels will initially rise, also known as flare-up phenomenon. After a few days, when the system senses the change, their concentration will begin to fall because of target tissue desensitization/down-regulation of pituitary GnRH receptor. The levels of LH and FSH will consequently decrease and the follicle maturity and ovulation is prevented. This principle was applied successfully for a long term reversible suppression of estrus in female dogs using another superagonist, nafarelin acetate (GnRH-[6-D-Nal(2)] acetate), via a subcutaneously implanted osmotic pump over 18 months treatment period[37]. Similar cycle blockage in the swine could be achieved with osmotic pumps delivering 1.06 µg/h or 2.12 µg/h GnRH [6-D-

Phe] acetate[38]. The high production costs and the difficulty to remove and terminate their action when necessary, renders the pump systems unsuitable for wider application in the veterinary sector. Therefore, the goal is the development of a new multidose depot formulation of GnRH [6-D-Phe], with a simple application, which is going to be administered once through an injection on the 11$^{th}$ day of the estrous cycle and will induce an estrous cycle blocking effect of two weeks or longer. This will inhibit the LH-surge at the beginning of the next estrous cycle and prolong the luteal phase until either a physiological or treatment induced ovulation occurs.

## 1.5 RESEARCH FOCUS, FORMULATION DEVELOPMENT REQUIREMENTS AND STUDIES

In order to achieve a two week physiological effect with GnRH [6-D-Phe] acetate, a number of factors should be taken into consideration. First, although the plasma half-life of GnRH [6-D-Phe] acetate, is prolonged in comparison to GnRH, it still reaches only hours[39–41] and the pharmacological effect should be maintained over days. Thus a suitable depot vehicle is required, which can deliver GnRH [6-D-Phe] in a controlled and sustained manner. Several approaches have been tried in the past for the long term delivery of peptide and protein drugs[42,43]. Among the wide variety of systems, a suspension is one of the easiest and cheapest pharmaceutical dosage form, which can offer a sustained release of a peptide from a subcutaneous or intramuscular depot at the injection site[44]. This was accomplished in 1948 by Buckwalter and Dickison with an oil depot suspension of procaine penicillin G suspended in peanut oil, gelled with 2 % aluminium monostearate[45]. The formulation was tested in 1000 human subjects and gave 96 h blood levels in 86 % of the patients. Similar results were obtained using a sesame oil vehicle instead of peanut oil and no significant difference regarding the absorption of the oil at the injection site was detected[46]. A great number of formulations were based on gelled oil vehicles as delivery systems for drugs[47,48,49,50]. In 1975 injectable oil peptide suspensions and methods for their preparation were patented. Another patent described the sustained release of proteins from a polyol/oil suspension, where spray-dried G-CSF (Granulocyte-Colony Stimulating Factor) was first suspended in glycerol and then dispersed in 1 % aluminium monostearate thickened sesame oil. At least a one week effect was accomplished[51]. The oily suspension of ACTH (adrenocorticotropic hormone) and MSH (melanocyte stimulating factor) gelled with 2 % aluminium monostearate achieved prolonged peptide action for several days[52]. Long acting oil depot formulations of 1 mg/mL GnRH salts in sesame oil gelled with 2 % aluminium monostearate were tested in rats. The acetate salt of GnRH showed a 38 day effect, whereas the zinc tannate salt and pamoate salt led to a return to estrous cycle after 120 days[53]. It is however to be noted that the estrous cycle within rodents is very short and spans only over 4-5 days, making the task of synchronizing the cycle easier in comparison to a swine cycle[54]. The above mentioned principles formed the basis for Posilac®, Monsanto. The formulation consists of N-methionyl-recombinant bovine somatotropin (rBSt) complexed with zinc salt and suspended in sesame oil with 5 % aluminium monostearate. It is injected every two weeks subcutaneously in lactating dairy cows to boost the milk production[55,56].

### *1.5.1 Selection and Composition of the Oily Vehicle*

Vegetable oils contain various triglycerides in different proportions. Their composition can influence vehicle viscosity, density and stability. Ideally the oils to be used as vehicles should be chemically and physically stable, inert to reactions with the peptide, relatively low in viscosity, resuspendable, syringeable, injectable, non-irritating and free of antigenic properties[57,58]. Oils, which potentially fulfill these characteristics and are suitable for injection, include: cottonseed oil, almond oil, olive oil, sesame oil, soybean oil, peanut oil, corn oil, castor oil, canola oil, coconut oil, sunflower oil, palm oil, palm kernel oil or linseed oil. Alternatively, synthetic fatty acid esters such as isopropyl myristate, ethyl oleate, benzyl benzoate and medium chain triglycerides can be incorporated. The fatty acid composition of selected oils is summarized in Table 1.1. The higher the amount and the degree of unsaturation of the fatty acids, the more susceptible the oils are to oxidation and autoxidation. The addition of oxygen to the double bonds produces hydroperoxides, susceptible to further reactions. It has been well established that the ease of formation of fatty acid radicals increases with increasing degree of unsaturation. Oleic acid for example has been estimated to be 10-40 times less susceptible to oxidation than linoleic acid[59]. Therefore, our focus lied on oils with a low percentage of oleic, linoleic and linolenic acid e.g. castor oil, peanut oil, sesame oil, wheat germ oil, cottonseed oil, corn oil, palm oil, palm kernel oil and coconut oil. Castor oil, which is characterized by a high content of ricinoleic acid shows a rather high oxidative stability due to an additional hydroxyl moiety preventing the formation of hydroperoxides. Furthermore, the hydroxyl group of ricinoleic acid similar to other hydrogen donating excipient such as n-octanol, dodecanol or myristic alcohol proved to significantly decrease the *in vitro* drug release from the oil vehicle[60]. As with regards to the *in vivo* release, the lipolysis of the oil vehicle at the injection site plays a major role [61]. Oils are cleared from the intramuscular and subcutaneous injection site within 2 to 30 days[62,63,64,65,66].

| Oils | Fatty acid composition [%] | | | | | |
|---|---|---|---|---|---|---|
| | Caproic/ Caprylic and Capric acid (C6, C8, C10) | Palmitoleic acid (C16:1) | Oleic acid (C18:1) | Linoleic acid (C18:2) | Linolenic acid (C18:3) | Arachidic acid (C20:0) |
| **Cottonseed oil** | – | 0.6–0.8 | 15.6–18.6 | 50.5–55.8 | 0.3 | 0.1 |
| **Almond oil** | – | < 1 | 68 | 25 | < 18.0 | - |
| **Olive oil** | – | 0.7 | 78 | 8.3 | 0.8 | 0.5 |
| **Sesame oil** | – | < 0.5 | 35–50 | 35–50 | < 1 | <1. |
| **Soybean oil** | – | – | 23 | 53 | 7 | |
| **Peanut oil** | – | – | 35.0–69.0 | 12–43 | | 1–2 |
| **Corn oil** | – | 0 | 24.2 | 58 | 0.7 | 0 |
| **Castor oil** | – | – | 87.7–Ricinoleic acid | 4.7 | 0.5 | 0.3 |
| **Canola oil** | – | 0.2 | 61.6 | 21.7 | 9.6 | 0.6 |
| **Coconut oil** | 0.5; 7.8; 6.7 | – | 6.2 | 1.6 | | |
| **Sunflower oil** | – | – | 14.0–39.4 | 48.3–74 | <0.3 | 0.1–0.5 |
| **Palm oil** | – | 0.1–0.3 | 37.3–40.8 | 9.1–11 | 0–0.6 | 0.2–0.7 |
| **Palm kernel oil** | – | – | | | | |
| **Linseed oil** | – | – | 27 | 29 | 60 | |

**Table 1.1| Chemical Composition of commonly used Vegetable Oils for Parenteral Drug Delivery**[67]

### *1.5.2 Incorporated GnRH [6-D-Phe] acetate and Micronization Process*

Shape, size and distribution of GnRH [6-D-Phe] acetate particles suspended in the oil phase can influence both the stability of the suspension, its injectability, syringeability as well the release characteristics. Therefore, spherical and smaller particles with narrow size distribution are desired since they offer the least surface area per volume, can be easily resuspended and can achieve better dose uniformity[68,69]. In addition, smaller particles offer a larger specific surface area for particle-particle interactions. For instance, in highly concentrated suspensions this effect promotes high viscosity and thixotropic character, which can reduce the spreading of the oil vehicle at the injection site and might counteract an initial burst release[70]. In contrast, larger particles in a suspension will increase the settling rate as explained by Stoke's law and decrease suspension stability. As the oil suspension is intended for a veterinary i.m. application, the suitable needle size range lies between 14 G and 18 G. According to a general rule it is advisable to avoid any particle greater than one forth to one third of the needle inner diameter[71]. This corresponds to an upper particle size limit for 18 G needle size of approximately 300 µm. An easy and fast reduction of the particle size can be achieved through a grinding process. Either a cryogenic grinding of GnRH [6-D-Phe] acetate avoiding thermal stress and increasing brittleness or a suspension-milling process in the dispersing medium can be viewed as suitable for GnRH [6-D-Phe] micronization[72].

### *1.5.3 Sustained Release*

Factors which can influence the release of GnRH [6-D-Phe] after intramuscular injection are peptide diffusion out of the oil vehicle, particle sedimentation at the oil–tissue fluids interface and subsequent dissolution as well as spreading and dispersion of the oil vehicle at the injection site[61]. The peptide liberation of the oil vehicle is influenced by the peptide particle size and solubility. A complexation of GnRH [6-D-Phe] acetate with metal salts or polymers can decrease its solubility and sustain peptide release. This strategy was traditionally used for the precipitation of insulin[73] and corticotropin (ACTH)[74] and more recently to achieve sustained release of recombinant hirudin[75,76]. Similarly, Posilac® (Monsanto) is a Zn-rBSt complex applied to increase the milk, fat and protein yield in cows with an effect over 14 days[77]. A substitution of the zinc gelled sesame oil base by vitamin E and lecithin based formulation Boostin-S® (LG Life Sciences) reduced the milk yield in dairy cattle due to a high variation and more inconsistent 14 day effect within the group[78]. Besides peptide solubility the oil vehicle fatty acid composition and viscosity may have a direct impact on the release characteristics of the suspension[62]. A suitable combination of oily components and additives may assure the long lasting *in vivo* effect of GnRH [6-D-Phe] acetate. Such compositions were mainly developed as production animal medicines and tend to be very profitable. Excede® is used for the treatment of respiratory diseases in herds and follows a sustained release pattern in order to deliver at least 7 days of therapeutic plasma levels of ceftiofur[79]. Excenel® RTU contains the hydrochloric salt of ceftiofur and is administered every 24h for 3-5 days. Adding aluminium monostearate to the sesame oil vehicle of the short-acting Excenel® RTU suspension provides therapeutically effective plasma concentrations similar to the long-acting Excede®[80].

### *1.5.4 Selection of a Suitable In Vitro Release Model*

The effect of the oil vehicle and additives on the GnRH [6-D-Phe] acetate release needs to be studied *in vitro* and *in vivo* in order to develop a formulation with the targeted two week pharmacological effect. For this purpose a suitable *in vitro* release model is mandatory and a number of factors needs to be taken into consideration. The release is estimated according to mass transport models and is highly dependent on the surface area between the oil vehicle and the tissue fluids at the injection site[81,82,83]. After intramuscular injection the oil is squeezed between the muscle fibers, increasing the surface area of the oil depot. The resulting surface area is much larger than the perfect sphere frequently used in mathematical calculation models[83]. The hydrophilic nature of GnRH [6-D-Phe] acetate and its low affinity for the vehicle make its release mostly dependent on the amount of tissue fluid available at the injection site, the oil/tissue fluid interfacial area and the diffusion distance[61].

Currently, no standard methods exist for testing drug release from parenteral depot products[84]. According to Larsen et al. a lipophilic solution floating on the top of the release medium[85], dialysis techniques[86,87] and continuous flow models[61] are the current methods of choice. As the injected oil depot is supposed to have an overall contact with the muscle tissue fluid the most suitable model appears to be the dialysis technique. This release model has its biggest advantage in the defined interfacial area for mass transfer, which equals the total membrane area covered by the oil donor phase[61]. One challenge this release model may pose is the lack of agitation within the donor cell, which can cause agglomeration of GnRH [6-D-Phe] acetate particles and sedimentation.

## 1.6 AIMS

Various hormonal products are currently available that allow for the manipulation of almost all key reproductive processes in the swine, making fixed time insemination possible. Recently different options for estrous synchronization in the form of osmotic pumps, releasing GnRH agonists, have been investigated. In the following chapters a development of a long acting oil depot formulation of GnRH [6-D-Phe] acetate has been anticipated, translating the veterinary requirements into a formulation which is more environmentally safe and at a reasonable cost (Figure 1.2).

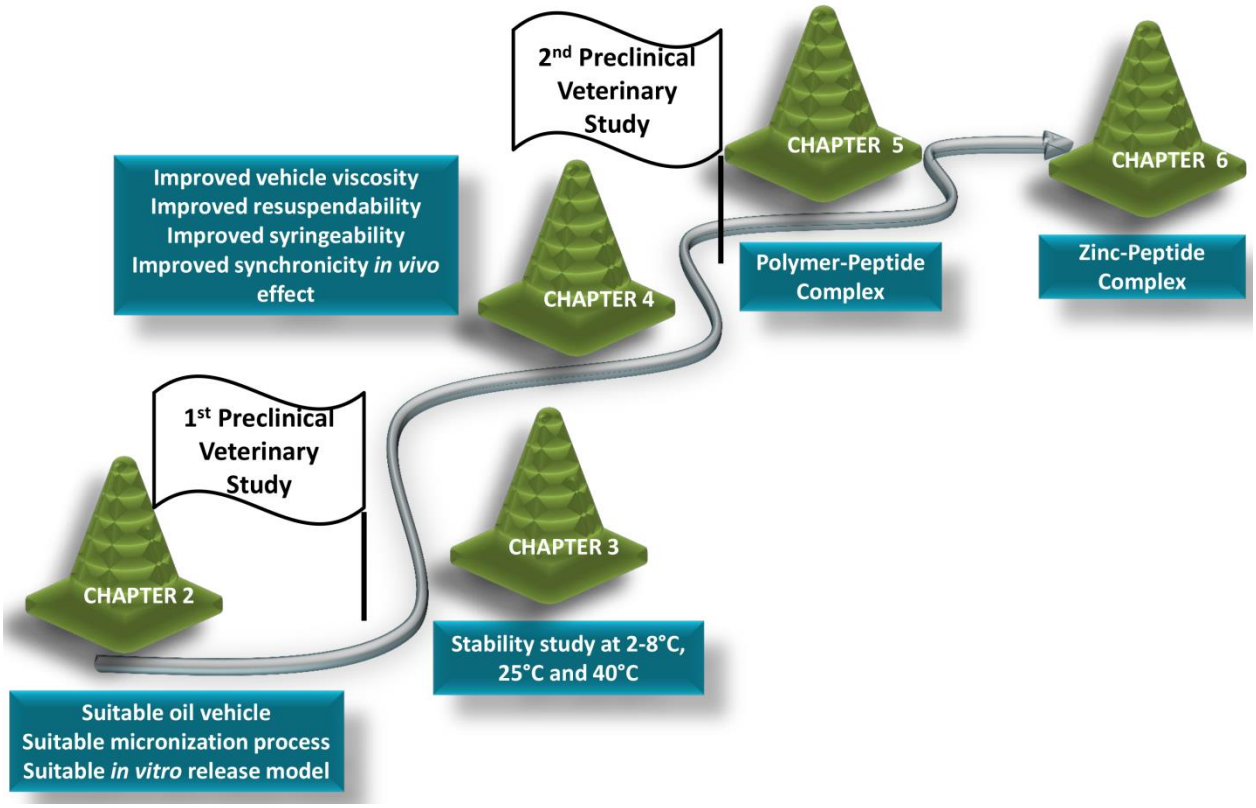


**Figure 1.2| Thesis outline**

In the first step, pure oil mixtures with incorporated GnRH [6-D-Phe] acetate were investigated. The effect of oil matrix viscosity on syringeability and injectability and the *in vitro* release rate of GnRH [6-D-Phe] acetate were explored. The focus lied on the development of a rugged *in vitro* release test that can be used to demonstrate formulations differences with regards to an initial burst effect. The *in vivo* effect of selected formulations was evaluated in the first preclinical study.

In the second step, the chemical and physical stability of GnRH [6-D-Phe] acetate formulations was evaluated.

Subsequently, the effect of oil thickening agent, as well as resuspendibility enhancers was analyzed. Using the advantages of Self-Emulsifying Drug Delivery Systems, a continuous and controlled release was envisioned. The *in vivo* effect of selected formulations was later analyzed in the second preclinical study.

Lastly, we investigated the effect of polymers and metal salt on GnRH [6-D-Phe] release prolongation.

## 1.7 REFERENCES


1. Tanabe, T. Y., Warnick, W. C., Casida, L. E. & Grummer, R. H. Effects of gonadotrophins administered to sows and gilts during different stages of the estrual cycle. *J. Anim. Sci.* **8,** 550–557 (1949).

2. Dziuk, P. J. & Baker, R. D. Induction and Control of Ovulation in Swine. *J. Anim. Sci.* **21,** 697 (1962).

3. Hühn, U. *et al.* Techniques developed for the control of estrus, ovulation and parturition in the East German pig industry: A review. *Theriogenology* **46,** 911–924 (1996).

4. Brüssow, K. P. *et al.* Studies on fixed-time ovulation induction in the pig. *Soc. Reprod. Fertil. Suppl.* **66,** 187–95 (2009).

5. Hazeleger, W., Kirkwood, R. N. & Soede, N. M. Synchronisation ofthe reproductive cycle in pigs. *Arch. Tierz. Dummerstorf* **44,** 71–76 (2001).

6. El-Zarkouny, S. Z. & Stevenson, J. S. Resynchronizing Estrus with Progesterone or Progesterone Plus Estrogen in Cows of Unknown Pregnancy Status. *J. Dairy Sci.* **87,** 3306–3321 (2004).

7. Brüssow, K.-P. & Wähner, M. Biological and Technological Background of Estrus Synchronization and fixed-time Ovulation in the Pig. *Biotechnol. Anim. Husb.* **27,** 533–545 (2011).

8. Gordon, I. R. *Controlled reproduction in pigs*. (Wallingford, Oxon, UK ; New York, NY, USA : CAB International, 1997).

9. Horsley, B. R. *et al.* Effect of P.G. 600 on the timing of ovulation in gilts treated with altrenogest. *J. Anim. Sci.* **83,** 1690–1695 (2005).

10. Webel, S. K. & Day, B. N. The Control of Ovulation, in *Control of Pig Reproduction* 197–210 (1982).

11. Martinat-Botte, F. *et al.* Control of oestrus in gilts II. Synchronization of oestrus with a progestagen, altrenogest (Regumate): Effect on fertility and litter size. *Anim. Reprod. Sci.* **22,** 227–233 (1990).

12. Blanchard, T. L. *et al.* Regulation of estrus and ovulation in mares with progesterone or progesterone and estradiol biodegradable microspheres with or without PGF2α. *Theriogenology* **38,** 1091–1106 (1992).

13. Mumford, E. L. *et al.* Use of deslorelin short-term implants to induce ovulation in cycling mares during three consecutive estrous cycles. *Anim. Reprod. Sci.* **39,** 129–140 (1995).

14. Meinert, C. *et al.* Advancing the time of ovulation in the mare with a short-term implant releasing the GnRH analogue deslorelin. *Equine Vet. J.* **25,** 65–68 (1993).

15. Figueiredo, T. *et al.* Induction of ovulation in quarter horse mares through the use of deslorelin acetate and human chorionic gonadotrophin (hCG). *Brazilian Arch. Biol. Technol.* **54,** 517–521 (2011).

16. Lübbecke, M., Klug, E., Hoppen, H. O. & Jöchle, W. Attempts to Synchronize Estrus and Ovulation in Mares Using Progesterone (CIDR-B) and GnRH-Analog Deslorelin. *Reprod. Domest. Anim.* **29,** 305–314 (1994).

17. Garcia, A., Estienne, M. J., Harper, A. F. & Knight, J. W. Failure of Gonadotropin Therapy to Induce Estrus in Gilts Treated with a GnRH Analog to Suppress Ovarian Activity. *Int. J. Appl.*

*Res. Vet. Med.* **2,** 195–199 (2004).

18. Kauffold, J., Schneider, F., Zaremba, W. & Brussow, K. P. Lamprey GnRH-III stimulates FSH secretion in barrows. *Reprod. Domest. Anim.* **40,** 475–479 (2005).

19. Engl, S., Kauffold, J., Sobiraj, A. & Zaremba, W. Investigations into the suitability of a GnRH-variant for estrus induction in pluriparous sows. *Reprod. Domest. Anim.* **41,** (2006).

20. Kauffold, J., Beckjunker, J., Kanora, A. & Zaremba, W. Synchronization of estrus and ovulation in sows not conceiving in a scheduled fixed-time insemination program. *Anim. Reprod. Sci*. **97,** 84–93 (2007).

21. Kirkwood, R. N. & Kauffold, J. Advances in Breeding Management and Use of Ovulation Induction for Fixed-time AI. *Reprod. Domest. Anim* **50,** 85–89 (2015).

22. Kumar, V. *et al.* The challenge presented by progestins in ecotoxicological research: A critical review. *Environ. Sci. Technol.* **49,** 2625–2638 (2015).

23. Safholm, M., Ribbenstedt, A., Fick, J. & Berg, C. Risks of hormonally active pharmaceuticals to amphibians: a growing concern regarding progestagens. *Philos. Trans. R. Soc. B Biol. Sci.* **369,** 20130577–20130577 (2014).

24. Zeilinger, J. *et al.* Effects of synthetic gestagens on fish reproduction. *Environ. Toxicol. Chem.* **28,** 2663 (2009).

25. Willmann, C., Schuler, G., Hoffmann, B., Parvizi, N. & Aurich, C. Effects of age and altrenogest treatment on conceptus development and secretion of LH, progesterone and eCG in early-pregnant mares. *Theriogenology* **75,** 421–428 (2011).

26. van Leeuwen, J. J. *et al.* The effect of different postweaning altrenogest treatments of primiparous sows on follicular development, pregnancy rates, and litter sizes. *J. Anim. Sci.* **89,** 397–403 (2011).

27. Squires, E. L., Heesemann, C. P., Webel, S. K., Shideler, R. K. & Voss, J. L. Relationship of altrenogest to ovarian activity, hormone concentrations and fertility of mares. *J. Anim. Sci.* **56,** 901–910 (1983).

28. Wammer, K. H. *et al.* Environmental Photochemistry of Altrenogest: Photoisomerization to a Bioactive Product with Increased Environmental Persistence via Reversible Photohydration. *Environ. Sci. Technol.* **50,** 7480–7488 (2016).

29. Orlando, E. F. & Ellestad, L. E. Sources, concentrations, and exposure effects of environmental gestagens on fish and other aquatic wildlife, with an emphasis on reproduction. *Gen. Comp. Endocrinol.* **203,** 241–249 (2014).

30. Dequattro, Z. A. *et al.* Effects of progesterone on reproduction and embryonic development in the fathead minnow (Pimephales promelas). *Environ. Toxicol. Chem.* **31,** 851–856 (2012).

31. Guthrie, H. D. Estrous synchronization and fertility in gilts treated with estradiol-benzoate and prostaglandin F2α. *Theriogenology* **4,** 69–75 (1975).

32. Soede, N. M., Raaphorst, C. J. M., Bouwman, E. G. & Kirkwood, R. N. Effects of injection of hCG during the estrous cycle on follicle development and the inter-estrous interval. *Theriogenology* **55,** 901–909 (2001).

33. Geary, T. W., Salverson, R. R. & Whittier, J. C. Synchronization of ovulation using GnRH or hCG with the CO-Synch protocol in suckled beef cows. *J. Anim. Sci.* **79,** 2536–2541 (2001).

34. Fricke, P. M., Reynolds, L. P. & Redmer, D. A. Effect of human chorionic gonadotropin administered early in the estrous cycle on ovulation and subsequent luteal function in cows. *J.*

*Anim. Sci.* **71,** 1242–1246 (1993).

35. Hoitink, M. A. *et al.* Degradation kinetics of gonadorelin in aqueous solution. *J. Pharm. Sci.* **85,** 1053–1059 (1996).

36. The European Agency for the Evaluation of Medicinal Products Veterinary Medicines Evaluation Unit. *D-Phe6-Luteinizing-Hormone-Releasing-Hormone Summary Report*. (1996).

37. McRae, G. I., Roberts, B. B., Worden, A. C., Bajka, A. & Vickery, B. H. Long-term reversible suppression of oestrus in bitches with nafarelin acetate, a potent LHRH agonist. *J. Reprod. Fertil.* **74,** 389–397 (1985).

38. Brüssow, K. P., Schneider, F. & Kanitz, W. Die Langzeitapplikation eines GnRH-Agonisten als eine alternative Methode zur Zyklussteuerung beim Schwein. (2000).

39. Kumar, P. & Sharma, A. Gonadotropin-releasing hormone analogs: Understanding advantages and limitations. *J. Hum. Reprod. Sci.* **7,** 170 (2014).

40. Agarwal, S. Comparative effects of GnRH agonist therapy - Review of clinical studies and their implications. *J. Reprod. Med.* **43,** 293–298 (1998).

41. Hayden, C. GnRH analogues: Applications in assisted reproductive techniques. *Eur. J. Endocrinol.* **159,** S17-25 (2008).

42. Bari, H. A prolonged release Parenteral drug delivery system - An overview. *International Journal of Pharmaceutical Sciences Review and Research* **3,** 1–11 (2010).

43. Patel, A., Cholkar, K. & Mitra, A. K. Recent developments in protein and peptide parenteral delivery approaches. *Ther. Deliv.* **5,** 337–365 (2014).

44. Davis, J. M., Metalon, L., Watanabe, M. D. & Blake, L. Depot Antipsychotic Drugs: Place in Therapy. *Drugs* **47,** 741–773 (1994).

45. Buckwalter, F. H., Dickison, H. L., Miller, H. C., Rhodehamel, H. W. & Al., E. A new absorption delaying vehicle for penicillin. *J. Am. Pharm. Assoc. Am. Pharm. Assoc. (Baltim).* **37,** 472–4 (1948).

46. Buckwalter, F. H. & Dickison, H. L. The Effect of Vehicle and Particle Size on the Absorption, by the Intramuscular Route, of Procaine Penicillin G Suspensions**Research Division, Bristol Laboratories, Inc., Syracuse 1, N. Y. *J. Am. Pharm. Assoc. (Scientific ed.)* **47,** 661–666 (1958).

47. Sieger, G. M., Krueger, J. E., Osterberg, A. C. & Tedeschi, D. H. Sustained release forms of certain oxazepines for parenteral administration. (1977).

48. Lachman, L., Reiner, R. H., Shami, E. & Spector, W. Long-acting narcotic antagonist formulations. (1971).

49. Anschel, J. Relaxin composition and process for preparing same. (1959).

50. Bramley, M. R. Somatotropin formulations. (1988).

51. Goldenberg, M. S. M. S., Shan, D. & Beekman, A. C. A. C. Polyol/Oil Suspensions for the Sustained Release of Proteins. (1999).

52. Geller, L. Injectable oily peptide preparations and processes for their manufacture. (1973).

53. Nestor, J. J. & Vickery, B. H. Long acting depot injectable formulations for LH-RH analogues. (1979).

54. Caligioni, C. S. Assessing reproductive status/stages in mice. *Curr. Protoc. Neurosci.*

Appendix 4I (2009).

55. Mitchell, J. W. Prolonged release of biologically active somatotropins. (1983).

56. Jeng, Y. N. & Patel, K. R. Non-aqueous injectable formulations for extended release of somatotropin. (2004).

57. Patel, R. Parenteral suspension: an overview. *Int J Curr Pharm Res* **2,** 4–13 (2010).

58. Spiegel, a J. & Noseworthy, M. M. Use of Nonaqueous Solvents in Parenteral Products. *J. Pharm. Sci.* **52,** 917–27 (1963).

59. Pratt, D. A., Tallman, K. A. & Porter, N. A. Free radical oxidation of polyunsaturated lipids: New mechanistic insights and the development of peroxyl radical clocks. *Acc. Chem. Res.* **44,** 458–467 (2011).

60. Larsen, D. B., Fredholt, K. & Larsen, C. Addition of hydrogen bond donating excipients to oil solution: Effect on in vitro drug release rate and viscosity. *Eur. J. Pharm. Sci.* **13,** 403–410 (2001).

61. Weng Larsen, S. & Larsen, C. Critical Factors Influencing the In Vivo Performance of Long-acting Lipophilic Solutions—Impact on In Vitro Release Method Design. *AAPS J.* **11,** 762–770 (2009).

62. Tanaka, T., Kobayashi, H., Okumura, K., Muranishi, S. & Sezaki, H. Intramuscular absorption of drugs from oily solutions in the rat. *Chem. Pharm. Bull. (Tokyo).* **22,** 1275–1284 (1974).

63. Larsen, S. W. *et al.* Determination of the disappearance rate of iodine-125 labelled oils from the injection site after intramuscular and subcutaneous administration to pigs. *Int. J. Pharm.* **230,** 67–75 (2001).

64. Schultz, K., Möllgaard, B., Fisher, A. N., Illum, L. & Larsen, C. Intramuscular rate of disappearance of oily vehicles in rabbits investigated by gamma-scintigraphy. *Int. J. Pharm.* **169,** 121–126 (1998).

65. Svendsen, O. & Aaes-Jørgensen, T. Studies on the fate of vegetable oit after intramuscular injection into experimental animals. *Acta Pharmacol. Toxicol. (Copenh).* **45,** 352–378 (1979).

66. Zhang, J. *et al.* Effect of Lipolysis on Drug Release from Self-microemulsifying Drug Delivery Systems (SMEDDS) with Different Core/Shell Drug Location. *Pharmscitech* **15,** 1–10 (2014).

67. *Long Acting Injections and Implants*. (Springer US, 2012).

68. Dogonchi, A. S., Hatami, M., Hosseinzadeh, K. & Domairry, G. Non-spherical particles sedimentation in an incompressible Newtonian medium by Pade´ approximation. *Powder Technol.* **278,** 248–256 (2015).

69. Nutan, M. T. H. & Reddy, I. K. General principles of suspensions. in *Pharmaceutical Suspensions: From Formulation Development to Manufacturing* 39–65 (Springer New York, 2010).

70. Borges, F. A., Cho, H. S., Santos, E., Oliveira, G. P. & Costa, A. J. Pharmacokinetics of a new long acting endectocide formulation containing 2.25% ivermectin and 1.25% abamectin in cattle. *J. Vet. Pharmacol. Ther.* **30,** 62–67 (2007).

71. Puthli, S. & Vavia, P. Stability Studies of Microparticulate System with Piroxicam as Model Drug. *AAPS PharmSciTech* **10,** 872–880 (2009).

72. Lizio, R., Damm, M., Sarlikiotis, A. W., Bauer, H. H. & Lehr, C.-M. Low-Temperature Micronization of a Peptide Drug in Fluid Propellant : Case Study Cetrorelix. *AAPS*

*PharmSciTech* **2,** (2001).

73. Anand, O., Almoazen, H., Mehrotra, N., Johnson, J. & Shukla, A. Controlled release of modified insulin glargine from novel biodegradable injectable gels. *AAPS PharmSciTech* **13,** 313–22 (2012).

74. Homan, J. D. H., Neutelings, J. P. J., Overbeek, G. A., Booij, C. J. & Van Der Vies, J. Corticotrophin zinc phosphate and hydroxide; long-acting aqueous preparations. *Lancet* **263,** 541–543 (1954).

75. Gietz, U., Arvinte, T., Häner, M., Aebi, U. & Merkle, H. P. Formulation of sustained release aqueous Zn-hirudin suspensions. *Eur. J. Pharm. Sci.* **11,** 33–41 (2000).

76. Gietz, U., Arvinte, T., Mader, E., Oroszlan, P. & Merkle, H. P. Sustained release of injectable zinc-recombinant hirudin suspensions: Development and validation of in vitro release model. *Eur. J. Pharm. Biopharm.* **45,** 259–264 (1998).

77. Yu, L. & Foster, T. Preparation, characterization, and in vivo evaluation of an oil suspension of a bovine growth hormone releasing factor analog. *J. Pharm. Sci.* **85,** 396–401 (1996).

78. de Morais, J. P. G. *et al.* Lactation performance of Holstein cows treated with 2 formulations of recombinant bovine somatotropin in a large commercial dairy herd in Brazil. *J. Dairy Sci.* **100,** 5945–5956 (2017).

79. Tang, S. *et al.* Preparation of a newly formulated long-acting ceftiofur hydrochloride suspension and evaluation of its pharmacokinetics in pigs. *J. Vet. Pharmacol. Ther.* **33,** 238–245 (2010).

80. Medlicott, N. J., Waldron, N. A. & Foster, T. P. Sustained release veterinary parenteral products. *Adv. Drug Deliv. Rev.* **56,** 1345–1365 (2004).

81. Ayres, J. W. & Tom Lindstrom, F. Diffusion model for drug release from suspensions I: Theoretical considerations. *J. Pharm. Sci.* **66,** 654–662 (1977).

82. Nelson, K. G. & Shah, A. C. Convective Diffusion Model for a Transport-Controlled Dissolution Rate Process. *J. Pharm. Sci.* **64,** 610–614 (1975).

83. Kalicharan, R. W., Baron, P., Oussoren, C., Bartels, L. W. & Vromans, H. Spatial distribution of oil depots monitored in human muscle using MRI. *Int. J. Pharm.* **505,** 52–60 (2016).

84. Shen, J. & Burgess, D. J. Accelerated in-vitro release testing methods for extended-release parenteral dosage forms. *J. Pharm. Pharmacol.* **64,** 986–996 (2012).

85. Larsen, S. W., Østergaard, J., Friberg-Johansen, H., Jessen, M. N. B. B. & Larsen, C. In vitro assessment of drug release rates from oil depot formulations intended for intra-articular administration. *Eur. J. Pharm. Sci.* **29,** 348–354 (2006).

86. Larsen, D. H., Fredholt, K. & Larsen, C. Assessment of rate of drug release from oil vehicle using a rotating dialysis cell. *Eur. J. Pharm. Sci.* **11,** 223–229 (2000).

87. Larsen, S. W., Frost, A. B., Østergaard, J., Marcher, H. & Larsen, C. On the mechanism of drug release from oil suspensions in vitro using local anesthetics as model drug compounds. *Eur. J. Pharm. Sci.* **34,** 37–44 (2008).

## 1.8 FIGURES AND TABLES

# CHAPTER TWO

# PURE OIL MIXTURES

# 2 Pure Oil Mixtures as a Delivery Vehicle for GnRH [6-D-Phe] acetate

Yordanka Yordanova[1], Johannes Kauffold[2], Wolfgang Zaremba[3], Wolfgang Friess[1]

1. Department of Pharmacy, Pharmaceutical Technology & Biopharmaceutics, Ludwig-Maximilians-Universitaet, Butenandtstrasse 5, 81377 Muenchen, Germany
2. University of Leipzig, Faculty of Veterinary Medicine, An den Tierkliniken 29, 04103 Leipzig, Germany
3. Veyx Pharma GmbH, Scientific Department, Soehreweg 6, 34639 Schwarzenborn, Germany

**Gonadorelin (GnRH) is a hypothalamic 10 amino acids long peptide hormone with a very short plasma half-life. In the search for suitable oil vehicles for its sustained release after i.m. injection, combinations of vegetable oils as well as synthetic fatty acid esters were prepared and evaluated for miscibility and physical stability. Physically stable and homogenous mixtures of castor oil and middle chain triglycerides (MCT) were selected for further tests. GnRH [6-D-Phe] acetate was incorporated in low viscosity castor oil: MCT 50:50 % (w/w) and high viscosity castor oil: MCT 90:10 % (w/w) mixtures. The result from the *in vitro* release showed an initial burst from both oil matrices. Approximately 50 % of the peptide were released within the first 48 hours. A slightly lower initial release was achieved with a higher concentration and viscosity. In the first *in vivo* preclinical study the low viscosity GnRH [6-D-Phe] formulation distinguished itself from the rest of the tested formulations with a longer and more consistent cycle blocking effect.**

## 2.1 INTRODUCTION

The nobel–prize winning discovery of GnRH peptide, involved in a number of physiological processes, transformed the understanding of the reproduction regulation and led to the development of effective treatments for many conditions[1,2]. Its clinical application, though, is limited by its short half-life. In order to overcome this drawback, chemical modifications to increase its potency and extend its half-life from minutes to hours as well as delivery methods have been studied thoroughly[3–6]. A modification or substitution in the amino acids at positions 6 and 10 of the native peptide gives rise to superagonists, which are more degradation resistant to the endopeptidase and the post-proline carboxyamide peptidase enzymes[7]. Although this allows for an increased receptor binding affinity and lowers the dose to reach half maximal receptor activation, a suitable depot vehicle for the controlled and prolonged delivery is still necessary.

Up until now, the delivery platforms mostly used for incorporating GnRH analogues for either human or veterinary purposes are polymeric microparticles and implants[8,9]. The products are widely used in oncology to induce reversible chemical castration in patients with advanced prostate cancer. Prominent examples are microsphere-based formulations such as Lupron Depot®, Enantone® and Trenantone® as well as gel-based implants Eligard® with Leuprolide acetate (GnRH-[6-D-Leu] [10-Pro-NHEt] acetate), Zoladex® implant with Goserelin acetate (GnRH-[6-D-Ser($Bu^t$)] [10-Pro-NH-$NHCONH_2$ acetate], Vantas® implant with Histerelin acetate (GnRH-[6-D-His($N^T$–Bzl)] [10-Pro-NHEt] acetate) and Pamorelin®, Trelstar®,

Decapeptyl SR ® with Triptorelin pamoate (GnRH-[6-D-Trp] pamoate). In the veterinary sector a number of products are used to promote ovulation as part of an artificial insemination process: Suprelorin® and Ovuplant® with Deslorelin acetate (GnRH-[6-D-Trp] [9-Pro-NHEt]) acetate) Dalmarelin® with Lecilerin acetate (GnRH-[6-Tle] acetate), Maprelin® (Perforelin acetate), Porceptal® with buserelin (GnRH-[6-D-Ser($Bu^t$)] [10-Pro-NHEt] acetate]) and Gonavet Veyx® (GnRH-[6-D-Phe] acetate). In recent years alternative depot delivery systems such as *insitu* forming gels[10], self-microemulsifying delivery systems[11,12], lipid microparticles, liposomes, microsphere, microcapsules, solid lipid nanoparticles have become the focus of research[13].

Lipids and oil vehicles have been used as depot vehicles since many years in the treatment of schizophrenia and in the hormone replacement therapy[14–18]. In the form of microparticles or oil suspensions, they can be an appealing alternative to the already mentioned polymeric matrices for incorporating peptides[8]. They are ideal to incorporate compounds with very low solubility, poor stability or compounds that may cause irritations if injected in aqueous vehicle[19,20,21,22]. In recent years, lipid microparticles were prepared and evaluated for sustained release of small molecules such as local anaesthetics and antibiotics as well as proteins and peptides[23–25]. They are easily administered, generally biocompatible and can provide a sustained release from several days up to months[26]. Simple oily suspensions are even easier to manufacture and to apply. Therefore, here we anticipate the idea of selecting a suitable oil vehicle for compounding a stable GnRH [6-D-Phe] oil depot suspension. The product could be used as a part of an artificial insemination protocol with its major use in veterinary medicine. The formulation should be able to offer a sustained release of GnRH [6-D-Phe] acetate with at least two week physiological effect after application.

## 2.2 RESULTS AND DISCUSSION

### *2.2.1 Oil mixtures for extended release of GnRH [6-D-Phe]*

The viscosity of the pure oils was measured and categorized according to the values in four groups. Castor oil displayed with 780 mPas the highest viscosity, followed by corn oil, sesame oil, peanut oil, wheat germ oil and cottonseed oil with viscosities in the range of 60 to 70 mPas. The middle chain triglycerides (MCT) viscosity of 30 mPas was second to the last. The synthetic fatty acid esters, ethyl oleate and isopropyl myristate were with 3-4 mPas by far the least viscous vehicles (Table 2.1). The high viscosity and Newtonian flow of castor oil makes its injection a strenuous task, requiring high pressure forces. This was solved by preparing blends with low viscosity oil. The resulting viscosity of the mixtures can be estimated by equation:

$$\log \eta = V_1 * \log \eta_1 + V_2 * \log \eta_2$$ [27]

**Equation 2.1| Viscosity of an oil mixture**
$V_1$ and $V_2$ and $\eta_1$ and $\eta_2$ represent the volume and viscosity of the individual oil vehicles and $\eta$ is the viscosity of the mixture

The process of oil mixing required temperature of 65° C in order to reduce the castor oil viscosity. Castor oil blends with corn oil, sesame oil and peanut oil were oxidized at this temperature. Coconut oil, palm oil and palm kernel oil mixtures were excluded from further examination, since they showed solid components separation below 10° C. Vehicles containing castor oil and MCT, ethyl oleate or isopropyl myristate with a targeted oil viscosity between 100 mPas and 600 mPas were clear and homogenous. For the following experiments, MCT was selected because of its low oxidation tendency as a triglyceride containing primarily saturated fatty acids and its common parenteral use. The mixtures with the highest and the lowest viscosity were selected for incorporation of GnRH [6-D-Phe] acetate (Table 2.2).

| Oily vehicle | viscosity at 25° C [mPas] ± SD | viscosity at 39° C [mPas] ± SD | $t_{1/2}$ i.m back [days] ± SD[28] |
|---|---|---|---|
| castor oil | 780.4 ± 3.3 | 331.1 ± 2.1 | 19.0 ± 2.9 |
| corn oil | 58.4 ± 0.7 | 37.9 ± 2.1 | |
| cottonseed oil | 61.4 ± 0.5 | 38.7 ± 0.2 | |
| wheatgerm oil | 2.1 ± 1.1 | 38.5 ± 0.6 | |
| peanut oil | 72.3 ± 0.4 | 45.2 ± 1.5 | 25 |
| sesame oil | 63.4 ± 0.6 | 39.4 ± 0.5 | 21.4 ± 5.5 |
| MCT | 27.6 ± 0.5 | 17.3 ± 0.3 | 11.6 ± 1.8 |
| ethyl oleate | 6.3 ± 0.5 | 4.7 ± 0.5 | 10 |
| isopropyl myristate | 4.9 ± 0.8 | 3.1 ± 1.1 | 18.3 ± 3.5 |

**Table 2.1| Viscosity and $t_{1/2}$ of oily vehicles for the incorporation of GnRH [6-D-Phe]**
(a) at 25° C (b) at 39° C

| oil mixtures | Viscosity [mPas] ± SD | |
|---|---|---|
| | 25° C | 39° C |
| castor oil: MCT 90:10 % (w/w) | 436.3 ± 2.9 | 163.5 ± 1.5 |
| castor oil: MCT 50:50 % (w/w) | 112.6 ± 9.6 | 53.5 ± 4.5 |

**Table 2.2| Viscosity of castor oil/MCT mixtures for the incorporation of GnRH [6-D-Phe]**
(a) at 25° C (b) at 39° C

### *2.2.2 Oil Spreading at the Injection Site*

The viscosity has a direct impact on the spreading and distribution of the oil vehicle at the injection site. A higher viscosity and consequently a reduced oil vehicle spreading could counteract a possible burst release upon injection. Absorption of aprotinin from a low viscosity emulsion, which spread more extensively within the muscle, was shown to be greater than from the high viscosity formulation[29].

Ultrasonography of the muscle tissue after injection provided the first insights into the spreading behaviour of oils with different viscosity and enabled to judge the ease of manual application. The low viscosity 50:50 % (w/w) castor oil/MCT mixture showed a greater spreading at the injection site in comparison to the high viscosity 90:10 % (w/w) castor oil/MCT vehicle. The low viscosity mixture formed an oblong shape, following the muscles fibers (Figure 2.1 a), while the high viscosity formulation counteracted the tissue pressure and resulted in a well-defined circular depot (Figure 2.1 b).

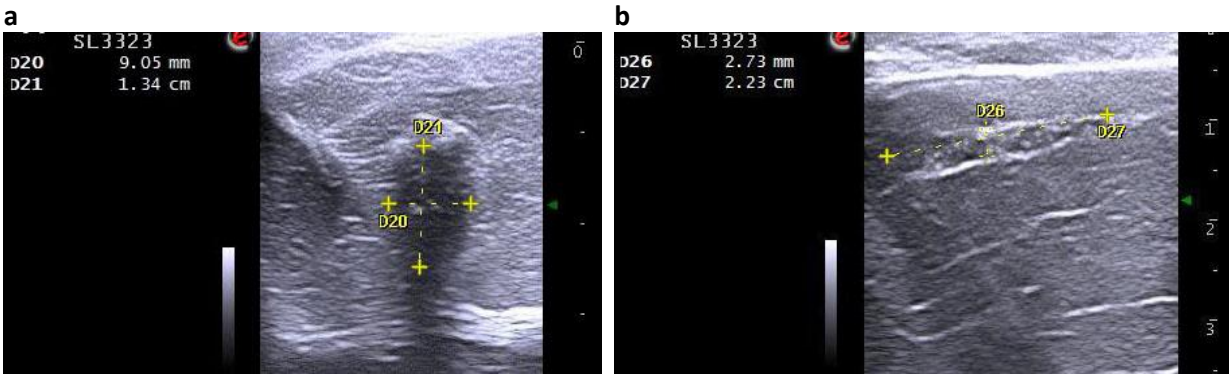


**Figure 2.1| Ultrasonography images at the injection site**
(a) castor oil/MCT 90:10 % (w/w) (b) castor oil/ MCT 50:50 % (w/w)

### *2.2.3 GnRH [6-D-Phe] Micronization and Particles Characterization*

In order to select a suitable GnRH [6-D-Phe] particle size range and micronization process, the particle size distribution of two commercially available oil suspensions for veterinary purposes, Cemay ® and Naxcel®, were analyzed and taken as reference. Cemay® is composed of 50 mg/mL ceftiofur hydrochloride salt in cottonseed oil, hydrogenated lecithin (Phospholipon®90H) and sorbitan monooleate with particles $D_{v50}$ 5.2 ± 0.1 µm; $D_{v90}$ = 32.7 ± 0.9. Naxcel® is composed of 200 mg/mL free crystalline acid of ceftiofur in cottonseed oil and MCT with particles $D_{v50}$ 5.2 ± 0.3 µm; $D_{v90}$ = 29.2 ± 0.2 (Table 2.3).

The GnRH [6-D-Phe] acetate bulk lyophilisate was cryo-and suspension-milled. A frequency increase from 15 Hz to 25 Hz in suspension-milling of GnRH [6-D-Phe] in castor oil: MCT 90:10 % (w/w) resulted in a decrease of the $D_{v50}$ particle size from 51.1 ± 1.9 µm to 38.5 ± 0.9 µm. Prolongation of the grinding time from 11 min to 15 min had less to no effect with $D_{v50}$ decrease from 43.3 ± 2.9 µm to 38.5 ± 0.9 µm (Figure 2.2 a). In comparison, the $D_{v50}$ particle size after cryogenic grinding of the lyophilisate was 8.7 ± 0.9 µm; $D_{v90}$ = 17.6 ± 0.3 (Figure 2.2 b). The particle size distribution of all measured fractions was non-symmetric. One major disadvantage of the cryogenic grinding process is that it requires an additional

dispersing step of the micronized peptide. Therefore cryogenic grinding was considered to be second choice. The suspension-milling for 11 min at 25 Hz was used for the preclinical sample preparation.

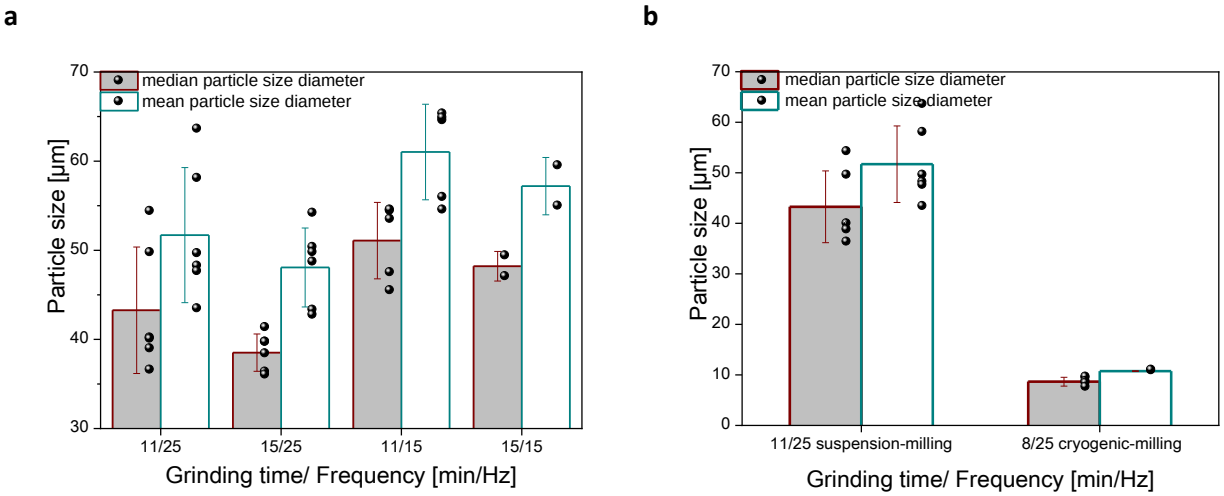


**Figure 2.2| Mean (the mean particle diameter over volume) and median particle size of GnRH [6-D-Phe]** after (a) suspension-milling (b) suspension- and cryogenic-milling

| Grinding Fraction | Grinding Parameters [Time/ Frequency] | $D_{V50}$ [µm] ± SD | $D_{V90}$ [µm] ± SD |
|---|---|---|---|
| GnRH [6-D-Phe] in castor oil: MCT 90:10 % (w/w) | 11 min /25 Hz | 43.3 ± 2.9 | 93.8 ± 5.9 |
| | 15 min/ 25 Hz | 38.5 ± 0.9 | 90.1 ± 4.9 |
| | 15 min / 15 Hz | 51.1 ± 1.9 | 113.9 ± 5.4 |
| | 11 min/ 15 Hz | 48.2 ± 1.2 | 104.9 ± 6.4 |
| GnRH [6-D-Phe] | 8 min/25Hz | 8.7 ± 0.9 | 17.6 ± 0.3 |
| Cemay® | - | 5.2 ± 0.1 | 32.7 ± 0.9 |
| Naxcel® | - | 5.2 ± 0.3 | 29.2 ± 0.2 |

**Table 2.3| Particle size distribution and $D_{v50}$ and $D_{v90}$ fractions**

### *2.2.4 Suspension-and Cryogenic-Milled GnRH [6-D-Phe]*

The particle morphology of suspension and cryogenic milled GnRH [6-D-Phe] was needle- and platelet-like and confirmed the broader particle size distribution of GnRH [6-D-Phe] in castor oil: MCT 90:10 % (w/w**) (**$D_{v50} \leq 50$ µm and $D_{v90} \leq 100$ µm ) in comparison to Cemay® and Naxcel® ($D_{v50} \leq 10$ µm $D_{v90} \leq 50$ µm) (Figure 2.3).

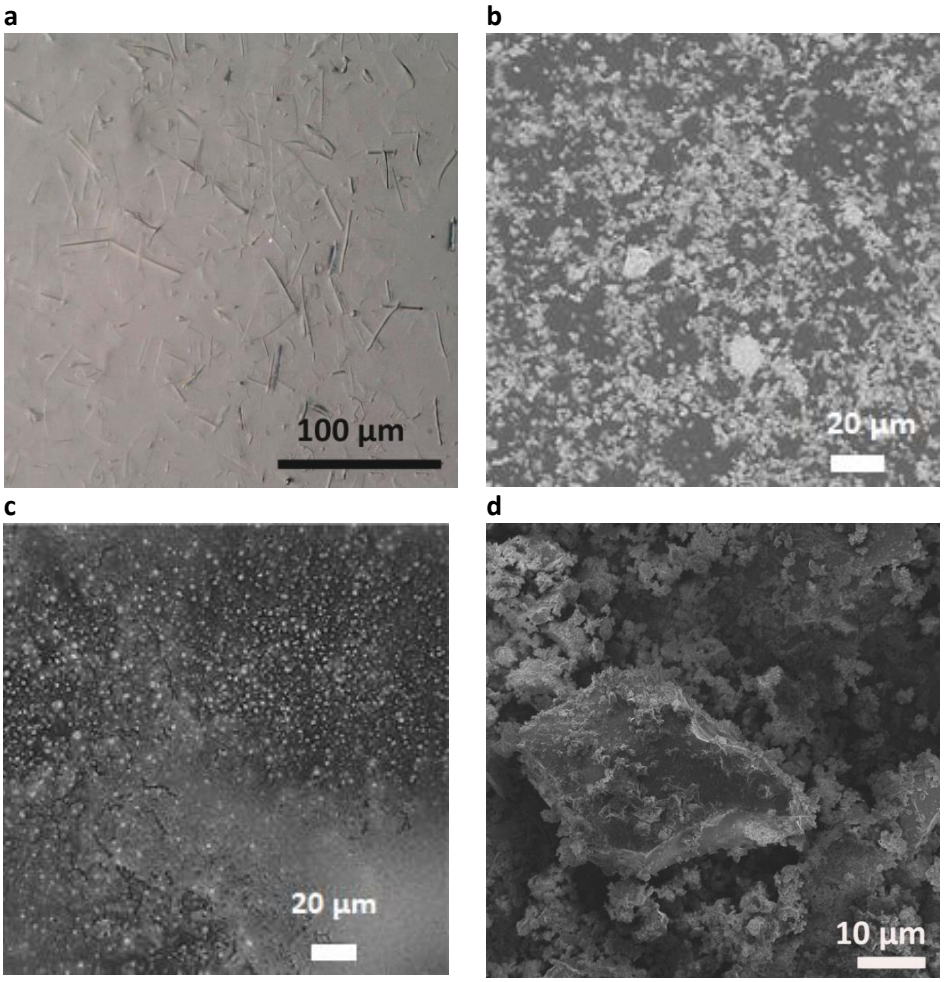


**Figure 2.3| Light microscopy and particles shape characterization**
(a) suspension-milled GnRH [6-D-Phe] (11min/25Hz in castor oil: MCT 90:10 % (w/w) (b) Cemay® (c) Naxcel® (d) scanning electron microscopy of cryoground GnRH [6-D-Phe] (8min/25Hz)

### *2.2.5 GnRH [6-D-Phe] Oil Depot Suspension*

In previous experiments ovulation was successfully blocked delivering 1.06 µg/h GnRH [6-D-Phe] over 14 days using an osmotic pump[30]. By taking this into account and compensating for an initial burst release from the suspension, 375 µg/mL and 1875 µg/mL suspensions were further evaluated (Figure 2.4).

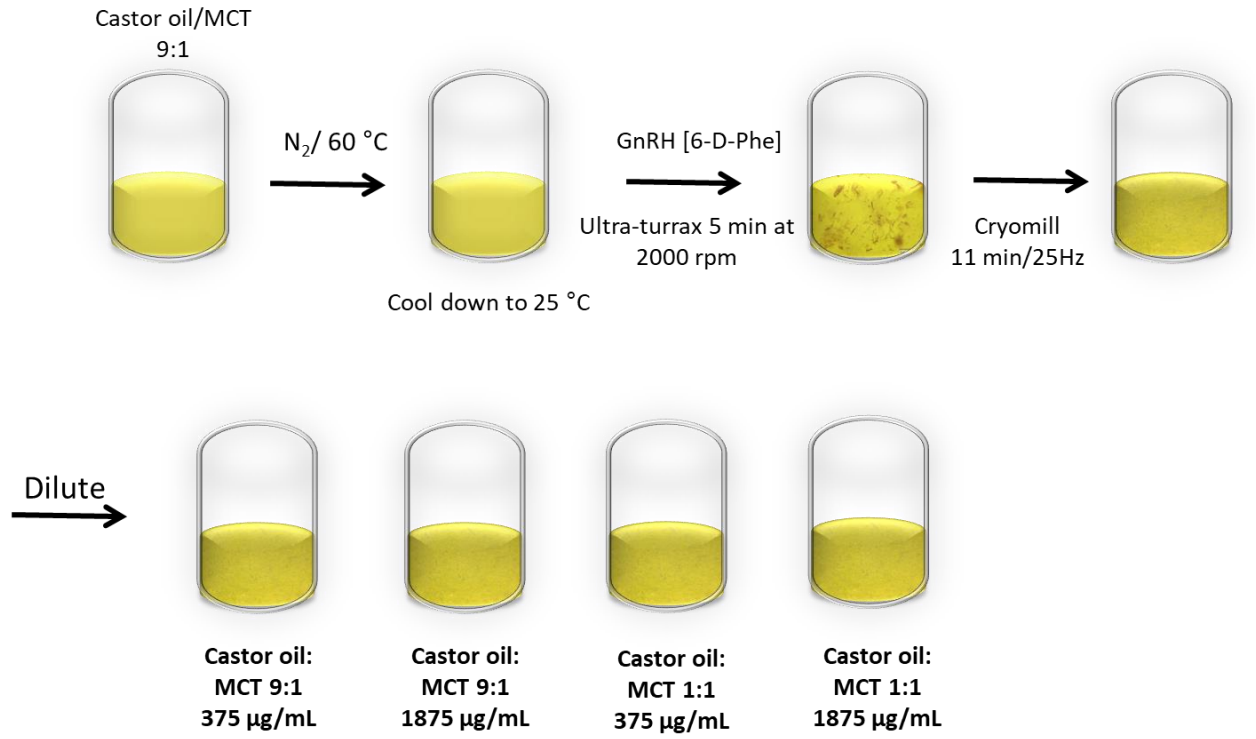


**Figure 2.4| 1st generation GnRH [6-D-Phe] oil depot suspension**

### *2.2.6 Rheology*

The four GnRH [6-D-Phe] formulations exhibited Newtonian flow. Because of their high particle concentrations, the references Cemay® and Naxcel® showed thixotropic behaviour with strong particle-particle interaction, which breaks at high shear rates (Figure 2.5 a). Formulations like this can be more easily administered, since the viscosity decreases at high shear rates, making the flow through the needle easier. Once it has been injected into the muscle, the reduction of shear rate leads to the formation of a more viscous oil depot. The measured viscosity at 1 $s^{-1}$ shear rate reflects the viscosity during formulation storage in the container and after application at the injection site. The viscosity at 500 $s^{-1}$ shear rate reflects the flow through the narrowest needle gauge at the slowest injection rate (Supplementary Data Table 2.4). The viscosity at 39° C reduced to half its value at 25° C, mimicking the *in vivo* behaviour after application (Figure 2.5 b).

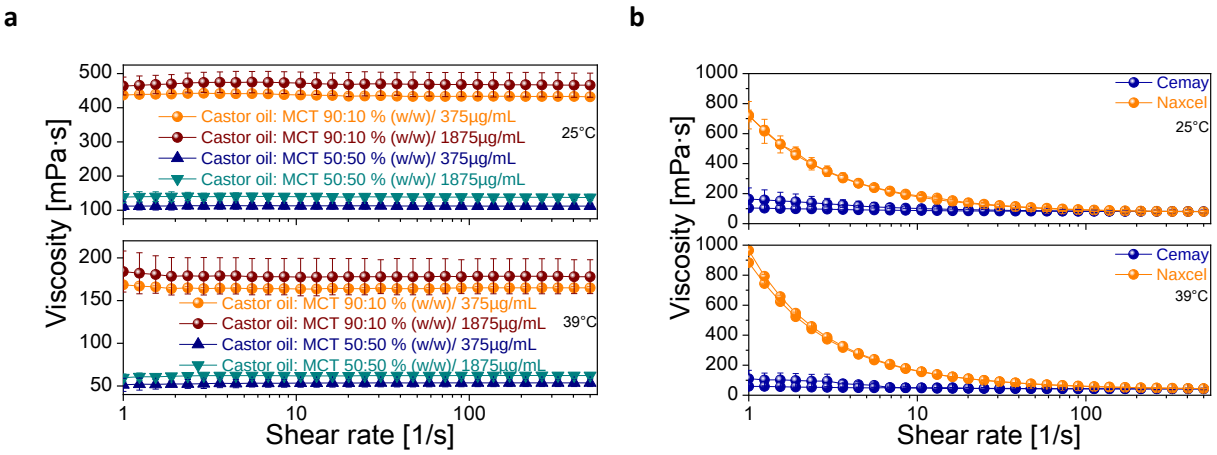


**Figure 2.5| Viscosity of (a) castor oil: MCT GnRH [6-D-Phe] oil depot suspension and (b) Cemay® and Naxcel®** at 25° C and at 39° C

### *2.2.7 Injection Force Determination*

In general, the expelling of a formulation out of a syringe can be divided in three different stages: the first is related to the force required to displace the plunger initially, the plunger-stopper break loose force (PBF). This force maximum is followed by a force plateau as the formulation bulk is continuously expelled through the needle, the dynamic glide force (DGF). Finally, the force rapidly increases as the syringe plunger pushes against the end of the syringe body[31]. This profile was visible with all formulations when injected through a 16 G needle (Figure 2.6 a). The PBF of all tested formulations was similar with the exception of the reference Naxcel®, which required higher PBF. The injection forces of the GnRH [6-D-Phe] formulations through a 16 G were lower in comparison to an 18 G needle (Figure 2.6 b) and indicated easy handling. This made 16 G the needle of choice for application.

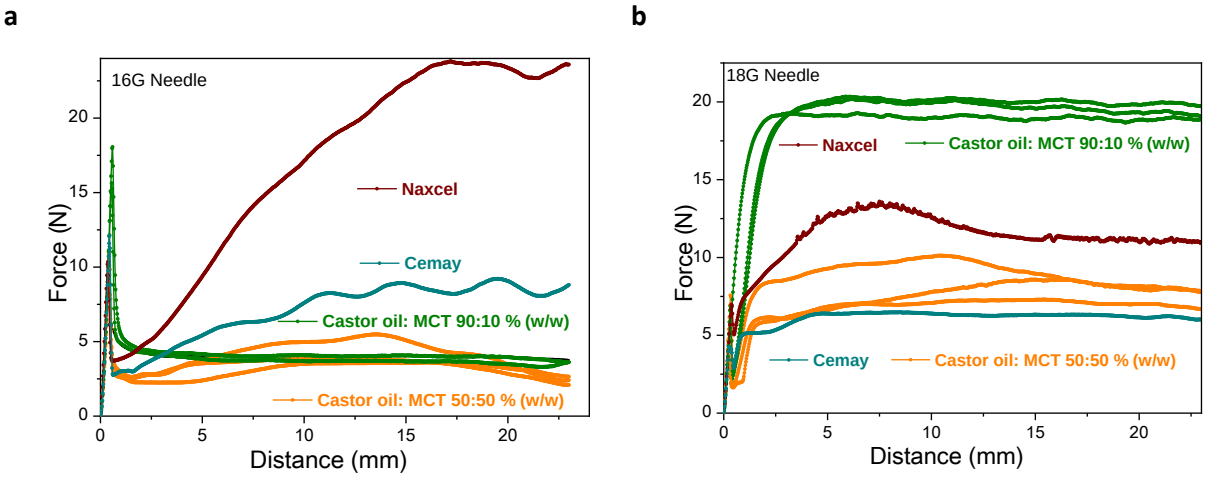


**Figure 2.6| Pressure required to expell the formulations (N) as a function of the distance (mm) of the syringe plunger** (a) 16 G (b) 18 G needle

### 2.2.8 *In vitro Release Model Selection and Studies*

In order to establish a robust *in vitro* release model able to differentiate between formulations, a Float-a-Lyzer® (FDS-Floating Dialysis System) and a dialysis bag method were tested. Preliminary experiments showed that an FDS with MWCO larger than 5 kD and preferably 300 kD and higher offered an unhindered diffusion of the GnRH [6-D-Phe], making the oil vehicle the rate limiting factor in the release (Supplementary Data Figure 2.9). Furthermore a 300 kD MWCO was compared with 12-14 kD MWCO dialysis bags.

Overall, the release from the FDS was incomplete (Figure 2.7 a). The suspended GnRH [6-D-Phe] particles in the oil phase settled on the FDS plastic bottom and the contact with the release medium was prevented. This was not the case with the test vehicle in the dialysis bag, where the oil vehicle stayed in contact with the release medium over the release time. For this reason, the dialysis system was selected for further *in vitro* testing.

The GnRH [6-D-Phe] formulations in the dialysis bag exhibited an initial burst release with approximately 50 % of the amount released within the first 48 hours. A slightly lower initial release was achieved with a higher concentration and viscosity. Thus increasing the concentration of GnRH [6-D-Phe] acetate or the viscosity could not compensate the burst effect completely and did not affect the *in vitro* release profile significantly (Figure 2.7 b).

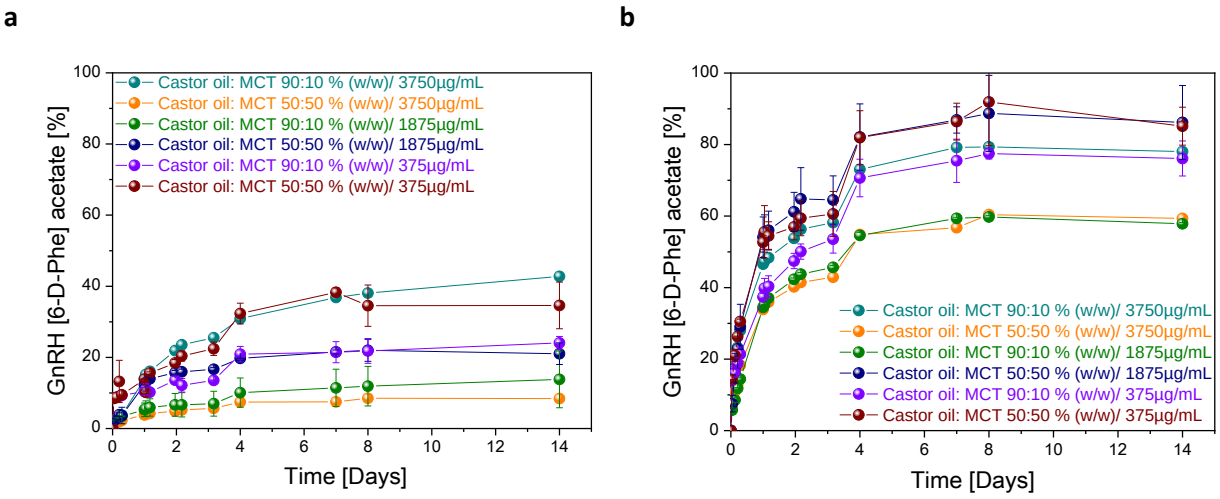


**Figure 2.7| *In vitro* release profiles of GnRH [6-D-Phe] formulations from castor oil: MCT**
(a) FDS MWCO 300 kD and (b) visking dialysis tubing, MWCO 12 – 14 kD

### 2.2.9 *In vivo 1st Preclinical Study*

The four formulations were tested *in vivo*:

castor oil: MCT 50:50 % (w/w) 375 µg/ml GnRH [6-D-Phe]

castor oil: MCT 50:50 % (w/w) 1875 µg/ml GnRH [6-D-Phe]

castor oil: MCT 90:10 % (w/w) 375 µg/ml GnRH [6-D-Phe]

castor oil: MCT 90:10 % (w/w) 1875 µg/ml GnRH [6-D-Phe]

The effect was evaluated and considered successful if first, the estrous cycle was blocked and there were no follicles larger than 5mm and second, the corpus luteum (CL) showed a reduced size in comparison to previous measurements. A CL regression was expected on days 15-17 of the estrous cycle, corresponding to 4-6 days post application. If a follicle growth, an ovulation or cyst development appeared, the cycle blockage was regarded as unsuccessful.

The control group received the oil matrix without GnRH [6-D-Phe]. Ultrasonography showed a follicle growth and no effect of the placebo (0.2 ± 0.4 days) (Figure 2.8)**.** Castor oil: MCT 50:50 % (w/w) 375 µg/ml GnRH [6-D-Phe] resulted in 2 to 3 days cycle blocking effect. One tested animal in the group displayed no cycle blocking effect and developed transient ovarian cysts 13 days after application. Thus the average effect was estimated to be 1.8 ± 1.1 days. The five animals injected with castor oil: MCT 50:50 % (w/w) 1875 µg/ml GnRH [6-D-Phe] showed follicle growth between day 9 and day 12, resulting in an effect of 2 to 5 days. One tested animal in the group showed an irreversible cycle blocking effect. After CL regression, the animal displayed an irregular follicle growth without ovulation. The average effect was 3.8 ± 1.3 days. The animals which received castor oil: MCT 90:10 % (w/w) 375 µg/ml GnRH [6-D-Phe] had an average cycle blocking effect of 1.2 ± 1.3 days. The animals treated with castor oil: MCT 90:10 % (w/w) 1875 µg/ml GnRH [6-D-Phe] showed the most irregularities. Cycle blockage for 11 and 12 days was seen in two animals, two others showed an irregular cycle and one developed multiple cysts with a permanent anestrus. The average effect lasted 6.0 ± 9.6 days (Supplementary Data Table 2.6).

Statistical analysis showed that the mean cycle blocking effect of castor oil: MCT 50:50 % (w/w) 375 µg/ml GnRH [6-D-Phe] and castor oil: MCT 50:50 % (w/w) 1875 µg/ml GnRH [6-D-Phe] was significantly longer than the one of the control group ($p<0.05$) (Supplementary Data Table 2.7, Table 2.8). There were no significant differences between castor oil: MCT 90:10 % (w/w) 375 µg/ml GnRH [6-D-Phe], castor oil: MCT 90:10 % (w/w) 1875 µg/ml GnRH [6-D-Phe] and placebo ($p>0.05$) (Supplementary Data Table 2.9, Table 2.10).

In summary, the *in vivo* study could confirm that a treatment with GnRH [6-D-Phe] oil depot suspension could successfully prolong the luteal phase of the estrous cycle and inhibit a follicle development and growth. The most pronounced cycle blocking effects, with regards to duration, synchronicity and observed adverse reactions, were detected in the groups castor oil: MCT 50:50 % (w/w) 1875 µg/ml GnRH [6-D-Phe] and castor oil: MCT 50:50 % (w/w) 375 µg/ml GnRH [6-D-Phe]. A longer effect was obtained with a higher peptide concentration (3.8 ± 1.3 days vs. 1.8 ± 1.1 days). The results of the *in vivo* study showed that a low viscosity GnRH [6-D-Phe] formulation could achieve a longer and more consistent cycle blocking effect compared to a high viscosity formulation.

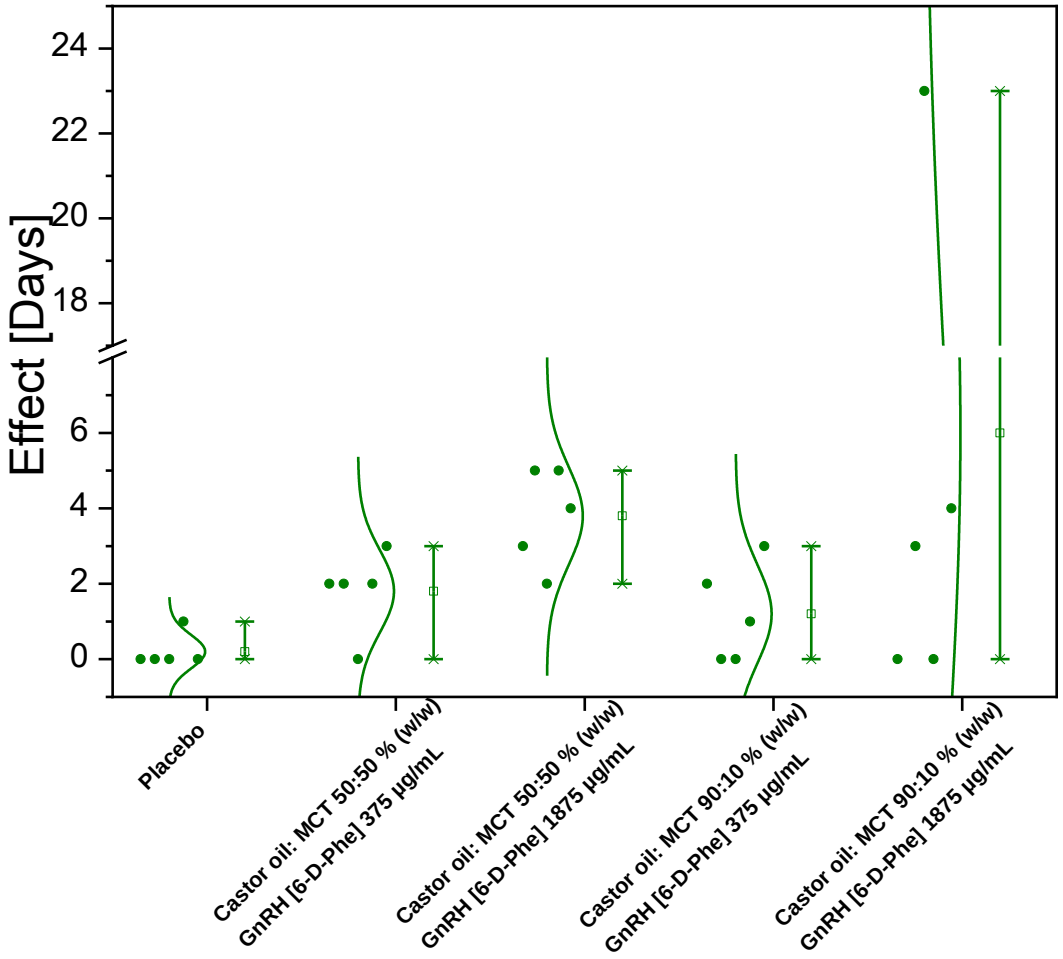


**Figure 2.8| *In vivo* effect of the oil depot GnRH [6-D-Phe] formulations**

## 2.3 CONCLUSION

The experiments demonstrated that sustained release of GnRH [6-D-Phe] can be achieved with castor oil/MCT oily vehicles. Still formulation optimization will be necessary to achieve a more consistent release rate and *in vivo* effect. Furthermore, the relatively high viscosity at 25° C and Newtonian flow behaviour of the formulations can pose a challenge for a multiple dose application. This might be resolved with Non-newtonian oily suspensions, e.g. incorporating an oil gelling additives such as aluminium stearate.

## 2.4 MATERIALS AND METHODS

**Gonadorelin [6-D-Phe] acetate peptide** (pE1–H2–W3–S4–Y5–(D)F6–L7–R8–P9–G10–NH2) or (pGlu-His-Trp-Ser-Tyr-D-Phe-Leu-Arg-Pro-Gly-NH2) was provided by BFC Biopept-Feinchemie as lyophilized powder and acetate salt (purity 99.76 %, water content 6.73 % and acetate peptide ratio (MW/MW) 1.8). **Oil vehicle**: miglyol®812 (MCT), ethyl oleate, isopropylmyristate (Caesar & Loretz, D-Hilden), castor oil, corn oil, sesame oil, peanut oil, coconut oil, palm oil, palm kernel oil (Gustav Heess,D-Leonberg).

**Oil mixtures preparation** The mixtures of castor oil and a second oily component (corn oil, sesame oil, peanut oil, coconut oil, palm oil, palm kernel oil, ethyl oleate, isopropyl myristate, MCT) were homogenized and heated at 65° C for 20 minutes without the addition of an antioxidant and under normal atmosphere in a silicone oil bath containing a metal holding plate with vials holder. In order to estimate the extent of miscibility of the oils, the prepared mixtures were visually evaluated.

**Ultrasonography images at the injection site** The formulations high viscosity castor oil/MCT 90:10 % (w/w) and low viscosity castor oil/MCT 50:50 % (w/w) were administered by intramuscular injection using a 18Gx1“1.2 mm x 25 mm needle in the post-auricular region of the neck of two swine carcasses of mature German Landrace x Piétrain. The ultrasonography images were taken with Fazone CB (Fujifilm) at 6 MHz frequency and 10 cm depth.

**GnRH [6-D-Phe] micronization** The suspension milling- and cryogenic micronization of GnRH [6-D-Phe] bulk lyophilisate were performed using a Retsch Cryo Mill (Retsch Technology, Haan, Germany). The suspension-milling was performed in the high viscosity medium castor oil/MCT 90:10 % (w/w) at room temperature and a concentration of 7.5 mg/mL. The grinding jar of 25 mL and 15 mm grinding balls was filled with each grinding fraction and cooled down in liquid nitrogen for 5 minutes in order to reduce the stress applied to GnRH [6-D-Phe] during the grinding process. The cryogenic grinding process was performed for the duration of 8 minutes at 25 Hz. The cryogenic cycle included a precooling phase of 10 min at 5 Hz.

**GnRH [6-D-Phe] particle size distribution and characterization** The particle size distribution was analysed employing a Laser Diffraction Particle Size Analyzer LA-950 (Retsch Technology, Haan). The samples were prepared in triplicate (n=3). 0.2 mL of the oil suspension was measured in a solution of 1 % sorbitan monooleate in isooctane (m/v) in a standard measuring cell with 10 mL volume.

**Light microscopy and Scanning Electron Microscopy** The SEM images of the cryoground GnRH [6-D-Phe] lyophilisate were taken with JSM 6500-F (Jeol, Peabody, MA, USA) and Inca Software (Oxford Instruments, Oxfordshire, UK). The SEM images were collected at a magnification 1000x and an accelerating voltage of 2.0 kV. The light microscopy images of the suspension milled GnRH [6-D-Phe] fractions, Cemay® and Naxcel® suspensions were taken with VHX – 500 FD (Keyence, Osaka, Japan).

**GnRH [6-D-Phe] oil depot suspension preparation** The high and low viscosity mixtures were heated and agitated under inert atmosphere ($N_2$) at 60° C and then cooled down to room temperature at 25° C. GnRH [6-D-Phe] was suspended in the oil vehicles using an Ultra-Turrax T-10 basic (IKA-Labortechnik, Staufen, Germany) for 5 min at 2000 rpm and later suspension-milled for 11 min at 25 Hz frequency in a grinding jar of 25 mL and 15 mm grinding balls with the Cryo Mill (Retsch Technology, Haan, Germany). Four castor oil/MCT formulations were composed: Castor oil: MCT 90:10 % (w/w) /1875 µg/mL; Castor oil: MCT 90:10 % (w/w) /375 µg/mL; Castor oil: MCT 50:50 % (w/w) /1875 µg/m and Castor oil: MCT 50:50 % (w/w) /375 µg/mL.

**Rheology** Viscosity measurement and flow curves evaluation of the pure oils and the mixtures were performed with MCR 100 (Anton Paar Germany, Ostfildern-Scharnhausen) cone plate system CP – 1 (50 mm diameter, a cone angle of 1 °, and a gap of 0.042 mm). The viscosity η was defined depending on the shear rate $\dot{\gamma}$ and measuring sections a) 0 – 500 $s^{-1}$ (30 points, 6 s per point; 180 s measurement time), b) 500 $s^{-1}$ (1 point, 6 s per point, 6 s measurement time), c) 500 – 0 $s^{-1}$ (30 points, 6 s per point, 180 s measurement time).

**Injection force determination** The injectability/syringeability experiments were performed with the TA.XT.plus Texture Analyser (Stable Micro Systems, Godlming, UK). The formulations were injected into air

using a terumo syringe 2.5 mL Luer Lock Tip (Terumo Europe N.V, Leuven, Belgium) with either a FINE-JECT 18Gx1'', 1.2x38mm needle (Henke-Sass-Wolf GmbH, Tuttlingen, Germany) or a FINE-JECT 16Gx1'', 1.6x25 mm needle (Henke-Sass-Wolf GmbH, Tuttlingen, Germany). The software Exponent was set to compression test mode with the parameters: 5.0 mm/sec pre-test speed, and 2.5 mm/sec test speed, and 20.00 mm/sec post-test speed, trigger force: 0.001 N. The applied force from the texture analyser was recorded in [N] against the distance of the syringe plunger (max. 24.5 mm).

**Preliminary *in vitro* release study and release model selection** The preliminary study was performed with a 100 µg/mL solution of GnRH [6-D-Phe] in 3.5-5 kD, 8-10 kD, 20 kD, 50 kD, 100 kD, 300 kD and 1000 kD Float-a-Lyzer® G2 systems (Spectrum Europe BV, Breda, Netherlands). The preparation and activation of the membrane required: 1. Pre-wetting the membrane of the Float-a-Lyzer, filling with a 10 % ethanol solution, soaking the filled membrane into 10 % ethanol solution for 10 min. Then the device was thoroughly flushed with deionized water, filled and soaked for 20 min in deionized water. The prepared membranes were stored in PBS (pH 7.4) (Na2HPO4x2H2O 1.44 mg/mL; KH2PO4 0.2 mg/mL; NaCL 8 mg/mL; KCL 0.2 mg/mL; Natriumazid 0.05 % (w/v)) at 2-8° C. 1.5 mL aqueous solution of GnRH [6-D-Phe] was filled in the Float-a-Lyzers. The release medium was 40 mL PBS buffer (pH 7.4). The experiment was performed in duplicate (n=2), in an incubated shaking water bath Julabo SW 21/2 (Julabo GmbH, Seelbach, Germany) at 39° C and agitation rate 90 $min^{-1}$.

***In vitro* release study** The *in vitro* release study was conducted using VISKING® dialysis tubing, MWCO 12 – 14 kD, RC, 28 mm (SERVA, Germany) and the Float-a-Lyzer® G2 300 kD, 1 mL 1.5 mL formulation was filled in the tube and the FDS (Floating Dialysis System) and released in 30 mL PBS (pH 7.4). The *in-vitro* evaluation was performed in duplicate (n=2), in an incubated shaker 3031 (GFL, Germany) at 39° C and 60 rpm. 1 mL sample was used for the RP-HPLC analysis at the following intervals 1 h, 3 h, 5 h, 7 h, 22 h, 25 h, 28 h, 46 h, 52 h, 76 h, 100 h, 172 h, 196 h, 220 h, and 336 h (14 days). The GnRH [6-D-Phe] content in the oil vehicle and in the donor cell was extracted using organic solvents, dichloromethane (DCM), where GnRH [6-D-Phe] is not soluble in combination with PBS (pH 7.4). 2 mL sample was weighted into a falcon tube, 4 mL DCM and 6 mL PBS (pH 7.4) were added. The tube was vortexed at room temperature (25° C) and put into an incubated shaker 3031 (GFL, Germany) at 39° C and 60 rpm for 24 h. The quantity of the peptide in the upper aqueous phase was analysed by RP-HPLC at 220 nm.

**Determination of the GnRH [6-D-Phe] (RP-HPLC)** The GnRH [6-D-Phe] content was analysed by RP-HPLC using a LUNA C8 (4.6 mm x 250 mm; size = 5 µm; Phenomenex, USA) column, with a C8 pre-column (4 mm x 3 mm; size = 5 µm) at an HPLC Agilent 1100/1200 series (Agilent Technologies, USA) (mobile phase A (water + 1 mL/L Trifluoroacetic acid (TFA) (v/v)) and mobile phase B (800 g Acetonitrile + 200 g water + 1.2 mL TFA), 1.1 mL/min flow, column temperature 40° C, and autosampler temperature 2 – 8° C. The Retention Time (RT) of GnRH [6-D-Phe] was 8.5 ± 1.5 minutes with UV detection at 220 nm. The HPLC Gonadorelin Quantification Method and Calibration curve, HPLC Gonadorelin Selectivity, HPLC Gonadorelin Linearity, HPLC Gonadorelin Accuracy, HPLC Intermediate Precision/Precision as well as HPLC LOD and LOQ were performed.

***In vivo* 1st preclinical study** The first *in vivo* testing and analysis of results were performed between 09.04.2014 and 25.06.2014 from the University in Leipzig by Prof. Dr. Johannes Kauffold with the support of Dr. Haukur Sigmarrson, Dr. Mathias Hoops, Rosa Stark and Catherine Poser. The number of tested animals was 25 (german landrace and pietrain breeds) with an average weight of 148 KG and 241- 243 days old. The gilts were administered with Altrenogest, eCG and GnRH in order to synchronize the estrus cycle of the gilts according to an established schedule (Supplementary Data Table 2.5). The sonography was performed with a Fazone CB (Fujifilm), C9-3 curved array type and 3-9 MHz frequency. The examination was done at 6 MHz frequency, 10 cm depth and a gain of 84 dB. The sonography examination represented a new method developed by Prof. Dr Johannes Kauffold[32,33]. The follicle, corpora hemorrhagica and corpora lutea were analyzed. Follicles with a diameter of 10 mm or larger, which did not ovulate were considered to be ovarian cysts. Single cysts were differentiated from polycystic ovarian syndrome. The ovulation included the collapse of the preovulatory follicle and the appearance of the corpora hemorrhagica.

**Statistical Analysis** The effect of treatment and a comparison between the formulations was performed using a t-test: two sample assuming unequal variances with the software QI Macros 2017 (Denver, USA).

## 2.5 REFERENCES AND ACKNOWLEDGMENTS


1. Magon, N. Gonadotropin releasing hormone agonists: Expanding vistas. *Indian J. Endocrinol. Metab.* **15,** 261–7 (2011).

2. Hayden, C. GnRH analogues: Applications in assisted reproductive techniques. *Eur. J. Endocrinol.* **159,** S17-25 (2008).

3. Morishita, M. & Peppas, N. A. Is the oral route possible for peptide and protein drug delivery? *Drug Discov. Today* **11,** 905–910 (2006).

4. Werle, M. & Bernkop-Schnuerch, A. Strategies to improve plasma half life time of peptide and protein drugs. *Amino Acids* **30,** 351–367 (2006).

5. Oh, E. J. *et al.* Target specific and long-acting delivery of protein, peptide, and nucleotide therapeutics using hyaluronic acid derivatives. *J. Control. Release* **141,** 2–12 (2010).

6. Witt, K. A., Gillespie, T. J., Huber, J. D., Egleton, R. D. & Davis, T. P. Peptide drug modifications to enhance bioavailability and blood-brain barrier permeability. *Peptides* **22,** 2329–2343 (2001).

7. Morgan, K., Leighton, S. P. & Millar, R. P. Probing the GnRH receptor agonist binding site identifies methylated triptorelin as a new anti-proliferative agent. *J. Mol. Biochem.* **1,** 86–98 (2012).

8. Del Curto, M. D. *et al.* Lipid microparticles as sustained release system for a GnRH antagonist (Antide). *J. Control. Release* **89,** 297–310 (2003).

9. Fontaine, C. Long-term contraception in a small implant: A review of Suprelorin (deslorelin) studies in cats. *J. Feline Med. Surg.* **17,** 766–71 (2015).

10. Wenzel, J. G. W. *et al.* Pluronic F127 gel formulations of deslorelin and GnRH reduce drug degradation and sustain drug release and effect in cattle. *J. Control. Release* **85,** 51–9 (2002).

11. Zhang, G., Li, J., Wang, T., Gao, L. & Quan, D. Oil-based formulation as a sustained-released injection for a novel synthetic peptide. *Curr. Pharm. Biotechnol.* **16,** 187–93 (2015).

12. Zhang, G., Wang, T., Gao, L. & Quan, D. Oral delivery of oil-based formulation for a novel synthetic cationic peptide of GnRH (gonadotropin-releasing hormone) antagonist for prostate cancer treatment. *Int. J. Pharm.* **450,** 138–144 (2013).

13. Patel, A., Cholkar, K. & Mitra, A. K. Recent developments in protein and peptide parenteral delivery approaches. *Ther. Deliv.* **5,** 337–365 (2014).

14. Zuidema, J., Kadir, F., Titulaer, H. A. C. & Oussoren, C. Release and absorption rates of intramuscularly and subcutaneously injected pharmaceuticals (II). *Int. J. Pharm.* **105,** 189–207 (1994).

15. Chien, Y. W. Long-acting parenteral drug formulations. *J. Parenter. Sci. Technol.* **35,** 106–39 (1981).

16. Benson, H. A. & Prankerd, R. J. Optimisation of Drug Delivery 6. Modified-Release Parenterals. *Aust. J. Hosp. Pharm.* **28,** 99–104 (1998).

17. Marder, S. R., Hubbard, J. W., Van Putten, T. & Midha, K. K. Pharmacokinetics of long-acting injectable neuroleptic drugs: clinical implications. *Psychopharmacology (Berl).* **98,** 433–439 (1989).

18. Davis, J. M., Metalon, L., Watanabe, M. D. & Blake, L. Depot Antipsychotic Drugs. *Drugs* **47,**

741–773 (1994).

19. Hoitink, M. A. *et al.* Degradation kinetics of gonadorelin in aqueous solution. *J. Pharm. Sci.* **85,** 1053–1059 (1996).

20. Helm, V. J. & Müller, B. W. Stability of Gonadorelin and Triptorelin in Aqueous Solution. *Pharm. Res. An Off. J. Am. Assoc. Pharm. Sci.* **7,** 1253–1256 (1990).

21. Hoitink, M. A. *et al.* Identification of the Degradation Products of Gonadorelin and Three Analogues in Aqueous Solution. *Anal. Chem.* **69,** 4972–4978 (1997).

22. Nema, S. & Ludwig, J. D. *Pharmaceutical dosage forms : parenteral medications. Volume 1, Formulation and packaging*. (Informa Healthcare, 2010).

23. Reithmeier, H., Herrmann, J. & Göpferich, A. Lipid microparticles as a parenteral controlled release device for peptides. *J. Control. Release* **73,** 339–350 (2001).

24. Reithmeier, H., Herrmann, J. & Göpferich, A. Development and characterization of lipid microparticles as a drug carrier for somatostatin. *Int. J. Pharm.* **218,** 133–143 (2001).

25. Li, L. C. *et al.* Effect of Solid State Transition on the Physical Stability of Suspensions Containing Bupivacaine Lipid Microparticles. *Pharm. Dev. Technol.* **10,** 309–318 (2005).

26. Shi, Y. & Li, L. C. Current advances in sustained-release systems for parenteral drug delivery. *Expert Opin. Drug Deliv.* **2,** 1039–1058 (2005).

27. Arrhenius, S. Über die innere Reibung verdünnter wässeriger Lösungen. *Zeitschrift für Phys. Chemie* **1,** 285–298 (1887).

28. Larsen, S. W. *et al.* Determination of the disappearance rate of iodine-125 labelled oils from the injection site after intramuscular and subcutaneous administration to pigs. *Int. J. Pharm.* **230,** 67–75 (2001).

29. Bjerregaard, S. *et al.* Parenteral water/oil emulsions containing hydrophilic compounds with enhanced in vivo retention: Formulation, rheological characterisation and study of in vivo fate using whole body gamma-scintigraphy. *Int. J. Pharm.* **215,** 13–27 (2001).

30. Brüssow, K. P., Schneider, F. & Kanitz, W. Die Langzeitapplikation eines GnRH-Agonisten als eine alternative Methode zur Zyklussteuerung beim Schwein. (2000).

31. Cilurzo, F. *et al.* Injectability Evaluation: An Open Issue. *AAPS PharmSciTech* **12,** 604–609 (2011).

32. Kauffold, J., Rautenberg, T., Richter, A., Waehner, M. & Sobiraj, A. Ultrasonographic characterization of the ovaries and the uterus in prepubertal and pubertal gilts. *Theriogenology* **61,** 1635–1648 (2004).

33. Kauffold, J. & Althouse, G. C. An update on the use of B-mode ultrasonography in female pig reproduction. *Theriogenology* **67,** 901–911 (2007).

This work was supported by Veyx Pharma D-Schwarzenborn and DBU (Deutsche Bundesstiftung Umwelt) D-Osnabrueck. We are also grateful to Gustav Heess for providing us with the oil compounds for the preliminary testing and to Christian Minke, Department Inorganic Chemistry LMU D-Munich, for recording the SEM images. We would like to thank BFC-BioPept Feinchemie D-Weinbergen for donating GnRH [6-D-Phe] acetate.

## 2.6 SUPPLEMENTARY DATA

| Injection rate [mL/s] | Shear rate [$s^{-1}$] | | |
|---|---|---|---|
| | 16G/1.194 mm | 17G/1.067mm | 18G/0.838mm |
| 0.05=0.078mm/s | 199.4 | 279.4 | 576.7 |
| 0.1=0.156mm/s | 398.8 | 558.8 | 1153.5 |
| 0.2=0.312mm/s | 797.5 | 1117.6 | 2306.9 |
| 0.4=0.624mm/s | 1595.1 | 2235.1 | 4613.8 |
| 2=3.12mm/s | 7975.4 | 11175.6 | 23069.2 |
| 2.5=3.9 mm/s | 9969.2 | 13969.5 | 28836.5 |

**Table 2.4| Shear rate through different needle sizes in correlation to injection rate**

The shear rate has been calculated using the equation:

$$\bar{\gamma} = \frac{2\partial V/\partial t}{\pi R_{needle}^3} \frac{3n+1}{2n+1}$$

**Equation 2.2| Shear rate through injection needle**
$\partial V/\partial t$ is the injection rate, $R$ is the radius of the needle, $n$ is a constant=1 for Newtonian flow behaviour

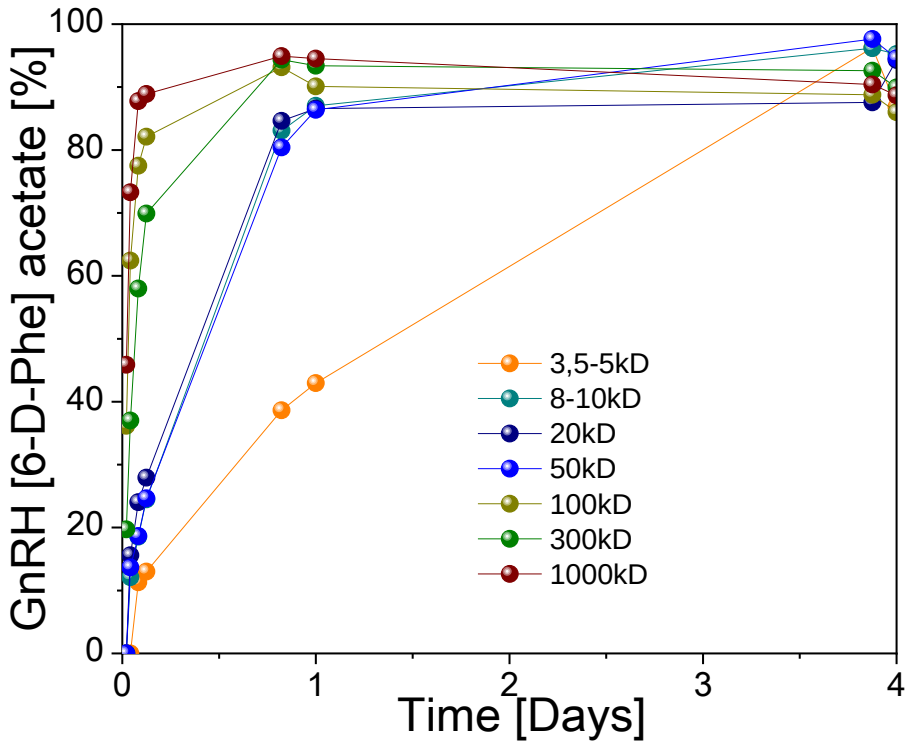


**Figure 2.9| Preliminary *in vitro* release study and release model selection**
Permeability of Floating Dialyis System (FDS) to GnRH [6-D-Phe] solution in correlation to the MWCO

| Step | | I. Preclinical Study<br>Oil Depot Suspension of Gonadorelin[6-D-Phe] acetate | | | | |
|---|---|---|---|---|---|---|
| **1** | 1. day | Sonographic examination of the 25 gilts to determine sexual maturity | | | | |
| **2** | 11.-28. day | Daily administration of 5 ml Regumate® 4 mg/ml (= 20 mg Altrenogest) per oral over 18 days to inhibit the follicle development | | | | |
| **3** | 30. day<br>(40 h after last Regumate administration) | 4,2 ml Intergonan® 240 I.E./ml intramuscular(i.m.) (= 1000 IE equine chorionic-gonadotropin (eCG)) to stimulate the folicle development | | | | |
| **4** | 33. day<br>(78 h after eCG administration) | 1,0 ml Gonavet Veyx® i.m. (= 50 µg Gonadorelin[6-D-Phe]) to induce ovulation | | | | |
| **5** | 35.-45. day | Daily clinical and sonographic examination of the 25 gilts | | | | |
| **6** | 46. day | Clinical and sonographic examination of the 25 gilts; separating the 25 gilts in 5 groups with different substances for application for intramuscular application | | | | |
| | | 5 Gilts<br>Group 1<br>375 µg/ml<br>Castor oil: MCT<br>50:50 % (w/w) | 5 Gilts<br>Group 2<br>1875 µg/ml<br>Castor oil: MCT<br>50:50 % (w/w) | 5 Gilts<br>Group 3<br>375 µg/ml<br>Castor oil: MCT<br>90:10 % (w/w) | 5 Gilts<br>Group 4<br>1875 µg/ml<br>Castor oil: MCT<br>90:10 % (w/w) | 5 Gilts<br>Group 5<br>Castor oil: MCT<br>90:10 % (w/w) |
| **7** | 47.-72. day | Daily clinical and sonographic examination of the 25 gilts | | | | |

**Table 2.5| *In vivo* Study Timetable**

| Group | Results |
|---|---|
| Placebo<br>**Castor oil: MCT 90:10 % (w/w)**<br>**n=5** | normal cycle 7 d p.i. and ovulation |
| | normal cycle 7 d p.i. and ovulation |
| | normal cycle 8 d p.i. and ovulation |
| | normal cycle 7 d p.i. and ovulation |
| | normal cycle 7 d p.i. and ovulation |
| GnRH [6-D-Phe] 375 µg/ml<br>**Castor oil: MCT 50:50 % (w/w)**<br>**n=5** | no cycle blocking effect |
| | 2 days cycle blocking effect |
| | 2 days cycle blocking effect |
| | 2 days cycle blocking effect |
| | 3 days cycle blocking effect |
| GnRH [6-D-Phe] 1875 µg/ml<br>**Castor oil: MCT 50:50 % (w/w)**<br>**n=5** | 2 days cycle blocking effect |
| | 3 days cycle blocking effect |
| | 4 days cycle blocking effect |
| | 5 days cycle blocking effect |
| | 5 days cycle blocking effect |
| GnRH [6-D-Phe] 375 µg/ml<br>**Castor oil: MCT 90:10 % (w/w)**<br>**n=5** | no cycle blocking effect |
| | no cycle blocking effect |
| | 1 day cycle blocking effect |
| | 2 days cycle blocking effect |
| | 3 days cycle blocking effect |
| GnRH [6-D-Phe] 1875 µg/ml<br>**Castor oil: MCT 90:10 % (w/w)**<br>**n=5** | no cycle blocking effect |
| | 3 days cycle blocking effect |
| | 4 days cycle blocking effect |
| | 23 days cycle blocking effect |
| | permanent cycle blocking effect |

**Table 2.6| *In vivo* Study Results**

| t-Test: Two-Sample Assuming Unequal Variances | | a=0.05 | | | |
|---|---|---|---|---|---|
| **Equal Sample Sizes** | | | | | |
| | ***Placebo*** | ***Treatment 1*** **GnRH [6-D-Phe] 375 µg/ml** Castor oil: MCT 50:50 % (w/w) | diff | 95 % Confidence Interval | |
| **Mean** | **0.2** | **1.8** | -1.600 | -2.960 | -0.240 |
| **Variance** | **0.2** | **1.2** | | | |
| **Observations** | 5 | 5 | | | |
| **Hypothesized Mean Difference** | 0 | | | | |
| **df** | 5 | | | | |
| **t Stat** | -3.024 | | | | |
| **P(T<=t) one-tail - Difference < Hypothesized Difference** | 0.015 | 0.985 | Difference > Hypothesized Difference | | |
| **T Critical one-tail** | 2.015 | | | | |
| **P(T<=t) two-tail** | 0.029 | | Reject Null Hypothesis because p < 0.05 (Means are Different) | | |
| **T Critical Two-tail** | 2.571 | | | | |

**Table 2.7| Statistical analysis t-test placebo-GnRH [6-D-Phe] 375 µg/ml Castor oil: MCT 50:50 % (w/w)**

| t-Test: Two-Sample Assuming Unequal Variances | α =0.05 | | | | |
|---|---|---|---|---|---|
| **Equal Sample Sizes** | | | | | |
| | ***Placebo*** | ***Treatment 2*** **GnRH [6-D-Phe] 1875 µg/ml** Castor oil: MCT 50:50 % (w/w) | diff | 95% Confidence Interval | |
| **Mean** | **0.2** | **3.8** | -3.600 | -5.312 | -1.888 |
| **Variance** | **0.2** | **1.7** | | | |
| **Observations** | 5 | 5 | | | |
| **Hypothesized Mean Difference** | 0 | | | | |
| **df** | 4 | | | | |
| **t Stat** | -5.840 | | | | |
| **P(T<=t) one-tail - Difference < Hypothesized Difference** | 0.002 | 0.998 | Difference > Hypothesized Difference | | |
| **T Critical one-tail** | 2.132 | | | | |
| **P(T<=t) two-tail** | 0.004 | | Reject Null Hypothesis because p < 0.05 (Means are Different) | | |
| **T Critical Two-tail** | 2.776 | | | | |

**Table 2.8| Statistical analysis t-test placebo-GnRH [6-D-Phe] 1875 µg/ml Castor oil: MCT 50:50 % (w/w)**

| t-Test: Two-Sample Assuming Unequal Variances | a=0.05 | | | | |
|---|---|---|---|---|---|
| **Equal Sample Sizes** | | | | | |
| | ***Placebo*** | ***Treatment 3*** **GnRH [6-D-Phe] 375 µg/ml** Castor oil: MCT 90:10 % (w/w) | diff | 95 % Confidence Interval | |
| **Mean** | **0.2** | **1.2** | -1.000 | -2.712 | 0.712 |
| **Variance** | **0.2** | **1.7** | | | |
| **Observations** | 5 | 5 | | | |
| **Hypothesized Mean Difference** | 0 | | | | |
| **df** | 4 | | | | |
| **t Stat** | -1.622 | | | | |
| **P(T<=t) one-tail - Difference < Hypothesized Difference** | 0.090 | 0.910 | Difference > Hypothesized Difference | | |
| **T Critical one-tail** | 2.132 | | | | |
| **P(T<=t) two-tail** | 0.180 | | Cannot Reject Null Hypothesis because p > 0.05 (Means are the same) | | |
| **T Critical Two-tail** | 2.776 | | | | |

**Table 2.9| Statistical analysis t-test placebo-GnRH [6-D-Phe] 375 µg/ml Castor oil: MCT 90:10 % (w/w)**

| t-Test: Two-Sample Assuming Unequal Variances | a=0.05 | | | | |
|---|---|---|---|---|---|
| **Equal Sample Sizes** | | | | | |
| | ***Placebo*** | ***Treatment 4*** **GnRH [6-D-Phe] 1875 µg/ml** Castor oil: MCT 90:10 % (w/w) | diff | 95 % Confidence Interval | |
| **Mean** | **0.2** | **6** | -5.800 | -17.819 | 6.219 |
| **Variance** | **0.2** | **93.5** | | | |
| **Observations** | 5 | 5 | | | |
| **Hypothesized Mean Difference** | 0 | | | | |
| **df** | 4 | | | | |
| **t Stat** | -1.340 | | | | |
| **P(T<=t) one-tail - Difference < Hypothesized Difference** | 0.126 | 0.874 | Difference > Hypothesized Difference | | |
| **T Critical one-tail** | 2.132 | | | | |
| **P(T<=t) two-tail** | 0.251 | | Cannot Reject Null Hypothesis because p > 0.05 (Means are the same) | | |
| **T Critical Two-tail** | 2.776 | | | | |

**Table 2.10| Statistical analysis t-test placebo-GnRH [6-D-Phe] 1875 µg/ml Castor oil: MCT 90:10 % (w/w)**

## 2.7 FIGURES AND TABLES

# CHAPTER THREE

# SUSPENSION STABILITY

# 3 GnRH [6-D-Phe] acetate Oil Depot Suspension Stability

Yordanka Yordanova[1], Wolfgang Zaremba[2], Sascha Schott[2],Wolfgang Friess[1]

1. Department of Pharmacy, Pharmaceutical Technology & Biopharmaceutics, Ludwig-Maximilians-Universitaet, Butenandtstrasse 5, 81377 Muenchen, Germany
2. Veyx Pharma GmbH, Scientific Department, Soehreweg 6, 34639 Schwarzenborn, Germany

**An oily depot suspension of a GnRH superagonist appears to be a promising alternative to the available on the market aqueous Gonavet Veyx® formulation for estrous control in swine. The stability of GnRH [6-D-Phe] suspended in castor oil: MCT 50:50 % (w/w) as a multi-dose vial was evaluated over 12 months at 2-8° C, 25° C and 40° C. The formulation was analysed in terms of GnRH [6-D-Phe] stability, content uniformity, particle size distribution, viscosity, injectability and oil vehicle oxidation. The study demonstrated that the stability and content uniformity were assured at all tested temperatures over the period of 12 months.**

## 3.1 INTRODUCTION

Formulating peptides and proteins in non-aqueous mediums such as oils can minimize the hydrolytic degradation pathways. For instance, hydrolytic degradation of leuprolide (LHRH) in dimethylsulfoxide (DMSO) was only 93 % compared to 75 % in aqueous solution after 2 years storage at 37° C[1,2]. One other example showed that the use of oil vehicle or DMSO could prevent the commonly observed aggregation and gelation of aqueous solutions of bovine growth hormone releasing factor[3].

In the case of GnRH [6-D-Phe] acetate, degradation is most pronounced under strong acidic (pH<3) and alkaline (pH>9) conditions, at which C-terminal deamidation and D-Ser[4] epimerization of the peptide occur[4,5,6,7]. For this reason, the aqueous injection solution of GnRH [6-D-Phe], Gonavet Veyx®, is formulated in acetate buffer pH 5[8,9].

The purpose of this study was to evaluate the stability of one exemplary oily suspension from the first preclinical study and compare it to the marketed aqueous Gonavet Veyx® formulation. The suspension vehicle is composed of castor oil with a high content of ricinoleic acid, representing a polar protic solvent and MCT, a polar aprotic medium. This matrix should be less prone to oxidative instability compared to other oily vehicles containing higher amounts of oleic, linoeic and linolenic acid esters[10]. The chemical stability of the peptide was analysed by RP-HPLC. Light microscopy, particle size distribution, rheology and oil vehicle oxidation were additionally evaluated.

## 3.2 RESULTS AND DISCUSSION

### *3.2.1 Content Uniformity*

The extraction recovery of GnRH [6-D-Phe] was calculated to be 95 % +/- 10 % (95 % CI). At 40° C storage temperature, some method-derived variability in the GnRH [6-D-Phe] content was visible (Figure 3.1).

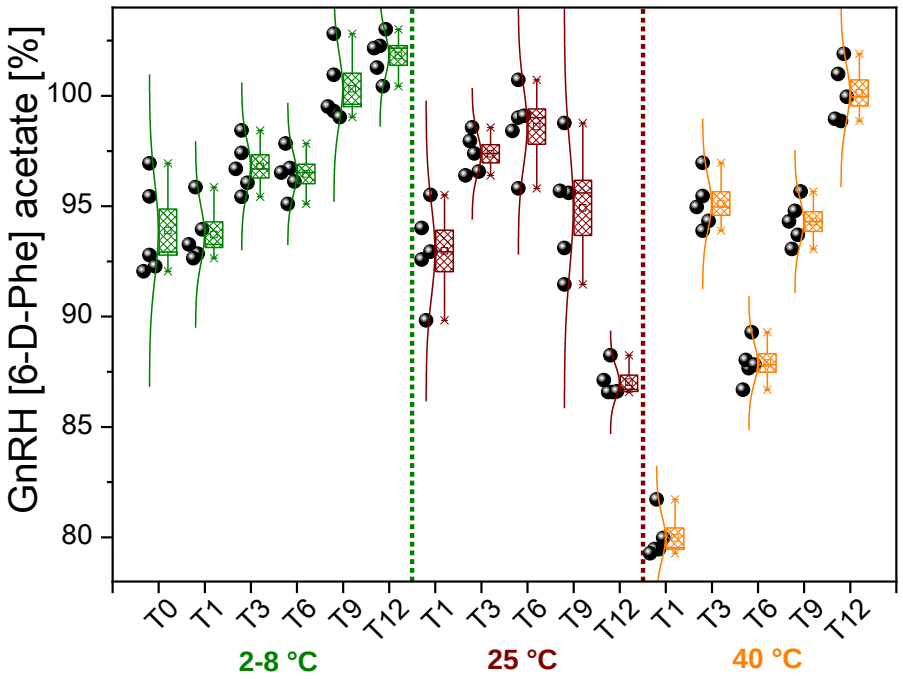


**Figure 3.1| Content uniformity of the castor oil: MCT 50:50 % (w/w) 1875 µg/ml GnRH [6-D-Phe] formulation**

Chromatograms analysis of GnRH [6-D-Phe] samples generated by treatment with alkali, acid, hydrogen peroxide and light revealed degradation products at relative retention time (RRT) 0.914, 0.509 and 0.789 (Table 3.1). These products did not appear in the recorded HPLC chromatograms of the suspension.

| GnRH [6-D-Phe] degradation | | GnRH [6-D-Phe] | |
|---|---|---|---|
| **Sample** | RT [min] | Nearest Peak RT [min] | Nearest Peak RRT [min] |
| **Blanc $H_20$ injected normal conditions** | - | - | - |
| **Chem. Stress 1N HCL 1.5% $H_20_2$ 12h** | 6.925 | 6.331 | 0.914 |
| **Chem. Stress 1N NaOH 1.5% $H_20_2$ 12h** | 8.068 | 4.111 | 0.509 |
| **Light Stress** | 8.235 | 6.503 | 0.789 |

**Table 3.1| HPLC analysis of GnRH [6-D-Phe] degradation**

### *3.2.2 Particle Size Distribution and Characterization*

Particle size serves as an indicator for the physical stability of the suspension over time. The increase of particle size might accelerate settling and lead to the caking of the sediment. Larger particles may clog the needle and affect the injection forces. For castor oil: MCT 50:50 % (w/w) 1875 µg/ml GnRH [6-D-Phe], the median and mean particle size of the dispersed samples remained under 50 µm at all storage temperatures. The particle size distribution of all measured samples was non-symmetric (Figure 3.2, Table 3.2). The microscopy images showed the formation of single large particles after 6 months of storage at 40° C (Figure 3.3). This might be due to some large but loosely connected particle agglomerates. Similarly at 9 and 12 months of storage the mean particle size was slightly increased. However, no negative impact on the injection force was observed (Figure 3.5).

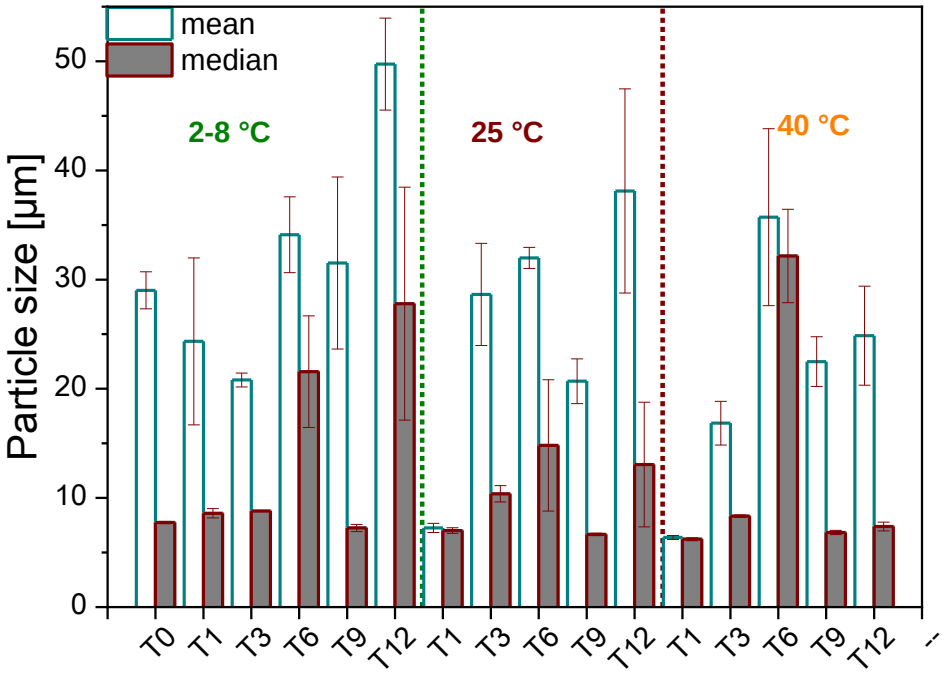


**Figure 3.2 |Mean (the mean particle diameter over volume) and median particle size of castor oil: MCT 50:50 % (w/w) 1875 µg/ml GnRH [6-D-Phe] oil depot suspension at 2-8° C, 25° C and 40° C over 12 months**

| | Temperature: 2-8° C | | Temperature: 25° C | | Temperature: 40° C | |
|---|---|---|---|---|---|---|
| Time [months] | $D_{v50}$ [µm] ± SD | $D_{v90}$ [µm] ± SD | $D_{v50}$ [µm] ± SD | $D_{v90}$ [µm] ± SD | $D_{v50}$ [µm] ± SD | $D_{v90}$ [µm] ± SD |
| **0** | 7.7 ± 0.1 | 108.1 ± 5.5 | 7.7 ± 0.1 | 108.1 ± 5.5 | 7.7 ± 0.1 | 108.1 ± 5.5 |
| **1** | 8.6 ± 0.2 | 93.6 ± 1.9 | 7.0 ± 0.1 | 13.2 ± 0.8 | 6.2 ± 0.1 | 11.9 ± 0.4 |
| **3** | 8.8 ± 0.2 | 56.2 ± 2.3 | 10.4 ± 0.4 | 108.7 ± 6.7 | 8.3 ± 0.1 | 16.0 ± 6.5 |
| **6** | 21.6 ± 2.9 | 74.3 ± 1.5 | 14.8 ± 3.5 | 75.1 ± 2.4 | 32.2 ± 2.5 | 55.3 ± 1.8 |
| **9** | 7.2 ± 0.2 | 102.8 ± 0.6 | 6.6 ± 0.1 | 17.8 ± 2.7 | 6.8 ± 0.1 | 10.4 ± 0.5 |
| **12** | 27.8 ± 6.2 | 119.4 ± 4.5 | 13.1 ± 3.3 | 91.3± 6.0 | 7.4 ± 0.2 | 98.7 ± 7.1 |

**Table 3.2| Particle size distribution and $D_{v50}$ and $D_{v90}$ fractions**

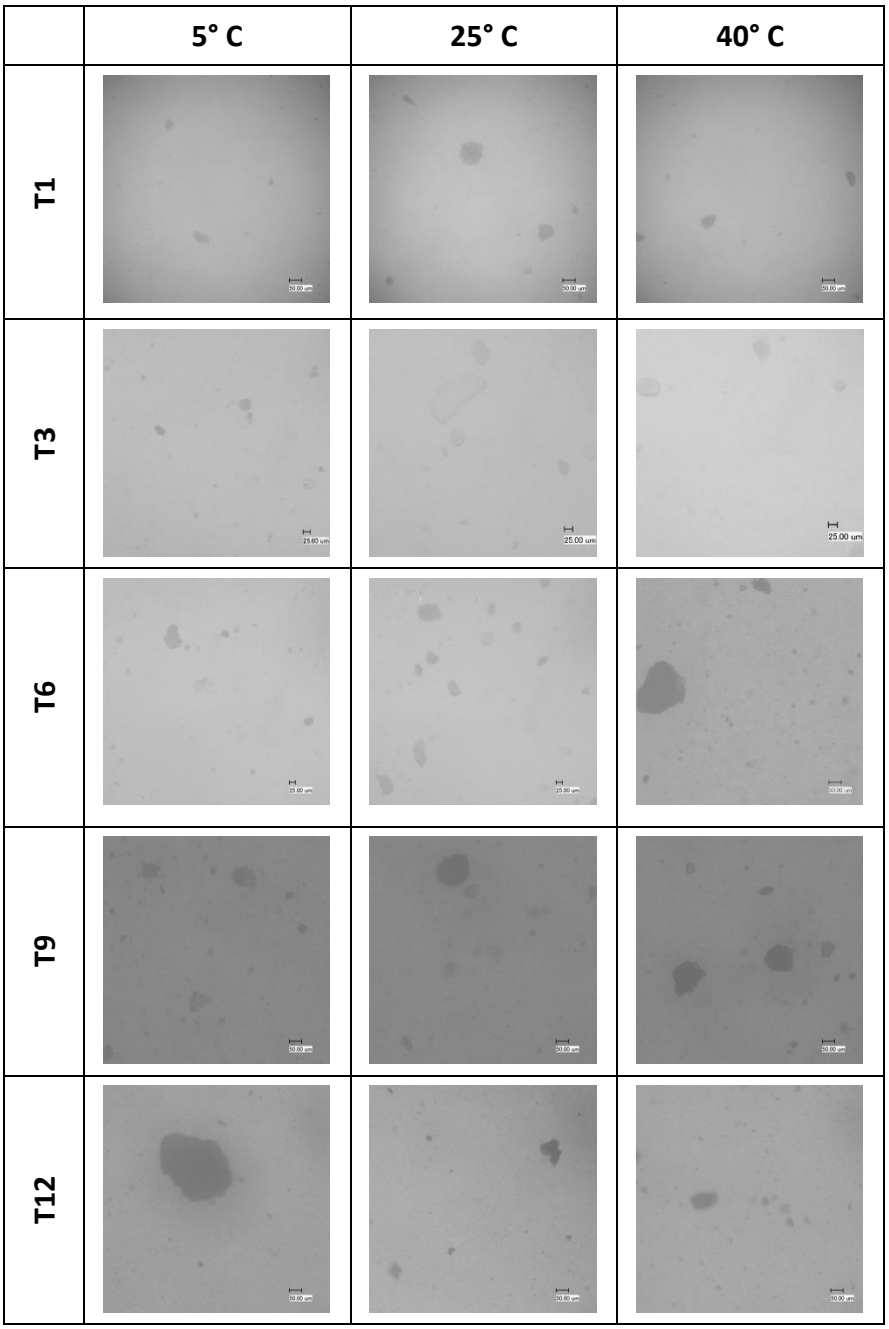


**Figure 3.3| Light microscopy of castor oil: MCT 50:50 % (w/w) 1875 µg/ml GnRH [6-D-Phe] oil depot suspension at 2-8° C, 25° C and 40° C over 12 months**

### *3.2.3 Rheology*

Additionally, neither the Newtonian flow behaviour nor the viscosity at 25° C as well as at 39° C changed over 12 months at the storage temperatures (Figure 3.4). The viscosity was approx. 120 mPas at 25° C and 60 mPas at 39° C.

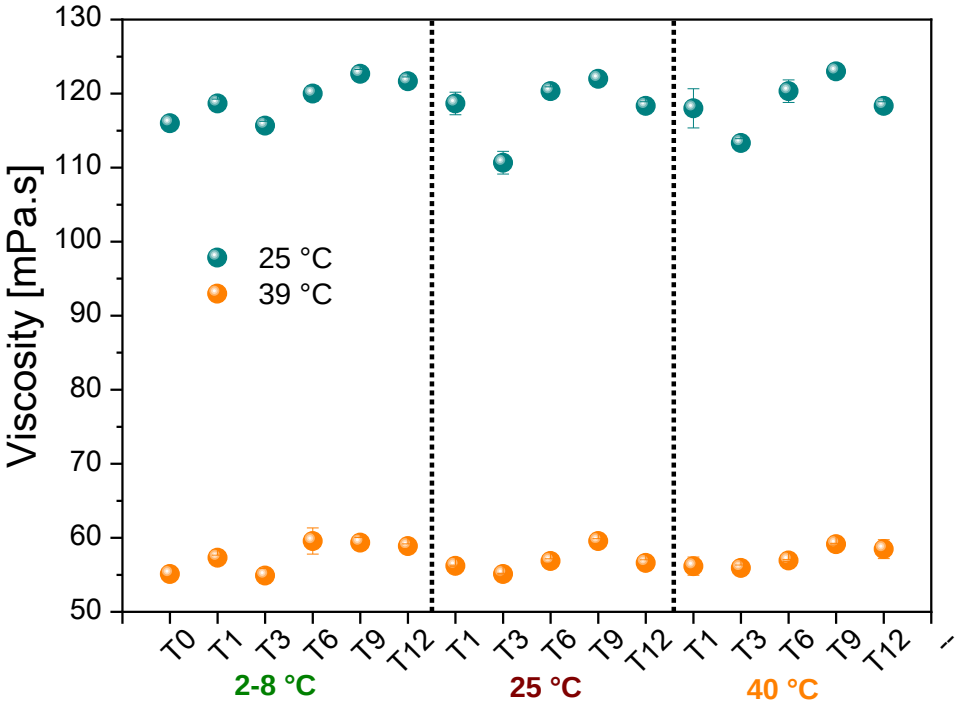


**Figure 3.4| Viscosity of castor oil: MCT 50:50 % (w/w) 1875 µg/ml GnRH [6-D-Phe] oil depot suspension at 2-8° C, 25° C and 40° C over 12 months at 25° C and 39° C**

Furthermore, oscillatory rheometry did not indicate any change upon storage. The loss modulus G" was greater than the storage modulus G', confirming the viscous character of the depot suspension (Table 3.3, Table 3.4)[11,12].

**25° C**

| Time [months] | 2-8° C G' [mPa] | 2-8° C G" [mPa] | 2-8° C tan δ | 25° C G' [mPa] | 25° C G" [mPa] | 25° C tan δ | 40° C G' [mPa] | 40° C G" [mPa] | 40° C tan δ |
|---|---|---|---|---|---|---|---|---|---|
| 0 (Start) | 5.4 | 303.7 | 56.2 | .4 | 303.7 | 56.2 | 5.4 | 303.7 | 56.2 |
| 1 | 16.6 | 488.6 | 29.4 | 12.6 | 530.1 | 42.1 | 13.7 | 540.7 | 39.5 |
| 3 | 13.9 | 492.3 | 35.4 | 10.3 | 4821 | 46.8 | 8.7 | 439.6 | 50.5 |
| 6 | 10. | 498.5 | 46.1 | 11.8 | 443. | 37.6 | 11.3 | 502.7 | 44.5 |
| 9 | 11.4 | 493.4 | 43.2 | 12.1 | 456.4 | 37.7 | 12.1 | 498.5 | 41.2 |
| 12 | 11.3 | 496.7 | 43.9 | 11.9 | 476.6 | 40.0 | 13.1 | 501.4 | 38.3 |

**39° C**

| Time [months] | 2-8° C G' [mPa] | 2-8° C G" [mPa] | 2-8° C tan δ | 25° C G' [mPa] | 25° C G" [mPa] | 25° C tan δ | 40° C G' [mPa] | 40° C G" [mPa] | 40° C tan δ |
|---|---|---|---|---|---|---|---|---|---|
| 0 (Start) | 4.5 | 163.3 | 36.3 | 4.5 | 163.3 | 36.3 | 4.5 | 163.3 | 36.3 |
| 1 | 12.3 | 246.0 | 20.0 | 13.8 | 275.0 | 19.9 | 10.2 | 264.0 | 25.8 |
| 3 | 8.9 | 244.1 | 27.4 | 8.2 | 248.7 | 30.3 | 5.4 | 224.0 | 41.5 |
| 6 | 10.7 | 257.3 | 24.0 | 8.6 | 230.3 | 26.7 | 11.2 | 166. | 14.8 |
| 9 | 10.4 | 244.2 | 23.5 | 8.3 | 248.9 | 29.9 | 12.3 | 224.0 | 18.2 |
| 12 | 10.2 | 257.5 | 25.2 | 8.7 | 230.7 | 26.5 | 12.6 | 246.0 | 19.5 |

**Table 3.3| Rheometer-Amplitude Sweep of castor oil: MCT 50:50 % (w/w) 1875 µg/ml GnRH [6-D-Phe] oil depot suspension at 2-8° C, 25° C and 40° C over 12 months at 25° C and 39° C**
G': storage modulus; G": loss modulus; tan δ= G"/ G', determined in the viscoelastic region (τ= 0.1-10 Pa)

**25° C**

| Time [months] | 2-8° C G' [mPa] | 2-8° C G" [mPa] | 2-8° C ŋ*[mPas] | 25° C G' [mPa] | 25° C G" [mPa] | 25° C ŋ*[mPas] | 40° C G' [mPa] | 40° C G" [mPa] | 40° C ŋ*[mPas] |
|---|---|---|---|---|---|---|---|---|---|
| 0 (Start) | 3.7E-6 | 4.0 | 112 | 3.7E-6 | 4.0 | 112 | 3.7E-6 | 4.0 | 112 |
| 1 | 2.5 | 3. | 113 | 5.5 | 3.2 | 150 | 3.3E-6 | 3.5 | 98.3 |
| 3 | 0.4 | 2.7 | 160 | 2.9E-6 | 3.2 | 106 | 2.8 | 2.8 | 106 |
| 6 | 4.2 | 3.1 | 114 | 3.9 | 2.9 | 137 | 1.32 | 3.3 | 97.8 |
| 9 | 2.6 | 3.3 | 115 | 5.8 | 3.4 | 112 | 3.1E-6 | 3.4 | 105 |
| 12 | 2.1E-6 | 2.2 | 113 | 1.5 | 2.6 | 115 | 0.9 | 2.5 | 98.9 |

**39° C**

| Time [months] | 2-8° C G' [mPa] | 2-8° C G" [mPa] | 2-8° C ŋ*[mPas] | 25° C G' [mPa] | 25° C G" [mPa] | 25° C ŋ*[mPas] | 40° C G' [mPa] | 40° C G" [mPa] | 40° C ŋ*[mPas] |
|---|---|---|---|---|---|---|---|---|---|
| 0 (Start) | 3.3E-6 | 3.5 | 76.6 | 3.3E-6 | 3.5 | 76.6 | 3.3E-6 | 3.5 | 76.6 |
| 1 | 3.1 | 1.4 | 74.7 | 3.1 | 1.4 | 74.7 | 3.2E-6 | 3.4 | 75.3 |
| 3 | 2.6E-6 | 2.8 | 77.7 | 2.6E-6 | 2.8 | 77.7 | 3.4E-6 | 3.6 | 79.6 |
| 6 | 2.8 | 3.6 | 78.7 | 1.9E-6 | 2.0 | 55.9 | 3.3 | 1.0 | 76.3 |
| 9 | 2.2E-6 | 2.4 | 75.6 | 2.2E-6 | 2.4 | 56.7 | 3.4E-6 | 3.6 | 56.8 |
| 12 | 2.4E-6 | 3.5 | 76.7 | 3.1 | 3.5 | 58.7 | 3.3 | 3.5 | 57.9 |

**Table 3.4| Rheometer-Frequency Sweep of castor oil: MCT 50:50 % (w/w) 1875 µg/ml GnRH [6-D-Phe] oil depot suspension at 2-8° C, 25° C and 40° C over 12 months at 25° C and 39° C**
G': storage modulus; G": loss modulus; ŋ*: complex viscosity determined in the viscoelastic region (f=0.1-10 Hz)

### *3.2.4 Injection Force Determination*

High viscosity and larger particles can lead to unstable injection forces and longer injection times, impacting negatively the syringeability and injectability. The Dynamic Glide Force (DGF) and the maximal glide force (F max) for castor oil: MCT 50:50 % (w/w) 1875 µg/ml GnRH [6-D-Phe] oil depot suspension remained ≤ 3 N and ≤ 5 N through 16 G and 18 G needles respectively, indicating an unproblematic manual application (Figure 3.5). 30 N is the value considered to be the maximum force for a manual injection[13].

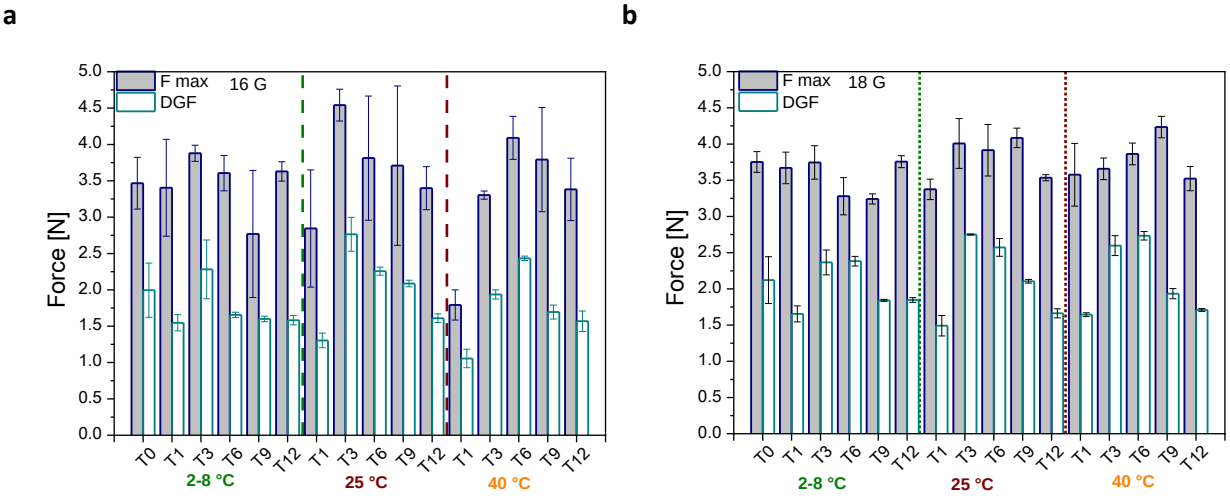


**Figure 3.5| Maximal force (F max) and dynamic glide force (DGF) of castor oil: MCT 50:50 % (w/w) 1875 µg/ml GnRH [6-D-Phe] oil depot suspension at 2-8° C, 25° C and 40° C over 12 months**
(a) 16 G (b) 18 G needle

### *3.2.5 Oil Vehicle Oxidation*

The peroxide value (PV) is an indicator of the oxidative level and the tendency of oils and fats to become rancid[14,15]. A PV between 1 – 5 meq/ kg is classified as low oxidation state, between 5 – 10 meq/ kg as moderate oxidation and above 10 meq/ kg as high oxidation state. The para-anisidine value (p-AV) expresses the degree of secondary degradation products of fats and oils after thermal stress and is a more reliable indicator of oxidation in the long term and should lie below 10 $g^{-1}$[16,17]. The total oxidation value (TOTOX) is the sum of PV and AV and an overall indicator of the oxidative degradation of lipids and oils[18]. Both PV and AV remained under 1 mEq/ kg and 1 $g^{-1}$ respectively, indicating the low oxidation state of the oil depot formulation. The TOTOX increased during the first months of the stability study at all storage temperatures. The lowest values were observed at 2-8° C storage temperature (Figure 3.6).

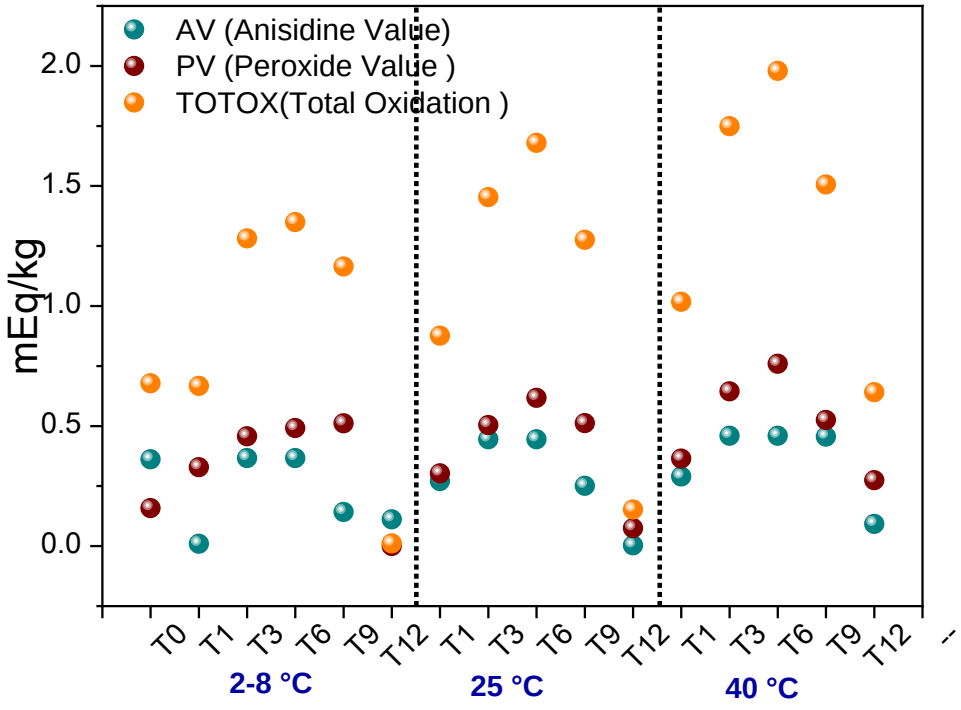


**Figure 3.6| PV, AV and TOTOX value of the castor oil: MCT 50:50 % (w/w) 1875 µg/ml GnRH [6-D-Phe] oil depot suspension at 2-8° C, 25° C and 40° C over 12 months**

## 3.3 CONCLUSION

No considerable decrease in the content of GnRH [6-D-Phe] in the castor oil/ MCT 50:50 % (w/w) matrix over 12 months at 2-8° C, 25° C and 40° C could be detected. The slight increase in GnRH [6-D-Phe] particle size after 6 months of storage might be due to some large but loosely connected particle agglomerates, which were also observed by microscopy. However, these particles did not have any negative impact on the physical stability of the suspension with regards to viscosity and injectability. The total oil vehicle oxidation was higher at 40° C storage temperature in comparison to 2-8° C and 25° C. Overall, the oxidation

was marginal and below the TOTOX limit[19]. Hydrogen peroxide induced degradation products of GnRH [6-D-Phe] with RRT (retention time) 0.914, 0.509 and 0.789 were not visible in the recorded HPLC chromatograms of the suspension. Thus the chemical and physical stability of castor oil: MCT 50:50 % (w/w) 1875 µg/ml GnRH [6-D-Phe] oil depot suspension at 2-8° C, 25° C and 40° C storage temperatures over 12 months can be assured.

## 3.4 MATERIALS AND METHODS

**Gonadorelin [6-D-Phe] acetate peptide** (pE1–H2–W3–S4–Y5–(D)F6–L7–R8–P9–G10–NH2) or (pGlu-His-Trp-Ser-Tyr-D-Phe-Leu-Arg-Pro-Gly-NH2) was provided by BFC Biopept-Feinchemie as lyophilized powder and acetate salt (purity 99.76 %, water content 6.73 % and acetate peptide ratio (MW/MW) 1.8); **Oil vehicle**: miglyol®812 (MCT) (Caesar & Loretz, D-Hilden), castor oil (Gustav Heess, D-Leonberg).

**Stability samples preparation & setup** Stability sample preparation was performed under a laminar flow cabinet in a two-step process. The GnRH [6-D-Phe] was cryo-ground with a precooling phase (10 min/ 5Hz) and a grinding phase (8 min/25 Hz) in 25 mL grinding jar with 15 mm grinding balls. Particle size of $D_{v50}$ 10.7 ± 0.2 µm was obtained. The mixture of castor oil and MCT in 50:50 % (w/w) was heated up at 60° C under N2 atmosphere and filtered at room temperature through a 1.2 µm Minisart® Single use filter unit. The cryo-ground GnRH [6-D-Phe] was suspended in the oil matrix using an Ultra-Turrax T-10 basic (IKA Labortechnik, Germany) for 5 minutes at 2000 rpm. The castor oil: MCT 50:50 % (w/w) 1875 µg/ml GnRH [6-D-Phe] oil depot suspension was aliquoted in 20 R glass vials, stoppered and crimped. In total, 20 vials were prepared and stored upright at 2-8° C, 25° C and 40° C over 12 months without applying agitation. Each vial contained 22 mL with a volume overfill of appr. 10 % (Supplementary Data Table 3.5). At 1, 3, 6, 9 and 12 months GnRH [6-D-Phe] content uniformity, suspension particle size distribution, morphology, injectability, rheology and oil vehicle oxidation were evaluated.

**GnRH [6-D-Phe] extraction from the oil matrix** GnRH [6-D-Phe] was extracted from castor oil: MCT 50:50 % (w/w) 1875 µg/ml GnRH [6-D-Phe] oil depot suspension using dichloromethane (DCM) and toluene, where GnRH [6-D-Phe] is not soluble, in combination with PBS (pH 7.4). **DCM Extraction**: 2 mL weighted oil suspension with added 4 mL DCM and 6 mL PBS (pH 7.4) was shaken at room temperature (25° C) and put into an incubated shaker 3031 (GFL, Germany) at 39° C and 60 rpm for 24 h. **Toluene extraction**: 2 mL weighted oil suspension with added 4 mL toluene and 6 mL PBS (pH 7.4) was shaken and centrifuged (12.000xg, 10 min) at room temperature (25° C). **PBS (pH 7.4) extraction**: 2 mL weighted oil suspension with added 6 mL PBS (pH 7.4) was shaken and centrifuged (12.000xg, 10 min) at room temperature (25° C). The preparation techniques using either PBS (pH 7.4) or toluene required centrifugation because of the organic solvent high density. **Reference sample**: weighted pure GnRH [6-D-Phe] was dissolved in 6 mL PBS (pH 7.4) and 4 mL DCM was added. The tube was shaken and put into an incubated shaker 3031 (GFL, Germany) at 39° C and 60 rpm for 24 h. The RP-HPLC analysis at 220 nm detection wavelength showed the highest recovery and was the method of choice for the analysis of the stability time points. The value of DCM extracted pure GnRH [6-D-Phe] was used to correct the obtained recovery values. The highest calculated recovery ratio of GnRH [6-D-Phe] was in DCM (Supplementary Data Table 3.6).

**GnRH [6-D-Phe] content uniformity and stability** The frequency of a normal human shaking and oscillating wrist lies at 6-12 Hz derived as a value from the Duhaime Study and represents the usual shoulder motion[20]. At each stability time point the formulation was shaken 2 minutes at 12 Hz with a Mixer Mill MM200 (Retsch Technologies, Germany) and 5 aliquots of 2 mL were withdrawn. The GnRH [6-D-Phe] content was analysed using RP-HPLC.

**Determination of the GnRH [6-D-Phe] content.** The GnRH [6-D-Phe] content was analysed by RP-HPLC using a LUNA C8 (4.6 mm x 250 mm; size = 5 µm; Phenomenex, USA) column, with a C8 pre-column (4 mm x 3 mm; size = 5 µm) at an HPLC Agilent 1100/1200 series (Agilent Technologies, USA) (mobile phase A (water + 1 mL/L Trifluoroacetic acid (TFA) (v/v)) and mobile phase B (800 g Acetonitrile + 200 g water + 1.2 mL TFA), 1.1 mL/min flow, column temperature 40° C, and autosampler temperature 2 – 8° C. The Retention Time (RT) of GnRH [6-D-Phe] was 8.5 ± 1.5 minutes with UV detection at 220 nm. In order to detect degradation products the following separations were performed: 1. A blanc run after injection of water to show that there is no signal found in the region of the RT of GnRH [6-D-Phe].2. A separation of 2.5 mL solution of GnRH [6-D-Phe] (50 µg/mL), 1mL $H_2O_2$ (30% v/v) and 2.5 mL HCL (1N) diluted to 25 mL with water, separation 12 hours after dilution. 3. A separation of 2.5 mL solution of GnRH [6-D-Phe] (50 µg/mL), 1 mL $H_2O_2$ (30% v/v) and 2.5 mL NaOH (1N) diluted to 25 mL with water, separation 10 minutes after dilution. 4. A separation of 2.5 mL

solution of GnRH [6-D-Phe] (50 µg/mL) after treatment with light (1.5mLux/h for 12 h in quartz dish), separation without dilution.

**GnRH [6-D-Phe] particle size distribution and characterization** The particle size distribution of the stability samples at each time point was analysed employing a Laser Diffraction Particle Size Analyzer LA-950 (Retsch Technology, Haan). The samples were prepared in triplicate (n=3). 0.2 mL of the oil suspension was withdrawn from the vial and measured in a solution of 1 % sorbitan monooleate in isooctane (m/v) in a standard measuring cell with 10 mL volume.

**Light microscopy and Scanning Electron Microscopy**. The light microscopy of castor oil: MCT 50:50 % (w/w) 1875 µg/ml GnRH [6-D-Phe] oil depot suspension was taken with VHX – 500 FD (Keyence, Osaka, Japan) at the 2-8° C, 25° C and 40° C storage temperature over 12 months.

**Rheology: Viscosity profile** Viscosity measurement and flow curves evaluation of the stability samples were performed with MCR 100 (Anton Paar Germany, Ostfildern-Scharnhausen) cone plate system CP – 1 (50 mm diameter, a cone angle of 1° and a gap of 0.042 mm). The viscosity η was defined depending on the shear rate $\dot{\gamma}$ and measuring sections a) 0 – 500 $s^{-1}$ (30 points, 6 s per point; 180 s measurement time), b) 500 $s^{-1}$ (1 point, 6 s per point, 6 s measurement time), c) 500 – 0 $s^{-1}$ (30 points, 6 s per point, 180 s measurement time). **Amplitude sweep** Amplitude sweep measurements were performed with cone plate system CP – 1 (50 mm diameter, a cone angle of 1°, and a gap of 0.2 mm). The storage and loss moduli G'/G'' were defined depending on strain γ or shear stress τ and the measuring sections a) $\tau = 0.01 \dots 0.1\ Pa\ ; f = 1\ Hz$ ; discarded (12 points, 5 s per point, 60 s measurement time), b) $\tau = 0.1 \dots 100\ Pa\ ; f = 1\ Hz$; (30 points, 15 s per point, 450 s measurement time), tan δ was determined in the viscoelastic region (τ= 0.1-10 Pa). **Frequency sweep** Frequency sweep measurements of the stability samples were performed with cone plate system CP – 1 (50 mm diameter, a cone angle of 1°, and a gap of 0.2 mm). The storage and loss moduli G'/G'' were defined depending on strain γ or shear stress τ and the measuring sections a) $\tau = 0.1\ Pa\ ; f = 0.01 \dots 0.1\ Hz$ ; discarded (12 points, 5 s per point, 60 s measurement time), b) $\tau = 0.1\ Pa\ ; f = 0.1 \dots 100\ Hz$; (30 points, 15 s per point, 450 s measurement time), ŋ* was determined in the viscoelastic region (f=0.1-10 Hz).

**Injection force determination** The injectability/syringeability were performed with the TA.XT.plus Texture Analyser (Stable Micro Systems, Godlming, UK). The formulations were injected into air using a NORM-JECT 1 mL Tuberkulin + Luer syringe (Henke-Sass-Wolf GmbH, Germany) with either a FINE-JECT 18 Gx2'', 1.2x50 mm needle (Henke-Sass-Wolf GmbH, Germany) or a FINE-JECT 16 Gx1½'', 1.6x40 mm needle (Henke-Sass-Wolf GmbH, Germany). The software Exponent was set to compression test mode with the parameters: 10 mm/sec pre-test speed, and 3.9 mm/sec test speed, and 10.00 mm/sec post-test speed, trigger force: 0.001 N. The applied force from the texture analyser was recorded in [N] against the distance of the syringe plunger (max. 64 mm).

**Oil vehicle oxidation The PV** at each stability time point was determined with the Pierce Quantitative Peroxide Assay Kit for lipid-compatible formulations. The assay consists of two reagents: Reagent A 25 mM ammonium ferrous (II) sulfate and 2.5 M $H_2SO_4$ and Reagent C 4 mM Butylhydroxytoluol (BHT) and 125 µM xylenol orange in methanol. The hydroperoxides convert $Fe^{2+}$ to $Fe^{3+}$. $Fe^{3+}$ reacts with xylenol orange dye and results in a coloured product, photometrically detectable at 595 nm. The working reagent was prepared from 1 volume Reagent A and 100 Volumes Reagent C and was stable for 12 h. The peroxide standards were prepared with 30 % (8.8 M) hydrogen peroxide in methanol (Supplementary Data Table 3.7**). The AV**: 0.5 – 4 g (w) of the oil suspension at each time point were dissolved in 25 mL isooctane and the absorbance of this fat solution ($A_1$) was measured against a blank of isooctane at 350 nm. 5 mL of the solution and 5 mL of the isooctane solution (as blank) were transferred in falcon tubes and 1 mL of the anisidine solution was added to each. After 10 min, the absorbance ($A_2$) was measured with the NanoDrop 2000 Spectrophotometer (Thermo Scientific, USA) at 350 nm. The p-AV was calculated according to the equation:

$$p - AV = 25 * \frac{1.2 * A_2 - A_1}{w}$$

**Equation 3.1| AV calculation**

The TOTOX value is the sum of both PV and AV

$$Totox\ Value = 2 * PV + p - AV$$

**Equation 3.2| TOTOX calculation**

## 3.5 REFERENCES AND ACKNOWLEDGMENTS


1. Hall, S. C., Tan, M. M., Leonard, J. J. & Stevenson, C. L. Characterization and comparison of leuprolide degradation profiles in water and dimethyl sulfoxide. *J Pept Res* **53,** 432–441 (1999).

2. Stevenson, C. L., Leonard, J. J. & Hall, S. C. Effect of peptide concentration and temperature on leuprolide stability in dimethyl sulfoxide. *Int. J. Pharm.* **191,** 115–129 (1999).

3. Yu, L. & Foster, T. Preparation, characterization, and in vivo evaluation of an oil suspension of a bovine growth hormone releasing factor analog. *J. Pharm. Sci.* **85,** 396–401 (1996).

4. Hoitink, M. A. *et al.* Identification of the Degradation Products of Gonadorelin and Three Analogues in Aqueous Solution. *Anal. Chem.* **69,** 4972–4978 (1997).

5. Motto, M. G., Hamburg, P. F., Graden, D. A., Shaw, C. J. & Cotter, M. Lou. Characterization of the degradation products of luteinizing hormone releasing hormone. *J. Pharm. Sci.* **80,** 419–23 (1991).

6. Okada, J., Seo, T., Kasahara, F., Takeda, K. & Kondo, S. New degradation product of des-Gly10-NH2-LH-RH-ethylamide (fertirelin) in aqueous solution. *J. Pharm. Sci.* **80,** 167–170 (1991).

7. Manning, M. C., Patel, K. & Borchardt, R. T. Stability of Protein Pharmaceuticals. *Pharm. Res. An Off. J. Am. Assoc. Pharm. Sci.* **6,** 903–918 (1989).

8. Powell, M. F., Sanders, L. M., Rogerson, A. & Si, V. Parenteral Peptide Formulations: Chemical and Physical Properties of Native Luteinizing Hormone-Releasing Hormone (LHRH) and Hydrophobic Analogues in Aqueous Solution. *Pharm. Res. An Off. J. Am. Assoc. Pharm. Sci.* **8,** 1258–1263 (1991).

9. Helm, V. J. & Müller, B. W. Stability of Gonadorelin and Triptorelin in Aqueous Solution. *Pharm. Res. An Off. J. Am. Assoc. Pharm. Sci.* **7,** 1253–1256 (1990).

10. Li, S., Patapoff, T. W., Nguyen, T. H. & Borchardt, R. T. Inhibitory effect of sugars and polyols on the metal-catalyzed oxidation of human relaxin. *J. Pharm. Sci.* **85,** 868–872 (1996).

11. Reboa, P. F. & Fryan, M. C. Rheological prediction of the physical stability of concentrated dispersions containing particulates. *J. Am. Oil Chem. Soc.* **69,** 71–79 (1992).

12. Method, R., Sedimentation, P. P. & Dispersions, L. Dispersion Rheology. 1–4

13. Burckbuchler, V. *et al.* Rheological and syringeability properties of highly concentrated human polyclonal immunoglobulin solutions. *Eur. J. Pharm. Biopharm.* **76,** 351–356 (2010).

14. Besbes, S. Quality Characteristics and Oxidative Stability of Date Seed Oil During Storage. *Food Sci. Technol. Int.* **10,** 333–338 (2004).

15. O'Brien, R. D. *Fats and oils: formulating and processing for applications*. *New York* (CRC Press, 2004).

16. Ojeh, O. A. Effect of refining on the physical and chemical properties of cashewkernel oil. *Int. J. Food Sci. Technol.* **16,** 513–517 (1981).

17. Muik, B., Lendl, B., Molina-Diaz, A. & Ayora-Canada, M. J. Direct monitoring of lipid oxidation in edible oils by Fourier transform Raman spectroscopy. *Chem. Phys. Lipids* **134,** 173–182 (2005).

18. Shahidi, F. & Wanasundara, U. N. Methods for Measuring Oxidative Rancidity in Fats and

Oils. in *Food Lipids: Chemistry, Nutrition, and Biotechnology* 387–407 (2002).

19. Irwin, J. W. & Hedges, N. 13 - Measuring lipid oxidation. in *Woodhead Publishing Series in Food Science, Technology and Nutrition* 289–316 (2004).

20. Xu, X. S. *et al.* Vibrations transmitted from human hands to upper arm, shoulder, back, neck, and head. *Int. J. Ind. Ergon.* (2016).

This work was supported by Veyx Pharma D-Schwarzenborn and DBU (Deutsche Bundesstiftung Umwelt) D-Osnabrueck. The authors wish to acknowledge Biopept Feinchemie D-Weinberg for their analytical support with the stability study.

## 3.6 SUPPLEMENTARY DATA

| Vial | Sample | Temperature [° C] | Filled Volume [mL] | % Overfill |
|---|---|---|---|---|
| 1 | Gona_t0 | 5, 25, 40 | 21.9 | 9.1 |
| 2 | Gona_t1_5° C | 5 | 22.1 | 9.4 |
| 3 | Gona_t1_25° C | 25 | 21.9 | 9.0 |
| 4 | Gona_t1_40° C | 40 | 22.2 | 9.7 |
| 5 | Gona_t3_5° C | 5 | 21.9 | 9.0 |
| 6 | Gona_t3_25° C | 25 | 21.9 | 9.0 |
| 7 | Gona_t3_40° C | 40 | 22.0 | 9.1 |
| 8 | Gona_t6_5° C | 5 | 22.1 | 9.3 |
| 9 | Gona_t6_25° C | 25 | 22.0 | 9.1 |
| 10 | Gona_t6_40° C | 40 | 22.0 | 9.2 |
| 11 | Gona_t9_5° C | 5 | 22.2 | 9.8 |
| 12 | Gona_t9_25° C | 25 | 22.1 | 9.3 |
| 13 | Gona_t9_40° C | 40 | 21.9 | 9.1 |
| 14 | Gona_t12_5° C | 5 | 22.0 | 9.1 |
| 15 | Gona_t12_25° C | 25 | 22.1 | 9.4 |
| 16 | Gona_t12_40° C | 40 | 22.1 | 9.3 |
| 17 | Gona_res | 5 | 20.9 | 4.7 |
| 18 | Gona_res | 25 | 20.9 | 4.5 |
| 19 | Gona_res | 40 | 20.9 | 4.5 |

**Table 3.5| Stability samples preparation**

| Extraction method | Extraction efficiency [%] ± SD | | | | | | |
|---|---|---|---|---|---|---|---|
| DCM | 81.9 | 81.9 | 78.2 | 78.2 | 84.8 | 81.2 | 81.1 ± 2.5 |
| Toluene | 77.4 | 77.4 | 82.4 | 82.3 | 75.2 | 75.1 | 78.3 ± 3.3 |
| PBS | 73.1 | 73.1 | 74.2 | 74.4 | 72.8 | 72.9 | 73.4 ± 0.7 |
| GnRH [6-D-Phe]_DCM | 89.9 | 89.8 | 93.2 | 93.1 | 92.9 | 92.9 | 91.9 ± 1.7 |

**Table 3.6| GnRH [6-D-Phe] extraction method efficiency from the castor oil/ MCT 50:50 % (w/w) matrix**

| Standard | µl $H_2O_2$ | $H_2O_2$ | MeOH |
|---|---|---|---|
| 1 | 1000 | 11 µl 8.8 M | 100 ml |
| 2 | 500 | 100 µl std.1 | 100 µl |
| 3 | 250 | 100 µl std.2 | 100 µl |
| 4 | 125 | 100 µl std.3 | 100 µl |
| 5 | 62.5 | 100 µl std.4 | 100 µl |
| 6 | 31.25 | 100 µl std.5 | 100 µl |
| 7 | 15.63 | 100 µl std.6 | 100 µl |
| 8 | 7.81 | 100 µl std.7 | 100 µl |
| 9 | 3.91 | 100 µl std.8 | 100 µl |
| 10 | 1.95 | 100 µl std.9 | 100 µl |
| **Sample** | | **Gona_$t_x$** | **MeOH** |
| Gona_tx_1 | | 90 µl | 10 µl |
| Gona_tx_2 | | 90 µl | 10 µl |
| Gona_tx_3 | | 90 µl | 10 µl |
| Gona_tx_blank | | 90 µl | 10 µl |

**Table 3.7| Pierce Quantitative Peroxide Assay, $t_x$, where x stands for 0, 1, 3, 6, 9 and 12 months**

## 3.7 FIGURES AND TABLES

# CHAPTER FOUR

# RELEASE ADDITIVES

# 4 GnRH [6-D-Phe] acetate Oil Depot Suspension: The Effect of Additives on the Release Characteristics

Yordanka Yordanova[1], Ivonne Seifert[1], Johannes Kauffold[2], Wolfgang Zaremba[3],Wolfgang Friess[1]

1. Department of Pharmacy, Pharmaceutical Technology & Biopharmaceutics, Ludwig-Maximilians-Universitaet, Butenandtstrasse 5, 81377 Muenchen, Germany
2. University of Leipzig, Faculty of Veterinary Medicine, An den Tierkliniken 29, 04103 Leipzig, Germany
3. Veyx Pharma GmbH, Scientific Department, Soehreweg 6, 34639 Schwarzenborn, Germany

**The release of GnRH [6-D-Phe] from low viscosity pure oil mixtures of castor oil and medium chain triglycerides (MCT) is superior to the high viscosity ones because of their more consistent *in vivo* effect. The formulation remains stable over 12 months at 5° C, 25° C and 40° C with respect to particle size, injection forces, viscosity and oxidation. The incorporation of gelling and stabilizing agents in the Newtonian formulation obtained a shear thinning behaviour. The *in vitro* release of GnRH [6-D-Phe] from the oil depot with additives, intended for swine reproduction cycle manipulation, was slower and consistent over 8 days. The *in vivo* effect of the formulation was tested in a second preclinical study and proved to resemble the observed *in vitro* effect.**

## 4.1 INTRODUCTION

Excipients in parenteral oil depot suspensions, e.g. gelling agents, resuspendibility enhancers, wetting agents and antioxidants, are used in order to enhance and maintain formulation stability, assure applicability and/or prolong the drug release. Gelling agents from the group of metallic stearates specifically aluminiummono or -distearate are known to improve the suspending properties and to reduce the spreading in the tissue after injection. The second can be related to the shear-thinning behaviour and increased formulation viscosity at rest[1]. The reduced spreading is further expected to delay the drug release. In 1950 an oil depot suspension of the antibiotic, penicillin G procaine in sesame oil and peanut oil gelled with 2 % aluminium monostearate produced prolonged therapeutic blood levels of penicillin G after i.m. injection[2]. Similar gelled oil matrices were applied successfully in the delivery of 50 % normorphinone and 40 % oxazepine either as free base or pamoate salt[3,4]. Subsequently, oil gelled formulations for the sustained release of proteins and peptides were tested, e.g. a 2 % suspension of relaxin gelled with aluminium monostearate[5] and a superagonist analogue of the luteinizing hormone-releasing hormone (LHRH) in peanut or sesame oil, gelled with aluminium stearate[6,7].

A 5 % aluminium monostearate gelled oil matrix forms the basis of Posilac®, a single-dose syringe of rbST-$Zn^{2+}$ (recombinant bovine somatotropin) oil depot suspension[8,9]. An alternative to using a gelling agent is to increase the drug concentration. Ivomec® Gold is 3.15 fold higher concentrated compared to a standard Ivomec® suspension. It exhibits unique thixotropic characteristics due to stronger particle-particle interactions, indirectly allowing the slow release of Ivermectin from the depot upon injection[10]. A structured vehicle approach,

using either a gelling agent or an increased compound concentration can keep the dispersed particles of the suspension in a deflocculated state, reducing the sedimentation rate. Wetting, dispersing and stabilizing agents are added to improve the resuspendibility and dose uniformity of the oil suspension and induce the formation of a stable flocculated system[11,12]. The main advantage of a stable flocculated system is the formation of loose particles aggregates in a network-like structure, which break up easily under the application of force or shear stress, allowing for an unproblematic multi-dose application. However, it should be noted that the stability of a suspension is influenced by the concentration of added flocculating agents. At higher concentration they make the resuspension of agglomerated particles difficult[13]. In the following study we tested suitable gelling agents and flocculating additives for the development of a stable oil GnRH [6-D-Phe] depot suspension with improved injectability and flow characteristic. We evaluated the effect of the additives on the *in vitro* release of GnRH [6-D-Phe]. The *in vivo* effect of the formulations was analysed in a preclinical study.

## 4.2 RESULTS AND DISCUSSION

### *4.2.1 Preliminary Study of Gelling Agent, Wetting Agent and Resuspendibility enhancer*

In the following the effect of added gelling, wetting agents and resuspendibility enhancer on the flow characteristics of middle chain triglycerides (MCT) was investigated. The measured viscosity of pure MCT is 27.6 ± 0.5 mPas at 25° C and 17.3 ± 0.3 mPas at 39° C (Chapter 2, Table 2.1). The addition of aluminium monostearate (Al-MonoSt), regardless of the concentration, displayed a nearly unchanged viscosity value and Newtonian flow behaviour with no gel and desirable thixotropic characteristics. An oil phase separation upon storage was visible. The addition of 3 % could achieve a marginal viscosity increase of the MCT oil from 28 mPas to 31 mPas (Figure 4.1 a, b). In contrast, samples with 3 % aluminium distearate (Al-DiSt) possessed a distinct thixotropic character at 25° C, which was preserved at higher temperatures, 39° C. The addition of 2 % and 3 % to MCT increased the viscosity to 53 mPas and 108 mPas at 500 $s^{-1}$, respectively (Figure 4.1 c, d). Both formulations were unproblematic for a manual injection. Mixtures composed of MCT + 3 % gelling agent Al-DiSt + 1 % wetting agent (hydrogenated lecithin) + 10 % resuspendibility enhancer (polyoxyl (PEG)-35 castor oil) were homogeneous upon visual inspection. The thixotropy of 3 % Al-DiSt was preserved after the addition of hydrogenated lecithin and PEG- 35 castor oil (Figure 4.1 e, f). Concentrations of the wetting agent and resuspendibility enhancer higher than 1 % and 10 % respectively, induced sedimentation and phase separation.

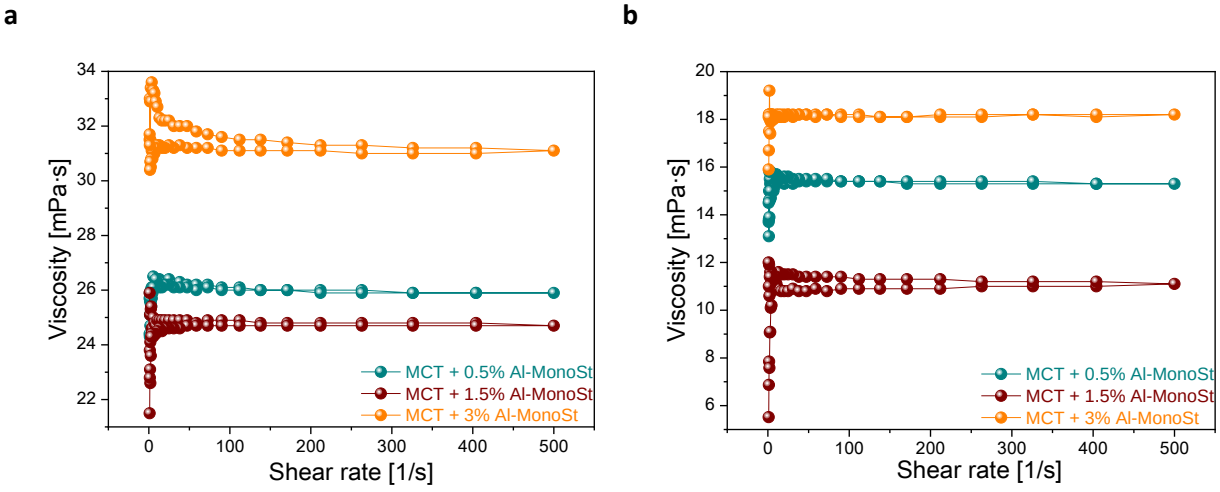

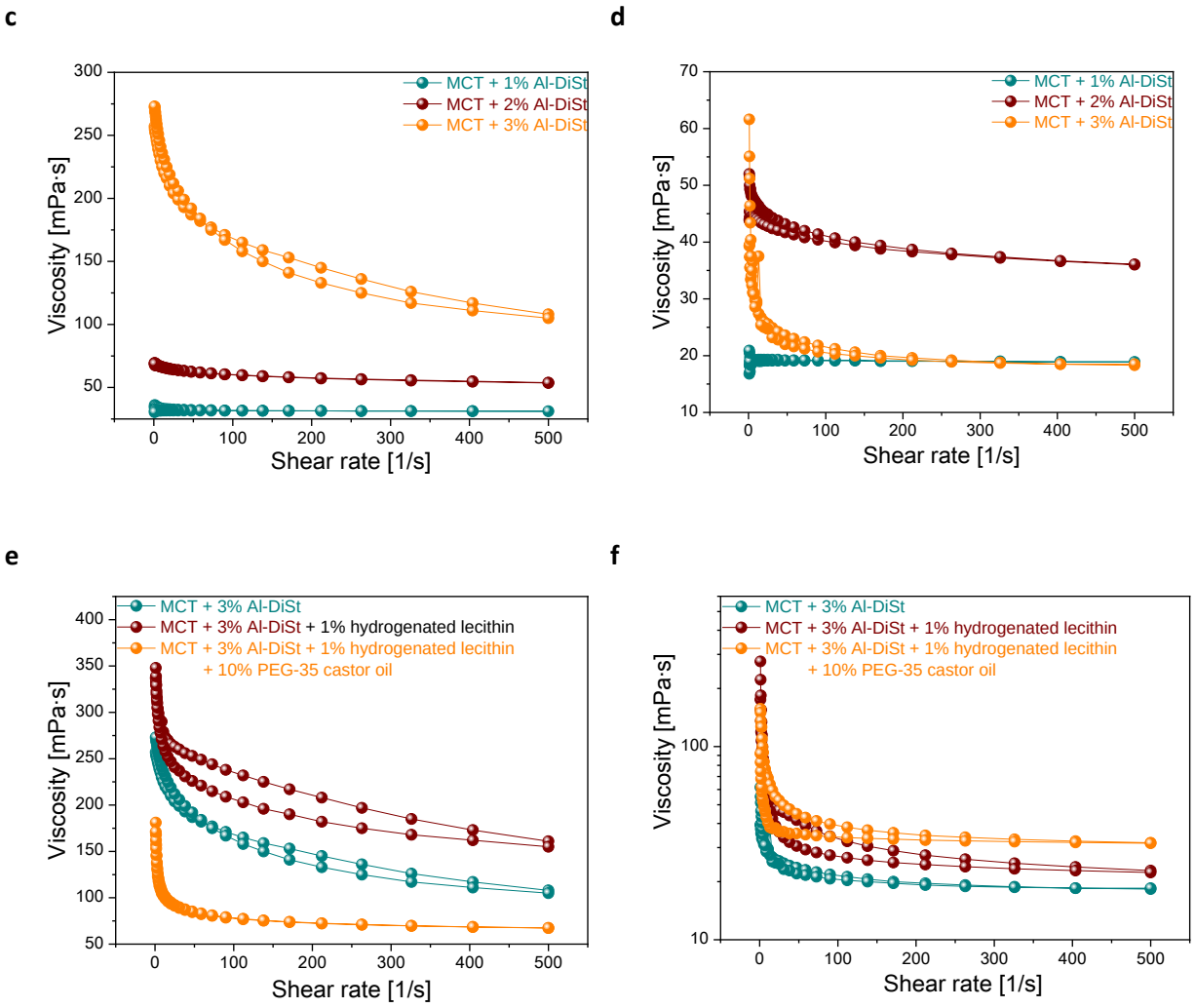


**Figure 4.1| Rheology of mixtures of MCT with a gelling agent and/or wetting agent and/or resuspendibility enhancer** (a), (c), (e) at 25° C (b),(d),(f) at 39° C

### *4.2.2 GnRH [6-D-Phe]-Additives Oil Depot Suspension*

The first preclinical study could show that a concentration of 1875 µg/mL GnRH [6-D-Phe] in castor oil: MCT 50:50 % (w/w) induced a synchronous *in vivo* effect of 2 days minimum and 5 days maximum (Chapter 2, Table 2.6). Thus formulations with 1875 µg/mL GnRH [6-D-Phe] were further evaluated (Figure 4.2). In total 11 formulations were composed (Table 4.1).

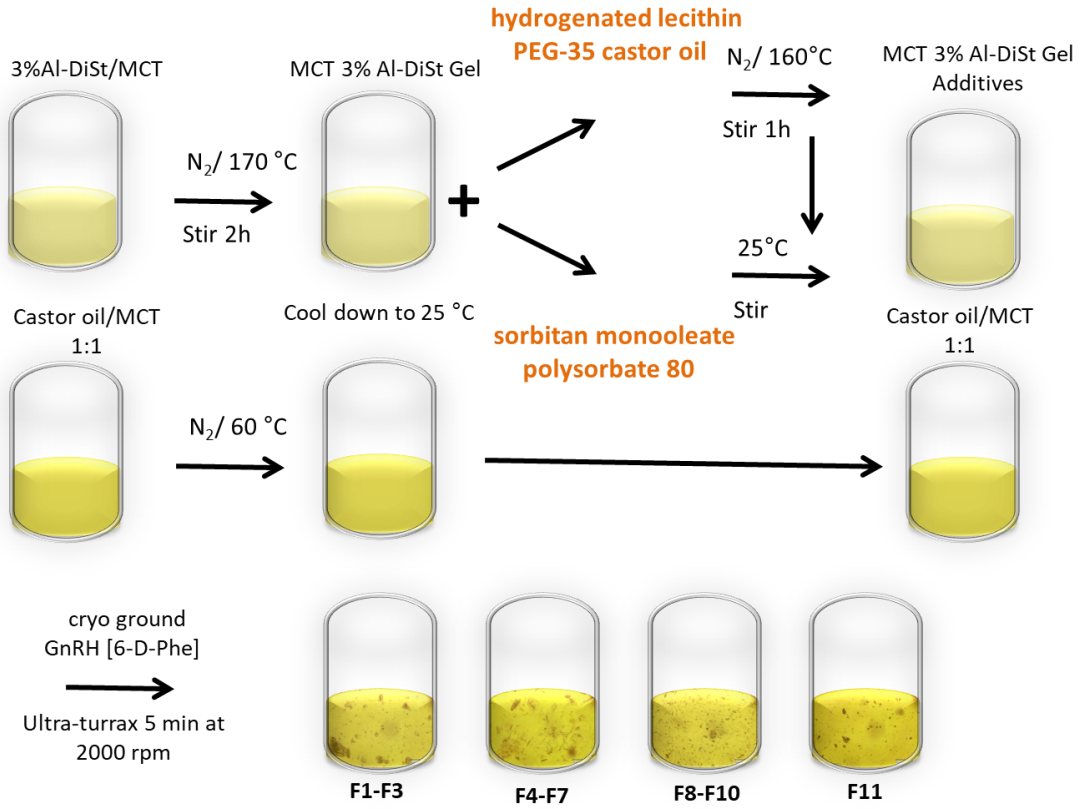


**Figure 4.2| 2nd generation GnRH [6-D-Phe] oil depot suspension**

| Formulation | Al-DiSt % (w/w) gelled MCT | Hydrogenated Lecithin (Phospholipon®90H) % (w/w) | Polyoxyl (PEG)-35 castor oil (Kolliphor®ELP) % (w/w) |
|---|---|---|---|
| **F1** | 1 | - | - |
| **F2** | 2 | - | - |
| **F3** | 3 | - | - |
| **F4** | 3 | 1 | 5 |
| **F5** | 3 | 2 | 5 |
| **F6** | 3 | 1 | 0.05 |
| **F7** | 3 | 1 | 10 |
| **Formulation** | **Al-DiSt % ( w/w) gelled MCT** | **Sorbitan monooleate (Span®80) % (w/w)** | **Ethoxylated sorbitan monooleate Polysorbate 80 (Tween ®80) % (w/w)** |
| **F8** | 3 | 5 | 5 |
| **F9** | 3 | 0.05 | 0.05 |
| **F10** | 3 | 2 | 2 |
| **Formulation** | **Castor oil: MCT 50:50 % (w/w)** | - | - |
| **F11** | - | - | - |

**Table 4.1| Composition of F1-F11 1875 µg/ml GnRH [6-D-Phe] oil depot formulation**

### *4.2.3 Rheology*

The GnRH [6-D-Phe] formulations gelled with 2 % (F2) and 3 % (F3) Al-DiSt showed a temperature independent shear-thinning behaviour compared to the previously tested Newtonian castor oil – MCT mix (F11) (Figure 4.3). The addition of hydrogenated lecithin and polyoxyl (PEG)-35 castor oil lowered the viscosity of the gelled matrix. The recorded high viscosity value of formulations F3 and F9 at 39° C in comparison to 25° C might be related to the absence or low concentrations of wetting and resuspendibility enhancer, inducing GnRH [6-D-Phe] particles agglomeration and increase in viscosity.

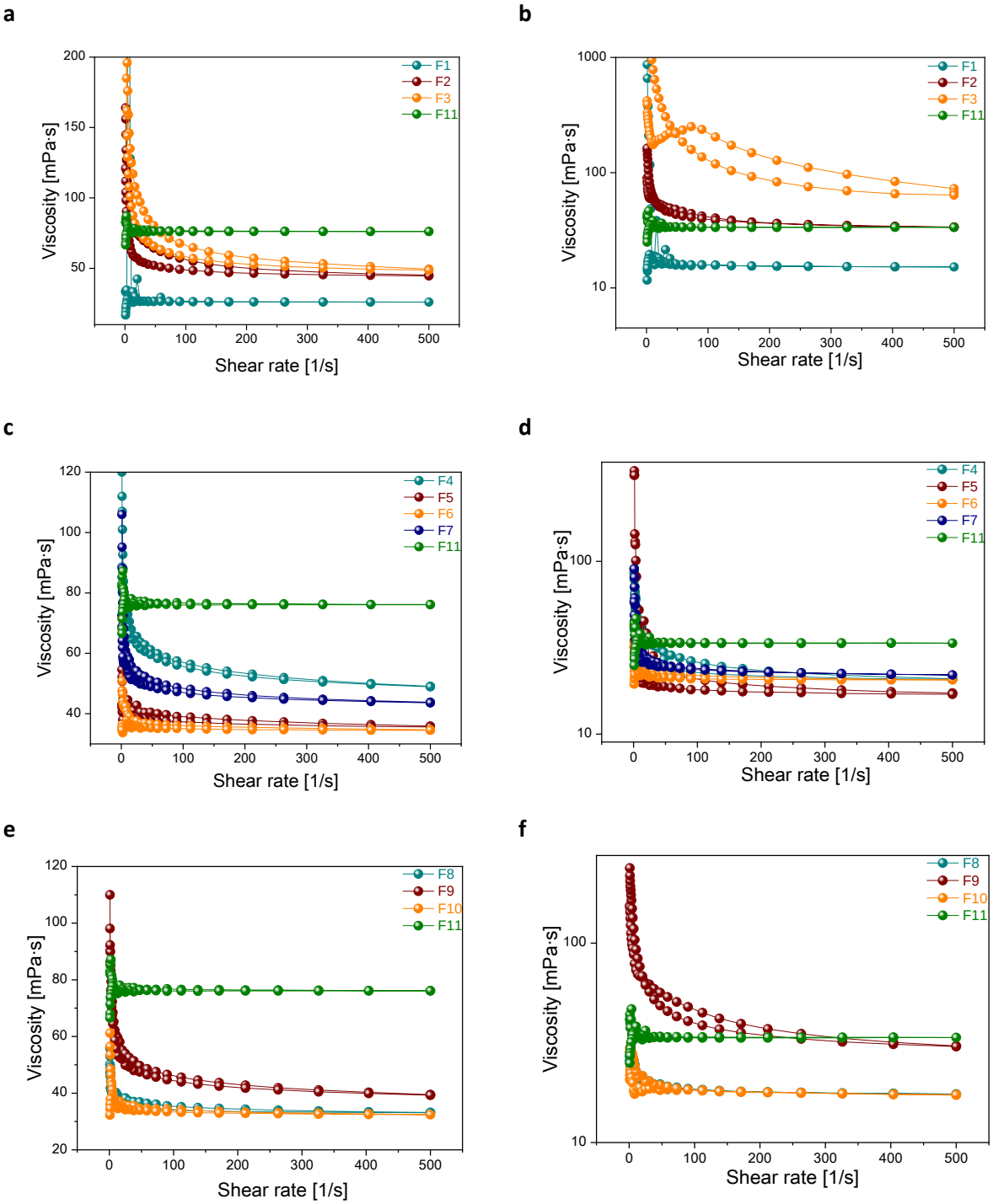


**Figure 4.3| Rheology of F1-F11 1875 µg/ml GnRH [6-D-Phe] oil depot formulations**
(a), (c), (e) at 25° C (b), (d), (f) at 39° C

Furthermore, oscillatory rheometry was applied. When applying stress on the vehicles, there are two possible scenarios which can result. The first one indicates a structure of loosely connected particles, where the applied mechanical force overrides the particle-particle interaction, breaking the structure and inducing the flow of the suspension (G“>G‘). The second possibility is strong gel structures, which are hard to separate through the induced mechanical stress (G‘>G“). Increasing the amount of the gelling agent from 1 % (F1) to 3 % (F3) led to the formation of a strong gel structure. This was further confirmed through a decreased tan δ value (Table 4.2). The formulation with 10 % PEG-35 castor oil showed increased tendency to break upon application of stress. Similar observations were made for the formulation with 5 % sorbitan monooleate and 5 % polysorbate 80 (Table 4.2, Table 4.3).

| Rheometer-Amplitude Sweep | | | | Rheometer-Amplitude Sweep | | | |
|---|---|---|---|---|---|---|---|
| 25° C | | | | 39° C | | | |
| Formulation | G’ [mPa] | G” [mPa] | tan $\delta$ | Formulation | G’ [mPa] | G” [mPa] | tan $\delta$ |
| F1 | 9.93 | 151 | 15.21 | F1 | 8.07 | 107 | 13.26 |
| F2 | 48.58 | 216 | 4.45 | F2 | 65.85 | 98 | 3.00 |
| F3 | 62 | 629.6 | 1.01 | F3 | 1217.5 | 670 | 0.55 |
| F4 | 1322 | 329.8 | 2.49 | F4 | 5.23 | 180 | 3.58 |
| F5 | 74.54 | 280 | 3.76 | F5 | 29.35 | 152 | 5.18 |
| F6 | 9.66 | 115.6 | 11.97 | F6 | 14.35 | 72.72 | 5.07 |
| F7 | 29.86 | 286.8 | 9.60 | F7 | 25.13 | 186 | 7.40 |
| F8 | 9.13 | 193.6 | 21.19 | F8 | 7.65 | 125 | 16.34 |
| F9 | 119.4 | 342 | 2.86 | F9 | 188.25 | 352.5 | 1.87 |
| F10 | 19.72 | 185.2 | 9.39 | F10 | 6.95 | 113.75 | 16.36 |
| F11 | 10.19 | 360.2 | 35.33 | F11 | 5.54 | 186.25 | 33.58 |

**Table 4.2| Rheometer-Amplitude Sweep of F1-F11 1875 µg/ml GnRH [6-D-Phe] oil depot formulations at 25° C and 39° C**
G’: storage modulus; G”: loss modulus; tan δ= G”/ G’, determined in the viscoelastic region (τ= 0.1-10 Pa) (Supplementary Data Figure 4.13)

| Frequency-Amplitude Sweep | | | | Frequency-Amplitude Sweep | | | |
|---|---|---|---|---|---|---|---|
| 25° C | | | | 39° C | | | |
| Formulation | G’ [mPa] | G” [mPa] | ŋ* [mPas] | Formulation | G’ [mPa] | G” [mPa] | ŋ* [mPas] |
| F1 | 7.10 | 97.81 | 1.03 | F1 | 7.46 | 75.45 | 25.06 |
| F2 | 17.51 | 116.75 | 37.27 | F2 | 38.04 | 122.75 | 41.72 |
| F3 | 437.31 | 378.23 | 228.82 | F3 | 737.15 | 637.54 | 448.31 |
| F4 | 91.32 | 187.6 | 71.98 | F4 | 45.22 | 116.52 | 43.87 |
| F5 | 45.42 | 158.48 | 50.72 | F5 | 8.20 | 72.52 | 24.30 |
| F6 | 9.78 | 99.85 | 26.25 | F6 | 114.28 | 243.40 | 76.58 |
| F7 | 25.01 | 153.15 | 49.28 | F7 | 22.91 | 108.57 | 35.48 |
| F8 | 10.98 | 135.61 | 40.96 | F8 | 11.62 | 97.84 | 31.12 |
| F9 | 81.48 | 218.11 | 76.95 | F9 | 44.82 | 195.37 | 69.89 |
| F10 | 18.53 | 129.95 | 40.15 | F10 | 17.84 | 92.09 | 29.92 |
| F11 | 13.30 | 272.44 | 79.45 | F11 | 5.26 | 143.29 | 2.92 |

**Table 4.3| Frequency-Amplitude Sweep of F1-F11 1875 µg/ml GnRH [6-D-Phe] oil depot formulations at 25° C and 39° C**
G’: storage modulus; G”: loss modulus; ŋ*: complex viscosity determined in the viscoelastic region (f=0.1-10 Hz); (Supplementary Data Figure 4.14)

Formulations F7 (MCT + 3 % Al-DiSt + 1 % hydrogenated lecithin + 10 % PEG-35 castor oil) and F8 (MCT + 3 % Al-DiSt + 5 % sorbitan monooleate + 5 % polysorbate 80) showed phase separation within 24 hours after preparation (Figure 4.4). The high concentrations of wetting and resuspendibility enhancer might induce the formation of flocculated system, where the sediment is rapidly formed.

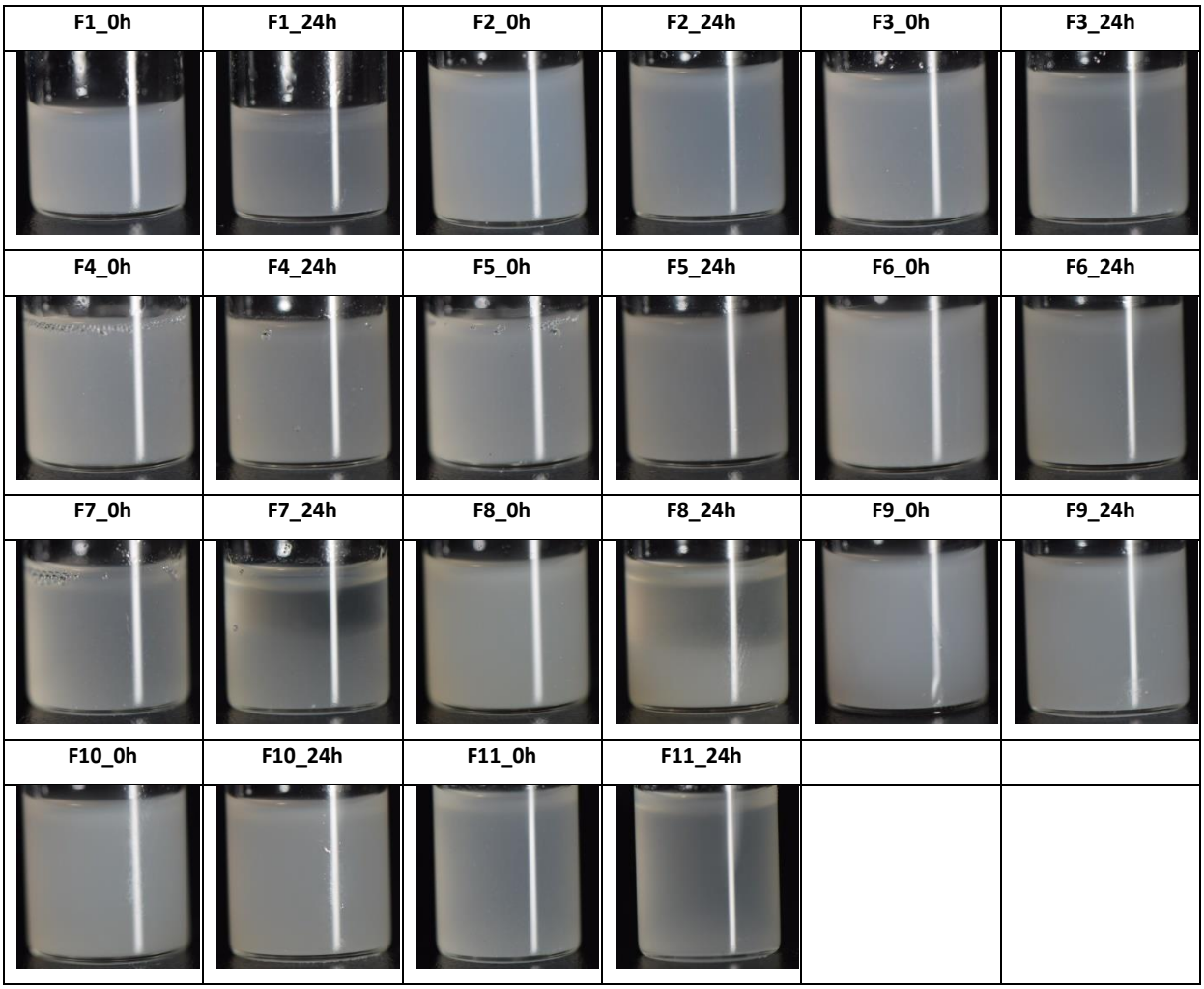


**Figure 4.4| Camera images of F1-F11 1875 µg/ml GnRH [6-D-Phe] oil depot formulations over 24 h**

### *4.2.4 Injection Force Determination*

Injecting a gelled oil vehicle can be a strenuous task and might require forces that can be hard to manage manually. Consequently, the injectability of F1-F11 was tested. Both the Dynamic Glide Force (DGF) and the maximal force (Fmax) for the injection of F1-F11 through 16 G and 18 G needles were below 3 N, 10 times lower than the estimated maximum force for manual injection, 30 N[14] (Figure 4.5).

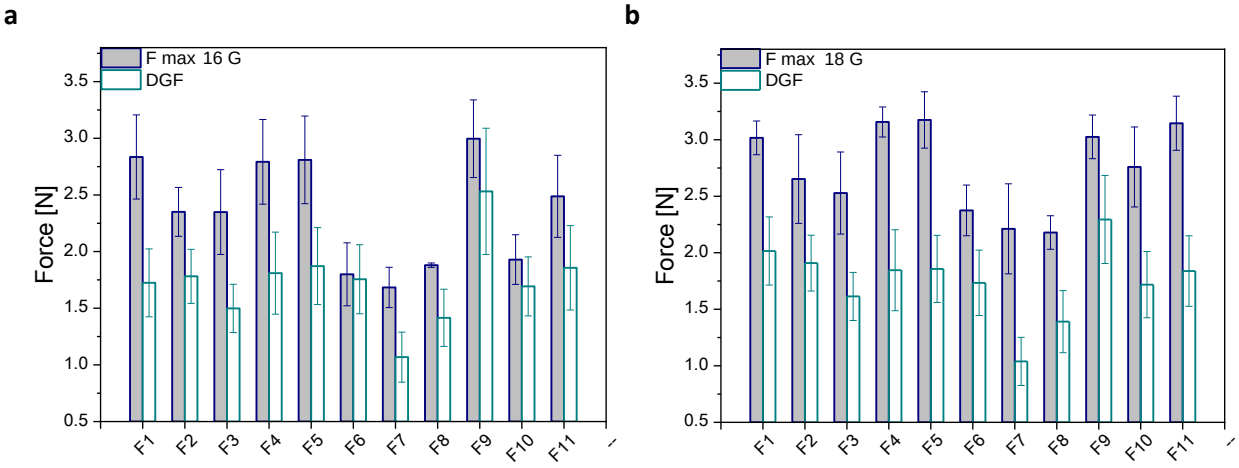


**Figure 4.5| F max and DGF of F1-F11 1875 µg/ml GnRH [6-D-Phe] oil depot formulations**
(a) 16 G (b) 18 G needle

### *4.2.5 Particle Size Distribution and Characterization*

GnRH [6-D-Phe] particle size can have an impact on the suspension sedimentation rate, stability and dose uniformity. The median particle size $D_{v50}$ for the dispersed formulations remained nearly unchanged. The particle size distribution of all measured samples was non-symmetric (Figure 4.6). Increasing the hydrogenated lecithin concentration to 2 % and reducing the concentration of PEG-35 castor oil to 0.1 % resulted in the formation of larger particles, visible through the increase of the $D_{v90}$ and mean particle size. There was no considerable difference between formulations with 5 % and 10 % PEG-35 castor oil. The dispersed formulations without wetting and resuspendibility agent showed an overall larger particle size (Table 4.4).

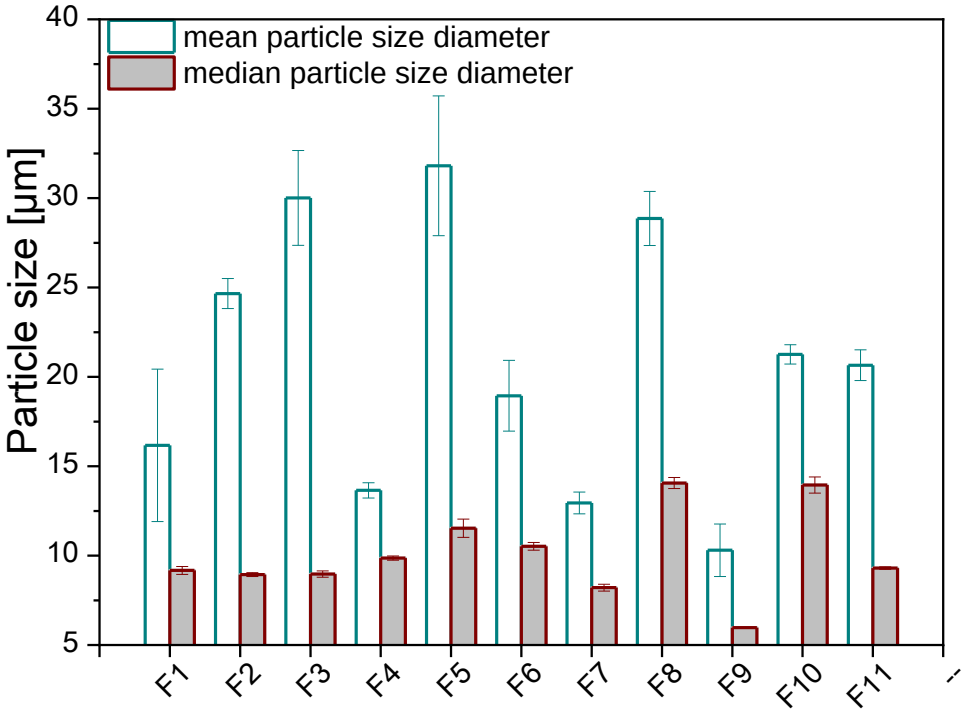


**Figure 4.6| Mean (the mean particle diameter over volume) and median particle size of F1-F11 1875 µg/ml GnRH [6-D-Phe] oil depot formulations**

| Formulation | $D_{v50}$ [µm] ± SD | $D_{v90}$ [µm] ± SD |
|---|---|---|
| **F1** | 9.17 ± 0.22 | 23.24 ± 9.54 |
| **F2** | 8.94 ± 0.11 | 71.92 ± 8.97 |
| **F3** | 8.97 ± 0.18 | 101.48 ± 9.69 |
| **F4** | 9.86 ± 0.12 | 29.99 ± 1.15 |
| **F5** | 11.53 ± 0.51 | 100.14 ± 28.38 |
| **F6** | 10.52 ± 0.22 | 48.49 ± 5.45 |
| **F7** | 8.21 ± 0.19 | 28.08 ± 2.00 |
| **F8** | 14.06 ± 0.31 | 64.00 ± 4.33 |
| **F9** | 5.97 ± 0.01 | 15.31 ± 0.45 |
| **F10** | 13.95 ± 0.45 | 48.39 ± 0.93 |
| **F11** | 9.30 ± 0.07 | 57.90 ± 0.04 |

**Table 4.4| Particle size distribution and $D_{v50}$ and $D_{v90}$ fractions**

### *4.2.6 Oil-Water Interface*

In order to visualize the behaviour of the formulations upon contact with aqueous phase, drop shape analysis and light microscopy of the formulation/water interface were performed. Formulations F1, F2, F3, and F11 without additives showed reduced spreading when injected into the PBS (pH 7.4). The surfactants led to a reduction of the surface tension promoting spreading of the oil vehicle (Figure 4.7).

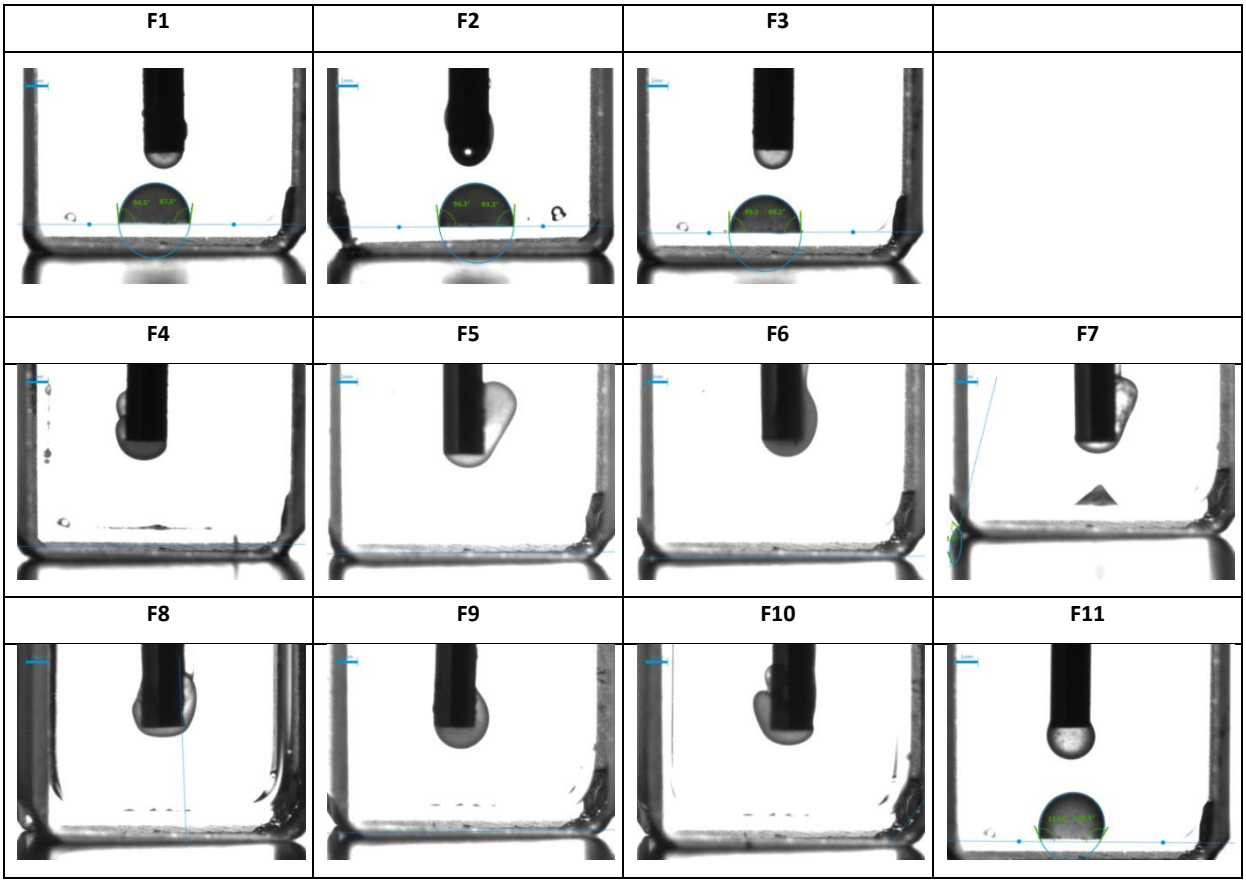


**Figure 4.7| Drop shape analysis in PBS (pH 7.4) of F1-F11 1875 µg/ml GnRH [6-D-Phe] oil depot formulations**

Formulations F4-F7 and F8-F10 with stabilizing agents got emulsified upon contact with aqueous buffer. The formulations with gelled oil or only oil, F1-F3 and F11, showed no emulsified oil drops in PBS (Figure 4.8).

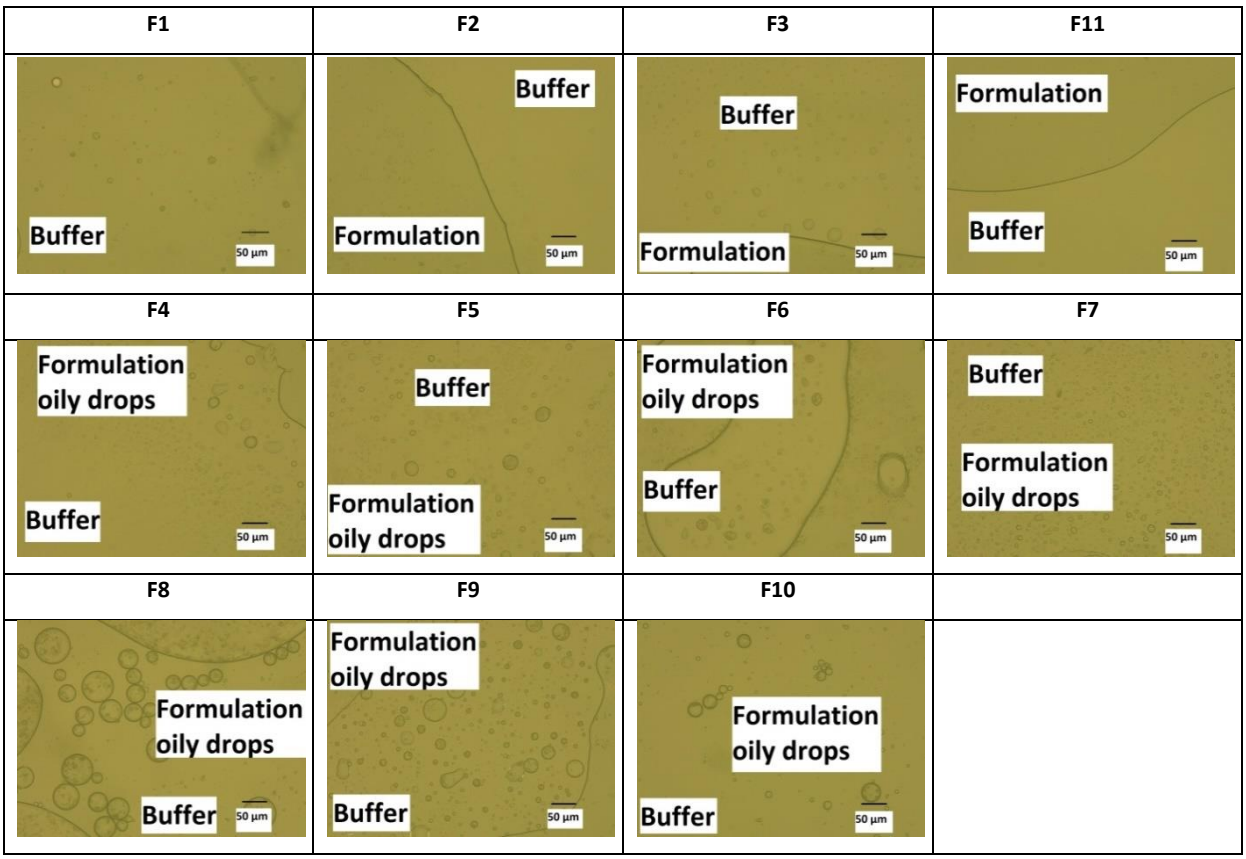


**Figure 4.8| Light microscopy of F1-F11 1875 µg/ml GnRH [6-D-Phe] oil depot formulations emulsified in PBS pH 7.4**

### *4.2.7 Self-Emulsifying Character*

F2, F4, F9 and F11 were injected into PBS to understand the *in vivo* behaviour upon contact with tissue fluid. F4 spontaneously formed an emulsion with droplet in the low micrometer range (Figure 4.9 a, b). The other formulations did not show this characteristic. Reduction of the hydrogenated lecithin concentration did not affect the formation of the microemulsion (Figure 4.9 e, f). The combination of PEG-35 castor oil and lecithin has been well established and applied into the formation of self-emulsifying systems. These are vehicles, which build a fine dispersed microemulsion using chemical rather than mechanical means[15–17]. A combination of a hydrophilic surfactant, PEG-35 castor oil (HLB=14-16), with a lipophilic surfactant hydrogenated lecithin (HLB ~ 3) in the oil phase, induces upon contact with the aqueous phase the formation of a mixed surfactant based self-emulsifying drug delivery system (SEDD) with incorporated GnRH [6-D-Phe][18,19] (Figure 4.9). This could assure a more consistent and controlled release of GnRH [6-D-Phe] from the oil matrix and improve its *in vivo* effect.

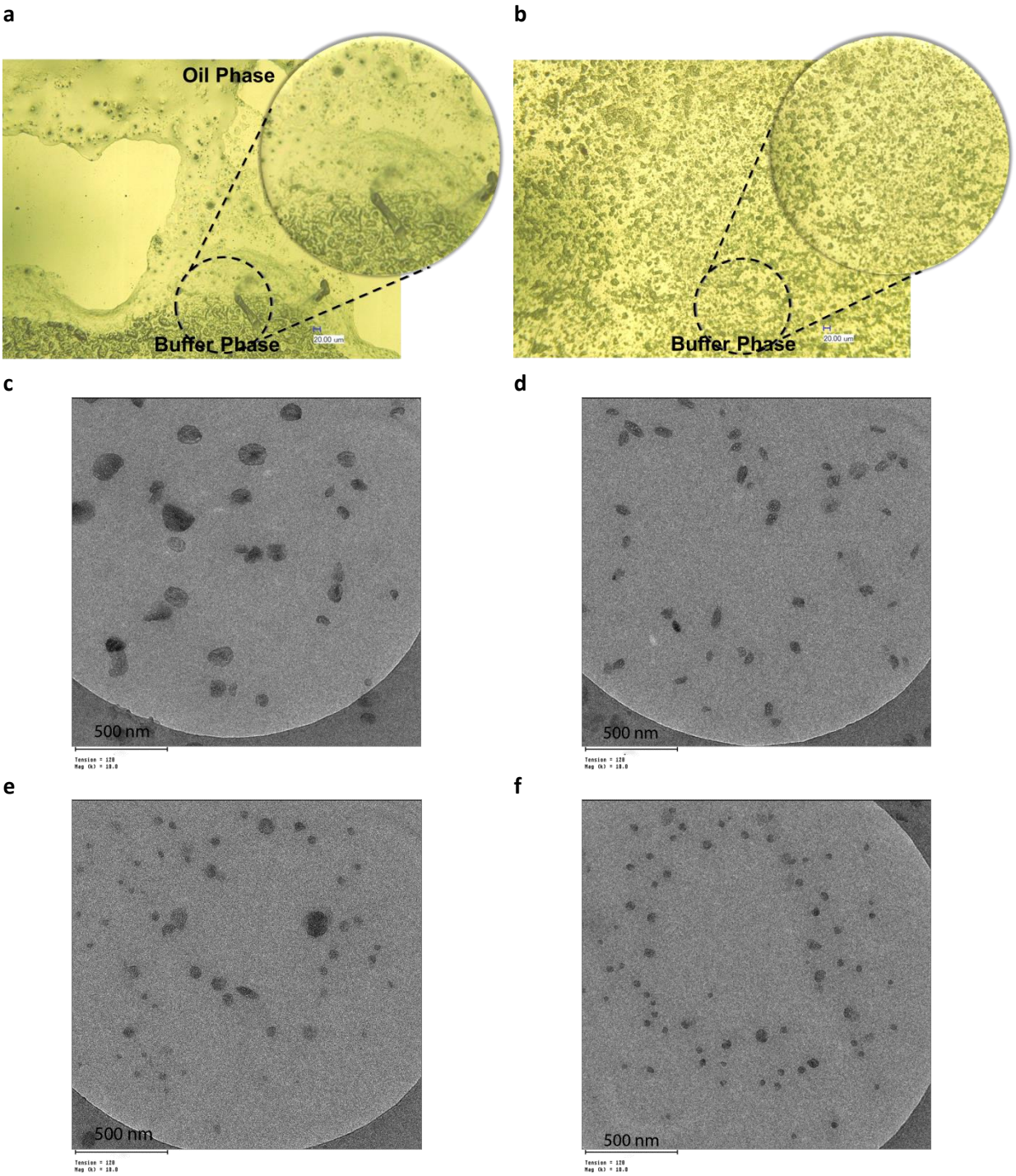


**Figure 4.9| Light microscopy and Transmission electron microscopy (TEM) of the oil phase and the microemulsified oil phase**
(a, b) F4 in PBS (pH 7.4)
(c, d) F4.0: MCT+ 3% Al-DiSt+ 1% hydrogenated lecithin+ 5% PEG-35 castor oil (e, f) F4.1: MCT+ 3% Al-DiSt+ 0.5% hydrogenated lecithin+ 2.5% PEG-35 castor oil injected in 6 mL PBS (pH 7.4) at 39° C in an incubated shaker after 24h

### *4.2.8 In vitro Release Studies*

In order to select formulations for the *in vivo* study an *in vitro* release experiment was performed.

This showed a correlation between the Al-DiSt content and the GnRH [6-D-Phe] release: the higher the Al-DiSt content, the more delayed the release of GnRH [6-D-Phe] (F1-F3) (Figure 4.10 a). The total amount of released GnRH [6-D-Phe] could be markedly increased by the addition of hydrogenated lecithin or PEG-35 castor oil (F4-F7, Figure 4.10 b). Hydrogenated lecithin and PEG-35 castor oil concentrations higher than 2 % and 10 % respectively induced a burst release of GnRH [6-D-Phe] from the oil depot. The third group (F8-F10) containing sorbitan monooleate/ polysorbate 80 mixtures showed higher burst with increasing concentration from 0.05 % in F9 to 5 % in F8, reaching the release values of castor oil: MCT 50:50 % (w/w) oil depot from the first preclinical study (F11, Figure 4.10 c).

For *in vivo* testing the following three formulations were selected:

MCT + 2 % (w/w) Al-DiSt (F2), displaying a shear-thinning behaviour with a relatively low viscosity.

MCT + 3 % (w/w) Al-DiSt + 1 % (w/w) hydrogenated lecithin + 5 % (w/w) PEG-35 castor oil (F4), showing narrow particle size distribution, no visible phase separation upon storage and good emulsification properties.

MCT + 3 % (w/w) Al-DiSt + 0.05 % (w/w) sorbitan monooleate + 0.05 % (w/w) polysorbate 80 (F9), exhibiting a low burst release, good rheological properties and good emulsification.

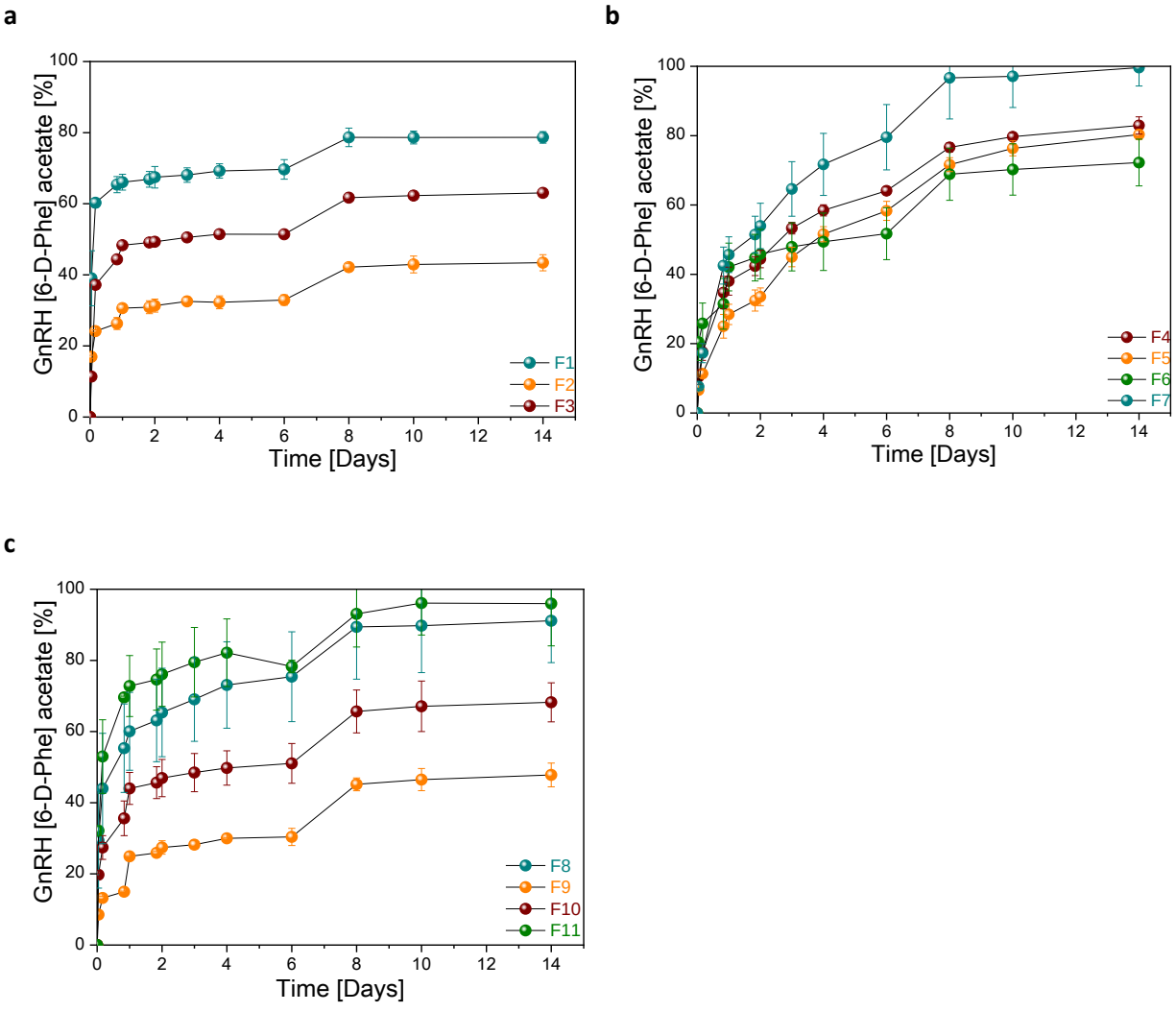


**Figure 4.10| *In vitro* release profiles of F1-F11 1875 µg/ml GnRH [6-D-Phe] oil depot formulations in visking dialysis tubing, MWCO 12 – 14 kD**

Increasing the concentration of GnRH [6-D-Phe] acetate to 3750 µg/mL could not compensate the burst effect and did not affect the *in vitro* release profile significantly (Figure 4.11). The established *in vitro* model could differentiate between the four formulations; however, it does not allow a prediction of their *in vivo* behaviour.

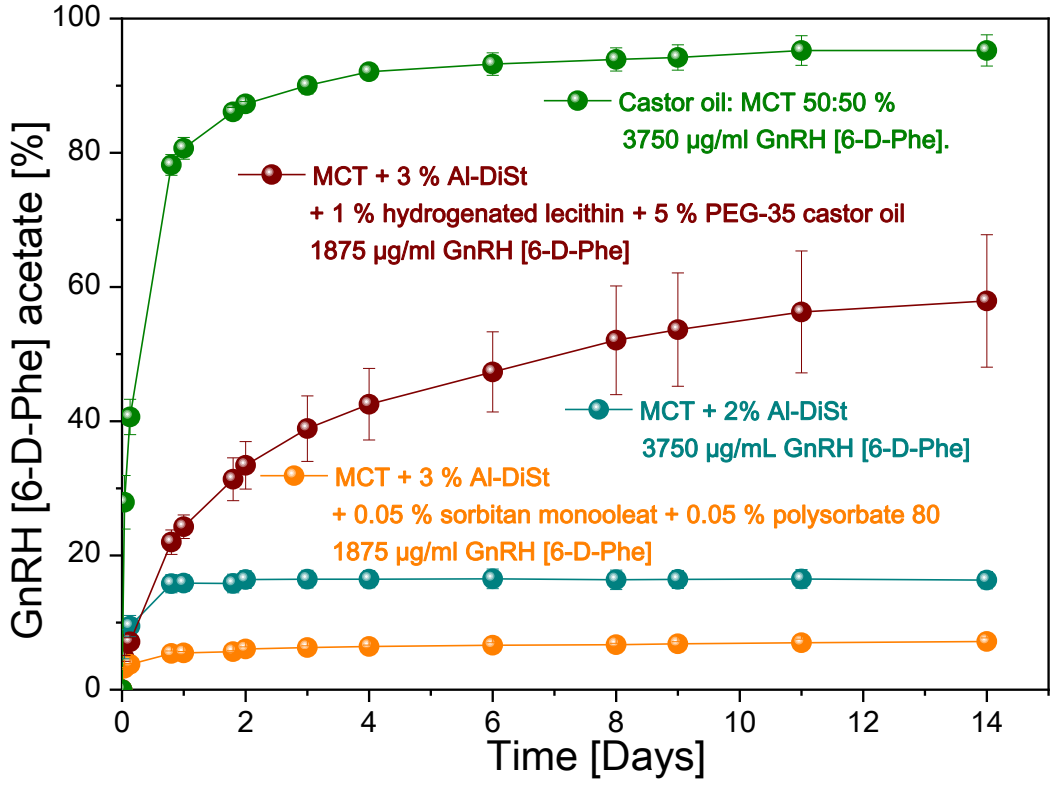


**Figure 4.11| *In vitro* release profiles of GnRH [6-D-Phe] oil depot formulations in visking dialysis tubing, MWCO 12 – 14 kD**

### *4.2.9 In vivo 2nd Preclinical Study*

The four formulations were tested *in vivo*:

MCT + 2 % (w/w) Al-DiSt 3750 µg/mL GnRH [6-D-Phe],

MCT + 3 % (w/w) Al-DiSt + 1 % (w/w) hydrogenated lecithin + 5 % (w/w) PEG-35 castor oil 1875 µg/ml GnRH [6-D-Phe]

MCT + 3 % (w/w) Al-DiSt + 0.05 % (w/w) sorbitan monooleat + 0.05 % (w/w) polysorbate 80 1875 µg/ml GnRH [6-D-Phe]

Castor oil: MCT 50:50 % (w/w) 3750 µg/ml GnRH [6-D-Phe]

The effect was evaluated and considered successful if first, the estrous cycle was blocked and there were no follicles larger than 5mm and second, Corpus luteum (CL) showed a reduced size in comparison to previous measurements. A CL regression was expected on days 15-17 of the estrous cycle, corresponding to 4-6 days post application. If a follicle growth, an ovulation or cyst development appeared, the cycle blockage was regarded as unsuccessful.

The control group received the oil medium without GnRH [6-D-Phe]. Ultrasonography showed a follicle growth and no effect of the placebo (0.2 ± 0.4 days) (Figure 4.12). MCT + 2 % (w/w) Al-DiSt 3750 µg/mL GnRH [6-D-Phe] resulted in 7 and 11 days of cycle blocking in two animals. Three animals displayed a permanent cycle blockage. Thus the average effect was 42.6 ± 30.7 days. Four animals injected with 1875 µg/mL GnRH [6-D-Phe] in the vehicle of MCT + 3 % (w/w) Al-DiSt + 1 % (w/w) hydrogenated lecithin + 5 % (w/w) PEG-35 castor oil showed follicle growth between day 10 and day 11 resulting in an effect of 4 to 5 days. One animal in the group displayed no cycle blocking effect. The average effect was 3.6 ± 2.1 days. Two animals treated with 1875 µg/mL GnRH [6-D-Phe] in the vehicle MCT + 3 % (w/w) Al-DiSt + 0.05 % (w/w) sorbitan monooleate + 0.05 % (w/w) polysorbate 80 showed 10 to 13 days of cycle blockage and three of the animals had permanent cycle blockage. This resulted in an average effect of 43.6 ± 29.3 days. The animals which received 3750 µg/ml GnRH [6-D-Phe] in castor oil: MCT 50:50 % (w/w) showed the most irregularities. Cycle blockage for 4 to 8 days was seen in three animals and two animals showed no effect. The average blockage lasted 3.4 ± 3.4 days (Supplementary Data Table 4.6).

Statistical analysis showed that the mean cycle blocking effect of the group MCT + 3 % (w/w) Al-DiSt + 1 % (w/w) hydrogenated lecithin + 5 % (w/w) PEG-35 castor oil was significantly longer than the one of the control group ($p<0.05$) (Supplementary Data Table 4.8). There were no significant differences between animals treated with castor oil: MCT 50:50 % (w/w) 3750 µg/ml GnRH [6-D-Phe] and placebo ($p>0.05$) (Supplementary Data Table 4.10).

In summary, the *in vivo* study confirmed that a treatment with GnRH [6-D-Phe] oil depot suspension could successfully prolong the luteal phase of the estrus cycle and inhibit a follicle development and growth. The most pronounced cycle blocking effect, with regards to effect synchronicity, length and observed adverse reactions, were detected in the group MCT + 3 % (w/w) Al-DiSt + 1 % (w/w) hydrogenated lecithin + 5 % (w/w) PEG-35 castor oil. In contrast the vehicles without self-emulsifying character, MCT + 3 % (w/w) Al-DiSt + 0.05 % (w/w) sorbitan monooleate + 0.05 % (w/w) polysorbate 80 and MCT + 2 % (w/w) Al-DiSt displayed irregular cycle blockage effect. Increased peptide concentration of 3750 µg/mL in castor oil: MCT 50:50 % (w/w) did not lead to a significant prolongation of the blocking effect (3.4 ± 3.4 days). The *in vivo* study results showed further that a mixed surfactant based SEDD of GnRH [6-D-Phe] with hydrogenated lecithin and PEG-35 castor oil achieved a more consistent cycle blocking effect compared to the pure gelled oil and pure oil vehicle formulations.

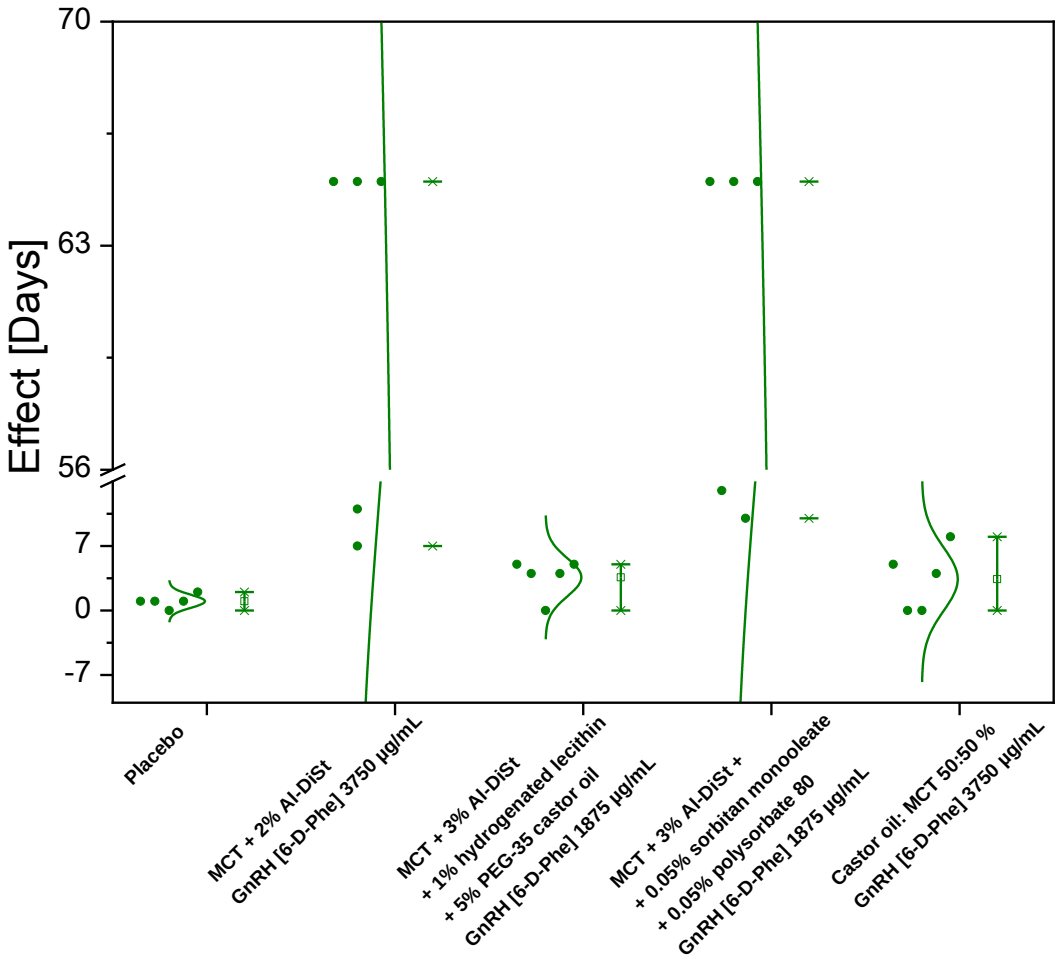


**Figure 4.12| *In vivo* effect of the oil depot GnRH [6-D-Phe] formulations**

## 4.3 CONCLUSION

The experiments demonstrated that the incorporation of additives to a pure MCT oil vehicle for the sustained delivery of GnRH [6-D-Phe] was favourable due to the following characteristics: First, the Al-DiSt gelled MCT oil displayed a clear shear-thinning behaviour in comparison to the pure oil, making the multiple dose withdrawal from a vial easier. Second, the incorporated hydrogenated lecithin as well as PEG-35 castor oil resulted in the formation of a self-emulsifying drug delivery system of GnRH [6-D-Phe], thus obtaining a more consistent and controlled release with reduced initial *in vitro* burst. The sustained release might be partially due to the gelled oil matrix. Although the 0.05% sorbitan monooleate/ polysorbate 80 mixture could achieve a longer *in vivo* blocking effect in comparison to 5% PEG-35 castor oil and 1% hydrogenated lecithin mixture, it was only of a moderate synchronicity. Therefore, in order to prolong the obtained consistent *in vivo* effect of MCT + 3 % (w/w) Al-DiSt + 1 % (w/w) hydrogenated lecithin + 5 % (w/w) PEG-35 castor oil, it might be beneficial to reduce the GnRH [6-D-Phe] solubility through salt or polymer complexation.

# 4.4 MATERIALS AND METHODS

**Gonadorelin [6-D-Phe] acetate peptide** (pE1–H2–W3–S4–Y5–(D)F6–L7–R8–P9–G10–NH2) or (pGlu-His-Trp-Ser-Tyr-D-Phe-Leu-Arg-Pro-Gly-NH2) was provided by BFC Biopept-Feinchemie as lyophilized powder and acetate salt (purity 99.76 %, water content 6.73 % and acetate peptide ratio (MW/MW) 1.8). **Gelling agents**: Aluminiumdistearte (Alugel30®HEP), Baerlocher, D-Unterschleissheim, Aluminium monostearate (Aluminiumstearate NF®), Ferro, D-Frankfurt; **Wetting agents**: hydrogenated phosphatidylcholine (lecithin) (Phospholipon®90H) Lipod D-Ludwigshafen, ethoxylated sorbitan monooleate;Polysorbate 80 (Tween®80) Sigma Aldrich, D- Taufkirchen, sorbitan monooleate (Span®80) Merck Schuchardt, D-Hohenbrunn and **Resuspendibility enhancer**: Polyoxyl (PEG) 35 castor oil (Kolliphor®ELP) BTC Europe, D-Burgbergheim; **Oil vehicle**: miglyol®812 (MCT) Caesar & Loretz, D-Hilden, castor oil (Gustav Heess, D-Leonberg).

**GnRH [6-D-Phe] micronization** The cryogenic micronization of GnRH [6-D-Phe] bulk lyophilisate was performed using a Retsch Cryo Mill (Retsch Technology, Haan, Germany). The grinding process was performed for the duration of 8 min at 25 Hz. The cycle included a precooling phase of 10 min at 5 Hz.

**GnRH [6-D-Phe] oil depot suspension preparation:** The gelling agent Aluminiumdistearte (Al-DiSt) was weighed and suspended in the MCT oil vehicle to a final weight of 9.5 g (corresponding to 10 mL). The prepared mixture was heated at 174° C for 2 hours under $N_2$. After cooling down to 25° C the wetting agent, hydrogenated lecithin and the resuspendibility enhancer PEG-35 castor oil were incorporated into the gelled oil matrix and stirred at 160° C for 1 hour under $N_2$. Sorbitan monooleate and polysorbate 80 were incorporated into the gelled oil matrix and stirred at 25° C for 1 hour under $N_2$. The castor oil: MCT 50:50 % (w/w) matrix was heated and agitated under inert atmosphere ($N_2$) at 60° C and then cooled down to room temperature at 25° C. The cryo-ground GnRH [6-D-Phe] lyophilizate was suspended in the prepared oil matrices at ambient temperature of 25° C using an Ultra-Turrax T-10 basic (IKA Labortechnik, Germany) for 5 minutes at 2000 rpm. The 1875 µg/mL GnRH [6-D-Phe] oil depot suspensions F1-F11 were aliquoted in 20R glass vials.

**Rheology: Viscosity profile** Viscosity measurement and flow curves evaluation of the F1-F11 formulations were performed with MCR 100 (Anton Paar Germany, Ostfildern-Scharnhausen) cone plate system CP – 1 (50 mm diameter, a cone angle of 1°, and a gap of 0.042 mm). The viscosity η was defined depending on the shear rate ẏ and measuring sections a) 0 – 500 $s^{-1}$ (30 points, 6 s per point; 180 s measurement time), b) 500 $s^{-1}$ (1 point, 6 s per point, 6 s measurement time), c) 500 – 0 $s^{-1}$ (30 points, 6 s per point, 180 s measurement time). **Amplitude sweep** Amplitude sweep measurements were performed with cone plate system CP – 1 (50 mm diameter, a cone angle of 1°, and a gap of 0.2 mm). The storage and loss moduli G'/G'' were defined depending on strain γ or shear stress τ and the measuring sections a) $\tau = 0.01 \dots 0.1\ Pa\ ; f = 1\ Hz$ ; discarded (12 points, 5 s per point, 60 s measurement time), b) $\tau = 0.1 \dots 100\ Pa\ ; f = 1\ Hz$; (30 points, 15 s per point, 450 s measurement time), tan δ was determined in the viscoelastic region (τ= 0.1-10 Pa). **Frequency sweep** Frequency sweep measurements of the stability samples were performed with cone plate system CP – 1 (50 mm diameter, a cone angle of 1°, and a gap of 0.2 mm). The storage and loss moduli G'/G'' were defined depending on strain γ or shear stress τ and the measuring sections a) $\tau = 0.1\ Pa\ ; f = 0.01 \dots 0.1\ Hz$ ; discarded (12 points, 5 s per point, 60 s measurement time), b) $\tau = 0.1\ Pa\ ; f = 0.1 \dots 100\ Hz$; (30 points, 15 s per point, 450 s measurement time), ŋ* was determined in the viscoelastic region (f=0.1-10 Hz).

**GnRH [6-D-Phe] particle size distribution and characterization** The particle size distribution of F1-F11 was analysed employing a Laser Diffraction Particle Size Analyzer LA-950 (Retsch Technology, Haan). The samples were prepared in triplicate (n=3). 0.2 mL of the oil suspension was withdrawn from the vial and measured in a solution of 1 % sorbitan monooleate in isooctane (m/v) in a standard measuring cell with 10 mL volume.

**Injection force determination** The injectability/syringeability of F1-F11 were performed with the TA.XT.plus Texture Analyser (Stable Micro Systems, Godlming, UK). The formulations were injected into air using a NORM-JECT 1 mL Tuberkulin + Luer syringe (Henke-Sass-Wolf GmbH, Germany) with either a FINE-JECT 18 Gx2'', 1.2x50 mm needle (Henke-Sass-Wolf GmbH, Germany) or a FINE-JECT 16 Gx1½'', 1.6x40 mm needle (Henke-Sass-Wolf GmbH, Germany). The software Exponent was set to compression test mode with the parameters: 10 mm/sec pre-test speed, and 3.9 mm/sec test speed, and 10.00 mm/sec post-test speed, trigger

force: 0.001 N. The applied force from the texture analyser was recorded in [N] against the distance of the syringe plunger (max. 64 mm).

**Camera images** The photographic images were taken with the Nikon D5300 reflex camera (Nikon, Japan), Nikon DX, AF-S Micro NIKKOR 85mm 1:3.5G EG (Nikon, Japan), and Nikon Speedlight SB910 with white filter (Nikon, Japan). A manual focusing function was used. Each formulation was shaken 2 minutes at 12 Hz with a Mixer Mill MM200 (Retsch Technologies, Germany) and filled into glass vials. To analyse the sedimentation rate of the 11 formulations, images were taken at the following time points: 0 h, 0.5 h, 2 h, 3 h, 4 h, 5 h, and 24 hours.

**Oil-Water Interface Tension and Drop Shape Analyser** The wettability and spreading of F1-F11 were analysed with sessile drop measurements on a Drop Shape Analyser (Krüss, Germany), using NORM-JECT 1 mL Tuberkulin + Luer syringes (Henke-Sass-Wolf, Germany) and a NE94 steel needle with 1.8 mm diameter (Krüss, Germany). The surrounding phase in the cuvette was PBS (pH 7.4), resembling the muscle tissue fluid of the swine.

**Light microscopy** 5 µL of F1-F11 formulation were injected in 10 µL PBS (pH 7.4) and filled into a 0.5 mL Eppendorf cap. The cap was gently wheeled around up to 5 times from left to right. The light micrographs were taken with VHX – 500 FD (Keyence, Osaka, Japan) using a 500x magnification.

**SEDD (Microemulsion) characterization** 1mL of the formulations was injected into 6 mL of PBS (pH 7.4) and shaken in an incubated shaker 3031 (GFL, Burgwedel, Germany) at 39° C and 60 rpm over 24 h. TEM was applied to analyse the microemulsion structures. 5 µl of the filtered but undiluted sample was pipetted on a Quantifoil ®Multi A holey carbon coated grid blotted and allowed to air dry at room temperature. A RT-TEM at a JEOL 200 kV JEM-FS2200 instrument and a RT EM-21010/EM-21311HTR specimen holder were used.

***In vitro* release study** In the *in vitro* release study 1.5 mL formulation were filled in VISKING® dialysis tubing, MWCO 12 – 14 kD, RC, 28 mm (SERVA, Germany). The release medium was 30 mL PBS (pH 7.4). The *in-vitro* evaluation was performed in duplicate and in an incubated shaker 3031 (GFL, Germany) at 39° C and 60 rpm. 1 mL sample was used for the RP-HPLC analysis at the following intervals 1 h, 3 h, 5 h, 7 h, 22 h, 25 h, 28 h, 46 h, 52 h, 76 h, 100 h, 172 h, 196 h, 220 h, and 336 h (14 days). The GnRH [6-D-Phe] content in the oil vehicle and in the donor cell was extracted using organic solvents, dichloromethane (DCM), where GnRH [6-D-Phe] is not soluble in combination with PBS (pH 7.4). 2 mL sample was weighted into a falcon tube, 4 mL DCM and 6 mL PBS (pH 7.4) were added. The tube was vortexed at room temperature (25° C) and put into an incubated shaker 3031 (GFL, Germany) at 39° C and 60 rpm for 24 h. The quantity of the peptide in the upper aqueous phase was analysed by RP-HPLC at 220 nm.

**Determination of the GnRH [6-D-Phe] (RP-HPLC)** The GnRH [6-D-Phe] content was analysed by RP-HPLC using a LUNA C8 (4.6 mm x 250 mm; size = 5 µm; Phenomenex, USA) column, with a C8 pre-column (4 mm x 3 mm; size = 5 µm) at an HPLC Agilent 1100/1200 series (Agilent Technologies, USA) (mobile phase A (water + 1 mL/L Trifluoroacetic acid (TFA) (v/v)) and mobile phase B (800 g Acetonitrile + 200 g water + 1.2 mL TFA), 1.1 mL/min flow, column temperature 40° C, and autosampler temperature 2 – 8° C. The Retention Time (RT) of GnRH [6-D-Phe] was 8.5 ± 1.5 minutes with UV detection at 220 nm.

***In vivo* 2nd preclinical study** The second *in vivo* testing as well as the analysis of the resulting data was performed between 09.04.2014 and 25.06.2014 from the University in Leipzig from Prof. Dr. Johannes Kauffold with the support of Dr. Haukur Sigmarrson, Dr. Mathias Hoops, Rosa Stark and Catherine Poser. The number of the tested animals was 25 (german landrace and pietrain breeds) with an average weight of 148 KG and 241 - 243 days old. The gilts were administered with Altrenogest, eCG and GnRH in order to synchronize the estrus cycle of the gilts according to an established schedule (Supplementary Data Table 4.5). The sonographic examination was performed with a Fazone CB (Fujifilm) with curved array type C9-3 with an ultrasound frequency of 3-9 MHz. The examination was performed at 6MHz frequency and 10 cm depth and a gain of 84 dB. The sonography examination represented a new method developed by Prof. Dr Johannes Kauffold[20,21]. The follicle, corpora hemorrhagica and corpora lutea were analyzed. Follicles with a diameter of 10 mm or larger, which did not ovulate were considered to be ovarian cysts. Single cysts were differentiated from polycystic ovarian

syndrome. The ovulation included the collapse of the preovulatory follicle and the appearance of the corpora hemorrhagica.

**Statistical Analysis** The effect of treatment and a comparison between the formulations was performed using a t-test: two sample assuming unequal variances with the software QI Macros 2017 (Denver, USA).

## 4.5 REFERENCES AND ACKNOWLEDGMENTS


1. Sims, E. E. & Worthington, H. E. C. Formulation studies on certain oily injection products. *Int. J. Pharm.* **24,** 287–296 (1985).

2. Buckwalter, F. H. & Dickison, H. L. The Effect of Vehicle and Particle Size on the Absorption, by the Intramuscular Route, of Procaine Penicillin G Suspensions. *J. Am. Pharm. Assoc. (Scientific ed.)* **47,** 661–666 (1958).

3. Sieger, G. M., Krueger, J. E., Osterberg, A. C. & Tedeschi, D. H. Sustained release forms of certain oxazepines for parenteral administration. (1977).

4. Lachman, L., Reiner, R. H., Shami, E. & Spector, W. Long-acting narcotic antagonist formulations. (1971).

5. Anschel, J. Relaxin composition and process for preparing same. (1959).

6. Nestor, J. J. & Vickery, B. H. Long acting depot injectable formulations for LH-RH analogues. (1979).

7. Geller, L. Injectable oily peptide preparations and processes for their manufacture. (1973).

8. Jeng, Y. N. & Patel, K. R. Non-aqueous injectable formulations for extended release of somatotropin. (2004).

9. Raymond, R. *et al. Recombinant Bovine Somatotropin ( rbST ): A Safety Assessment Recombinant Bovine Somatotropin ( rbST ): A Safety Assessment*. (2009).

10. Otranto, D. *et al.* Treatment and control of bovine hypodermosis with ivermectin long-acting injection (IVOMEC® GOLD). *Parasites and Vectors* **9,** 1–6 (2016).

11. Foster, Todd P.; Kiefer, D. L. Antibiotic oil suspensions. (1996).

12. Jindal, Kour Chand; Razzak, Majid; Sen, N. Novel pharmaceutical composition of ceftiofur. (2002).

13. Patel, R. Parenteral suspension: an overview. *Int J Curr Pharm Res* **2,** 4–13 (2010).

14. Burckbuchler, V. *et al.* Rheological and syringeability properties of highly concentrated human polyclonal immunoglobulin solutions. *Eur. J. Pharm. Biopharm.* **76,** 351–356 (2010).

15. Jethara, S. I., Patel, A. D. & Patel, M. R. Recent Patents Survey on Self Emulsifying Drug Delivery System. *Recent Pat. Drug Deliv. Formul.* **8,** 233–243 (2014).

16. Seljak, K. B. *et al.* A self-microemulsifying drug delivery system to overcome intestinal resveratrol toxicity and presystemic metabolism. *J. Pharm. Sci.* **103,** 3491–3500 (2010).

17. Momoh, M. A. & Esimone, C. O. Phospholipon 90H (P90H)-based PEGylated microscopic lipospheres delivery system for gentamicin: an antibiotic evaluation. *Asian Pac. J. Trop. Biomed.* **2,** 889–94 (2012).

18. Degalindez, M. J. G. and D. A. The self-emulsifying action of mixed surfactants in oil. *Acta Pharm. Suec* **13,** 361–372. (1976).

19. Weerapol, Y., Limmatvapirat, S., Nunthanid, J. & Sriamornsak, P. Self-Nanoemulsifying Drug Delivery System of Nifedipine: Impact of Hydrophilic–Lipophilic Balance and Molecular Structure of Mixed Surfactants. *AAPS PharmSciTech* **15,** 456–464 (2014).

20. Kauffold, J., Rautenberg, T., Richter, A., Waehner, M. & Sobiraj, A. Ultrasonographic characterization of the ovaries and the uterus in prepubertal and pubertal gilts. *Theriogenology*

**61,** 1635–1648 (2004).

21. Kauffold, J. & Althouse, G. C. An update on the use of B-mode ultrasonography in female pig reproduction. *Theriogenology* **67,** 901–911 (2007).

This work was supported by Veyx Pharma D-Schwarzenborn and DBU (Deutsche Bundesstiftung Umwelt) D-Osnabrueck. We would like to thank Aloys Hutten, Baerlocher GmBH, D-Unterschleissheim for donating Aluminium Stearate Alugel 30HEP with pharmaceutical quality for the preliminary studies as well as the *in vivo* studies. We are also grateful to Dr. Marie-Sousai Appavou, Julich Centre for Neutron Science JCNS Garching, D-Muenchen and Dr. Marianne Hanzlik, Technische Universitaet München, Fakultaet fuer Chemie, FG Elektronenmikroskopie Garching, D-Muenchen for performing TEM.

## 4.6 SUPPLEMENTARY DATA

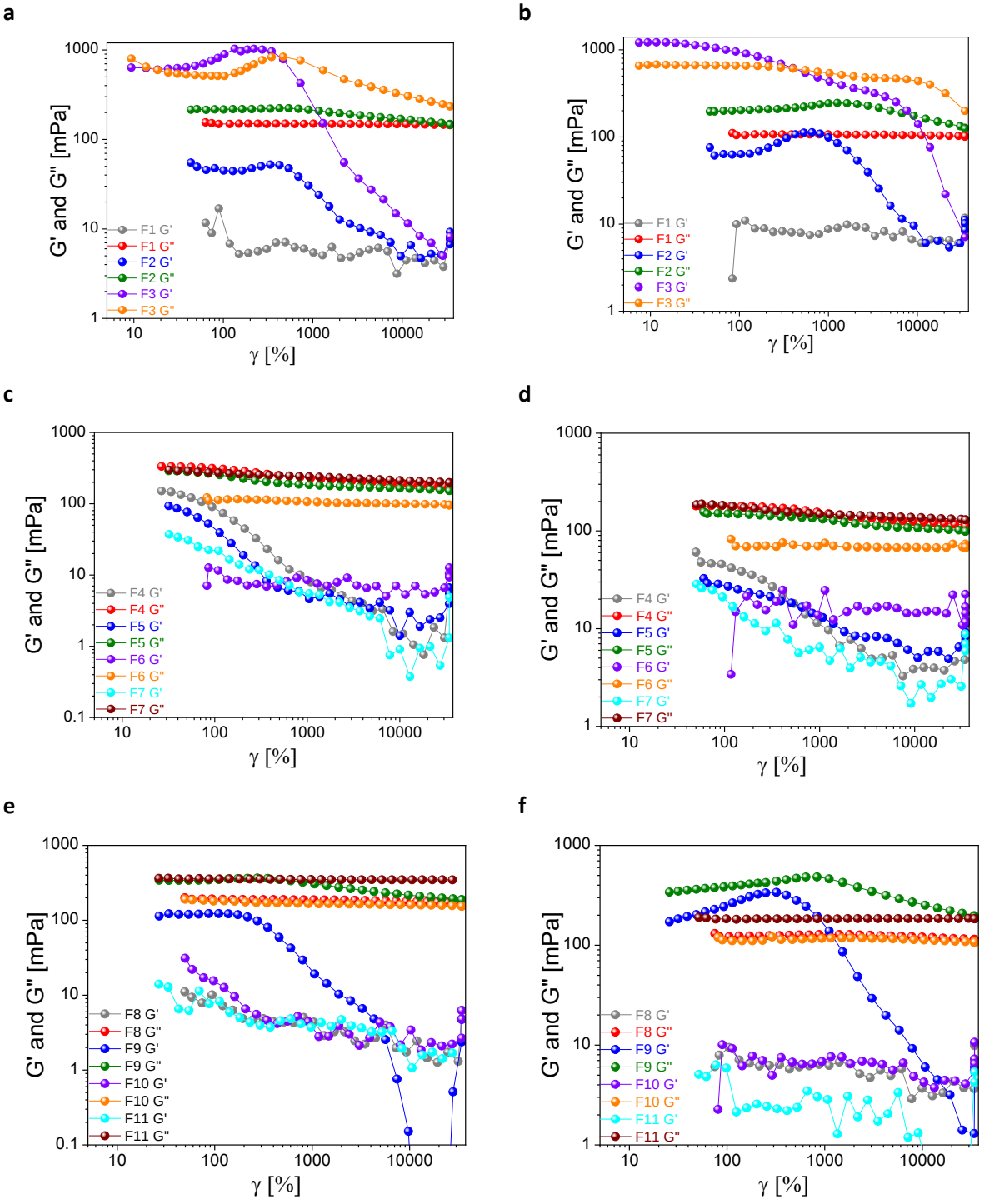


**Figure 4.13| Rheometer-Amplitude Sweep of F1-F11 1875 µg/ml GnRH [6-D-Phe] oil depot formulations**
(a), (c), (e) at 25° C (b), (d), (f) at 39° C

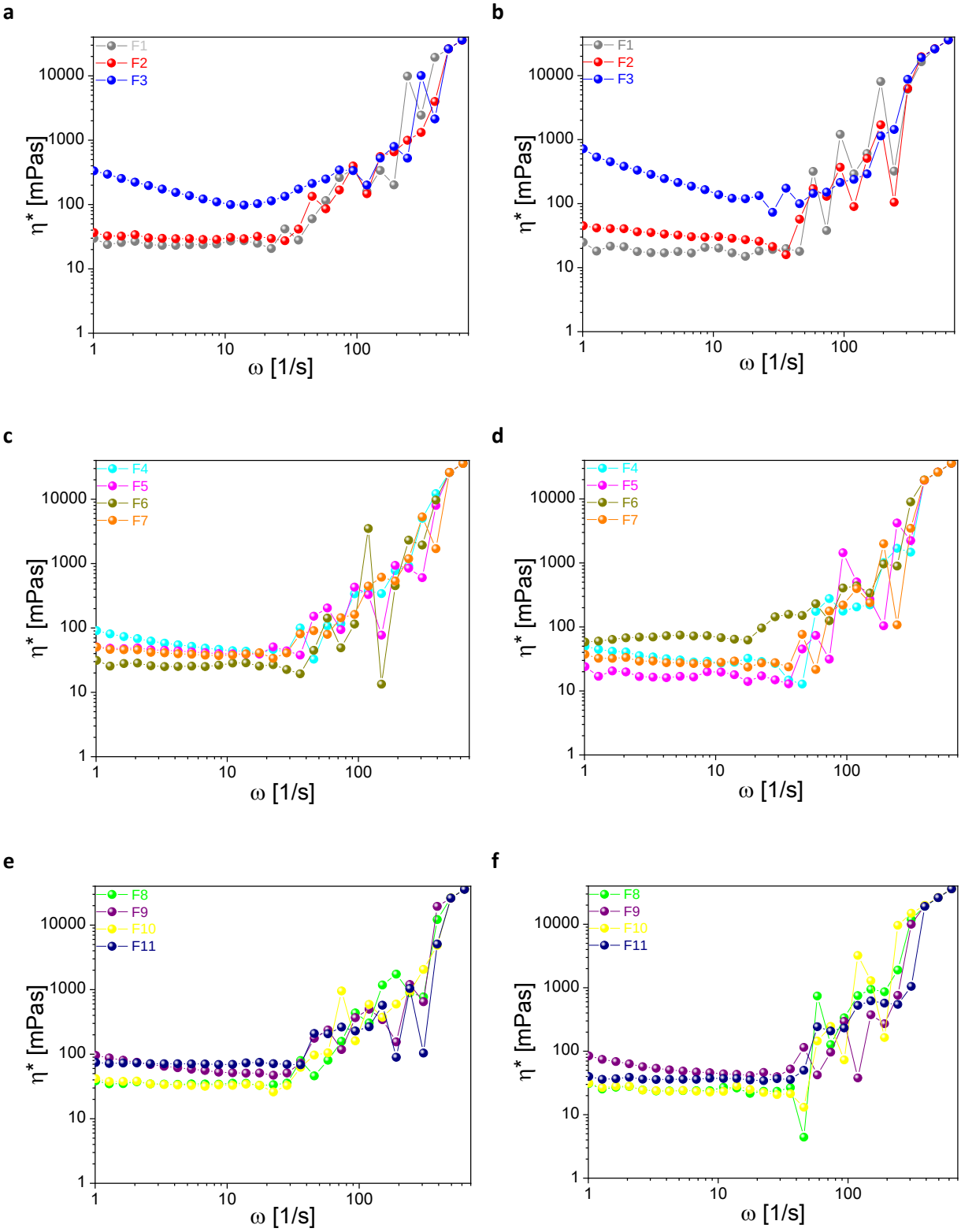


**Figure 4.14| Rheometer-Frequency Sweep of F1-F11 1875 µg/ml GnRH [6-D-Phe] oil depot formulations**
(a), (c), (e) at 25° C (b), (d), (f) at 39° C

| Step | | II. Preclinical Study<br>Oil Depot Suspension of Gonadorelin[6-D-Phe] | | | | |
|---|---|---|---|---|---|---|
| **1** | 1. day | Sonographic examination of the 25 gilts to determine sexual maturity | | | | |
| **2** | 11.-28. day | Daily administration of 5 ml Regumate® 4 mg/ml (= 20 mg Altrenogest) per oral over 18 days to inhibit the folicle development | | | | |
| **3** | 30. day<br>(40 h after last Regumate administration) | 4,2 ml Intergonan® 240 I.E./ml intramuscular(i.m.) (= 1000 IE equine chorionic-gonadotropin (eCG)) to stimulate the follicle development | | | | |
| **4** | 33. day<br>(78 h after eCG administration) | 1,0 ml Gonavet Veyx® i.m. (= 50 µg Gonadorelin[6-D-Phe]) to induce ovulation | | | | |
| **5** | 35. - 45. day | Daily clinical and sonographic examination of the 25 gilts | | | | |
| **6** | 46. day | Clinical and sonografic examination of the 25 gilts; separating the 25 gilts in 5 groups with different substances for application for intramuscular application | | | | |
| | | 5 Gilts<br>Group 1<br>1875 µg/mL<br>MCT + 3 % (w/w) Al-DiSt + 0.05 % (w/w) sorbitan monooleate + 0.05 % (w/w) polysorbate 80 | 5 Gilts<br>Group 2<br>1875 µg/mL<br>MCT + 3 % (w/w) Al-DiSt + 1 % (w/w) hydrogenated lecithin + 5 % (w/w) PEG-35 castor oil | 5 Gilts<br>Group 3<br>MCT | 5 Gilts<br>Group 4<br>3750µg/ml<br>MCT + 2 % (w/w) Al-DiSt | 5 Gilts<br>Group 5<br>3750µg/ml Castor oil: MCT 50:50 % (w/w) |
| **7** | 47. - 72. day | Daily clinical and sonographic examination of the 25 gilts | | | | |

**Table 4.5| *In vivo* Study Timetable**

| Group | Results |
|---|---|
| Placebo<br>**MCT**<br>**n=5** | normal cycle 6 d.p.i. and ovulation<br>normal cycle 7 d.p.i. and ovulation<br>normal cycle 7 d.p.i. and ovulation<br>normal cycle 7 d.p.i. and ovulation<br>normal cycle 8 d.p.i. and ovulation |
| GnRH [6-D-Phe] 3750 µg/ml<br>**MCT + 2 % (w/w) Al-DiSt**<br>**n=5** | 7 days cycle blocking effect<br>11 days cycle blocking effect<br>permanent cycle blocking effect<br>permanent cycle blocking effect<br>permanent cycle blocking effect |
| GnRH [6-D-Phe] 1875 µg/ml<br>**MCT + 3 % (w/w) Al-DiSt + 1 % (w/w) hydrogenated lecithin +**<br>**5 % (w/w) PEG-castor oil**<br>**n=5** | no cycle blocking effect<br>4 days cycle blocking effect<br>4 days cycle blocking effect<br>5 days cycle blocking effect<br>5 days cycle blocking effect |
| GnRH [6-D-Phe] 1875 µg/ml<br>**MCT + 3 % (w/w) Al-DiSt + 0.05 % (w/w) sorbitan monooleate + 0.05 % (w/w) polysorbate 80**<br>**n=5** | 10 days cycle blocking effect<br>13 days cycle blocking effect<br>permanent cycle blocking effect<br>permanent cycle blocking effect<br>permanent cycle blocking effect |
| GnRH [6-D-Phe] 3750 µg/ml<br>**Castor oil: MCT 50:50 % (w/w)**<br>**n=5** | no cycle blocking effect<br>no cycle blocking effect<br>4 days cycle blocking effect<br>5 days cycle blocking effect<br>8 days cycle blocking effect |

**Table 4.6| *In vivo* Study Results**

| t-Test: Two-Sample Assuming Unequal Variances | | a=0.05 | | | |
|---|---|---|---|---|---|
| **Equal Sample Sizes** | | | | | |
| | ***Placebo*** | ***Treatment 1*** **GnRH [6-D-Phe] 3750 µg/ml** MCT + 2 % (w/w) Al-DiSt | diff | 95% Confidence Interval | |
| **Mean** | **0.2** | **42.6** | -42.400 | -80.529 | -4.271 |
| **Variance** | **0.2** | **942.8** | | | |
| **Observations** | 5 | 5 | | | |
| **Hypothesized Mean Difference** | 0 | | | | |
| **df** | 4 | | | | |
| **t Stat** | -3.087 | | | | |
| **P(T<=t) one-tail - Difference < Hypothesized Difference** | 0.018 | 0.982 | Difference > Hypothesized Difference | | |
| **T Critical one-tail** | 2.132 | | | | |
| **P(T<=t) two-tail** | 0.037 | | Reject Null Hypothesis because p < 0.05 (Means are Different) | | |
| **T Critical Two-tail** | 2.776 | | | | |

**Table 4.7| Statistical analysis t-test placebo-GnRH [6-D-Phe] 3750 µg/ml MCT + 2 % (w/w) Al-DiSt**

| t-Test: Two-Sample Assuming Unequal Variances | | a=0.05 | | | |
|---|---|---|---|---|---|
| **Equal Sample Sizes** | | | | | |
| | ***Placebo*** | ***Treatment 2*** **GnRH [6-D-Phe] 1875 µg/ml** MCT + 3 % (w/w) Al-DiSt + 1 % (w/w) hydrogenated lecithin + 5 % (w/w) PEG-35 castor oil | diff | 95% Confidence Interval | |
| **Mean** | **0.2** | **3.6** | -3.400 | -6.034 | -0.766 |
| **Variance** | **0.2** | **4.3** | | | |
| **Observations** | 5 | 5 | | | |
| **Hypothesized Mean Difference** | 0 | | | | |
| **df** | 4 | | | | |
| **t Stat** | -3.584 | | | | |
| **P(T<=t) one-tail - Difference < Hypothesized Difference** | 0.012 | 0.988 | Difference > Hypothesized Difference | | |
| **T Critical one-tail** | 2.132 | | | | |
| **P(T<=t) two-tail** | 0.023 | | Reject Null Hypothesis because p < 0.05 (Means are Different) | | |
| **T Critical Two-tail** | 2.776 | | | | |

**Table 4.8| Statistical analysis t-test placebo-GnRH [6-D-Phe] 1875 µg/ml MCT + 3 % (w/w) Al-DiSt + 1 % (w/w) hydrogenated lecithin + 5 % (w/w) PEG-35 castor oil**

| t-Test: Two-Sample Assuming Unequal Variances | | a=0.05 | | | |
|---|---|---|---|---|---|
| **Equal Sample Sizes** | | | | | |
| | ***Placebo*** | ***Treatment 3*** **GnRH [6-D-Phe] 1875 µg/ml** MCT + 3 % (w/w) Al-DiSt + 0.05 % (w/w) sorbitan monooleate + 0.05 % (w/w) polysorbate 80 | diff | 95% Confidence Interval | |
| **Mean** | **0.2** | **43.6** | -43.400 | -79.813 | -6.987 |
| **Variance** | **0.2** | **859.8** | | | |
| **Observations** | 5 | 5 | | | |
| **Hypothesized Mean Difference** | 0 | | | | |
| **df** | 4 | | | | |
| **t Stat** | -3.309 | | | | |
| **P(T<=t) one-tail - Difference < Hypothesized Difference** | 0.015 | 0.985 | Difference > Hypothesized Difference | | |
| **T Critical one-tail** | 2.132 | | | | |
| **P(T<=t) two-tail** | 0.030 | | Reject Null Hypothesis because p < 0.05 (Means are Different) | | |
| **T Critical Two-tail** | 2.776 | | | | |

**Table 4.9| Statistical analysis t-test placebo-GnRH [6-D-Phe] 1875 µg/ml MCT + 3 % (w/w) Al-DiSt + 0.05 % (w/w) sorbitan monooleate + 0.05 % (w/w) polysorbate 80**

| t-Test: Two-Sample Assuming Unequal Variances | | a=0.05 | | | |
|---|---|---|---|---|---|
| **Equal Sample Sizes** | | | | | |
| | ***Placebo*** | ***Treatment 4*** **GnRH [6-D-Phe] 3750 µg/ml** Castor oil: MCT 50:50 % (w/w) | diff | 95% Confidence Interval | |
| **Mean** | **0.2** | **3.4** | -3.200 | -7.501 | 1.101 |
| **Variance** | **0.2** | **11.8** | | | |
| **Observations** | 5 | 5 | | | |
| **Hypothesized Mean Difference** | 0 | | | | |
| **df** | 4 | | | | |
| **t Stat** | -2.066 | | | | |
| **P(T<=t) one-tail - Difference < Hypothesized Difference** | 0.054 | 0.946 | Difference > Hypothesized Difference | | |
| **T Critical one-tail** | 2.132 | | | | |
| **P(T<=t) two-tail** | 0.108 | | Cannot reject Null Hypothesis because p > 0.05 (Means are the same) | | |
| **T Critical Two-tail** | 2.776 | | | | |

**Table 4.10| Statistical analysis t-test placebo-GnRH [6-D-Phe] 3750 µg/ml Castor oil: MCT 50:50 % (w/w)**

## 4.7 FIGURES AND TABLES

# CHAPTER FIVE

# RELEASE POLYMERS

# 5 GnRH [6-D-Phe] acetate Oil Depot Suspension: The Effect of Polymers on the Release Characteristics

Yordanka Yordanova[1], Laura Liberto[1], Kathrin Hoffmann[1], Wolfgang Zaremba[2] Wolfgang Friess[1]

1. Department of Pharmacy, Pharmaceutical Technology & Biopharmaceutics, Ludwig-Maximilians-Universitaet, Butenandtstrasse 5, 81377 Muenchen, Germany
2. Veyx Pharma GmbH, Scientific Department, Soehreweg 6, 34639 Schwarzenborn, Germany

**The incorporation of gelling agent, wetting agent and resuspendibility enhancer considerably improves the applicability and homogeneity of oily suspensions of GnRH [6-D-Phe]. The self-emulsifying character of vehicles based on medium chain triglycerides (MCT) with aluminiumdistearate (Al-DiSt), hydrogenated lecithin and macrogol-hydrogenated castor oil led to sustained and controlled release of GnRH [6-D-Phe]. It provided an estrus cycle blockage in swine for 4 to 5 days with adequate synchronicity. To further sustain the effect, HPC, HPMC and HP-β-CD polymers were added to the formulation. The resulting suspensions were evaluated *in vitro* with respect to rheology, particles size and release. The incorporation of HPMC and HPC resulted in a higher viscosity in castor oil-MCT in comparison to the Al-DiSt gelled MCT with hydrogenated lecithin and PEG-35 castor oil. The median particle size $D_{v50}$ for the formulations with HPMC and HPC remained nearly unchanged in comparison to the formulation with pure GnRH [6-D-Phe]. 2 % of low and high molecular HPMC, HPC and HP-β-CD were insufficient to sustain the further release of GnRH [6-D-Phe] and to achieve a higher percentage of total released GnRH [6-D-Phe].**

## 5.1 INTRODUCTION

Many different vehicles including microparticles, liposomes and nanoparticles have been investigated for the parenteral delivery of proteins and peptides. The biodegradable microparticles are in most cases based on poly (D,L-lactide-co-glycolide) (PLGA) because of its long safety history. The success of PLGA is evidenced by the numerous marketed formulations such as Lupron Depot®, Decapeptyl®, Sandostatin LAR® Depot and Somatuline® LA[1].

Over the last years self-emulsifying drug delivery systems have emerged as a vital strategy to formulate poor water-soluble compounds for oral bioavailability enhancement[2]. Only recently have they gained on importance as delivery strategy for proteins and peptides, where the hydrophilic macromolecules get entrapped in the oil phase of the emulsion, protecting them from enzymatic degradation[3]. Our current formulation approach uses the advantages of such a formulation for the controlled and sustained release of GnRH [6-D-Phe]. The self-emulsifying system is composed of aluminiumdistearate (Al-DiSt) gelled MCT and two surfactants, hydrogenated lecithin and PEG-35 castor oil[4]. The incorporation of Al-DiSt inhibited a burst release. However, a major challenge of the gelled matrix remains its ability to encapsulate the GnRH [6-D-Phe] peptide upon contact with the aqueous medium, inhibiting the peptide

release[2]. This problem might be solved by adding polymeric precipitation inhibitors, which have been shown to improve the bioavailability and absorption variability of poorly water soluble compounds, e.g. hydroxypropylmethyl cellulose (HPMC) in dispersion formulations[5–8] and a supersaturable self-emulsifying drug delivery system of paclitaxel[9].

In the current study GnRH [6-D-Phe] acetate was combined with hydrophilic polymers, freeze-dried and incorporated into Al-DiSt gelled MCT with hydrogenated lecithin and PEG-35 castor oil and into a castor oil-MCT mix. The effect of HPMC, hydroxypropyl cellulose (HPC), hydroxypropyl-beta-cyclodextrin (HP-β-CD) and their interaction with GnRH [6-D-Phe] and Al-DiST gelled oil matrix was analyzed. The results were used to identify a polymer_GnRH [6-D-Phe] combination with prolonged and complete release characteristics. Furthermore, HPMC of different viscosity grades was investigated as to determine whether longer chain length and hence higher viscosity might be beneficial for the complete and sustained release of GnRH [6-D-Phe].

## 5.2 RESULTS AND DISCUSSION

### *5.2.1 GnRH [6-D-Phe]_Polymer Oil Depot Suspension*

Mixtures of 0.2 % (w/w) GnRH [6-D-Phe] and 2 % (w/w) HPMC, HPC and HP-β-CD were freeze-dried and incorporated at 1875 µg/ml GnRH [6-D-Phe] in the oil vehicles. Oil vehicle 1 (OV1) consists of MCT + 3 % (w/w) Al-DiSt + 1 % (w/w) hydrogenated lecithin + 5 % (w/w) polyoxyl (PEG)-35 castor oil. Oil vehicle 2 (OV2) is composed of castor oil: MCT 50:50 % (w/w) (Figure 5.1). In total 12 formulations were composed (Table 5.1).

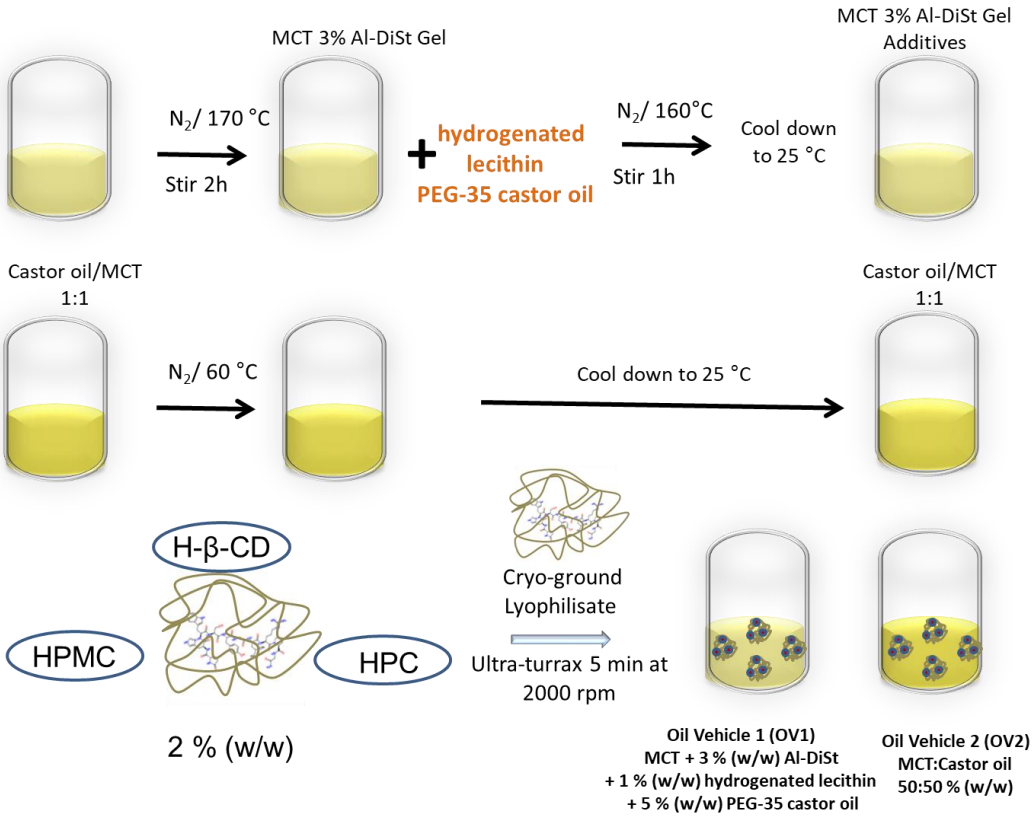


**Figure 5.1| GnRH [6-D-Phe]_Polymer oil depot suspension**

| Formulations | Polymer % (w/w) | GnRH [6-D-Phe] % (w/w) |
|---|---|---|
| GnRH [6-D-Phe]_HPMC K4M_OV1 | 2 | 0.2 |
| GnRH [6-D-Phe]_HPMC K4M_OV2 | 2 | 0.2 |
| GnRH [6-D-Phe]_HPMC K100M_OV1 | 2 | 0.2 |
| GnRH [6-D-Phe]_HPMC K100M_OV2 | 2 | 0.2 |
| GnRH [6-D-Phe]_HPMC K200_OV1 | 2 | 0.2 |
| GnRH [6-D-Phe]_HPMC K200M_OV2 | 2 | 0.2 |
| GnRH [6-D-Phe]_HPC_OV1 | 2 | 0.2 |
| GnRH [6-D-Phe]_HPC_OV2 | 2 | 0.2 |
| GnRH [6-D-Phe]_HP-β-Cyclodextrin_OV1 | 2 | 0.2 |
| GnRH [6-D-Phe]_HP-β-Cyclodextrin_OV2 | 2 | 0.2 |
| GnRH [6-D-Phe]_OV1 | | 0.2 |
| GnRH [6-D-Phe]_OV2 | | 0.2 |

**Table 5.1| Composition of GnRH [6-D-Phe]_Polymer oil depot formulations**

### *5.2.2 Rheology*

Aqueous solutions of GnRH [6-D-Phe]_HPMC and HPC showed thixotropic behaviour with increasing viscosity in the order HPMC K4M~HPC< HPMC K100M< HPMC K200M (Supplementary Data Figure 5.8). GnRH [6-D-Phe]_HPMC K4M and HPC showed nearly identical shear-thinning behaviour at 25° C and 39° C. The incorporation of GnRH [6-D-Phe]_HPMC and GnRH [6-D-Phe]_HPC into the oil vehicles led to a weakened polymer network and viscosity decrease[10].

Whereas the inclusion of HPC and HPMC at 2 % (w/w) resulted in a higher viscosity in Castor oil-MCT in comparison to pure GnRH [6-D-Phe], it did not influence the viscosity of the Al-DiSt gelled MCT with hydrogenated lecithin and PEG-35 castor oil (Figure 5.2). Fluctuations in viscosity values are related to individual large particles or particle agglomerates exceeding the size of the measuring gap of 0.042 mm resulting in a stick-slip phenomenon. This emerged primarily with castor oil – MCT based formulations and can be explained by the absence of stabilizing agents, resulting in the formation of difficult to separate particle agglomerates.

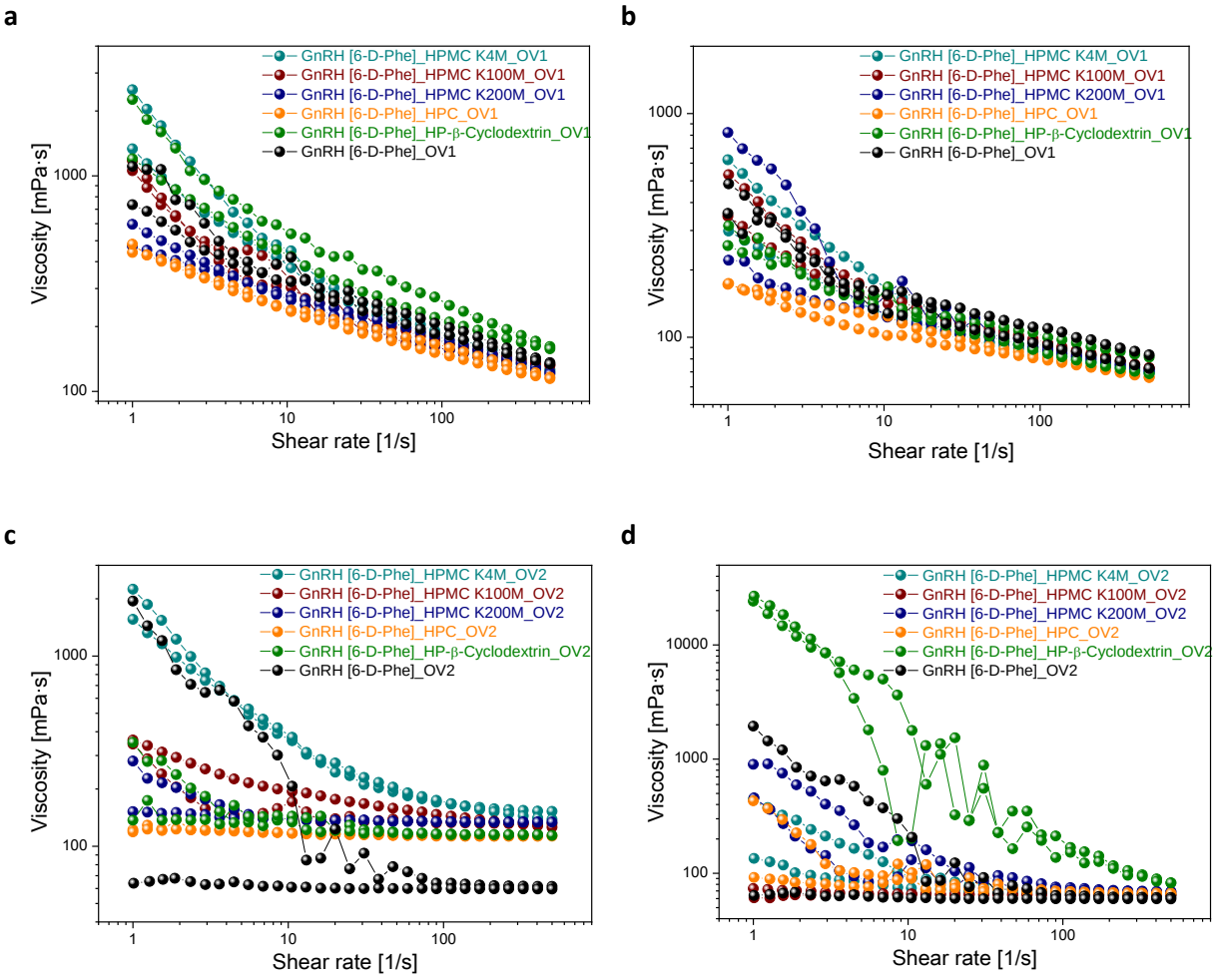


**Figure 5.2| Rheology of GnRH [6-D-Phe]_Polymer oil depot formulations**
(a), (c) at 25° C (b), (d) at 39° C

### *5.2.3 Particle Size Distribution and Characterization*

The median particle size $D_{v50}$ of the dispersed formulations with HPMC and HPC was comparable (Figure 5.3). GnRH [6-D-Phe]_HP-β-CD displayed particles in the lowest $D_{v50}$ range of 4.7-5.7 µm (Table 5.2). The larger particles of HPMC and HPC resulted most probably from agglomeration. However, their size did not exceed the critical value of 0.325 mm required for an unproblematic application through 16 G needle[11,12].

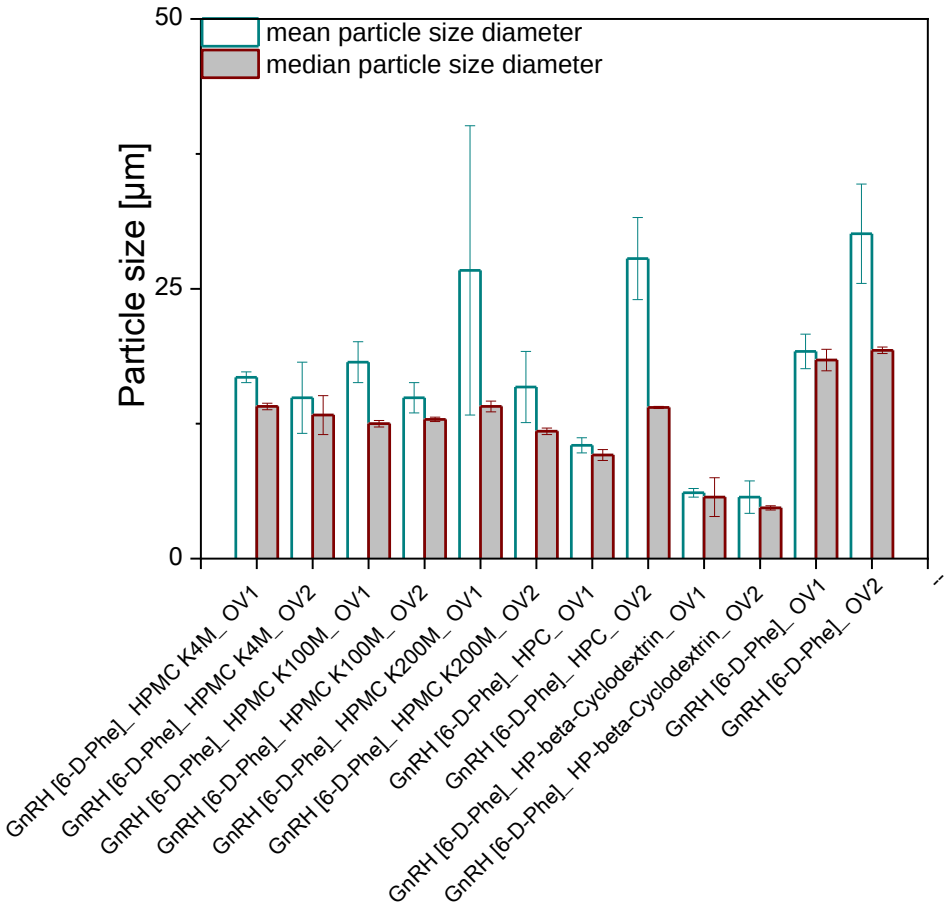


**Figure 5.3| Mean (the mean particle diameter over volume) and median particle size of GnRH [6-D-Phe]_Polymer oil depot formulations**

| Formulation | $D_{v50}$ [µm] ± SD | $D_{v90}$ [µm] ± SD |
|---|---|---|
| GnRH [6-D-Phe]_HPMC K4M_OV1 | 14.1 ± 0.3 | 29.1 ± 1.6 |
| GnRH [6-D-Phe]_HPMC K4M_OV2 | 13.3 ± 1.8 | 25.5 ± 7.4 |
| GnRH [6-D-Phe]_HPMC K100M_OV1 | 12.5 ± 0.3 | 20.3 ± 3.9 |
| GnRH [6-D-Phe]_HPMC K100M_OV2 | 12.9 ± 0.2 | 22.2 ± 0.9 |
| GnRH [6-D-Phe]_HPMC K200_OV1 | 14.1 ± 0.3 | 34.3 ± 1.5 |
| GnRH [6-D-Phe]_HPMC K200M_OV2 | 11.8 ± 0.3 | 19.9 ± 1.3 |
| GnRH [6-D-Phe]_HPC_OV1 | 9.6 ± 0.1 | 16.3 ± 0.1 |
| GnRH [6-D-Phe]_HPC_OV2 | 14.0 ± 0.5 | 30.4 ± 1.7 |
| GnRH [6-D-Phe]_HP-β-Cyclodextrin_OV1 | 5.7 ± 0.2 | 10.2 ± 0.9 |
| GnRH [6-D-Phe]_HP-β-Cyclodextrin_OV2 | 4.7 ± 0.5 | 9.4 ± 1.4 |
| GnRH [6-D-Phe]_OV1 | 18.4 ± 1.0 | 27.1 ± 2.3 |
| GnRH [6-D-Phe]_OV2 | 19.3 ± 1.8 | 34.5 ± 9.1 |

**Table 5.2| Particle size distribution and $D_{v50}$ and $D_{v90}$ fractions**

The cryoground GnRH [6-D-Phe]_polymer lyophilisate was platelet-like in case of HPMC and in the higher µm range in comparison to HPC and HP-β-CD (Figure 5.4).

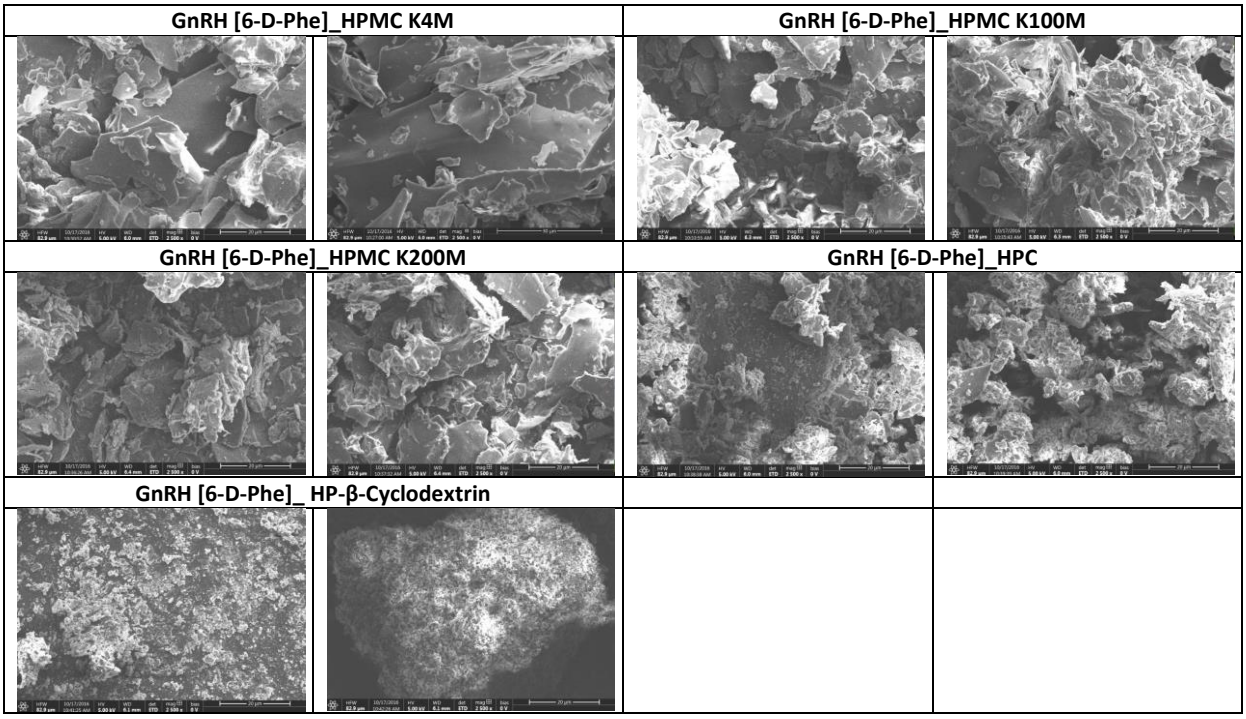


**Figure 5.4| Scanning electron microscopy (SEM) of the cryoground GnRH [6-D-Phe]_polymer**

### *5.2.4 Self-Emulsifying Character*

GnRH [6-D-Phe]_HPMC and GnRH [6-D-Phe]_HPC in MCT + 3 % (w/w) Al-DiSt + 1 % (w/w) hydrogenated lecithin + 5 % (w/w) PEG-35 castor oil formed nanostructures upon injection in PBS (pH 7.4) (Figure 5.5). In contrast, GnRH [6-D-Phe]_HPC in castor oil: MCT 50:50 % (w/w) formed individual large HPC structures in the µm range. HPMC and HPC might interact with hydrogenated lecithin and PEG-35 castor oil at the aqueous/oil interface after injection, leading to the formation of micelles of surfactant or polymer as well as mixed micelles[13]. HPMC and HPC absorb at the oil/water interface creating a diffuse corona around emulsion droplets with a steric repulsive effect[14,15].

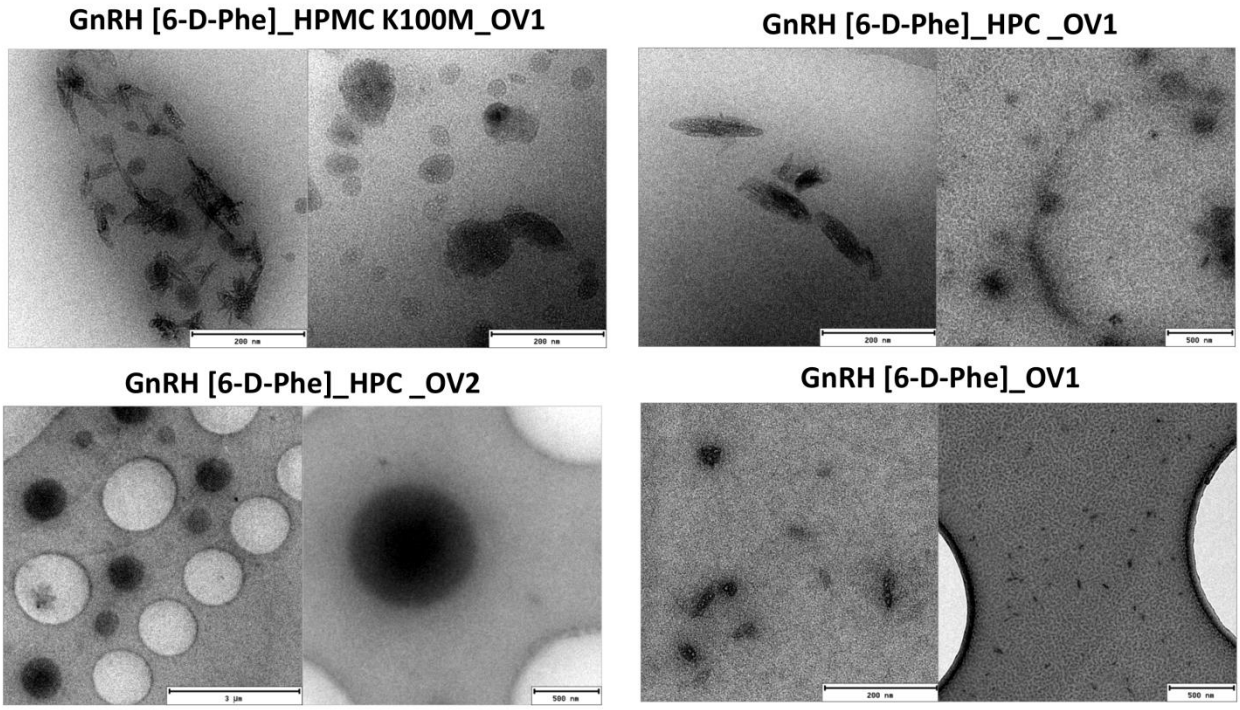


**Figure 5.5| Transmission electron microscope (TEM) images after injection in 6 mL PBS (pH 7.4) at 39° C in an incubated shaker after 24h**

MCT + 3 % (w/w) Al-DiSt + 1 % (w/w) hydrogenated lecithin + 5 % (w/w) PEG-35 castor oil act as a self-emulsifying drug delivery system[16,17,18]. Upon injection into PBS (pH 7.4), all formulations formed small droplets under 200 nm. In contrast, the majority of castor oil: MCT 50:50 % (w/w) formulations generated an unstable emulsion with droplet size larger than 600nm (Table 5.3).

| Formulation | Z-average d ± SD [nm] | PDI ± SD |
|---|---|---|
| GnRH [6-D-Phe]_HPMC K4M_OV1 | 233.1 ± 24.7 | 0.519 ± 0.1 |
| GnRH [6-D-Phe]_HPMC K4M_OV2 | 7090.3 ± 809.2 | 0.355 ± 0.2 |
| GnRH [6-D-Phe]_HPMC K100M_OV1 | 85.8 ± 5.4 | 0.567 ± 0.1 |
| GnRH [6-D-Phe]_HPMC K100M_OV2 | 673.9 ± 134.7 | 0.638 ± 0.1 |
| GnRH [6-D-Phe]_HPMC K200M_OV1 | 172.0 ± 26.9 | 0.329 ± 0.1 |
| GnRH [6-D-Phe]_HPMC K200M_OV2 | 660.8 ± 83.3 | 0.518 ± 0.1 |
| GnRH [6-D-Phe]_HPC_OV1 | 94.3 ± 12.2 | 0.317 ± 0.1 |
| GnRH [6-D-Phe]_HPC_OV2 | 650.2 ± 109.9 | 0.483 ± 0.1 |
| GnRH [6-D-Phe]_ HP-β-Cyclodextrin_OV1 | 78.6 ± 2.3 | 0.391 ± 0.1 |
| GnRH [6-D-Phe]_ HP-β-Cyclodextrin_OV2 | 637.7 ± 93.1 | 0.493 ± 0.1 |
| GnRH [6-D-Phe]_OV1 | 97.4 ± 0.7 | 0.446 ± 0.1 |
| GnRH [6-D-Phe]_OV2 | 677.5 ± 30.9 | 0.609 ± 0.1 |

**Table 5.3| Droplet size determination after injection of GnRH [6-D-Phe]_polymer oil depot formulations in 6 mL PBS (pH 7.4) at 39° C in an incubated shaker after 24h**

The MCT + 3 % (w/w) Al-DiSt + 1 % (w/w) hydrogenated lecithin + 5 % (w/w) PEG-35 castor oil tends to spread upon injection into a hydrogel to a greater extent in comparison to castor oil: MCT 50:50 % (w/w). This was not affected by the addition of polymer (Figure 5.6).

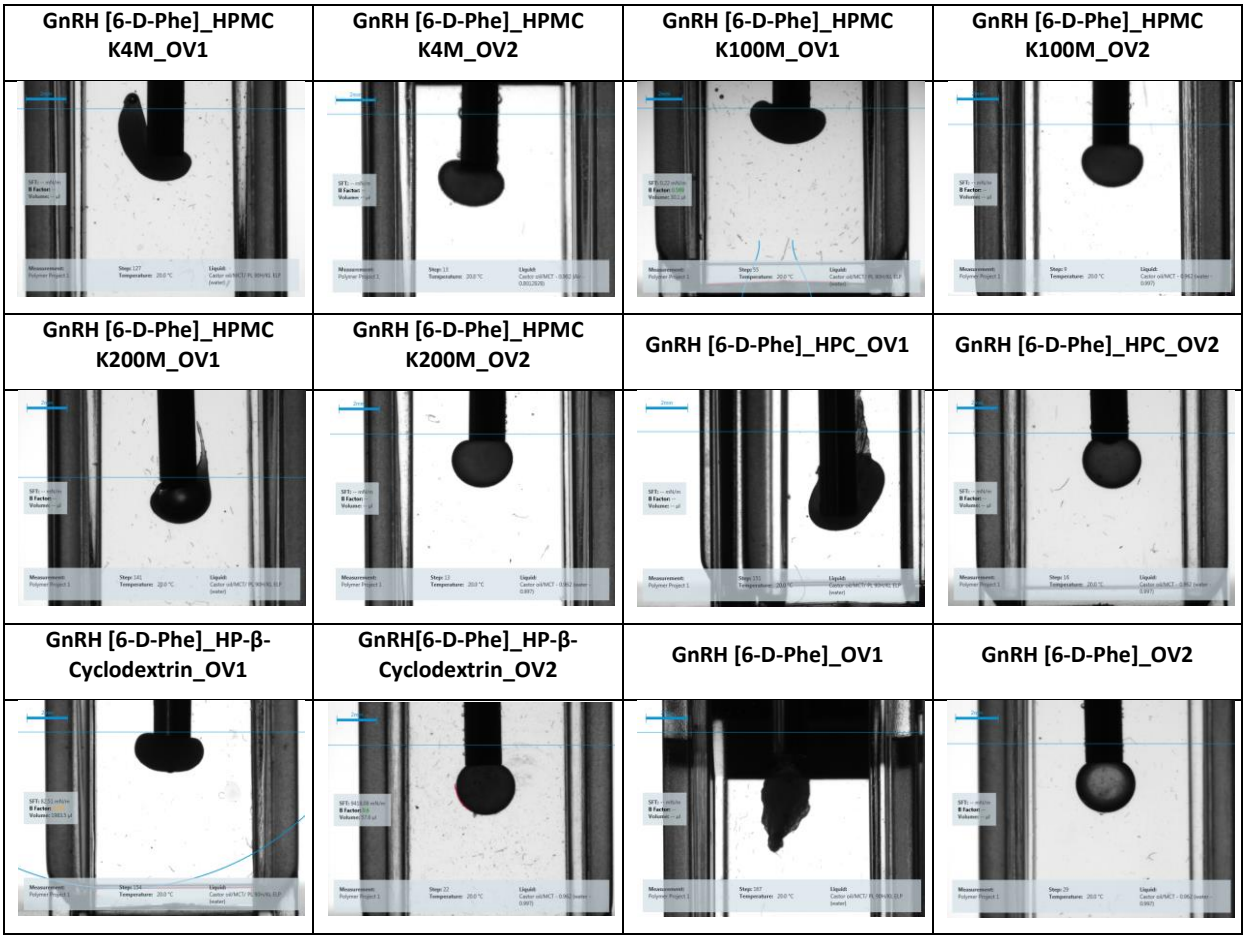


**Figure 5.6| Drop shape analysis in 0.5 % Benecel K100M in PBS (pH 7.4) of GnRH [6-D-Phe]_Polymer oil depot formulations**

### *5.2.5 In vitro Release Studies*

Both the purely oil based vehicle castor oil: MCT 50:50 % (w/w) and the formulation based on MCT, hydrogenated lecithin and PEG-35 castor oil exhibited a substantial initial burst. Approximately 80 % GnRH [6-D-Phe] was released in the first 3 hours. In contrast adding 3 % Al-DiSt to the latter formulation resulted in suppression of the burst release of GnRH [6-D-Phe] (Figure 5.7). Al-DiSt gelled oil vehicle might increase the water repellence and hence slow down the diffusion of the aqueous phase into the oil depot[4]. Contrary to our initial assumption of achieving a more complete and sustained release of GnRH [6-D-Phe] through HPMC, HPC and HP-β-CD incorporation, after 3 – 4 days the release came to rest similar to the reference (Supplementary Data Figure 5.9).

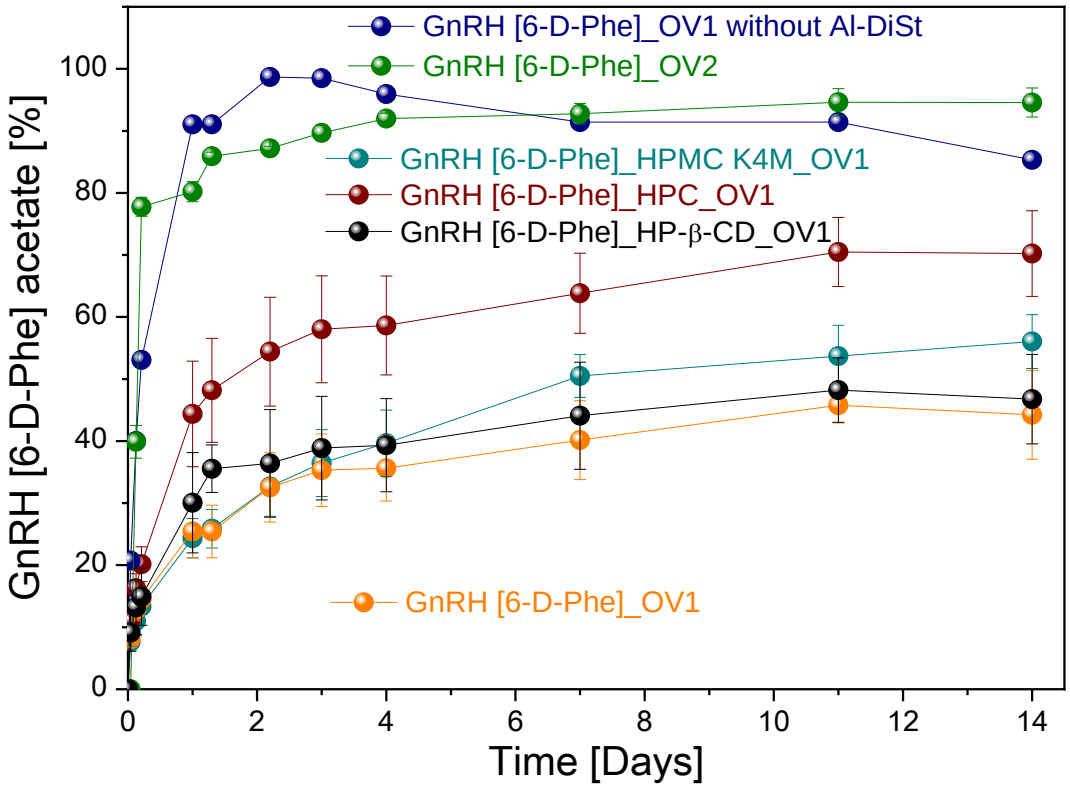


**Figure 5.7| *In vitro* release profiles of GnRH [6-D-Phe] Polymer oil depot formulations in visking dialysis tubing, MWCO 12 – 14 kD**

## 5.3 CONCLUSION

The effect of the incorporated 2 % HPMC, HPC and HP-β-CD into GnRH [6-D-Phe] on the suspension viscosity was more pronounced with castor oil: MCT 50:50 % (w/w). When suspended in gelled self-emulsifying vehicle of MCT + 3 % (w/w) Al-DiSt + 1 % (w/w) hydrogenated lecithin+ 5 % (w/w) PEG-35 castor oil, a shear thinning behaviour resulted, which was independent of polymer class or chain length. Upon injection in PBS pH 7.4, 3 % Al-DiSt gelled MCT with hydrogenated lecithin and PEG-35 castor oil formed multiple nanostructures in the 200-1000 nm range, whereas castor oil – MCT displayed individual structures in the higher µm range. *In vitro* burst release was suppressed with the self-emulsifying vehicle in comparison to the pure oil. 2 % of low and high molecular HPMC as well as HPC and HP-β-CD were insufficient to achieve a higher percentage of the total released GnRH [6-D-Phe]. Therefore to further extend the release interval and achieve a more complete release of GnRH [6-D-Phe], the addition of complex forming metal salts may be advantageous.

## 5.4 MATERIALS AND METHODS

**Gonadorelin [6-D-Phe] acetate peptide** (pE1–H2–W3–S4–Y5–(D)F6–L7–R8–P9–G10–NH2) or (pGlu-His-Trp-Ser-Tyr-D-Phe-Leu-Arg-Pro-Gly-NH2) was provided by BFC Biopept-Feinchemie as lyophilized powder and acetate salt (purity 99.76 %, water content 6.73 % and acetate peptide ratio (MW/MW) 1.8). **Gelling agents**: Aluminiumdistearte (Alugel 30 ®HEP), Baerlocher, D-Unterschleissheim; **Wetting agents**: hydrogenated phosphatidylcholine(lecithin) (Phospholipon®90H) Lipod D-Ludwigshafen; **Resuspendibility enhancer**: Polyoxyl (PEG)-35 castor oil (Kolliphor®ELP) BTC Europe, D-Burgbergheim; **Polymers**: Hydroxypropylmethylcellulose (HPMC) K4M, hydroxypropylmethylcellulose (HPMC) K100M, hydroxypropylmethylcellulose (HPMC) K200M, hydroxypropylcellulose (HPC), 2-hydroxypropyl-β-cyclodextrin HP7 (Ashland, D-Düsseldorf); **Oil vehicle**: miglyol®812 (MCT) Caesar & Loretz, D-Hilden, castor oil (Gustav Heess, D-Leonberg).

**GnRH [6-D-Phe]_polymer complexes preparation** Solution of 0.2 % (w/w) GnRH [6-D-Phe] with 2 % (w/w) polymer were prepared. GnRH [6-D-Phe] -polymer mixtures were freeze dried using a Christ Epsilon 2-6 D freeze-dryer (Martin Christ Gefriertrocknungsanlagen GmbH, D-Osterode) (ambient pressure; freezing 3 h, −50° C, 150 mTorr; primary drying: 60 h,−20° C; secondary drying: 18 h, 20° C) with process and plant control LPC plus SCADA software.

**GnRH [6-D-Phe] polymer lyophilisate micronization** The cryogenic micronization of GnRH [6-D-Phe] polymer lyophilisate was performed using a Retsch Cryo Mill (Retsch Technology, Haan, Germany). The grinding process was performed for the duration of 2 minutes at 25Hz with a precooling phase of 5 min in liquid nitrogen.

**GnRH [6-D-Phe] polymer oil depot preparation** The GnRH [6-D-Phe] polymer formulations preparation was performed in a two-step process. The gelling agent Al-DiSt was weighed and suspended in the oil vehicle MCT to a final weight of 95 g (corresponding to 100 mL). The prepared mixture was heated at 174° C for 2 hours under inert atmosphere ($N_2$). After cooling down to 25° C hydrogenated lecithin and PEG-35 castor oil were incorporated into the gelled oil matrix and stirred at 160° C for 1 hour under $N_2$. The castor oil: MCT 50:50 % (w/w) matrix was heated and agitated under inert $N_2$ at 60° C and then cooled down to room temperature at 25° C. 200 mg cryoground GnRH [6-D-Phe]_polymer lyophilisate was suspended in the prepared oil matrices at temperature of 25° C using an Ultra-Turrax T-10 basic (IKA Labortechnik, Germany) for 5 minutes at 2000 rpm. The GnRH [6-D-Phe] Polymer oil depot suspensions were aliquoted in 20R glass vials. References GnRH [6-D-Phe] were prepared using bulk GnRH [6-D-Phe] lyophilisate.

**Rheology: Viscosity profile** Viscosity measurement and flow curves evaluation was performed with MCR 100 (Anton Paar Germany, Ostfildern-Scharnhausen) cone plate system CP – 1 (50 mm diameter, a cone angle of 1°, and a gap of 0.042 mm). The viscosity η was defined depending on the shear rate $\dot{\gamma}$ and measuring sections a) 0 – 500 $s^{-1}$ (30 points, 6 s per point; 180 s measurement time), b) 500 $s^{-1}$ (1 point, 6 s per point, 6 s measurement time), c) 500 – 0 $s^{-1}$ (30 points, 6 s per point, 180 s measurement time).

**GnRH [6-D-Phe] extraction from the polymer and oil matrix** The GnRH [6-D-Phe] was extracted from the prepared GnRH [6-D-Phe] polymer oil depot suspensions using dichloromethane (DCM) in combination with PBS (pH 7.4). 2 mL oil depot suspension was weighted into a falcon tube, 4 mL DCM and 6 mL PBS-buffer (pH 7.4) were added. The tube was shaken or vortexed at room temperature (25° C) and put into a horizontal shaker 3017 (GFL, Germany) at 25° C and 100 rpm for 48 h. The RP-HPLC analysis was performed at 220 nm.

**GnRH [6-D-Phe] polymer particle size distribution and characterization** The particle size distribution of GnRH [6-D-Phe] polymer oil depot suspensions was analysed employing a Laser Diffraction Particle Size Analyzer LA-950 (Retsch Technology, Haan). The samples were prepared in triplicate (n=3). 0.2 mL of the oil suspension withdrawn from the vial and measured in a solution of 1 % span 80 in isooctane (m/v) in a standard measuring cell with 10 mL volume.

**Scanning Electron Microscopy**. The SEM images of the cryoground GnRH [6-D-Phe]_polymer lyophilisate were taken with FEI Helios G3 UC instrument with EDX detector (Hillboro, Oregon, USA) with Microscope Control Version 10.1.1 software. SEM micrographs were collected at a magnification of 2500 and accelerating voltage of 5.0KV

**Oil-Water Interface Tension and Drop Shape Analyser** The wettability and spreading were analysed with pendant drop measurements on a Drop Shape Analyser (Krüss, Germany), using NORM-JECT 1 mL Tuberkulin + Luer syringes (Henke-Sass-Wolf, Germany) and a NE94 steel needle with 1.8 mm diameter (Krüss, Hamburg, Germany). The surrounding phase in a semi-micro PMMA cuvettes (Brand GmBH, Wertheim, Germany) was 0.5 % (m/m) Benecel K100M in PBS-buffer (pH 7.4), resembling the muscle tissue of the swine.

**SEDD (Microemulsion) characterization** The microemulsion droplet size was determined by dynamic light scattering using Zetasizer Nano-ZS (Malvern Instruments Ltd., Herrenberg, Germany). 1 mL of the formulations was injected into 6 mL in PBS-buffer (pH 7.4) and shaken in an incubated shaker 3031 (GFL, Burgwedel, Germany) at 39° C and 60 rpm over 24 h. The diluted and filtered samples were measured in disposable Plastibrand semi-micro PMMA cuvettes (Brand GmBH, Wertheim, Germany) after 20 seconds equilibration time at 25° C and with PBS as dispersant. Positioning, attenuation selection and measuring duration as well as number of sub runs for the three performed measurements per sample were optimised automatically for each run by the Zetasizer Software 6.32. Z-average and polydispersity index (PdI) were calculated applying the general purpose (normal resolution) analysis model. TEM was applied to analyse the microemulsion structures. 5 µl of the filtered sample but undiluted sample was pipetted on a Quantifoil ®Multi A holey carbon coated grid blotted and allowed to air dry at room temperature. A RT-TEM at a JEOL 200 kV JEM-FS2200 instrument and a RT EM-21010/EM-21311HTR specimen holder were used.

***In vitro* release study** In the *in vitro* release study 1.5 mL formulation were filled in VISKING® dialysis tubing, MWCO 12 – 14kD, RC, 28 mm (SERVA, Germany). The release medium was 30 mL PBS-buffer (pH 7.4). The *in vitro* evaluation was performed in duplicates and in an incubated shaker 3031 (GFL, Germany) at 39° C and 60 rpm. 1 mL sample was used for the RP-HPLC analysis at the following intervals 1 h, 3 h, 5 h, 7 h, 22 h, 25 h, 28 h, 46 h, 52 h, 76 h, 100 h, 172 h, 196 h, 220 h, and 336 h (14 days). The GnRH [6-D-Phe] content in the oil vehicle and in the donor cell was extracted using 2 mL DCM and 2 mL PBS (pH 7.4). After 24 hours of an equilibration of the drug between the two phases the drug quantity in the supernatant was determined with RP-HPLC.

**Determination of the GnRH [6-D-Phe] (RP-HPLC)** The GnRH [6-D-Phe] content was analysed by RP-HPLC using a LUNA C8 (4.6 mm x 250 mm; size = 5 µm; Phenomenex, USA) column, with a C8 pre-column (4 mm x 3 mm; size = 5 µm) at an HPLC Agilent 1100/1200 series (Agilent Technologies, USA) (mobile phase A (water + 1 mL/L Trifluoroacetic acid (TFA) (v/v)) and mobile phase B (800 g Acetonitrile + 200 g water + 1.2 mL TFA), 1.1 mL/min flow, column temperature 40° C, and autosampler temperature 2 – 8° C. The Retention Time (RT) of GnRH [6-D-Phe] was 8.5 ± 1.5 minutes with UV detection at 220 nm.

## 5.5 REFERENCES AND ACKNOWLEDGMENTS


1. Sinha, V. R. & Trehan, A. Biodegradable microspheres for protein delivery. *J. Control. Release* **90,** 261–280 (2003).

2. Dokania, S. & Joshi, A. K. Self-microemulsifying drug delivery system (SMEDDS) – challenges and road ahead. *Drug Deliv.* **22,** 675–690 (2015).

3. AboulFotouh, K., Allam, A. A., El-Badry, M. & El-Sayed, A. M. Role of self-emulsifying drug delivery systems in optimizing the oral delivery of hydrophilic macromolecules and reducing interindividual variability. *Colloids Surfaces B Biointerfaces* **167,** 82–92 (2018).

4. Buckwalter, F. H., Dickison, H. L., Miller, H. C., Rhodehamel, H. W. & Al., E. A new absorption delaying vehicle for penicillin. *J. Am. Pharm. Assoc. Am. Pharm. Assoc. (Baltim).* **37,** 472–4 (1948).

5. Won, D. H., Kim, M. S., Lee, S., Park, J. S. & Hwang, S. J. Improved physicochemical characteristics of felodipine solid dispersion particles by supercritical anti-solvent precipitation process. *Int. J. Pharm.* **301,** 199–208 (2005).

6. Kim, M. S. *et al.* Supersaturatable formulations for the enhanced oral absorption of sirolimus. *Int. J. Pharm.* **445,** 108–116 (2013).

7. Han, H. K., Lee, B. J. & Lee, H. K. Enhanced dissolution and bioavailability of biochanin A via the preparation of solid dispersion: In vitro and in vivo evaluation. *Int. J. Pharm.* **415,** 89–94 (2011).

8. Engers, D. *et al.* A solid-state approach to enable early development compounds: Selection and animal bioavailability studies of an itraconazole amorphous solid dispersion. *J. Pharm. Sci.* **99,** 3901–3922 (2010).

9. Gao, P. *et al.* Development of a supersaturable SEDDS (S-SEDDS) formulation of paclitaxel with improved oral bioavailability. *J. Pharm. Sci.* **92,** 2386–2398 (2003).

10. Katona, J. *et al.* Rheological properties of hydroxypropylmethyl cellulose/sodium dodecylsulfate mixtures. *J. Serbian Chem. Soc.* **79,** 457–468 (2014).

11. Patel, R. Parenteral suspension: an overview. *Int J Curr Pharm Res* **2,** 4–13 (2010).

12. Puthli, S. & Vavia, P. Stability Studies of Microparticulate System with Piroxicam as Model Drug. *AAPS PharmSciTech* **10,** 872–880 (2009).

13. Mezdour, S., Lepine, A., Erazo-Majewicz, P., Ducept, F. & Michon, C. Oil/water surface rheological properties of hydroxypropyl cellulose (HPC) alone and mixed with lecithin: Contribution to emulsion stability. *Colloids Surfaces A Physicochem. Eng. Asp.* **331,** 76–83 (2008).

14. Zimmermann, A. *et al.* Adsorption of pharmaceutical excipients onto microcrystals of siramesine hydrochloride: Effects on physicochemical properties. *Eur. J. Pharm. Biopharm.* **71,** 109–116 (2009).

15. Tadros, T. Polymeric surfactants in disperse systems. *Adv. Colloid Interface Sci.* **147–148,** 281–299 (2009).

16. Narang, A. S., Delmarre, D. & Gao, D. Stable drug encapsulation in micelles and microemulsions. *Int. J. Pharm.* **345,** 9–25 (2007).

17. Eastoe, J. 3. Microemulsions. *Surfactant Chem.* 59–95 (2003).

18. Talegaonkar, S. *et al.* Microemulsions: a novel approach to enhanced drug delivery. *Recent Pat. Drug Deliv. Formul.* **2,** 238–257 (2008).

This work was supported by Veyx Pharma D-Schwarzenborn and DBU (Deutsche Bundesstiftung Umwelt) D-Osnabrueck. We are also grateful to Karin Zehetner, Fresenius Kabi A-Linz, as well as Dr. Christian Muehlenfeld, Ashland Inc D-Duesseldorf for providing us with the polymeric compounds for the preliminary testing and the *in vitro* evaluation. We are also grateful to Dr. Marie-Sousai Appavou, Julich Centre for Neutron Science JCNS Garching, D-Muenchen for performing TEM.

## 5.6 SUPPLEMENTARY DATA

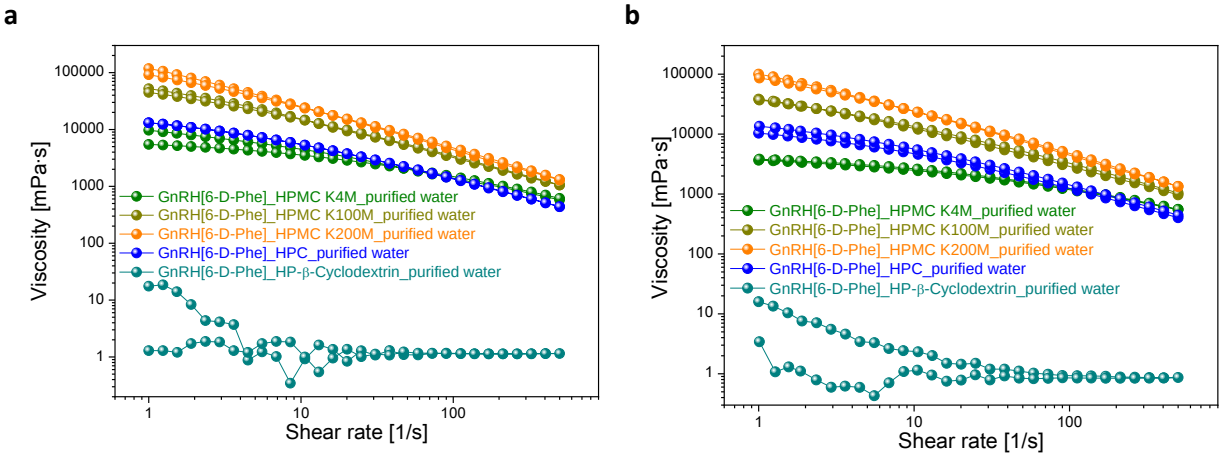


**Figure 5.8| Rheology of GnRH [6-D-Phe]_Polymer aqueous solution**
(a) at 25° C (b) at 39° C

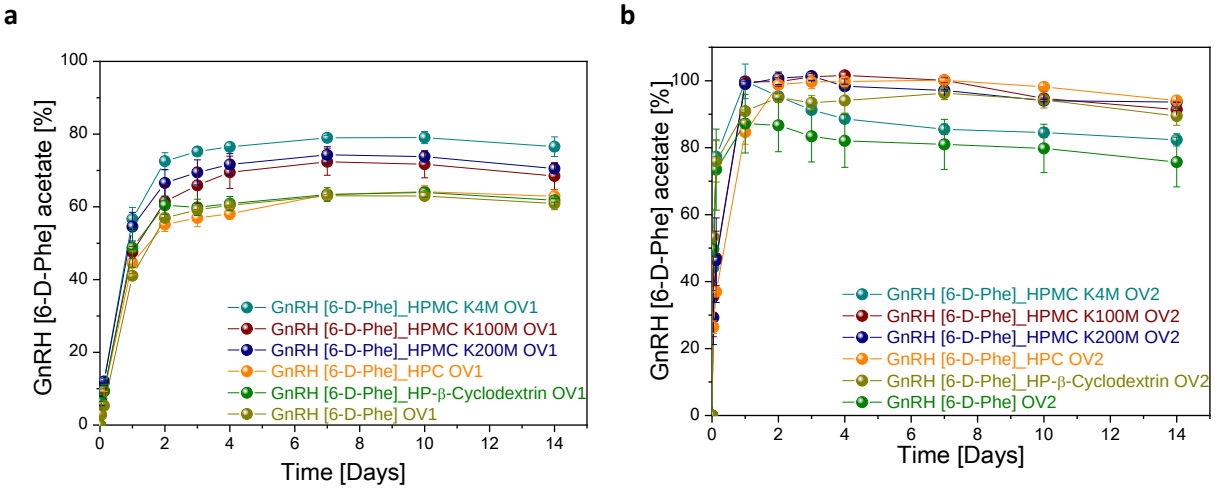


**Figure 5.9| *In vitro* release profiles of GnRH [6-D-Phe] Polymer oil depot formulations in visking dialysis tubing, MWCO 12 – 14 kD**

## 5.7 FIGURES AND TABLES

# CHAPTER SIX

# RELEASE ZINC

*Parts of this chapter have been published in Nature Scientific Reports 2018 vol: 8 (1) pp: 11280*

# 6 GnRH [6-D-Phe] acetate Oil Depot Suspension: The Effect of Zinc on the Release Characteristics

Yordanka Yordanova[1], Willem Vanderlinden[2], Raphael Stoll[3], Daniel Ruediger[4], Andreas Tosstorff[1], Wolfgang Zaremba[5], Gerhard Winter[1], Stefan Zahler[4], Wolfgang Friess[1]

1. Department of Pharmacy, Pharmaceutical Technology & Biopharmaceutics, Ludwig-Maximilians-Universitaet, Butenandtstrasse 5, 81377 Muenchen, Germany
2. Department of Applied Physics and Centre for NanoScience, Ludwig-Maximilian-Universitaet, Amalienstrasse 54, 80799 Muenchen, Germany
3. Department of Chemistry and Biochemistry, Biomolecular NMR Spectroscopy and RUBiospek, Universitaetsstrasse 150, 44780 Bochum, Germany
4. Department of Pharmacy, Pharmaceutical Biology, Ludwig-Maximilians-Universitaet, Butenandtstrasse 5, 81377 Muenchen, Germany
5. Veyx Pharma GmbH, Scientific Department, Soehreweg 6, 34639 Schwarzenborn, Germany

**The incorporation of cellulosic polymers into GnRH [6-D-Phe] could not increase the amount of released peptide in a sustained manner. Therefore $Zn^{2+}$: GnRH [6-D-Phe] complexation was tested. Attenuated Total Reflection Fourier Transform Infrared spectroscopy (ATR–FTIR) revealed the existence of higher order assembly of $Zn^{2+}$: GnRH [6-D-Phe]. Nuclear Magnetic Resonance spectroscopy (NMR) indicated a weak interaction between $Zn^{2+}$ and GnRH [6-D-Phe]. Atomic Force Microscopy (AFM) showed the existence of GnRH [6-D-Phe] oligomers and fibrils. In contrast to already existing short peptide fibrils, GnRH [6-D-Phe] nanostructures and fibrils form in a Tris-buffered pH environment in a controlled manner through a temperature reduction and a pH shift. Molecular Dynamic (MD) simulation of the 10:1 $Zn^{2+}$: GnRH [6-D-Phe] explored the interaction and dimerization processes. The $Zn^{2+}$: GnRH [6-D-Phe] assembly was tested as a platform for the sustained delivery of GnRH [6-D-Phe] and incorporated into castor oil-medium chain triglycerides (MCT) mixture and 3% aluminiumdistearate (Al-DiSt) gelled MCT with hydrogenated lecithin and macrogol-hydrogenated castor oil. The *in vitro* release from the lyophilized $Zn^{2+}$: GnRH [6-D-Phe] was slow and continuous over 14 days and not influenced by the oil matrix.**

## 6.1 INTRODUCTION

A non-covalent complexation of peptides with metal ions controlling their release is a method, which resembles their storage in vesicles at physiological conditions. Insulin, for instance, is a prominent example for a peptide stored in the pancreas in the form of insoluble zinc complex[1]. The extended availability of insulin from an insoluble zinc complex has been long known and utilized. The development of insulin sustained release formulations for injection originated from studies of the insulin solubility in acetate and phosphate buffer[2]. The studies found the efficiency of insulin precipitation to be a function of pH and zinc salt concentration. Recently, a similar approach was adopted with other peptide compounds in order to achieve their controlled and sustained release. A non-covalently bound adduct of glucagon-like peptide 1 (GLP-1) agonist with zinc acetate could prolong its terminal half-life $t_{1/2}$ after subcutaneous application from 2 h to 8.5 h. It further reduced the initial burst release of GLP-1 from the formulation vehicle, indicating its potential for long term release[3]. A

precipitation of recombinant Hirudin (rHir) by zinc salt at neutral pH was as well shown to result in $Zn^{2+}$-rHir suspension with a prolonged biological activity in rats[4]. The prepared suspension was then further optimized with regards to pH and zinc salt[5]. Similarly, corticotrophin (ACTH) was precipitated with zinc salt[6]. The addition of zinc induced the dimerization of human growth hormone (hGH). The $Zn^{2+}$-hGH dimer was more stable than the monomeric hGH form[7,8]. The formed structures of $Zn^{2+}$-hGH were later found to be fibrils of amyloidogenic nature, able to release monomers upon dilution[9]. Various studies have investigated short amyloidogenic peptides and their assemblies that mimic the amyloidosis process[10,11,12,13,14]. The amyloid structures have also been considered as a possible source for sustained release of small peptides, e.g. the GnRH analogue Leuprorelin (LHRH)[15]. In this connection, LHRH was complexed and precipitated with $Zn^{2+}$, using sodium hydroxide (NaOH) solution for the pH adjustment. The lyophilizate was then incorporated into *in situ* forming implants[16]. The same technique for complexation and precipitation was applied in another study with GnRH, tyroliberin (TRH), dalarelin and ACTH for the formation of $Zn^{2+}$-peptide aqueous suspension[17]. Comparable to hGH, LHRH exhibited a similar tendency to form β-sheet rich aggregates with amyloid-like character[15]. In both cases, peptides with the ability to form amyloids were investigated. The amyloid structures are highly organized stable aggregates, which in most cases are associated with neurodegenerative diseases[18]. However, in the studies with hGH and LHRH, the concept of amyloids was applied to prepare complexes capable of slowly releasing the active peptide.

Based on the "amyloid concept" from these studies, we investigated two approaches to complex GnRH [6-D-Phe] with $Zn^{2+}$. The first method was performed in a Tris buffer temperature controlled environment and applied the reciprocal relationship between temperature and pH of the Tris buffer in order to simultaneously precipitate and freeze-dry the $Zn^{2+}$: GnRH [6-D-Phe] complex. The second *in situ* method used similar concept with exception of the Tris buffer salt, which was added to the oil vehicle. Thus precipitation takes place after application. Both $Zn^{2+}$: GnRH [6-D-Phe] complexes were characterized and evaluated (Figure 6.1).

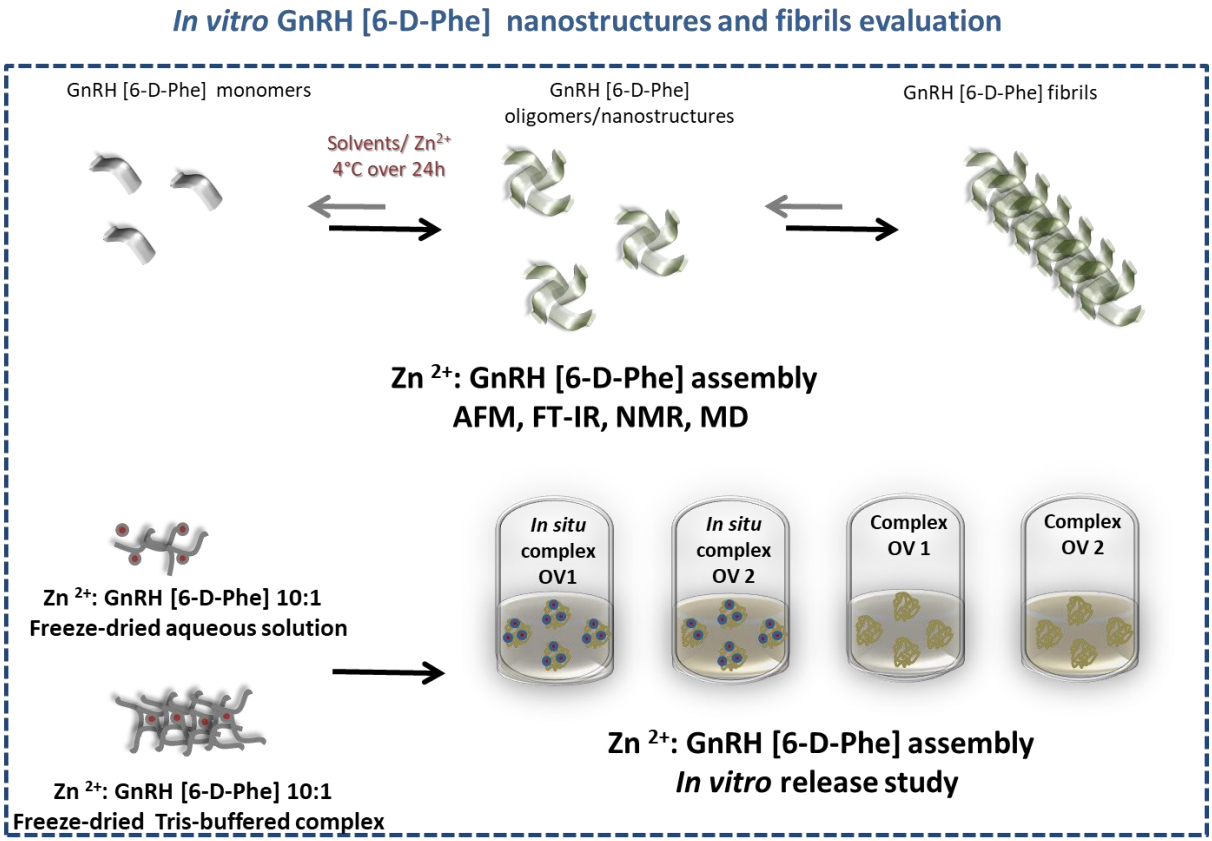


**Figure 6.1| Overview of the *in vitro* GnRH [6-D-Phe] nanostructures and fibrils formation and evaluation**

## 6.2 RESULTS AND DISCUSSION

### *6.2.1 New approach to complex GnRH [6-D-Phe] by $Zn^{2+}$ and controlled pH shift*

In the current study we applied two techniques to complex GnRH [6-D-Phe] and compared them to each other in order to select the most suitable one. The percentage of free GnRH [6-D-Phe] was analyzed by Reversed-Phase Chromatography (RP-HPLC).

The first technique was the method of choice used in earlier studies of precipitating LHRH, rHir, ACTH, TRH etc. and involved increasing the pH of the peptide solution containing $Zn^{2+}$ from 7.2 to 8.2 by the addition of NaOH[5,16,19,17]. The GnRH [6-D-Phe] was complexed at 2.5 mg/mL from 5 mg/mL bulk concentration. Below pH 7.8 the percentage of precipitated GnRH [6-D-Phe] remained low at all $Zn^{2+}$: GnRH [6-D-Phe] molar ratios and no correlation between molar ratio and pH could be acertained. Above pH 7.8, we observed an increase and a maximum of precipitated GnRH [6-D-Phe] of 95.9 ± 0.1 % at a 10:1 $Zn^{2+}$: GnRH [6-D-Phe] molar ratio (Figure 6.2 a; Supplementary Data Table 6.6). The high percentage of precipitated peptide might be due to the interaction of the histidine (His) side chain with $Zn^{2+}$ through its imidazole group. One major drawback of the technique is the unsatisfactory accuracy using the pH-adjustment with NaOH solution due to lack of buffer capacity at the pH value of interest. Thus upon addition of NaOH extremely unstable and high local pH values may result. This can lead on the one hand to the coinciding precipitation of $Zn(OH)_2$ from a mixture of complexed, free peptide and unbound $Zn^{2+}$ and on the other to epimerization at the serine (Ser) of GnRH [6-D-Phe], preceding a Ser hydroxyl group triggered peptide bond hydrolysis[20].

The second technique was based on a recent study of Valery *et al.*, which showed that a change of pH value and thus deprotonation of the His residue in the GnRH agonist, TRH, could trigger a self-assembly of the peptide into nanotubes[21]. This pH dependent switch can be applied in the bottom-up development of pH-responsive nanomaterials as well as for the *in vitro* induced conformational change and fibrillation of GnRH [6-D-Phe]. In our study, this was achieved through a temperature controlled pH-shift between 7.2 and 8.2 with a Tris-buffered system, as an alternative to NaOH[22].

The percentage of precipitated peptide reached 99.2 ± 0.2 % at a 10:1 $Zn^{2+}$: GnRH [6-D-Phe] ratio in 0.05 M Tris buffer pH 7.8 after temperature reduction from 25° C to 5° C, over 24 h. In contrast, the precipitation efficiency in a 0.05 M Tris buffer pH 7.2 reached only 36.2 ± 0.1 % (Figure 6.2 b). This could be explained by the measured-temperature-induced pH increase of the Tris-buffered system with 0.03 pH units per 1° C[23]. Cooling the $Zn^{2+}$: GnRH [6-D-Phe] in Tris buffer (pH 7.8) from 25° C to 5° C promoted a pH increase from pH 7.3 to pH 7.9. At this pH the His-side chain is in a deprotonated state and can form hydrogen bonds or enhance the peptide interaction with $Zn^{2+}$ and the formation of an assembly. In contrast the solution of $Zn^{2+}$: GnRH [6-D-Phe] in Tris buffer with pH 7.2 reached pH 7.3 at 5° C (Supplementary Data Table 6.7).

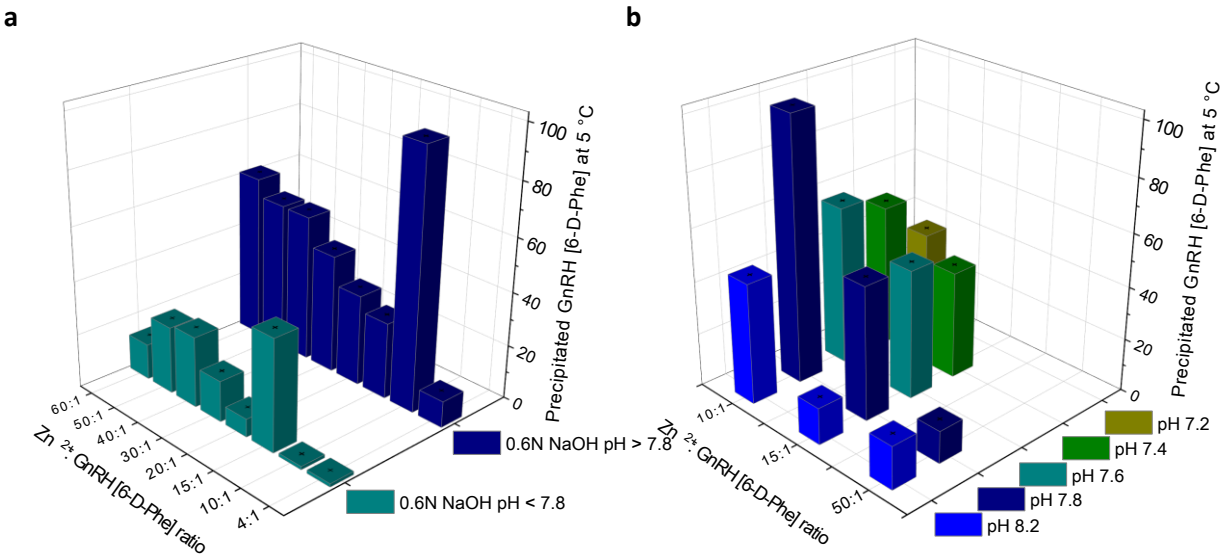


**Figure 6.2| Precipitated GnRH [6-D-Phe] from Zn 2+: GnRH [6-D-Phe] solution**
(a) with 0.6 N NaOH at pH > 7.8 and pH<7.8 (b) in 0.05 M Tris buffer at 5° C (starting pH at 25° C); the left panel illustrates an increased, but uncontrolled, precipitation at molar ratio Zn 2+:GnRH [6-D-Phe] 10:1 at pH > 7.8 with 0.6 N NaOH; the right panel illustrates a new method of a temperature controlled Tris buffer precipitation of Zn 2+:GnRH [6-D-Phe] 10:1 at 5° C

### *6.2.2 Existence of higher-order assembly of GnRH [6-D-Phe]*

In order to study the conformational changes and secondary structures, resulting upon adding different molar concentrations of $Zn^{2+}$ to GnRH [6-D-Phe], we used Attenuated Total Reflection Fourier Transform Infrared spectroscopy (ATR–FTIR). The bands at 1416 $cm^{-1}$ and 1434-1454 $cm^{-1}$ indicated an increase in the C-H bending and -C=O stretching vibration, respectively[24–26](Figure 6.3 a). Absorbance spectra analysis in the amide II range (1500-1600 $cm^{-1}$) yielded two major peaks at ~1520 $cm^{-1}$ and 1560 $cm^{-1}$. The peak at 1560 $cm^{-1}$ can be assigned to the N-H bend in plane and stretch. The peak at 1520 $cm^{-1}$ has been associated in earlier studies with vibrations of heterocyclic compounds, e.g. furan ring, phenyl ring, imidazole ring and can be attributed to the stretching vibration of the –C=N bond in the imidazole heterocycle of the His side chain[27–29](Figure 6.3 a). The amide I region (1600-1700 $cm^{-1}$) presented one major band at 1650 $cm^{-1}$ as an indicator of an alpha-helical structure. The characteristic beta-sheet regions of 1610-1630 $cm^{-1}$ and 1680-1700 $cm^{-1}$ were visibly overlapped from the major alpha-helical peak. A deconvolution of the absorbance spectra could unveil a beta-sheet peak in the 1604-1617 $cm^{-1}$ range (Supplementary Data Figure 6.13). With increasing $Zn^{2+}$ molar concentrations, most stunning appears to be the change in the percentage of beta-sheet and carbonyl stretching area. The observed changes are good indicators of the initiation of oligomer formation at 4:1 and the maximum stretching of the carbonyl group at 10:1 $Zn^{2+}$: GnRH [6-D-Phe] molar ratios (Figure 6.3 a, Table 6.1). With higher $Zn^{2+}$ concentrations the beta-sheet peak disappeared and an increase of the carbonyl stretching due to the formation of ZnO/ $Zn(OH)_2$ resulted. Its strong peak at 1560 $cm^{-1}$ coincides with the peptide amide II region. Analysis of the second-derivative amide I region showed bands at~1611 $cm^{-1}$ and at ~1690 $cm^{-1}$, typical for oligomers in solution[30–35](Figure 6.3 b). This supports the hypothesis that the oligomeric structure of GnRH [6-D-Phe] forms with increasing molar concentration of $Zn^{2+}$.

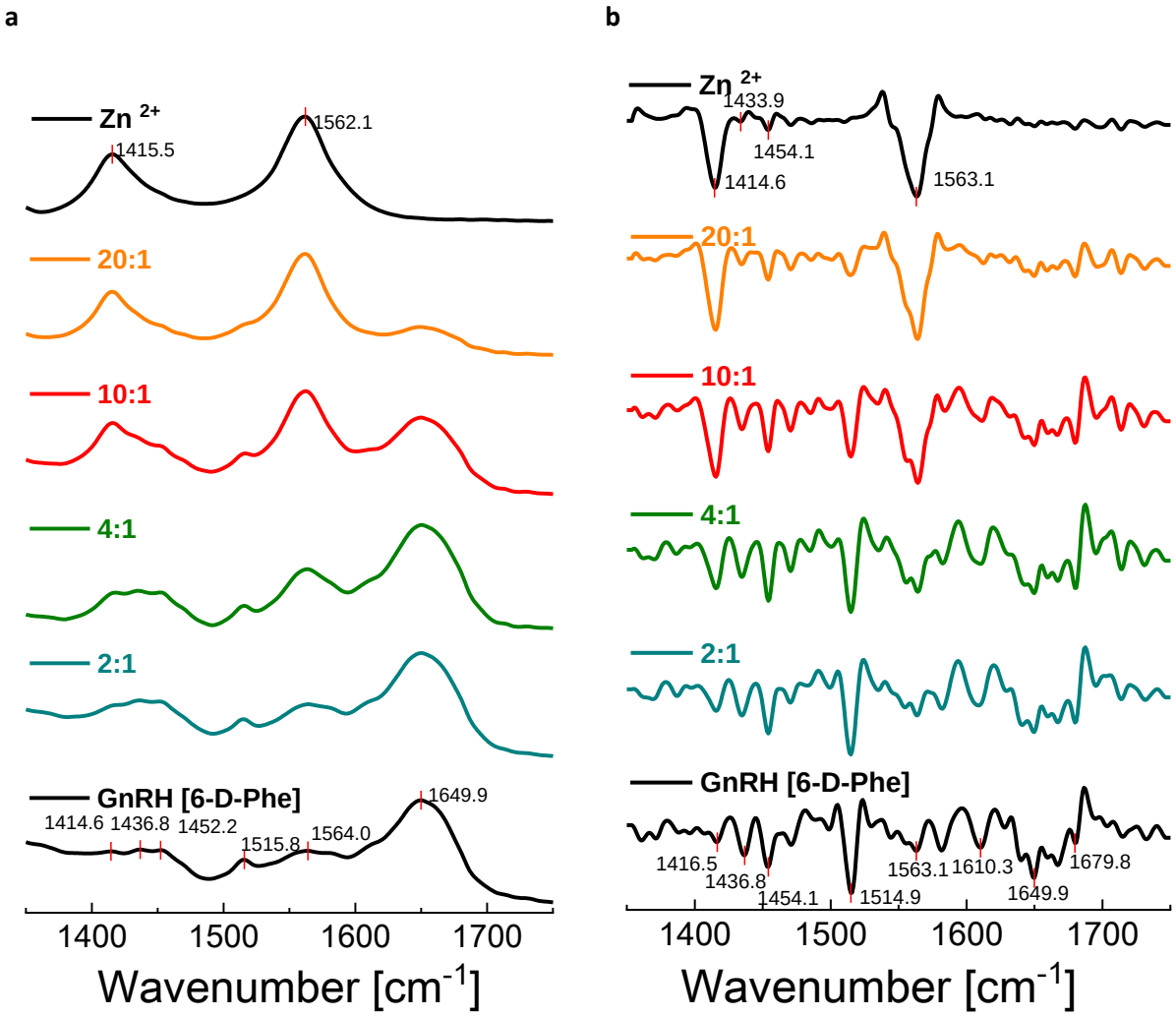


**Figure 6.3| FT-IR Spectra of the $Zn^{2+}$: GnRH [6-D-Phe] assemblies in comparison to GnRH [6-D-Phe]**
(a) normalized, absorbance spectra (b) normalized second derivative of the absorbance spectra

| | Main peaks $cm^{-1}$ (% Area) | | | | |
|---|---|---|---|---|---|
| | -C-H bending and C=O stretching | -C=N (Imidazole) | Amide II | Beta-sheet | Amide I |
| **GnRH [6-D-Phe]** | 1416 (2%)<br>1434 (2%)<br>1454 (6%) | 1514 (3%) | 1568 (27%) | 1612 (6%) | 1652 (54%) |
| **$Zn^{2+}$:GnRH [6-D-Phe] 2_1** | 1414 (4%)<br>1435 (5%)<br>1456 (7%) | 1514 (2%) | 1563 (17%) | 1608 (10%) | 1653 (54%) |
| **$Zn^{2+}$:GnRH [6-D-Phe] 4_1** | 1417 (8%)<br>1435 (1%)<br>1452 (8%) | 1515 (3%) | 1560 (20%) | 1617 (20%) | 1657 (40%) |
| **$Zn^{2+}$:GnRH [6-D-Phe] 10_1** | 1416 (13%)<br>1435 (1%)<br>1450 (7%) | 1517 (4%) | 1561 (32%) | 1604 (9%) | 1653 (35%) |
| **$Zn^{2+}$: GnRH [6-D-Phe] 20_1** | 1415 (20%)<br>1447 (5%) | - | 1560 (40%) | - | 1653 (15%) |

**Table 6.1| Main peaks and integrated peak area in the deconvoluted normalized absorbance spectra of $Zn^{2+}$: GnRH [6-D-Phe] assemblies in comparison to GnRH [6-D-Phe]**

### *6.2.3 Binding of Zn 2+ to GnRH [6-D-Phe]*

The LHRH interactions with $Zn^{2+}$, $Ni^{2+}$ and $Cu^{2+}$ were studied in the 1980s[19,17]. The results of the $^{1}$H-NMR spectroscopy favoured a view that the coordination between $Zn^{2+}$ and LHRH takes place at the carbonyl oxygen of the His-Trp peptide bond[19]. In addition, the imidazole of the His residue coordinates to the $Zn^{2+}$ ligand. This coordination to $Zn^{2+}$ happens in a fast proton exchange. The changes of the chemical shift in the aromatic part of the $^{1}$H-NMR in correlation to the added molar concentration of $Zn^{2+}$ can be traced back to two distinct occurrences. The first one involves the already mentioned His and Trp residue interaction with $Zn^{2+}$ (Supplementary Data Figure 6.12). The second one can be due to a stronger peptide-peptide interaction[36,37]. Using the observed change in the chemical shift ($\Delta\delta$), we fitted the data to a hyperbolic function with the following equation:

$$\Delta\delta = \frac{\Delta\delta_{max} * Zn^{2+}}{K_d + Zn^{2+}}$$

**Equation 6.1| Chemical shift Δδ in correlation to $Zn^{2+}$**

This allowed us to determine the dissociation constants ($K_d$) of the $Zn^{2+}$: GnRH [6-D-Phe] assembly, assuming a 1:1 stoichiometry. The calculated value of the dissociation constant $K_d$ (38.4 ± 4.8 mM[1]) indicated a weak interaction between $Zn^{2+}$ and GnRH [6-D-Phe]. The $Zn^{2+}$ ligand concentration for the interaction with GnRH [6-D-Phe] was in the range of 4-160 mM (Figure 6.4).

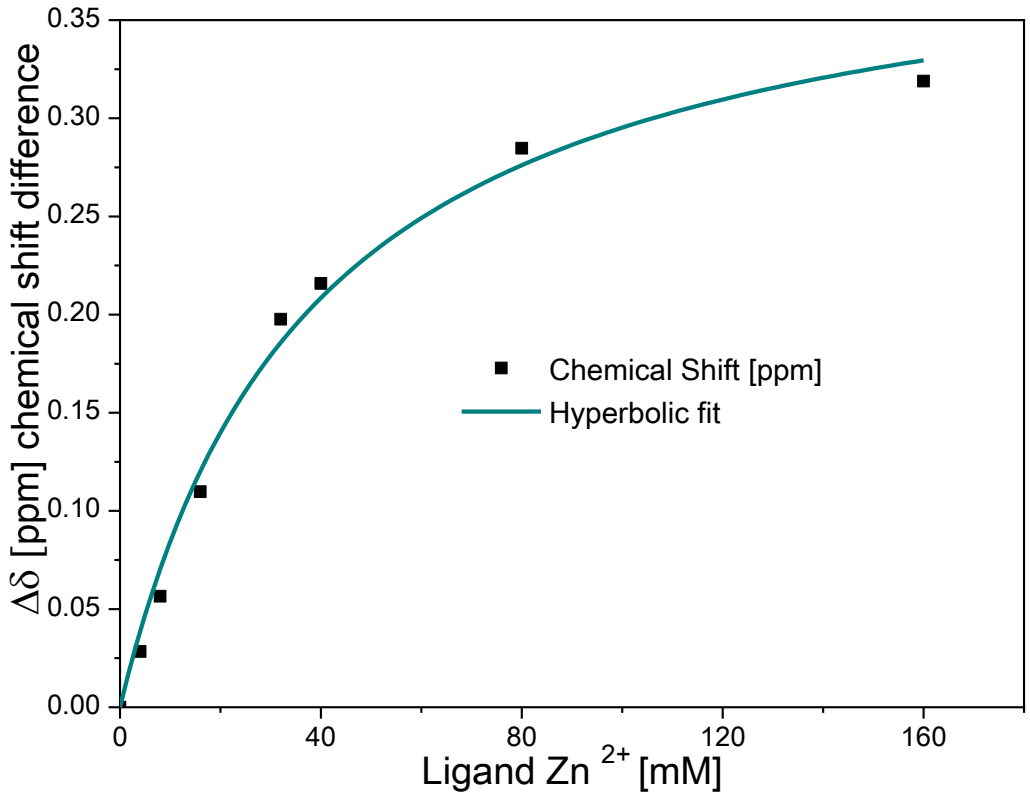


**Figure 6.4| NMR shift in solution-state NMR spectra vs. $Zn^{2+}$ concentration for the determination of the dissociation constant $K_d$ of the $Zn^{2+}$:GnRH [6-D-Phe] 1:1 stoichiometry**

### *6.2.4 $Zn^{2+}$: GnRH [6-D-Phe] assembly: nanostructures and fibrils*

In order to visualize the formation process of the assembly, we took atomic force microscopy (AFM) images in solution and in dry state at the highest precipitation efficiency, $Zn^{2+}$: GnRH [6-D-Phe] 10:1. The observed fast proton exchange and interaction in the $^{1}$H-NMR spectra required the use of a $D_2O$: DMSO-d6 (80:20) solvent in order to capture the images. In solution, nanostructures with a diameter of up to 5nm in the presence of $Zn^{2+}$ were recorded (Figure 6.5 a, b; Supplementary Data Figure 6.14). The assembly process appeared to be dynamic and going through different stages: immediately after preparation large circular aggregates formed (Figure 6.5 a), which resulted after 48h in 5 nm nanostructures (Figure 6.5 b). The smaller size oligomers might be due to solvation of peptide chains from the preliminary formed large aggregate back into solution. In dry state, $Zn^{2+}$: GnRH [6-D-Phe] small fibrils with a diameter of up to 10 nm were observed (Figure 6.5 c, d).

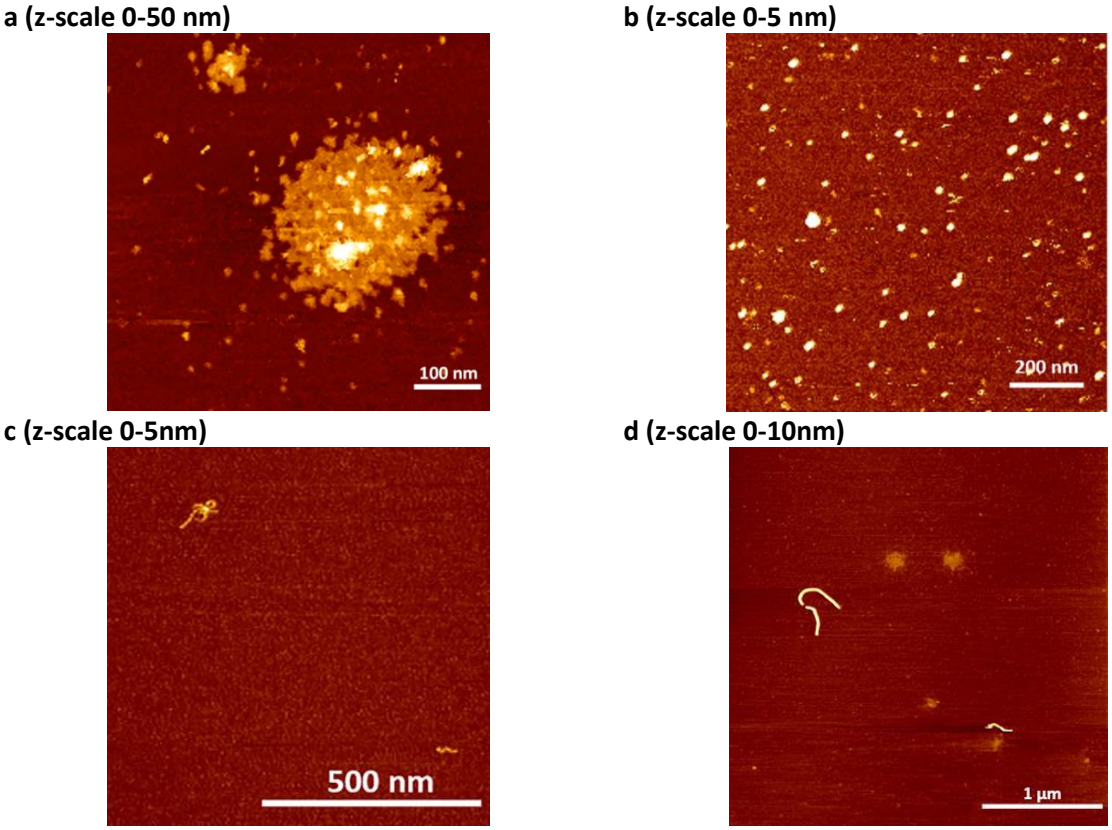


**Figure 6.5| AFM image of the $Zn^{2+}$: GnRH [6-D-Phe] 10:1 complex**
(a), (b) oligomers after preparation with tapping mode in Tris buffer solution (c), (d) fibrils with tapping mode in air (z-scale indicates the average size of the formed oligomers and fibrils)

The effect of increasing $Zn^{2+}$ ion concentration on GnRH [6-D-Phe] fibrillization was further studied with Thioflavin T (ThT) assay. ThT is a benzothiazole dye used to visualize and quantify misfolded protein fibrils or amyloid both *in vitro* and *in vivo*[38]. The assay could show the formation of secondary structures with increasing $Zn^{2+}$ concentration. Above a 10:1 $Zn^{2+}$: GnRH [6-D-Phe] ratio, the obtained fluorescence values decreased. Pure GnRH [6-D-Phe] and aggregated Aβ42 were included and served as negative and positive control, respectively (Table 6.2).

| | ThT Fluorescence [a.u.] ± SD | | | | |
|---|---|---|---|---|---|
| | 0h | 1h | 3h | 5h | 24h |
| GnRH [6-D-Phe] | **1.1** ± 5.6E-03 | **1.2** ± 2.8E-03 | **1.2** ± 1.8E-03 | **1.1** ± 4.6E-03 | **1.1** ± 2.1E-03 |
| 2:1 | **5.7** ± 8.7E-03 | **5.6** ± 2.5E-02 | **5.3** ± 1.6E-02 | **6.4** ± 5.9E-02 | **5.8** ± 1.6E-02 |
| 4:1 | **7.9** ± 1.3E-02 | **6.3** ± 2.0E-02 | **7.3** ± 9.2E-03 | **5.6** ± 3.4E-02 | **5.8** ± 1.7E-02 |
| 10:1 | **2.5** ± 6.3E-03 | **2.8** ± 4.1E-03 | **3.3** ± 3.9E-02 | **4.9** ± 4.1E-02 | **2.4** ± 8.6E-03 |
| 20:1 | **1.2** ± 3.1E-03 | **1.0** ± 5.2E-03 | **1.2** ± 7.7E-03 | **1.1** ± 9.4E-03 | **1.0** ± 7.4E-03 |
| Aβ 42 | **5.1** ± 1.8E-02 | **3.9** ± 1.1E-02 | **5.9** ± 1.2E-01 | **4.7** ± 1.9E-01 | **4.7** ± 1.9E-01 |

**Table 6.2| ThT fluorescence recorded over 24h of the $Zn^{2+}$: GnRH [6-D-Phe] assemblies in comparison to GnRH [6-D-Phe] and Aβ 42**

### *6.2.5 Molecular dynamics simulation of $Zn^{2+}$: GnRH [6-D-Phe] 10:1 assembly*

Using molecular dynamics (MD) simulations, we further explored the interaction between $Zn^{2+}$ and GnRH [6-D-Phe] in the 10:1 ratio. Analysis of the trajectory with the linear interaction energy method showed three dimerization events driven by VdW and electrostatic interactions in the $Zn^{2+}$: GnRH [6-D-Phe] 10:1 (Supplementary Data Figure 6.15). These interactions could further confirm the observed weak coordination of $Zn^{2+}$ to GnRH [6-D-Phe] in the $^{1}$H-NMR spectra[39,40]. In the first dimerization event, the Arg8 residue of peptide 1 was engulfed by the second peptide. The dimer's interface consists of Leu7, Arg8 and Pro9 of peptide 1 and pGlu1, Ser4, Pro9, Gly-$NH_2$10 of peptide 2 (Figure 6.6 a). The second and third dimerization events present a flatter interface, which is composed of residues pGlu1, His2 Tyr5 D-Phe6 Pro9 of peptide 1 and Trp3 Ser4 Tyr5 of peptide 2 (Figure 6.6 b). During the first dimerization event there was a pronounced conformational change of peptide 1, reflected from the RMSD values (Figure 6.6 c, d). A cluster analysis showed that the dimer formed in the first dimerization event (at around 10000 frames) is the most prominent species in the course of the simulation. MD simulations showed that the dimer formation is furthermore driven by hydrogen bond formation between the peptide residues (Supplementary Data Figure 6.16).

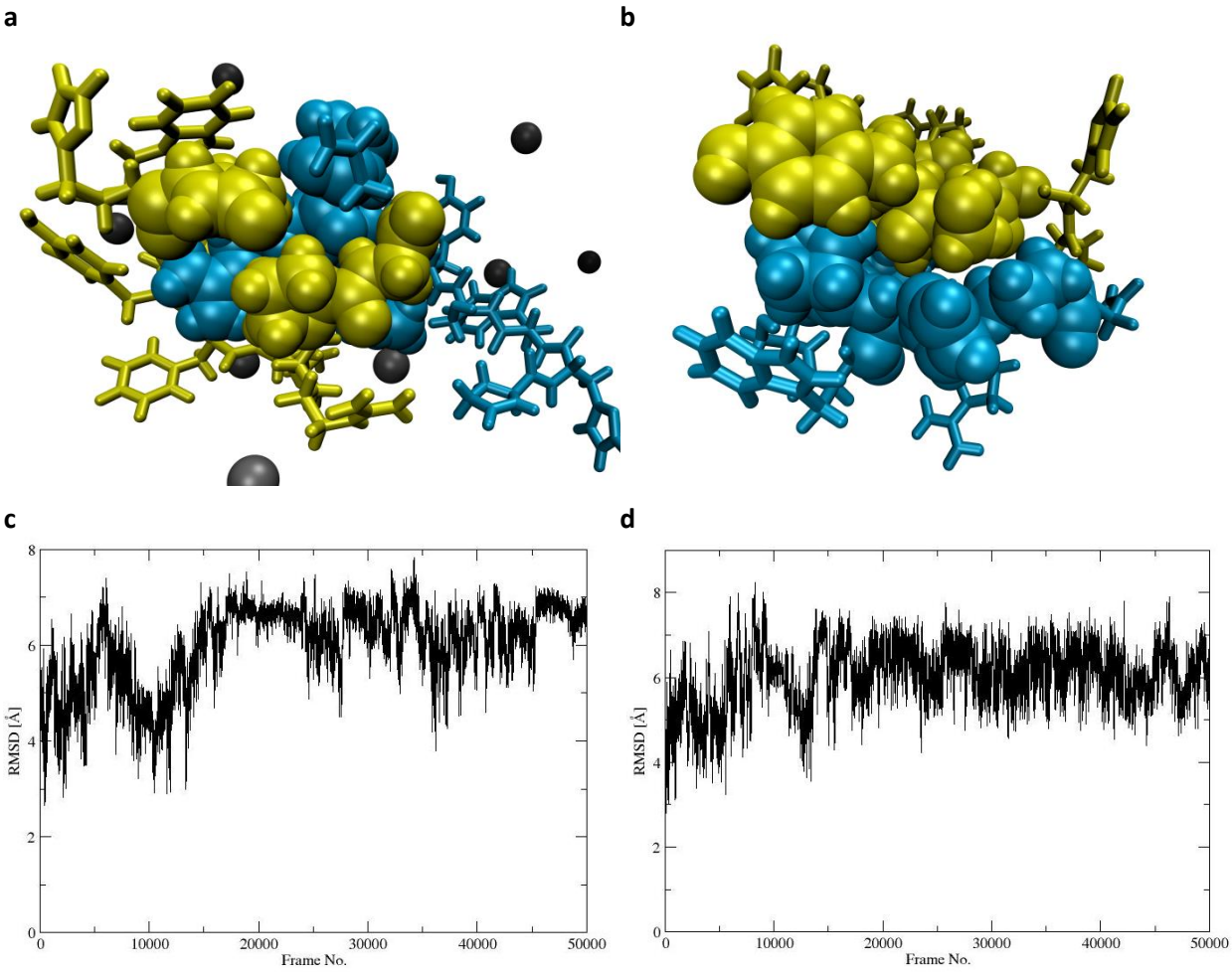


**Figure 6.6| MD simulation**
(a), (b) Dimer structures of GnRH [6-D-Phe]-1 in blue, GnRH [6-D-Phe]-2 in yellow, $Zn^{2+}$ in black, interfacial residues pictured as VdW spheres (c), (d) RMSD value peptide 1 and RMSD value peptide 2

### *6.2.6 $Zn^{2+}$: GnRH [6-D-Phe] complex and oil depot suspension preparation*

In order to generate a GnRH-depot system two new approaches were evaluated. In the first setup, complexation of GnRH [6-D-Phe] in the presence of $Zn^{2+}$ was directly performed in the freezing phase of a lyophilization process. The temperature-dependent pH switch of the Tris buffer system led to the formation of $Zn^{2+}$: GnRH [6-D-Phe] complex 10:1, which was simultaneously stabilized in a 3D freeze-dried matrix (Figure 6.7). The complex was then incorporated in medium chain triglycerides (MCT) + 3 % (w/w) aluminium distearate (Al-DiSt) + 1 % (w/w) hydrogenated lecithin + 5 % (w/w) PEG-35 castor oil (OV1) or in castor oil: MCT 50:50 % (w/w) (OV2) oil vehicle. For the second *in situ* method, the Tris buffer salt was added to the oil vehicle separately from GnRH [6-D-Phe], enabling a possible precipitation as dissolution of both suspended water soluble compounds takes place after *in vivo* application (Figure 6.7). Both $Zn^{2+}$: GnRH [6-D-Phe] complexes in the oil vehicles were characterized and evaluated.

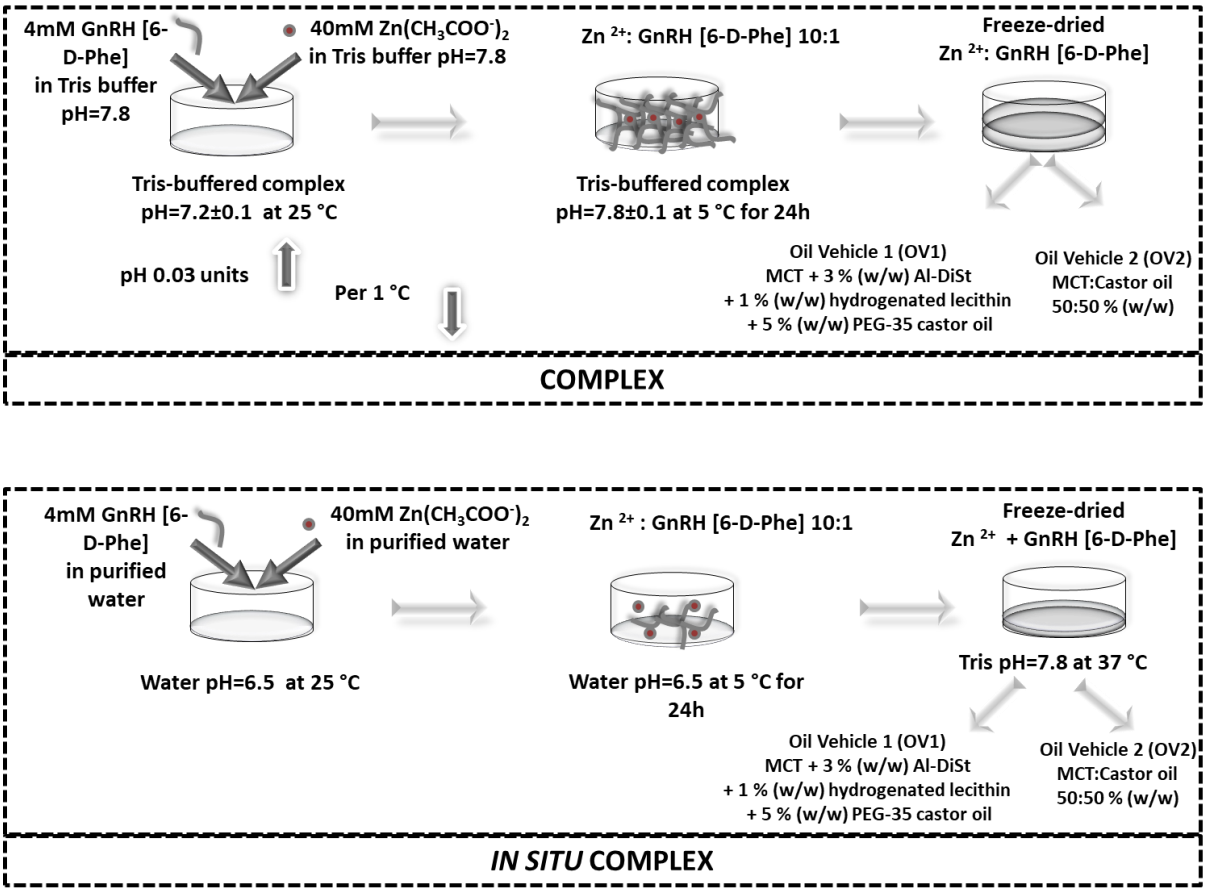


**Figure 6.7| Zn $^{2+}$: GnRH [6-D-Phe] complex and oil depot preparation**

### *6.2.7 Rheology*

The freeze-dried Zn $^{2+}$: GnRH [6-D-Phe] 10:1 complex in MCT + 3 % (w/w) Al-DiSt + 1 % (w/w) hydrogenated lecithin + 5 % (w/w) PEG-35 castor oil displayed a thixotropic profile at 25° C (Figure 6.8). Fluctuations in viscosity values are related to individual large particles or particles agglomerates exceeding the size of the measuring gap of 0.042 mm resulting in a stick-slip phenomenon. This emerged primarily with castor oil-MCT based formulations and can be explained by the absence of stabilizing agents, resulting in the formation of difficult to separate particle agglomerates.

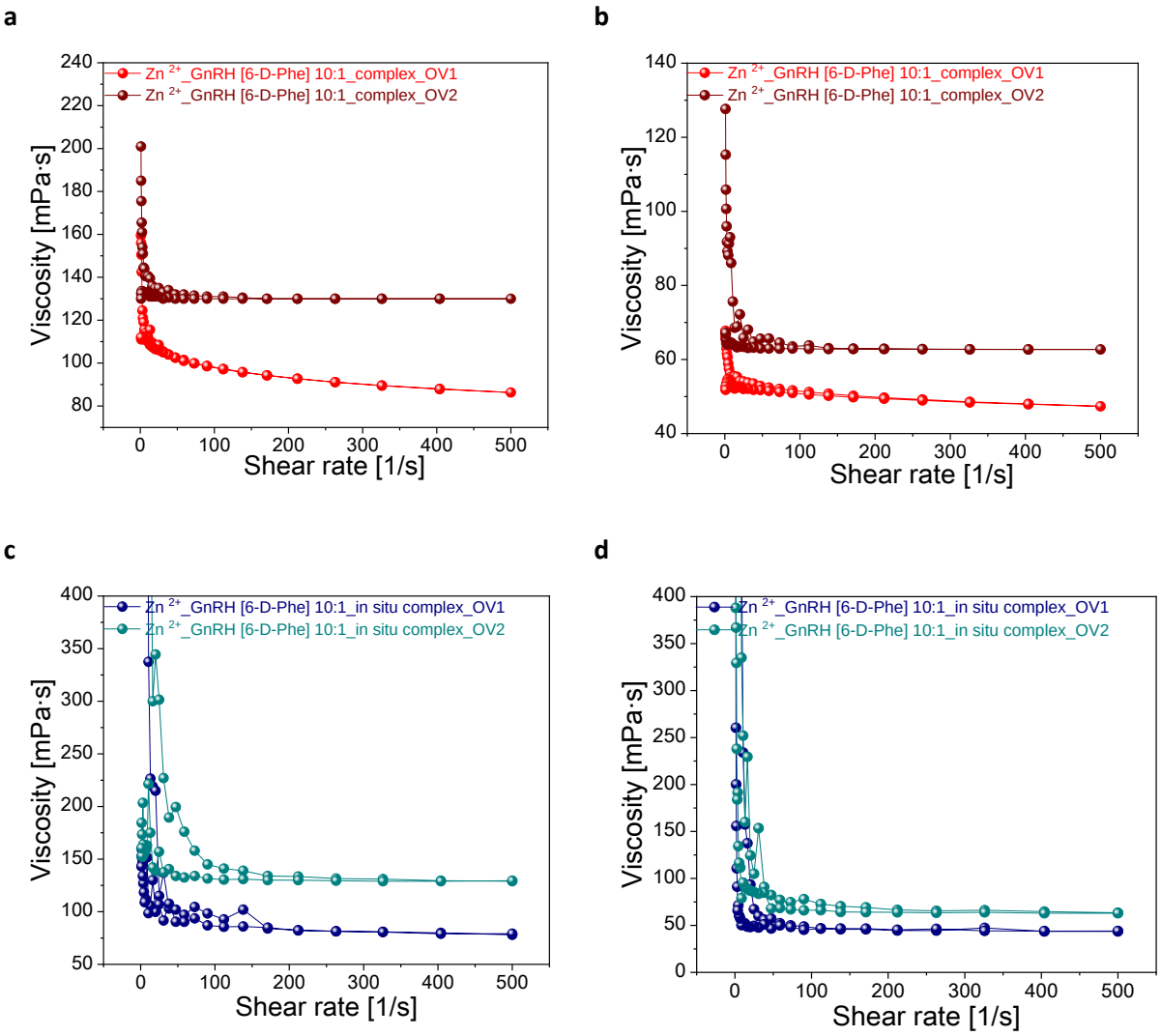


**Figure 6.8| Rheology of $Zn^{2+}$: GnRH [6-D-Phe] oil depot formulations for $Zn^{2+}$: GnRH [6-D-Phe] 10:1 complex and *in situ* complex in OV1 and OV2**
(a), (c) at 25° C (b), (d) at 39° C

### *6.2.8 Particle Size Distribution and Characterization*

The median particle size $D_{v50}$ for the dispersed freeze-dried $Zn^{2+}$: GnRH [6-D-Phe] 10:1 complex was comparable in both oil vehicles (Table 6.3). The particle size distribution was symmetric (Figure 6.9). Their size did not exceed the critical value of 0.325 mm required for an unproblematic application through 16 G needle[41,42].

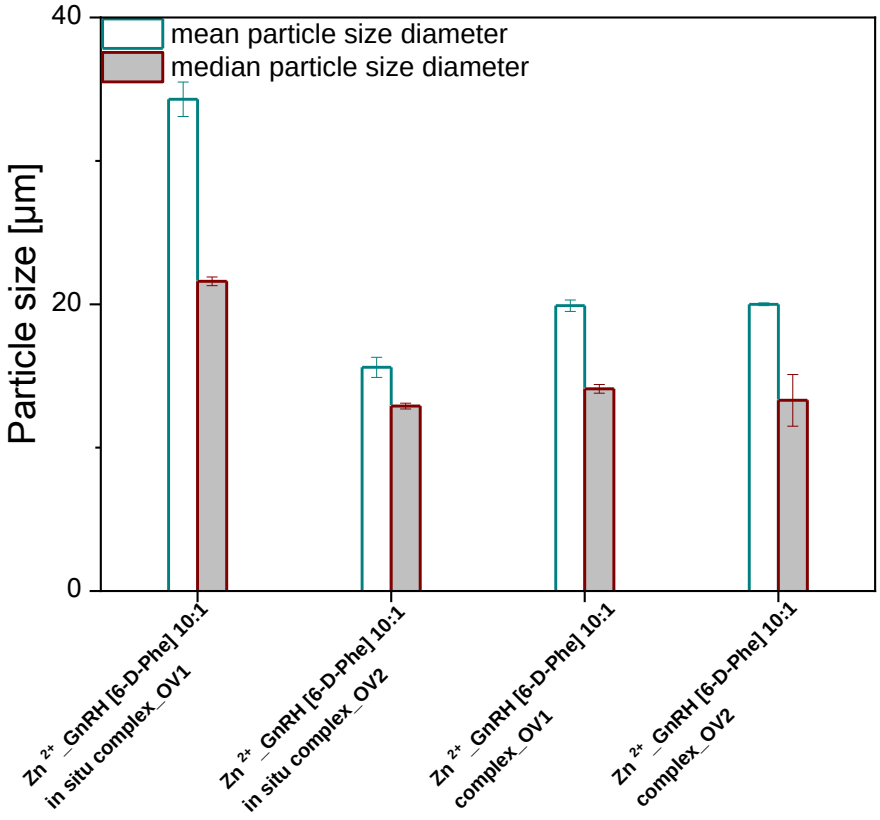


**Figure 6.9| Mean (the mean particle diameter over volume) and median particle size of GnRH [6-D-Phe]_Polymer oil depot formulations**

| Formulation | $D_{v50}$ [µm] ± SD | $D_{v90}$ [µm] ± SD |
|---|---|---|
| $Zn^{2+}$-GnRH [6-D-Phe] 10:1_in situ complex_OV1 | 21.6 ± 0.3 | 79.9 ± 3.6 |
| $Zn^{2+}$-GnRH [6-D-Phe] 10:1_in situ complex_OV2 | 12.9 ± 0.2 | 35.8 ± 5.4 |
| $Zn^{2+}$-GnRH [6-D-Phe] 10:1_complex_OV1 | 14.1 ± 0.3 | 107.9 ± 3.4 |
| $Zn^{2+}$-GnRH [6-D-Phe] 10:1_complex_OV2 | 13.3 ± 1.8 | 114.0 ± 23.2 |

**Table 6.3| Particle size distribution and $D_{v50}$ and $D_{v90}$ fractions**

Upon injection into PBS (pH 7.4), the 3% Al-DiSt gelled MCT with hydrogenated lecithin and hydrogenated macrogol-castor oil formed small droplets under 100 nm. In contrast, the formulations based on the pure mixture of castor oil and MCT generated an unstable emulsion with droplet size above 300 nm (Table 6.4). This trend was observed regardless of the incorporated $Zn^{2+}$: GnRH [6-D-Phe] complex and can be related to MCT + 3 % (w/w) Al-DiSt + 1 % (w/w) hydrogenated lecithin + 5 % (w/w) PEG-35 castor oil acting as a self-emulsifying drug delivery system[43,44,45].

| Formulation | Z-Average d ± SD [nm] | PDI ± SD |
|---|---|---|
| $Zn^{2+}$-GnRH [6-D-Phe] 10:1_complex_OV2 | 734.2 ± 122.5 | 0.620 ± 0.1 |
| $Zn^{2+}$-GnRH [6-D-Phe] 10:1_complex_OV1 | 56.4 ± 8.8 | 0.394 ± 0.1 |
| $Zn^{2+}$-GnRH [6-D-Phe] 10:1_in situ complex_OV2 | 370.9 ± 35.6 | 0.418 ± 0.1 |
| $Zn^{2+}$-GnRH [6-D-Phe] 10:1_in situ complex_OV1 | 66.4 ± 0.5 | 0.504 ± 0.1 |

**Table 6.4| Droplet size determination after injection of $Zn^{2+}$: GnRH [6-D-Phe] oil depot formulations in 6 mL PBS (pH 7.4) at 39° C in an incubated shaker after 24h**

### *6.2.9 In vitro Release Studies*

The *in vitro* release of the GnRH [6-D-Phe] peptide formed by *in situ* complexation with $Zn^{2+}$ in the oil vehicle OV1: MCT + 3 % (w/w) Al-DiSt+ 1 % (w/w) hydrogenated lecithin + 5 % (w/w) PEG-35 castor oil or OV2 : castor oil: MCT 50:50 % (w/w) reached a maximum of 40 % after 2-3 days (Figure 6.10). In contrast, the preformed complex formulations in OV1 and OV2 showed slow and continuous *in vitro* release profiles over 14 days with a minor burst effect. The release from the reference formulation based on pure GnRH [6-D-Phe] in castor oil: MCT 50:50 % (w/w) was fast and almost complete within 24 h. In contrast the release was more sustained over 4 days from Al-DiSt gelled MCT with hydrogenated lecithin and PEG-35 castor oil.

In order to determine the release kinetics from the $Zn^{2+}$:GnRH [6-D-Phe] formulations, the data was fitted to first-order, Higuchi, zero-order and Korsemeyer-Peppas models[46]. The formulations clearly did not follow zero order release kinetics (Figure 6.11). The model that best fitted the release data was evaluated by correlation coefficient ($R^2$) (Table 6.5). The release profile of the preformed complex formulation in OV1 could be best explained by the Higuchi model, as the plot showed linearity with $R^2$ value of 0.9416. The Korsmeyer-Peppas plots of all formulations showed fair linearity ($R^2$ values between 0.95-0.97) with a considerably high slope value (n). This indicated a coupling of diffusion and erosion mechanisms or so called anomalous diffusion[47].

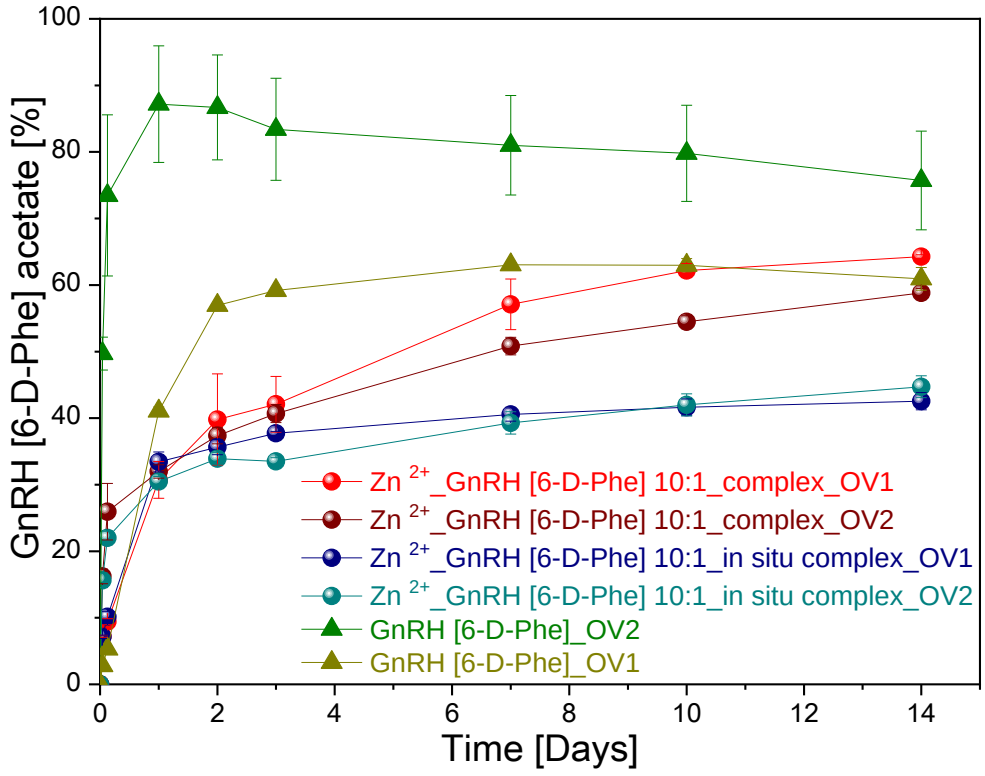


**Figure 6.10| *In vitro* release profiles of Zn 2+: GnRH [6-D-Phe] oil depot formulations in visking dialysis tubing, MWCO 12 – 14 kD**

| Formulation | First-order[1] $R^2$ | Higuchi[2] $R^2$ | Zero-order[3] $R^2$ | Korsmeyer-Peppas[4] $R^2$ | n |
|---|---|---|---|---|---|
| 10:1_complex_OV1 | 0.8574 | 0.9416 | 0.7589 | 0.9784 | 24.342 |
| 10:1_complex_OV2 | 0.8214 | 0.8848 | 0.7087 | 0.9296 | 18.314 |
| 10:1_in situ complex_OV1 | 0.5505 | 0.7552 | 0.5092 | 0.9533 | 16.491 |
| 10:1_in situ complex_OV2 | 0.6654 | 0.7891 | 0.5836 | 0.8960 | 13.566 |
| GnRH [6-D-Phe]_OV1 | 0.5405 | 0.7460 | 0.4949 | 0.9471 | 27.433 |
| GnRH [6-D-Phe]_OV2 | 0.0721 | 0.2894 | 0.1229 | 0.5010 | 19.913 |

**Table 6.5| *In vitro* release kinetic values of GnRH [6-D-Phe] from selected Zn 2+: GnRH [6-D-Phe] oil depot formulations**
[1]First-order equation, log Q=Log $Q_0$ –kt/2.303; [2]Higuchi equation, Q=kt ½; [3]Zero-order equation, Q=Q + kt; [4]Korsmeyer-Peppas equation, $Q_t/Q_\mu=kt^n$

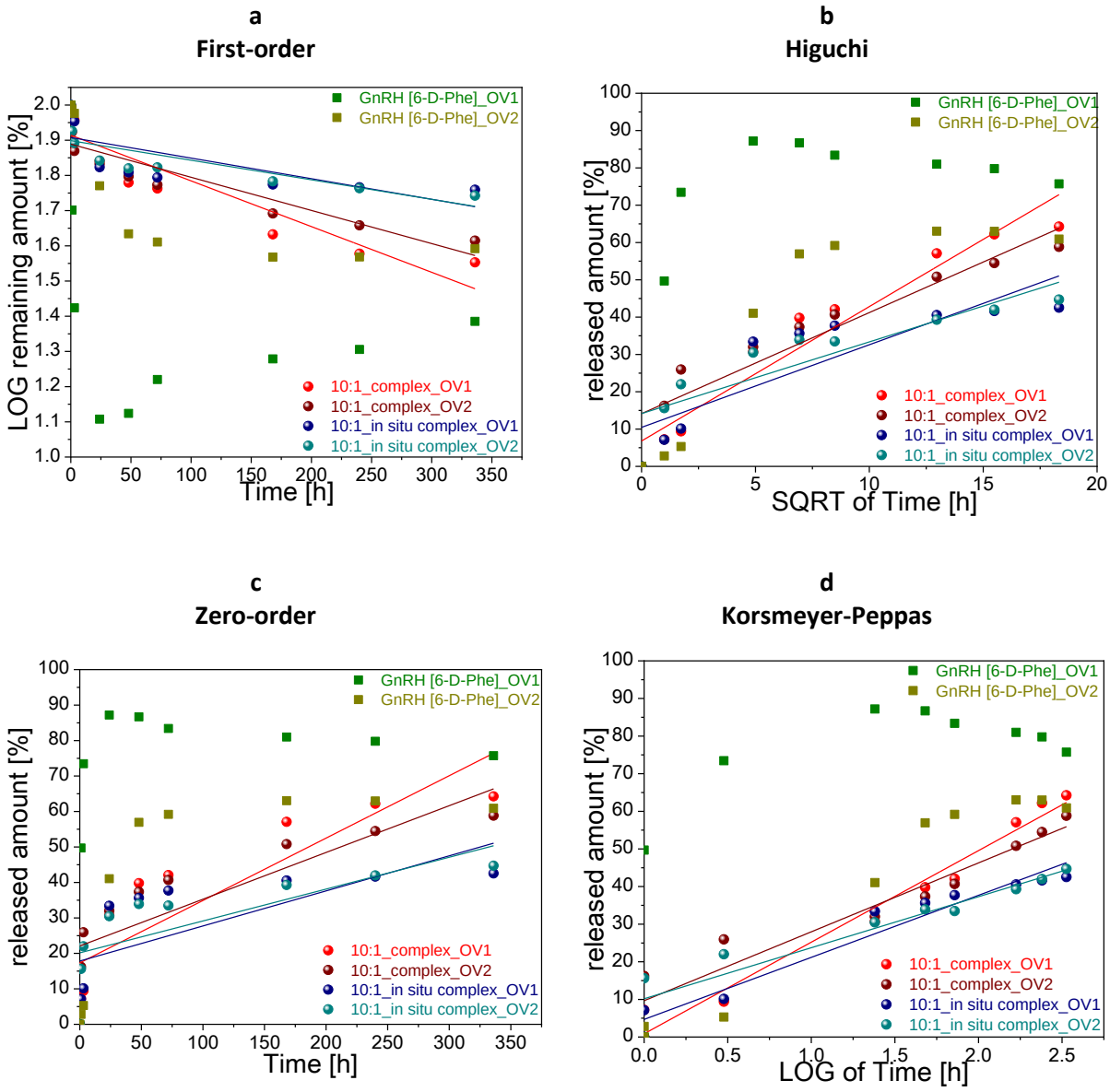


**Figure 6.11| Linear fit of *in vitro* release kinetic values of GnRH [6-D-Phe] from selected Zn $^{2+}$: GnRH [6-D-Phe] and GnRH [6-D-Phe] oil depot formulations**
(a) [1]First-order equation, log Q=Log $Q_0$ –kt/2.303; (b) [2]Higuchi equation, Q=kt ½; (c) [3]Zero-order equation, Q=Q + kt; (d) [4]Korsmeyer-Peppas equation, $Q_t/Q_\mu=kt^n$

Compared to the reference formulations without $Zn^{2+}$, the release profiles of the complex and *in situ* complex formulations were not influenced by the oil matrix. Thus the interaction of $Zn^{2+}$ with GnRH [6-D-Phe] in a preformed lyophilized complex could accomplish a superior controlled release of GnRH [6-D-Phe] with minor burst effect. It represents a simple and scalable formulation approach.

## 6.3 CONCLUSION

As illustrated above a short synthetic decapeptide, GnRH [6-D-Phe] can form nanostructures and fibrils *in vitro* through the addition of $Zn^{2+}$ ions. The aggregation tendency seems to depend on $Zn^{2+}$ concentration, reaching a maximum efficiency of almost 100% at a 10:1 $Zn^{2+}$: GnRH [6-D-Phe] ratio. The oligomerization and mature fibrils formation of GnRH [6-D-Phe] are $Zn^{2+}$ induced. GnRH [6-D-Phe] fibrils form in a Tris-buffered pH 7.8-8.2 environment in a controlled manner through temperature reduction and a pH shift. The *in vitro* release of the GnRH [6-D-Phe] peptide from the freeze-dried assembly was sustained and continuous over 14 days and can be viewed as a promising platform for the controlled delivery of peptides.

Recent articles have highlighted the numerous fields of application of similar self-assembled peptide –based nanostructures[48–50]. The further investigation of the GnRH [6-D-Phe]: $Zn^{2+}$ self-assembling/oligomerization process is necessary in order to evaluate to what extent it can find application in other research fields.

## 6.4 MATERIALS AND METHODS

**Gonadorelin [6-D-Phe] acetate peptide** (pE1–H2–W3–S4–Y5–(D)F6–L7–R8–P9–G10–NH2) or (pGlu-His-Trp-Ser-Tyr-D-Phe-Leu-Arg-Pro-Gly-NH2) was provided by BFC Biopept-Feinchemie as lyophilized powder and acetate salt (purity 99.76 %, water content 6.73% and acetate peptide ratio (MW/MW) 1.8). **Amyloid β-Protein (1-42)** (H-Asp-Ala-Glu-Phe-Arg-His-Asp-Ser-Gly-Tyr-Glu-Val-His-His-Gln-Lys-Leu-Val-Phe-Phe-Ala-Glu-Asp-Val-Gly-Ser-Asn-Lys-Gly-Ala-Ile-Ile-Gly-Leu-Met-Val-Gly-Gly-Val-Val-Ile-Ala-OH) was provided by Bachem Holding AG as lyophilizied powder; **Gelling agents**: Aluminiumdistearte (Alugel 30 ®HEP), Baerlocher, D-Unterschleissheim); **Wetting agents**: hydrogenated phosphatidylcholine(lecithin) (Phospholipon®90H) Lipod D-Ludwigshafen; **Resuspendibility enhancer**: Polyoxyl (PEG)-35 castor oil (Kolliphor®ELP) BTC Europe, D-Burgbergheim; **Complexing agent**: Zinc acetate dehydrate (Zn $(CH_3COO^-)_2$ (Merck KGaA, D-Darmstadt); **Oil vehicle**: miglyol 812 (MCT) (Caesar & Loretz, D-Hilden), castor oil (Gustav Heess, D-Leonberg).

**Formation of the $Zn^{2+}$: GnRH [6-D-Phe] assembly with 0.6 N NaOH.** Equal amounts of 4 mM GnRH [6-D-Phe] and 16 mM, 40 mM, 60 mM, 80 mM, 120 mM, 160 mM, 200 mM and 240 mM $Zn(CH_3COO^-)_2$ aqueous solutions were combined. The pH adjustment was performed using a 0.6 N NaOH under stirring carefully with a dropwise addition along the side wall. The formed precipitate was centrifuged at 12000 x g for 10 min, washed with highly purified water. GnRH [6-D-Phe] in the supernatant as well as in the precipitate was analyzed through a Reversed Phase Chromatography (RP-HPLC) (Supplementary Data Table 6.6).

**Formation of the $Zn^{2+}$: GnRH [6-D-Phe] assembly in Tris buffer.** Equal amounts of 4 mM GnRH [6-D-Phe] and 40 mM, 60 mM, 200 mM $Zn(CH_3COO^-)_2$ solution in 0.05 M Tris buffer (pH=7.2, 7.4, 7.6, 7.8, 8.2) were combined. Precipitation was performed at reduced temperature, 5° C. The formed precipitate was centrifuged at 12000 x g for 10 min, washed with highly purified water. GnRH [6-D-Phe] in the supernatant as well as in the precipitate was analyzed through a RP-HPLC (Supplementary Data Table 6.7).

**ATR-FTIR** Equal amounts of 4 mM GnRH [6-D-Phe] and 8 mM, 16 mM, 40 mM, 80 mM $Zn(CH_3COO^-)_2$ solution in a 0.05 M Tris buffer (pH 7.8) were combined. Aliquots of 30µl of each prepared solution were loaded and the spectra were recorded with a Tensor 27 FTIR spectrometer (Bruker Optics, Ettlingen, Germany) using a Bio-ATR unit at 20° C. Corresponding blank spectra were subtracted. Spectra were recorded at 4 $cm^{-1}$ resolution and the second derivative spectrum was generated (OPUS, Bruker Optics, Ettlingen, Germany).The spectra data analysis and Fourier Self-Deconvolution (FSD) was performed with Origin 2018 software. FSD was performed using bandwidth of 10 $cm^{-1}$ and noise suppression factor of 0.3. The structure content of the deconvoluted peaks was determined using Gaussian band shapes by an iterative curve fitting.

**NMR Spectroscopy** Solution $^1$H-NMR zinc titration of the peptide in $D_2O$: DMSO-d6 (80:20) solvent was performed in a 0.05 M Tris buffer (pH 7.8) at 25° C on a Bruker Avance III HD 800 MHz and at a reduced temperature 5° C on a Varian NMR System 400 MHz. The binding efficiency of $Zn^{2+}$ to peptide was determined through the NMR analysis of the $Zn^{2+}$: GnRH [6-D-Phe] assemblies. The spectra were evaluated using the MestReNova Software 10.0.2-15465 (Supplementary Data Figure 6.12).

**Atomic force microscopy (tapping in Air)** The 10:1 $Zn^{2+}$: GnRH [6-D-Phe] (20 ng/µL; 20 µL volume) was deposed onto poly-L-lysine coated mica for 2 min, followed by gentle rinsing with water and dried in a $N_2$-gas stream. Coating the mica with (+) charged poly-L-lysine repulsed the (+) charged arginine peptide residues of chains not involved in the dimerization process, allowing better imaging. AFM imaging was performed on a Multimode AFM, equipped with a Nanoscope III controller and a type E scanner. Images were recorded on dried samples, under ambient conditions, and using Silicon cantilevers (Olympus; AC160TS; resonance frequency ≈300 kHz). Typical scans were recorded at 1–3 Hz line frequency, with optimized feedback parameters and at 512 × 512 pixels. For image processing and analysis, Scanning Probe Image Processor (v6.4; Image Metrology) was employed. Image processing involved background correction using global fitting with a third-order polynomial and line-by-line correction through the histogram alignment routine.

**Atomic force microscopy (tapping in Tris buffer solution)** The AFM images were performed using the AFM NanoWizard® 4 from JPK Instruments with SPM software and an integrated Axiovert 200 inverted microscope

from Zeiss. As cantilever the qp-BioAC CB3 (Nanosenors; resonance frequency ≈ 30 kHz) was used. A mica-chip was glued on a microscope slide and 20 µl of the 10:1 $Zn^{2+}$: GnRH [6-D-Phe] was added. After 5 min incubation time, the mica-substrate was washed with Tris buffer. The imaging was performed in 1 ml Tris buffer and with the tapping mode (QI™ Advanced Imaging). The following values have been set: Z-length 50 - 70 nm; duration 2 ms and pixel size 256x256. All images were processed and optimized with Data Processing Software from JPK. The processing involved removing incorrect lines, replacing outlier pixel values with the median value of neighbouring pixels and line-by-line correction with a first-order polynomial fit. A histogram is calculated for each line and only the data between the lower and upper limits is used for fitting the polynomial.

**Thioflavin-T Binding Assay.** The fluorescence intensity was measured in multi-well plates in an Agilent Cary Eclipse Fluorescence Spectrophotometer (exc.at 440 nm (slit width 5nm), em. at 482 nm (slit width 10 nm), and averaging over 60 s). 100 µl of each $Zn^{2+}$: GnRH [6-D-Phe] sample, prepared in 0.05 M Tris buffer pH 7.8 containing 20 % DMSO, was vortexed gently and mixed with 200 µL 50 µM ThT solution prepared in the same buffer and stored at 5° C. Aβ42 lyophilizate was dissolved in 0.05 M Tris pH 7.8 containing 20 % DMSO and stored at 5° C over 24 h for the purpose of forming minimal peptide aggregation. 100 µl of 150µM Aβ42 and 100 µl of 4mM GnRH [6-D-Phe] were used as controls and treated the same way as the $Zn^{2+}$: GnRH [6-D-Phe] samples. The fluorescence intensity of all samples was measured over 24 hours.

**MD simulations** Molecular dynamic simulations were performed using the Amber 16 suite[51]. Non-standard residue files were generated using antechamber and the peptide structure was generated with t-leap. Two identical GnRH [6-D-Phe] molecules and 20 zinc ions were placed at random coordinates in a TIP3P water box using 10 Å of padding. Energy minimization was performed with pmemd. MPI with the steepest descent method for 5000 cycles and with the conjugate gradient method at constant volume for the remaining 45000 cycles. The system was then heated from 0 to 300 K and equilibrated for 200 ps with pmemd.cuda. A Langevin thermostat with a collision frequency set to 5 $ps^{-1}$ was used. Pressure was kept constant using isotropic position scaling and a Monte Carlo barostat. The SHAKE algorithm was turned on. After equilibration, a 500 ns production run was performed with the same thermostat and barostat settings as during equilibration. VdW and electrostatic interaction energies were calculated using the LIE method as implemented in cpptraj and plotted with matplotlib[39,40,52].

**$Zn^{2+}$: GnRH [6-D-Phe] complex preparation** $Zn^{2+}$:GnRH [6-D-Phe] 10:1 preformed complex was prepared from equal amounts of 4 mM GnRH [6-D-Phe] and 40 mM $Zn(CH_3COO^-)_2$ in 0.05 M Tris buffer pH 7.8. The pH of the resulting mixture at 25° C was 7.2. The temperature was then reduced to 5° C and resulted in a pH increase to pH 7.8. The mixture was kept at 5° C for 24 h and then freeze dried. The *in situ* $Zn^{2+}$: GnRH [6-D-Phe] 10:1 complex was prepared from equal amounts of 4 mM GnRH [6-D-Phe] and 40 mM Zn $(CH_3COO^-)_2$ in water. The pH of the resulting mixture at 25° C was 6.5. Similarly to the preformed complex the temperature was reduced to 5° C. The pH stayed constant. The mixture was kept at the same conditions as the preformed complex and freeze dried. Both complexes were freeze dried using a Christ Epsilon 2-6 D freeze-dryer (Martin Christ Gefriertrocknungsanlagen GmbH, D-Osterode) (ambient pressure; freezing 3 h, −50° C; 150 mTorr; primary drying: 60 h,−20° C; secondary drying: 18 h, 20° C) with process and plant control LPC plus SCADA software.

**$Zn^{2+}$: GnRH [6-D-Phe] lyophilisate micronization** The cryogenic micronization of $Zn^{2+}$: GnRH [6-D-Phe] lyophilisate and the separately added Tris buffer were performed using a Retsch Cryo Mill (Retsch Technology, Haan, Germany). The grinding process was performed for the duration of 1 minute at 25 Hz with a precooling phase of 10 min in liquid nitrogen.

**$Zn^{2+}$: GnRH [6-D-Phe] oil depot preparation** The $Zn^{2+}$: GnRH [6-D-Phe] oil depot formulations preparation was performed under a laminar flow cabinet in a two-step process. The gelling agent Aluminiumdistearte (Al-DiSt) was weighed and suspended in the oil vehicle miglyol 812 (MCT) to a final weight of 95 g (corresponding to 100 mL). The prepared mixture was heated at 174° C for 2 hours under $N_2$. After cooling down to 25° C hydrogenated lecithin and PEG-35 castor oil were incorporated into the gelled oil matrix and stirred at 160° C for 1 hour under $N_2$. The castor oil: MCT 50:50 % (w/w) matrix was heated and agitated under inert atmosphere ($N_2$) at 60° C and then cooled down to room temperature at 25° C. The cryo-ground $Zn^{2+}$: GnRH [6-D-Phe] lyophilizate was suspended in the prepared oil matrices at ambient temperature of 25° C using an Ultra-Turrax

T-10 basic (IKA Labortechnik, Germany) for 5 minutes at 2000 rpm. 139.8 mg of Tris buffer salt consisting of 2.01 g Trizma HCl and 1.485 g Trizma Base was added to the *in-situ* complex formulation. The 5000 µg/ml $Zn^{2+}$: GnRH [6-D-Phe] oil depot suspensions were aliquoted in 20R glass vials. Both reference suspensions were prepared using bulk GnRH [6-D-Phe] lyophilisate at the same concentration.

**Rheology: Viscosity profile** Viscosity measurement and flow curves evaluation were performed with MCR 100 (Anton Paar Germany, Ostfildern-Scharnhausen) cone plate system CP – 1 (50 mm diameter, a cone angle of 1 °, and a gap of 0.042 mm). The viscosity η was defined depending on the shear rate ẏ and measuring sections a) 0 – 500 $s^{-1}$ (30 points, 6 s per point; 180 s measurement time), b) 500 $s^{-1}$ (1 point, 6 s per point, 6 s measurement time), c) 500 – 0 $s^{-1}$ (30 points, 6 s per point, 180 s measurement time).

**$Zn^{2+}$: GnRH [6-D-Phe] particle size distribution and characterization** The particle size distribution of $Zn^{2+}$: GnRH [6-D-Phe] oil depot suspensions was analysed employing a Laser Diffraction Particle Size Analyzer LA-950 (Retsch Technology, Haan). The samples were prepared in triplicate (n=3). 0.2 mL of the oil suspension withdrawn from the vial and measured in a solution of 1 % span 80 in isooctane (m/v) in a standard measuring cell with 10 mL volume.

**SEDD (Microemulsion) characterization** The microemulsion droplet size was determined by dynamic light scattering using Zetasizer Nano-ZS (Malvern Instruments Ltd., Herrenberg, Germany). 1mL of the formulations was injected into 6mL of PBS (pH=7.4) and shaken in an incubated shaker 3031 (GFL, Burgwedel, Germany) at 39° C and 60 rpm over 24h. The diluted and filtered samples were measured in disposable Plastibrand semi-micro PMMA cuvettes (Brand GmBH, Wertheim, Germany) after 20 seconds equilibration time at 25° C and with buffer as dispersant. Positioning, attenuation selection and measuring duration as well as number of sub runs for the three performed measurements per sample were optimised automatically for each run by the Zetasizer Software 6.32. Z-average and polydispersity index (PdI) were calculated applying the general purpose (normal resolution) analysis mode

**GnRH [6-D-Phe] extraction from the complex and oil matrix** In order to establish a suitable extraction method for the determination of the GnRH [6-D-Phe] content in the oil depot suspension the following extraction experiments were performed: the GnRH [6-D-Phe] was extracted from the prepared $Zn^{2+}$: GnRH [6-D-Phe] oil depot suspensions using dichloromethane (DCM), where GnRH [6-D-Phe] is not soluble in combination with HEPES (pH 7.4). HEPES was selected as medium instead of PBS buffer, since phosphate can precipitate the zinc salt from the complex. 2 mL oil depot suspension was weighted into a falcon tube, 4 mL DCM and 6 mL HEPES (pH 7.4) were added. The tube was shaken or vortexed at room temperature (25° C) and put into an incubated shaker 3031 (GFL, Germany) at 39° C and 60 rpm for 48 h. The RP-HPLC analysis was performed at 220 nm. A second extraction method was applied: 2 ml of each formulation were pipetted into 6 ml HEPES (pH 7.4). The falcon tubes were placed in an incubated shaker 3031 (GFL, Germany) at 39° C and 60 rpm for 48 h. The tubes were then centrifuged for 60 minutes at 4000 rpm and 5° C. 1 ml of the lower aqueous phase was used for RP-HPLC at 220 nm. The extraction with HEPES (pH 7.4) delivered results of nearly 100% and indicated high extraction efficiency.

***In vitro* release study** The *in vitro* release study was conducted using VISKING® dialysis tubing, MWCO 12 – 14 kD, RC, 28 mm (SERVA, Germany). The tubes were filled with 1.5 mL formulation. The release medium was 20 mL HEPES (pH 7.4). HEPES was selected as release medium instead of PBS buffer, since phosphate can precipitate the zinc salt from the complex. The *in vitro* evaluation was performed in duplicates and in an incubated shaker 3031 (GFL, Germany) at 39° C and 60 rpm. 1 mL sample was used for the RP-HPLC analysis at the following time points: 1 h, 3 h, 5 h, 7 h, 22 h, 25 h, 28 h, 46 h, 52 h, 76 h, 100 h, 172 h, 196 h, 220 h, and 336 h (14 days). The GnRH [6-D-Phe] content in the oil vehicle and in the donor cell was extracted using 2mL HEPES buffer (pH 7.4). After 48 hours of an equilibration of the peptide between the two phases the emulsion was centrifuged for 60 minutes at 4000 rpm and 5° C. The quantity of the peptide in the lower aqueous phase was analysed by RP-HPLC at 220 nm.

**Determination of the GnRH [6-D-Phe] (RP-HPLC)** The GnRH [6-D-Phe] content in the formed precipitate/fibrils was analysed by RP-HPLC after dissolution in 0.1 % acetic acid, using a LUNA C8 (4.6 mm x 250 mm; size = 5 µm; Phenomenex, USA) column, with a C8 pre-column (4 mm x 3 mm; size = 5 µm) at an

HPLC Agilent 1100/1200 series (Agilent Technologies, USA) (mobile phase A (water + 1 mL/L Trifluoroacetic acid (TFA) (v/v)) and mobile phase B (800 g Acetonitrile + 200 g water + 1.2 mL TFA), 1.1 mL/min flow, column temperature 40° C, and autosampler temperature 2 – 8° C. The Retention Time (RT) of GnRH [6-D-Phe] was 8.5 ± 1.5 minutes with UV detection at 220 nm.

## 6.5 REFERENCES AND ACKNOWLEDGMENTS


1. Cai, L., Hogue, D., Lin, Z. & Filvaroff, E. H. A slow release formulation of insulin as a treatment for osteoarthritis. *Osteoarthr. Cartil.* **10,** 692–706 (2002).

2. Hallas-Møller, K., Petersen, K. & Schlichtkrull, J. Crystalline and amorphous insulin-zinc compounds with prolonged action. *Science* **116,** 394–398 (1952).

3. Qian, F. *et al.* Sustained release subcutaneous delivery of BMS-686117, a GLP-1 receptor peptide agonist, via a zinc adduct. *Int. J. Pharm.* **374,** 46–52 (2009).

4. Tudor, A. Pharmaceutical compositions containing hirudin. (2002).

5. Gietz, U., Arvinte, T., Häner, M., Aebi, U. & Merkle, H. P. Formulation of sustained release aqueous Zn-hirudin suspensions. *Eur. J. Pharm. Sci.* **11,** 33–41 (2000).

6. Homan, J. D. H., Neutelings, J. P. J., Overbeek, G. A., Booij, C. J. & Van Der Vies, J. Corticotrophin zinc phosphate and hydroxide; long-acting aqueous preparations. *Lancet* **263,** 541–543 (1954).

7. Cai, Y., Xu, M., Yuan, M., Liu, Z. & Yuan, W. Developments in human growth hormone preparations: Sustained-release, prolonged half-life, novel injection devices, and alternative delivery routes. *Int. J. Nanomedicine* **9,** 3527–3538 (2014).

8. Brodbeck, K. J., Pushpala, S. & McHugh, A. J. Sustained Release of Human Growth Hormone from PLGA Solution Depots. *Pharm. Res.* **16,** 1825–1829 (1999).

9. Jacob, R. S. *et al.* Amyloid formation of growth hormone in presence of zinc: Relevance to its storage in secretory granules. *Sci. Rep.* **6,** 23370 (2016).

10. Matthes, D., Gapsys, V., Brennecke, J. T. & de Groot, B. L. An Atomistic View of Amyloidogenic Self-assembly: Structure and Dynamics of Heterogeneous Conformational States in the Pre-nucleation Phase. *Sci. Rep.* **6,** 33156 (2016).

11. Gilead, S. & Gazit, E. Self-organization of short peptide fragments: From amyloid fibrils to nanoscale supramolecular assemblies. in *Supramolecular Chemistry* **17,** 87–92 (2005).

12. Zanuy, D., Ma, B. & Nussinov, R. Short Peptide Amyloid Organization: Stabilities and Conformations of the Islet Amyloid Peptide NFGAIL. *Biophys. J.* **84,** 1884–1894 (2003).

13. Gazit, E. Self Assembly of Short Aromatic Peptides into Amyloid Fibrils and Related Nanostructures. *Prion Mini-Review* **1,** (2007).

14. Rufo, C. M. *et al.* Short peptides self-assemble to produce catalytic amyloids. *Nat. Chem.* **6,** 303–309 (2014).

15. Maji, S. K. *et al.* Amyloid as a Depot for the Formulation of Long-Acting Drugs. *PLoS Biol.* **6,** e17 (2008).

16. Astaneh, R., Nafissi-Varcheh, N. & Erfan, M. Zinc-leuprolide complex: Preparation, physicochemical characterization and release behaviour from in situ forming implant. *J. Pept. Sci.* **13,** 649–654 (2007).

17. Dolińska, B. & Ryszka, F. Preparation and properties of selected Zn(II)–peptide complexes in suspension. *Farm.* **58,** 1131–1136 (2003).

18. Chiti, F. & Dobson, C. M. Protein Misfolding, Functional Amyloid, and Human Disease. *Annu. Rev. Biochem.* **75,** 333–366 (2006).

19. Bal, W., Kozlowski, H., Masiukiewicz, E., Rzeszotarska, B. & Sóvágó, I. LHRH interaction with Zn(II) ions. *J. Inorg. Biochem.* **37,** 135–139 (1989).

20. Hoitink, M. A. *et al.* Identification of the Degradation Products of Gonadorelin and Three Analogues in Aqueous Solution. *Anal. Chem.* **69,** 4972–4978 (1997).

21. Valéry, C. *et al.* Atomic view of the histidine environment stabilizing higher-pH conformations of pH-dependent proteins. *Nat. Commun.* **6,** 7771 (2015).

22. Carrell, R. W. & Lehmann, H. Zinc acetate as a precipitant of unstable haemoglobins. *J. Clin. Pathol.* **34,** 796–9 (1981).

23. Sigma-Aldrich Company. Trizma ® Buffers. *Supelco* 9–10 (1996).

24. Ami, D. *et al.* In situ characterization of protein aggregates in human tissues affected by light chain amyloidosis: a FTIR microspectroscopy study. *Sci. Rep.* **6,** 29096 (2016).

25. Kurouski, D., Van Duyne, R. P. & Lednev, I. K. Exploring the structure and formation mechanism of amyloid fibrils by Raman spectroscopy: a review. *Analyst* **140,** 4967–4980 (2015).

26. Majid, A., Patil-Sen, Y., Ahmed, W. & Sen, T. Tunable Self-Assembled Peptide Structure: A Novel Approach to Design Dual-Use Biological Agents. in *Materials Today: Proceedings* **4,** 32–40 (2017).

27. Zubyk, H., Plonska-Brzezinska, M., Shyshchak, O., Astakhova, O. & Bratychak, M. Study of Phenol-Formaldehyde Oligomers Derivatives Structure by IR- and NMR-Spectroscopy. *Chem. Chem. Technol.* **9,** (2015).

28. Şen, P. *et al.* Fluorescence and FTIR spectra analysis of trans-A2B2-substituted di- and tetra-phenyl porphyrins. *Materials (Basel).* **3,** 4446–4475 (2010).

29. Skushnikova, A. I. *et al.* Antidote and Antihypoxant Activity of 1-Organylimidazole Complexes with Zinc Salts. *Khimiko-Farmatsevticheskii Zhurnal* **37,** 28–30 (2003).

30. Sarroukh, R., Goormaghtigh, E., Ruysschaert, J. M. & Raussens, V. ATR-FTIR: A 'rejuvenated' tool to investigate amyloid proteins. *Biochim. Biophys. Acta - Biomembr.* **1828,** 2328–2338 (2013).

31. Shivu, B. *et al.* Distinct β-sheet structure in protein aggregates determined by ATR-FTIR spectroscopy. *Biochemistry* **52,** 5176–5183 (2013).

32. Karjalainen, E.-L., Ravi, H. K. & Barth, A. Simulation of the Amide I Absorption of Stacked β-Sheets. *J. Phys. Chem. B* **115,** 749–757 (2011).

33. Miller, L. M., Bourassa, M. W. & Smith, R. J. FTIR spectroscopic imaging of protein aggregation in living cells. *Biochim. Biophys. Acta - Biomembr.* **1828,** 2339–2346 (2013).

34. Chimie, R. R. De, Adochitei, A. & Drochioiu, G. Rapid Characterization of Peptide Secondary Structure By FTIR Spectroscopy. *Rev. Roum. Chim.* **56,** 783–791 (2011).

35. Zandomeneghi, G., Krebs, M. R. H., McCammon, M. G. & Fändrich, M. FTIR reveals structural differences between native β-sheet proteins and amyloid fibrils. *Protein Sci.* **13,** 3314–3321 (2009).

36. Alies, B. *et al.* Zinc(II) Binding Site to the Amyloid-β Peptide: Insights from Spectroscopic Studies with a Wide Series of Modified Peptides. *Inorg. Chem.* **55,** acs.inorgchem.6b01733 (2016).

37. Nedumpully-Govindan, P., Yang, Y., Andorfer, R., Cao, W. & Ding, F. Promotion or

Inhibition of Islet Amyloid Polypeptide Aggregation by Zinc Coordination Depends on Its Relative Concentration. *Biochemistry* **54,** 7335–7344 (2015).

38. Gregoire, S., Irwin, J. & Kwon, I. Techniques for monitoring protein misfolding and aggregation in vitro and in living cells. *Korean J Chem Eng* **29,** 693–702 (2012).

39. Brandsdal, B. O. *et al.* Free energy calculations and ligand binding. *Advances in Protein Chemistry* **66,** 123–158 (2003).

40. Aqvist, J., Luzhkov, V. B. & Brandsdal, B. O. Ligand binding affinities from MD simulations. *Acc. Chem. Res.* **35,** 358–365 (2002).

41. Patel, R. Parenteral suspension: an overview. *Int J Curr Pharm Res* **2,** 4–13 (2010).

42. Puthli, S. & Vavia, P. Stability Studies of Microparticulate System with Piroxicam as Model Drug. *AAPS PharmSciTech* **10,** 872–880 (2009).

43. Narang, A. S., Delmarre, D. & Gao, D. Stable drug encapsulation in micelles and microemulsions. *Int. J. Pharm.* **345,** 9–25 (2007).

44. Eastoe, J. 3. Microemulsions. *Surfactant Chem.* 59–95 (2003).

45. Talegaonkar, S. *et al.* Microemulsions: a novel approach to enhanced drug delivery. *Recent Pat. Drug Deliv. Formul.* **2,** 238–257 (2008).

46. Basak, S. C., Kumar, K. S. & Ramalingam, M. Design and release characteristics of sustained release tablet containing metformin HCl. *Rev. Bras. Ciencias Farm. J. Pharm. Sci.* **44,** 477–483 (2008).

47. Kalam, A., Kabir, L., Biswas, B. K., Shara, A. & Rouf, S. Design , Fabrication and Evaluation of Drug Release Kinetics from Aceclofenac Matrix Tablets using Hydroxypropyl Methyl Cellulose. *Dhaka Univ. J. Pharm. Sci.* **8,** 23–30 (2009).

48. Wan, S. *et al.* Self-assembling peptide hydrogel for intervertebral disc tissue engineering. *Acta Biomater.* **46,** 29–40 (2016).

49. Lian, M., Chen, X., Lu, Y. & Yang, W. Self-Assembled Peptide Hydrogel as a Smart Biointerface for Enzyme-Based Electrochemical Biosensing and Cell Monitoring. *ACS Appl. Mater. Interfaces* **8,** 25036–25042 (2016).

50. Habibi, N., Kamaly, N., Memic, A. & Shafiee, H. Self-assembled peptide-based nanostructures: Smart nanomaterials toward targeted drug delivery. *Nano Today* **11,** 41–60 (2016).

51. Maingi, V., Jain, V., Bharatam, P. V. & Maiti, P. K. Dendrimer building toolkit: Model building and characterization of various dendrimer architectures. *J. Comput. Chem.* **33,** 1997–2011 (2012).

52. Roe, D. R. & Cheatham, T. E. PTRAJ and CPPTRAJ: Software for processing and analysis of molecular dynamics trajectory data. *J. Chem. Theory Comput.* **9,** 3084–3095 (2013).

This work was supported by Veyx Pharma D-Schwarzenborn and DBU (Deutsche Bundesstiftung Umwelt) D-Osnabrueck. The authors wish to acknowledge Dr. David. S. Stephenson and Claudia Dubler Department of Chemistry, LMU D-Munich, for recording the solution state NMR spectra and for their support. We are also grateful to Dr. Dimitar Stamov, JPK Instruments D-Berlin, for his help and troubleshooting during the AFM measurements with tapping mode in solution. I would like to thank Nikola Z. Kolev Department of Molecular Biology, Umea University for his support and help.

## 6.6 SUPPLEMENTARY DATA

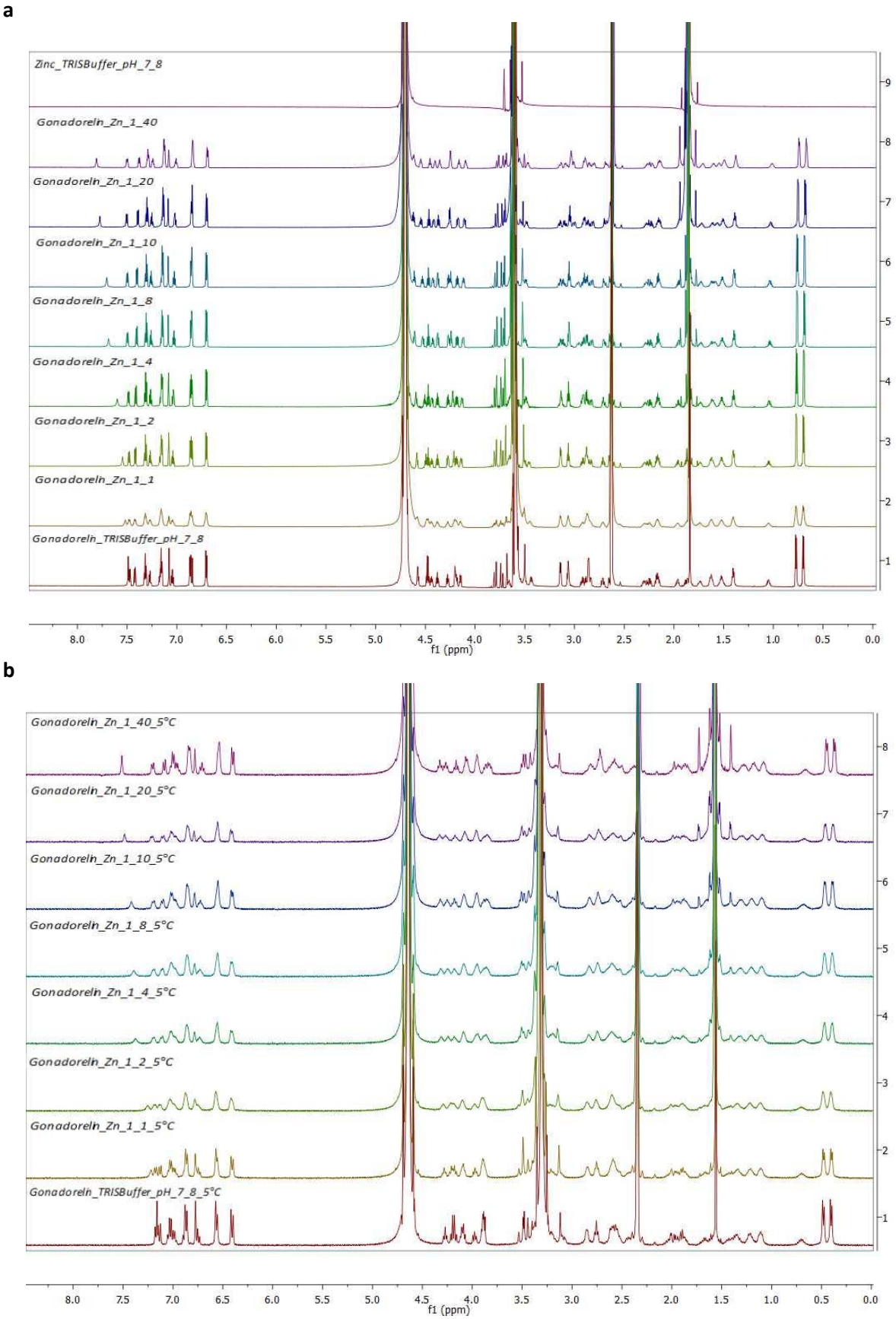


**Figure 6.12| Solution-state NMR Spectra of $Zn^{2+}$: GnRH [6-D-Phe] assemblies**
molar ratio 1:1 , 2:1, 4:1, 8:1,10:1, 20:1, 40:1, GnRH [6-D-Phe] in Tris buffer (pH 7.8) **(a)** at 25° C **(b)** at 5° C

| 1 | 2 | 3 | | 4 | |
|---|---|---|---|---|---|
| **Ratio $Zn^{2+}$: GnRH** | pH at 25° C | pH adjusted with 0.6 N NaOH | GnRH [6-D-Phe] [ % ] ± SD | pH adjusted with 0.6 N NaOH | GnRH [6-D-Phe] [ % ] ± SD |
| **4:1** | 6.4 | 7.0 | 1.2 ± 0.2 | 8.2 | 9.8 ± 0.2 |
| **10:1** | 6.4 | 7.0 | 1.2 ± 0.2 | 8.3 | 95.9 ± 0.1 |
| **15:1** | 6.5 | 7.8 | 41.5 ± 0.1 | 8.3 | 28.4 ± 0.1 |
| **20:1** | 6.5 | 7.1 | 6.8 ± 0.1 | 8.1 | 33.9 ± 0.3 |
| **30:1** | 6.6 | 7.2 | 15.2 ± 0.2 | 8.1 | 44.2 ± 0.1 |
| **40:1** | 6.6 | 7.3 | 26.3 ± 0.1 | 8.2 | 54.7 ± 0.3 |
| **50:1** | 6.6 | 7.2 | 24.9 ± 0.2 | 8.0 | 54.9 ± 0.2 |
| **60:1** | 6.6 | 6.8 | 13.3 ± 0.1 | 8.1 | 61.2 ± 0.3 |

**Table 6.6| Precipitation of the $Zn^{2+}$: GnRH [6-D-Phe] assembly with 0.6 N NaOH**
**Column 1** indicates the $Zn^{2+}$: GnRH molar ratios. **Column 2** represents the pH of the corresponding aqueous $Zn^{2+}$: GnRH at 25° C. **Column 3** represents the adjusted pH at ~ 7.0 with 0.6N NaOH and corresponding % precipitated peptide. **Column 4** represents the adjusted pH at ~ 8.0 with 0.6N NaOH and corresponding % precipitated peptide. The titration with NaOH did not offer enough precision to adjust the pH value of the solutions in the range of pH=7.2- 8.2 at 0.2 pH units step

| 1 | 2 | 3 | 4 | 5 | 2 | 3 | 4 | 5 | 2 | 3 | 4 | 5 |
|---|---|---|---|---|---|---|---|---|---|---|---|---|
| **pH Tris Buffer** | Ratio Zn2+: GnRH | pH 25° C | pH 5° C | GnRH [6-D-Phe] at 5° C [ % ] ± SD | Ratio Zn2+: GnRH | pH 25° C | pH 5° C | GnRH [6-D-Phe] at 5° C [ % ] ± SD | Ratio Zn2+: GnRH | pH 25° C | pH 5° C | GnRH [6-D-Phe] at 5° C [ % ] ± SD |
| **7.2** | 10:1 | 6.7 | 7.3 | 36.2 ±0.1 | 15:1 | 6.7 | 7.3 | no precipitation | 50:1 | 6.3 | 6.9 | no precipitation |
| **7.4** | | 6.9 | 7.5 | 53.6 ±0.1 | | 6.8 | 7.4 | 40.5 ±0.1 | | 6.4 | 7.0 | no precipitation |
| **7.6** | | 7.1 | 7.7 | 59.9 ±0.1 | | 7.0 | 7.6 | 48.8 ±0.1 | | 6.6 | 7.2 | no precipitation |
| **7.8** | | 7.3 | 7.9 | 99.9 ±0.2 | | 7.1 | 7.7 | 50.5 ±0.1 | | 6.8 | 7.4 | 12.2 ±0.1 |
| **8.2** | | 7.5 | 8.1 | 45.7 ±0.1 | | 7.2 | 7.8 | 13.9 ±0.1 | | 6.7 | 7.3 | 16.2 ±0.1 |

**Table 6.7| Precipitation of the $Zn^{2+}$: GnRH [6-D-Phe] assembly in Tris buffer (pH 7.8) at 5° C**
**Column 1** represents the pH of the used Tris-buffer. **Column 2** indicates the $Zn^{2+}$: GnRH molar ratio. **Column 3** represents the pH of $Zn^{2+}$: GnRH [6-D-Phe] assembly in the corresponding Tris-buffer at 25° C. **Column 4** represents the pH of $Zn^{2+}$: GnRH [6-D-Phe] assembly in the corresponding Tris-buffer at 5° C. **Column 5** represents the corresponding % precipitated peptide after reduction of 25° C to 5° C over 24 h.

**a**

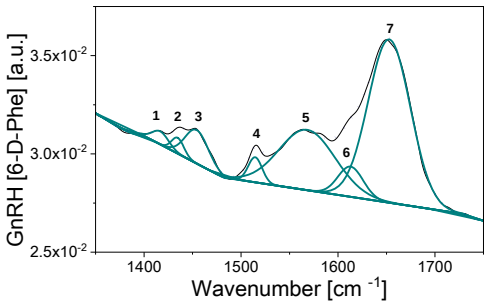


| Index | Center | FWHM | Height | Area |
|---|---|---|---|---|
| 1 | 1416.74 | 19.96 | 6.64E-0 | 1.71 |
| 2 | 1434.73 | 14.92 | 8.01E-0 | 1.54 |
| 3 | 1454.28 | 28.35 | 1.70E-0 | 6.24 |
| 4 | 1514.58 | 16.89 | 1.28E-0 | 2.78 |
| 5 | 1568.23 | 67.85 | 3.07E-0 | 26.94 |
| 6 | 1612.96 | 30.58 | 1.54E-0 | 6.07 |
| 7 | 1652.86 | 50.98 | 8.31E-0 | 54.72 |

**b**

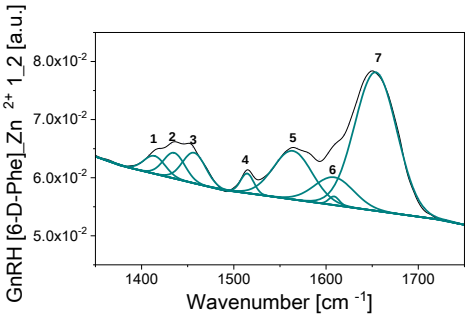


| Index | Center | FWHM | Height | Area |
|---|---|---|---|---|
| 1 | 1414.00 | 27.12 | 3.07E-0 | 3.53 |
| 2 | 1435.36 | 27.34 | 4.41E-0 | 5.11 |
| 3 | 1456.98 | 29.45 | 5.25E-0 | 6.55 |
| 4 | 1514.51 | 16.68 | 3.37E-0 | 2.38 |
| 5 | 1563.86 | 49.33 | 8.35E-0 | 17.46 |
| 6 | 1608.72 | 49.95 | 4.79E-0 | 10.15 |
| 6 | 1608.72 | 13.33 | 1.49E-0 | 0.84 |
| 7 | 1653.84 | 53.38 | 2.38E-0 | 53.98 |

**c**

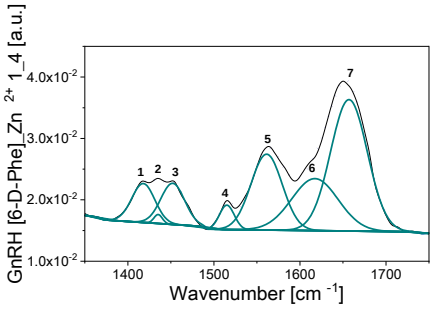


| Index | Center | FWHM | Height | Area |
|---|---|---|---|---|
| 1 | 1417.99 | 31.42 | 6.34E-0 | 7.52 |
| 2 | 1435.26 | 11.28 | 1.46E-0 | 0.62 |
| 3 | 1452.18 | 32.62 | 6.70E-0 | 8.25 |
| 4 | 1515.06 | 20.21 | 3.98E-0 | 3.03 |
| 5 | 1561.29 | 42.77 | 1.24E-0 | 19.93 |
| 6 | 1617.46 | 63.33 | 8.47E-0 | 20.23 |
| 7 | 1657.03 | 50.06 | 2.14E-0 | 40.42 |

**d**

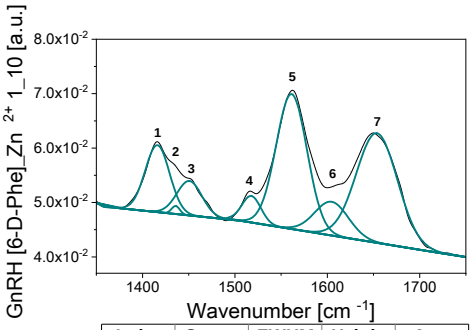


| Index | Center | FWHM | Height | Area |
|---|---|---|---|---|
| 1 | 1416.08 | 30.86 | 1.23E-02 | 12.65 |
| 2 | 1435.92 | 10.30 | 1.47E-03 | 0.50 |
| 3 | 1450.71 | 31.73 | 6.33E-03 | 6.70 |
| 4 | 1517.83 | 24.16 | 4.86E-03 | 3.92 |
| 5 | 1561.35 | 39.17 | 2.48E-02 | 32.38 |
| 6 | 1604.70 | 42.78 | 6.20E-03 | 8.84 |
| 7 | 1653.68 | 52.12 | 2.01E-02 | 35.00 |

**e**

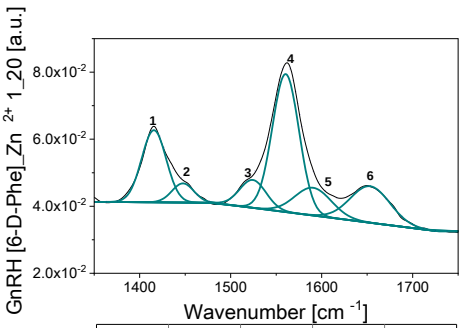


| Index | Center | FWHM | Height | Area |
|---|---|---|---|---|
| 1 | 1415.62 | 31.65 | 2.15E-02 | 19.56 |
| 2 | 1447.52 | 28.24 | 5.71E-03 | 4.64 |
| 3 | 1524.39 | 34.14 | 8.31E-03 | 8.16 |
| 4 | 1560.47 | 34.26 | 4.11E-02 | 40.51 |
| 5 | 1590.54 | 47.04 | 8.26E-03 | 11.17 |
| 6 | 1653.32 | 51.00 | 1.09E-02 | 15.96 |

**Figure 6.13| Deconvoluted FT-IR absorbance spectra**
(a) GnRH [6-D-Phe] and (b) 2:1; (c) 4:1; (d) 10:1 ; (e) 20:1 Zn 2+: GnRH [6-D-Phe] assemblies

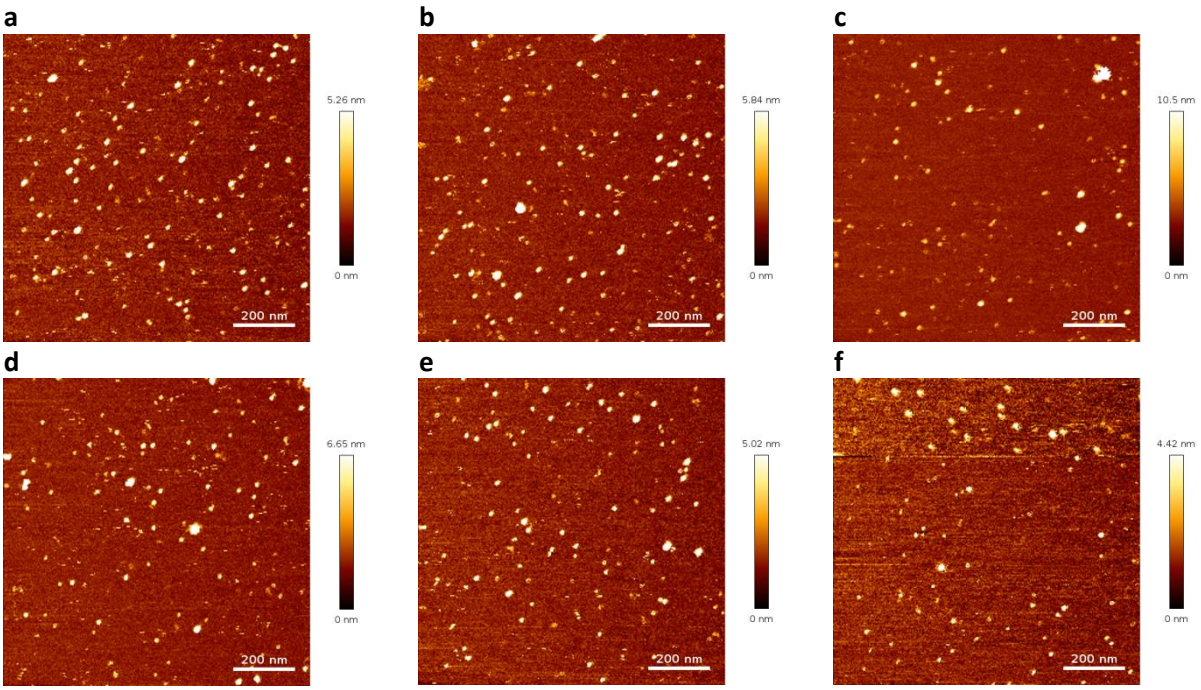


**Figure 6.14| AFM image of the $Zn^{2+}$: GnRH [6-D-Phe]**
(a)-(e) tapping mode Tris buffer solution with dilution 1:1000 after 48h

a

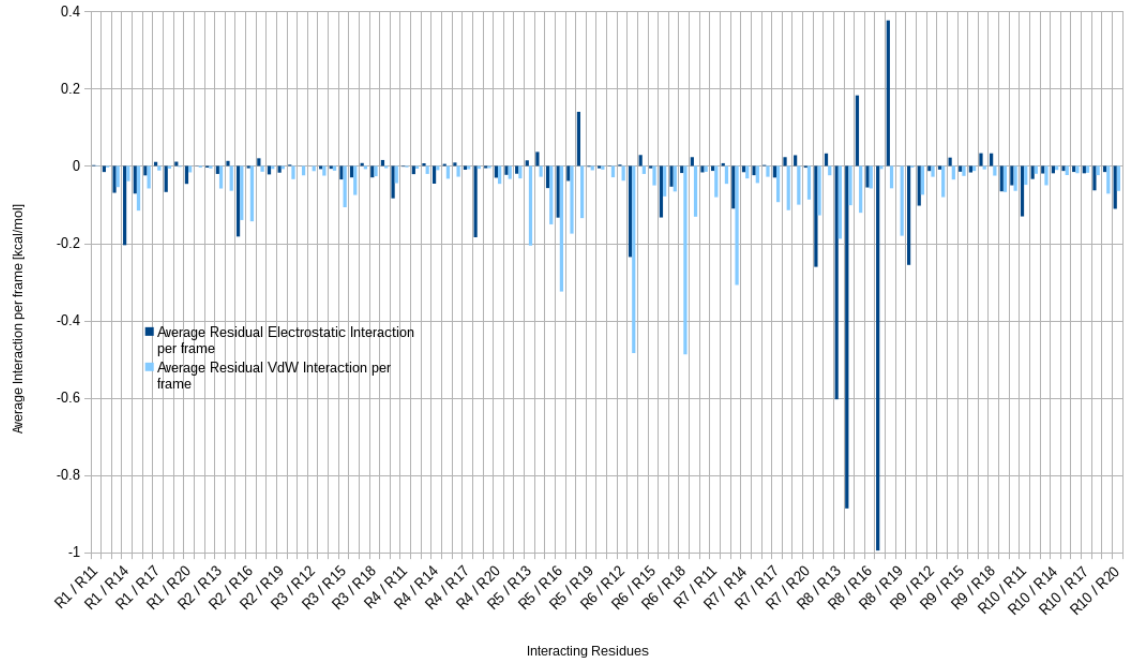


b

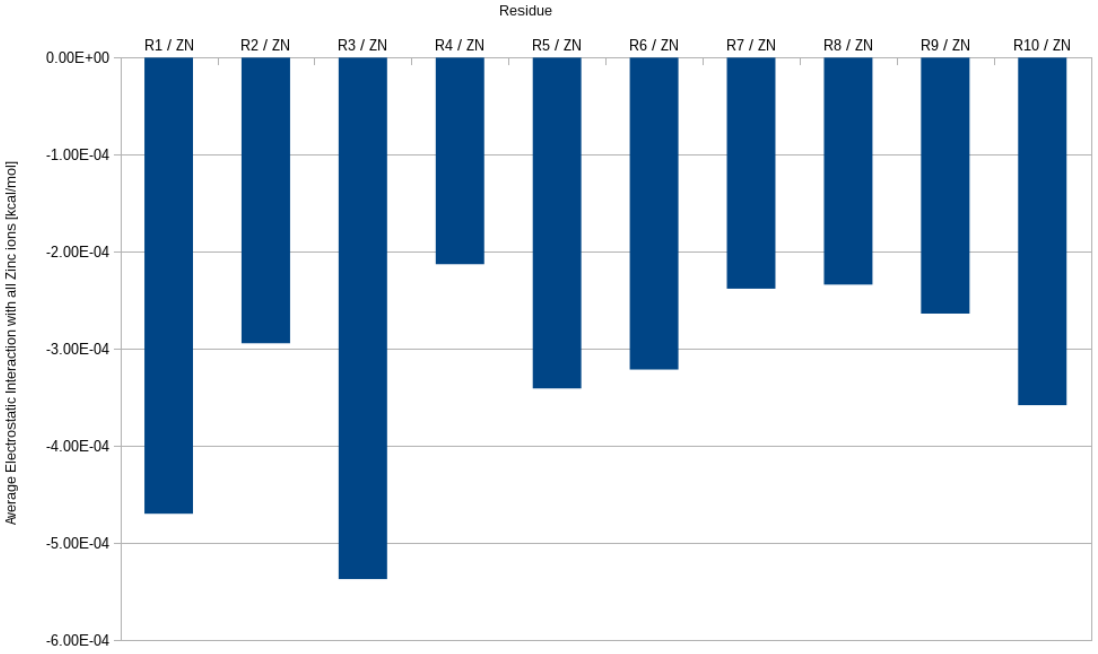


**Figure 6.15| Average linear interaction energy**
(a) VdW and electrostatic of R1-R10 amino acid residue of the first peptide chain and R11-R20 amino acid residue of the second peptide chain (b)electrostatic of all amino acid residue with $Zn^{2+}$

**a**

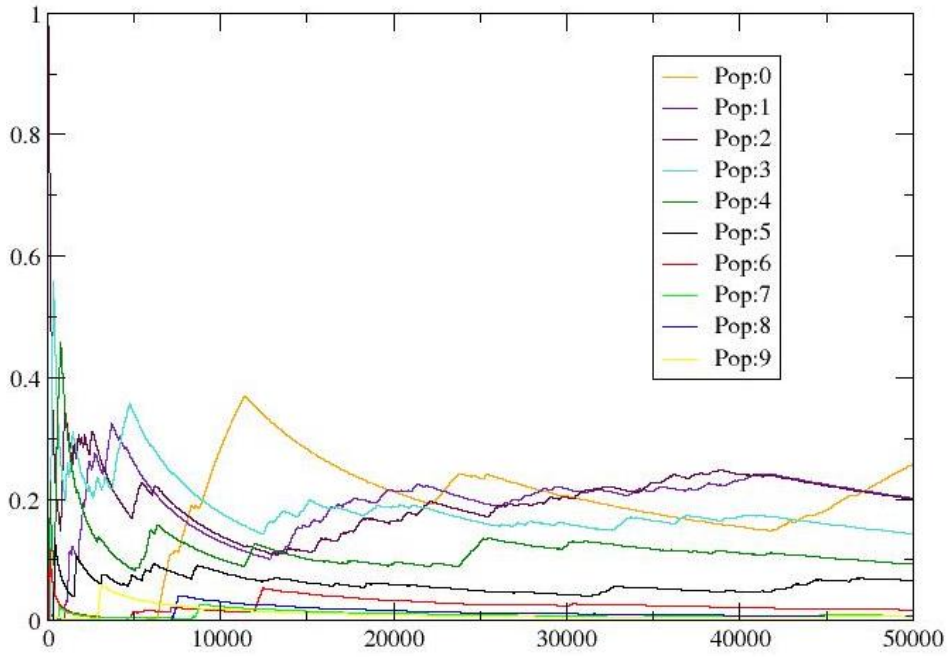


**b**

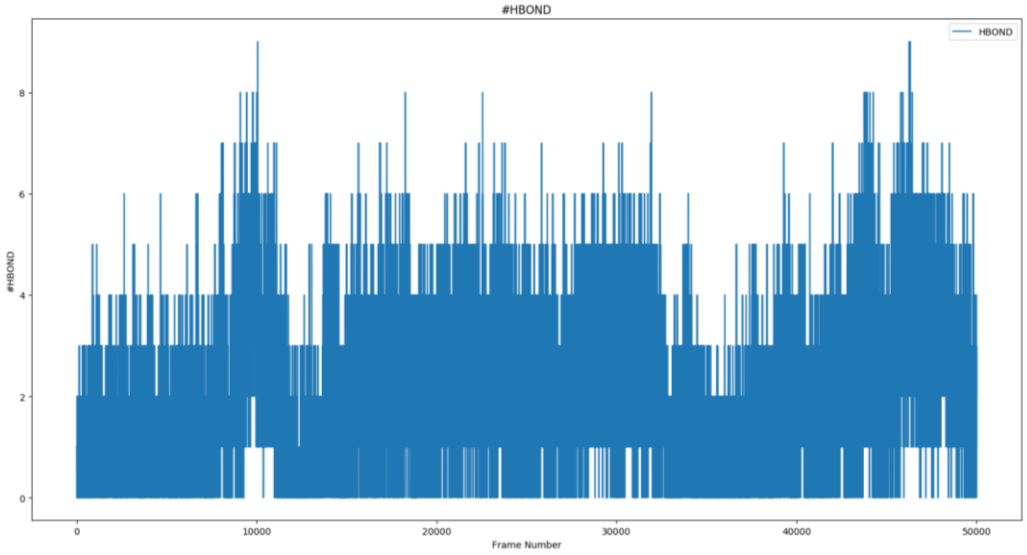


**Figure 6.16| Peptide dimerization**
(a) Cluster analysis of the formed dimer (b) Total number of hydrogen bonds formed between peptide residues during a 500 ns MD simulation.

## 6.7 FIGURES AND TABLES

# SUMMARY

The goal of this thesis was to obtain an environmentally safe and economically-priced formulation for swine estrous cycle synchronization. Based on the veterinary requirements, a GnRH [6-D-Phe] acetate multi – dose oil depot formulation was pursued.

Due to the short GnRH [6-D-Phe] plasma half – life of up to 2 hours, a suitable depot vehicle was necessary to achieve sustained release with at least two week physiological effect. For this purpose, low viscosity 50:50 % (w/w) castor oil/ MCT and high viscosity 90:10 % (w/w) castor oil/MCT were investigated at first. The required two week physiological effect demanded to establish a suitable *in vitro* model. The established model could differentiate between formulations with regards to vehicle viscosity and peptide concentration effect. The first *in vivo* study showed the most pronounced cycle blocking effect with castor oil: MCT 50:50 % (w/w) 1875 µg/ml GnRH [6-D-Phe], which lasted an average of 3.8 ± 1.3 days. 1875 µg/mL GnRH [6-D-Phe] in low viscosity castor oil: MCT 50:50 % (w/w) achieved a longer and more consistent cycle blocking effect compared to 1875 µg/mL GnRH [6-D-Phe] in high viscosity castor oil: MCT 90:10 %.

Formulating GnRH [6-D-Phe] in a less prone to oxidation oily mixture of castor oil/MCT proved to be beneficial. Storage of the castor oil: MCT 50:50 % (w/w) 1875 µg/ml GnRH [6-D-Phe] oil depot suspension at 2-8° C, 25° C and 40° C over 12 months did not affect its chemical or physical integrity.

At an effective concentration of 1875 µg/mL GnRH [6-D-Phe], the incorporation of aluminium distearate as gelling agent, hydrogenated lecithin as well as PEG-35 castor oil to pure MCT oil resulted in a favourable shear-thinning behaviour. This may potentially reduce the spreading of the formulation at the injection site and facilitate easier withdrawal from a multi – dose container. The combination of hydrogenated lecithin and PEG-35 castor oil resulted in the formation of a self-emulsifying drug delivery system of GnRH [6-D-Phe]. As a result, the release was more consistent and controlled with reduced initial *in vitro* burst. The second *in vivo* study could confirm that the best cycle blocking effect of 4 to 5 days with regards to synchronicity, length and adverse reactions, was achieved with 1875 µg/mL GnRH [6-D-Phe] in MCT + 3 % aluminium distearate + 1 % hydrogenated lecithin + 5 % PEG-35 castor oil.

In order to achieve a sustained and more complete release from the self-emulsifying oil vehicle, GnRH [6-D-Phe] acetate was combined with 2 % HPMC, HPC and HP-β-CD polymers, freeze-dried and incorporated into the Al-DiSt gelled MCT with hydrogenated lecithin and PEG-35 castor oil and into a castor oil-MCT mix. The addition of polymers of different grades to GnRH [6-D-Phe] increased the viscosity when incorporated in the pure mixture of castor oil: MCT 50:50 % (w/w) in comparison to self-emulsifying vehicle. Multiple nanostructures in the 200-1000 nm range formed upon injection of the self-emulsifying vehicle into PBS, whereas castor oil – MCT displayed single structures of self-assembled polymer in the higher µm range. The tested 2 % of low and high molecular HPMC, HPC and HP-β-CD were insufficient to achieve a more sustained and complete release of GnRH [6-D-Phe].

Interestingly, $Zn^{2+}$ ions and GnRH [6-D-Phe] formed nanostructures and fibrils *in vitro*. The association efficiency was maximal at a 10:1 $Zn^{2+}$: GnRH [6-D-Phe] ratio. The GnRH [6-D-Phe] fibrils could be formed in a Tris-buffer in a controlled manner through temperature reduction resulting in a pH shift of the buffer. This approach allowed simultaneously precipitating and freeze-drying the $Zn^{2+}$: GnRH [6-D-Phe] complex. A second *in situ* method used similar concept with exception of the Tris buffer salt, which was added to the oil vehicle. Thus association takes place after application. The release profiles of the complex and *in situ* complex formulations were not influenced by the oil matrix. The *in vitro* release of GnRH [6-D-Phe] from the freeze-dried assembly was sustained and continuous over 14 days and can be viewed as a promising platform for the controlled delivery of peptides.

In summary, the work in the thesis highlighted exemplary steps towards the development of a stable GnRH [6-D-Phe] oil depot suspension. It further underlies the importance of combining the oily vehicle development approach with the modification of the GnRH [6-D-Phe] peptide in order to successfully deliver the peptide in a sustained and controlled manner.

*When the dissertation is not the single thing that you can remember from the last couple of years, than you know you have done it the right way…..*

# ACKNOWLEDGMENTS

I would like to acknowledge our cooperation partners Veyx Pharm GmbH and in particular Dr. Sascha Schott and Dr. Wolfgang Zaremba for the vibrant scientific discussions concerning the project. I would also like to thank our collaboration partners in Leipzig, Prof. Kauffold and Dr. Haukur Sigmarrson for their valuable scientific input in the field of veterinary medicine and their constructive feedback, which improved the quality of the obtained results. I am glad DBU gave us the opportunity to collaborate on a project exploring the future sustainability of veterinary medicine.

I would like to thank Prof. Gerhard Winter and Andreas Tosstorff, Prof. Raphael Stoll, Prof. Stefan Zahler and Daniel Rüdiger for their help, support, recommendations and interesting additions for our collaboration on a published article, helping us bring the publication to fruition.

Above all, I want to thank my PhD supervisor, Prof. Wolfgang Friess, who somehow found a way to work with a single – minded free spirit such as myself. I want to thank him for his patience, his constant support and for helping me get through the disappointing and frustrating times of failed experiments. During the years I learned that research work, results and life in general are not always as expected but this only means you have to start looking somewhere else and never give up. I think I would never have become the researcher and person that I am right now without his guidance.

I would like to thank both working groups and I would not have made it without my best friend and lab partner, Christoph Marschall, aka Oli Cannoli- Giraffen Buddy. Dear Oli, you know, you helped me see some things clearer and my research became 100 times better when we were working together, though on different projects.

I want to thank my mathematics teachers, who taught me the value of mathematics as a tool to learn logical thinking and not just for the sake of solving problems. I want to thank all my professors at the university in Frankfurt, where I studied pharmacy for their passion and inspiration, which I found to be very contagious and made me follow the path of scientific research. I want to thank the one chemistry PhD student from Poland who recommended to me the best book of organic chemistry in English. I want to thank Dr. Marino Mania and Prof. Sabine Köpper for my first opportunity to go to a conference while still at university, where I wrote my first article. I would like to thank Dr. Wolfgang Schatton for the chance to do some experimental work in the pharmacy. I want to thank my supervisors during my practical year Dr. Daniel Wagner and Dr. Jörn Möckel, who gave me the opportunity to lead, teach and create, while working on a project. I would like to thank Gabriele Elser for her warmth welcome in the Rosen Pharmacy and for her constant support and help.

I would like to thank Inas ElBialy, Ivonne Seifert, Frida Gorreja, Vladimir Georgiev and Julia Meiereder who were there for me whenever I needed advice or someone to talk to. I would like to thank my dearest best friend, Ekaterina Bakardzhieva, for her uplifting and motivating words, and for always being there for me. I would also like to thank Nikola Kolev, who is a dear friend of mine and a fellow researcher for his feedback, his help and support. I would like to thank Elenka Dobreva, for her support in difficult moments.

I would like to dedicate all my work to my parents: Zhivko Zhelezov and Penka Zhelezova and to my sister: Nadezhda Yordanova. They were always there for me and have always supported me. My heart goes to them, because they were the ones who were with me in the worst and best moments in my life. I would not have made it so far without them. I would like to dedicate the last chapter of my thesis to my late grandmother, Radka Chaneva Raeva.

I think I would need more than these two pages to thank you all and I am sure I need to thank even more people, since life is a journey and not a destination.

“There are only two days in the year that nothing can be done. One is called Yesterday and the other is called Tomorrow. Today is the right day to Love, Believe, Do and mostly Live.” ― Dalai Lama XIV